Nuclear Safety
NEA/CSNI/R(2000)21
February 2001

OECD

In-Vessel Core Degradation Code Validation Matrix **Update 1996-1999**

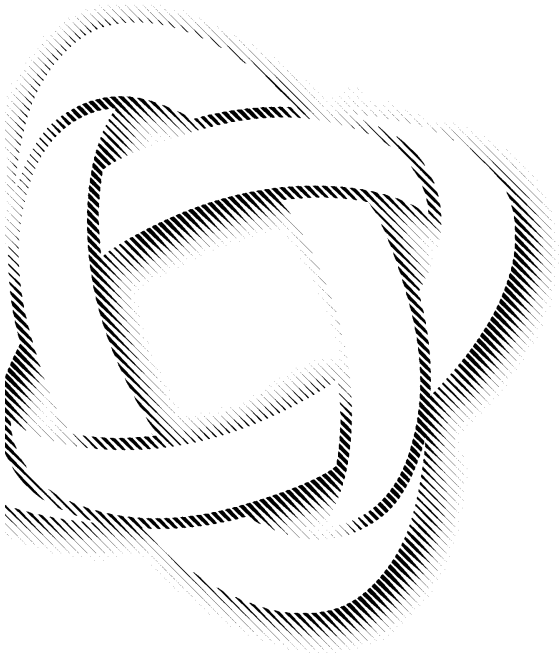

Report by an
OECD/NEA
Group of Experts

October 2000

OECD Nuclear Energy Agency
Le Seine Saint-Germain - 12, boulevard des Îles
F-92130 Issy-les-Moulineaux, France
Tél. +33 (0)1 45 24 82 00 - Fax +33 (0)1 45 24 11 10
Internet: http://www.nea.fr

AEN NEA

N U C L E A R • E N E R G Y • A G E N C Y

Additional copies of this CD-ROM, and paper copies, can be obtained from:

Dr. Jacques Royen
Nuclear Safety Division
OECD Nuclear Energy Agency
Le Seine - Saint Germain
12 Boulevard des Iles
F-92130 Issy-les-Moulineaux
France

E-mail: jacques.royen@oecd.org

IN-VESSEL CORE DEGRADATION CODE VALIDATION MATRIX
NEA/CSNI/R(2000)21

CONTENTS OF CD-ROM

IN-VESSEL CORE DEGRADATION
CODE VALIDATION MATRIX
Update 1996-1999

31. October 2000

Authors

K Trambauer - GRS Garching, Germany

T J Haste - EC, Joint Research Centre, Ispra, Italy

B Adroguer - IPSN, Cadarache, France

Z Hózer - AEKI, Budapest, Hungary

D Magallon - EC, Joint Research Centre, Ispra, Italy

A Zurita - EC, DG Research, Brussels, Belgium

Empty page

IN-VESSEL CORE DEGRADATION CODE VALIDATION MATRIX Update 1996-1999

K Trambauer (GRS, Garching), T J Haste (JRC, Ispra), B Adroguer (IPSN, Cadarache),
Z Hózer (AEKI, Budapest), D Magallon (JRC, Ispra) and A Zurita (EC, DG Research)

EXECUTIVE SUMMARY

In 1991 the Committee on the Safety of Nuclear Installations (CSNI) issued a State-of-the-Art Report (SOAR) on In-Vessel Core Degradation in Light Water Reactor (LWR) Severe Accidents. Based on the recommendations of this report a Validation Matrix for severe accident modelling codes was produced. Experiments performed up to the end of 1993 were considered for this validation matrix. To include recent experiments and to enlarge the scope, an update was formally inaugurated in January 1999 by the Task Group on Degraded Core Cooling, a sub-group of Principal Working Group 2 (PWG-2) on Coolant System Behaviour, and a selection of writing group members was commissioned. The present report documents the results of this study.

The objective of the Validation Matrix is to define a basic set of experiments, for which comparison of the measured and calculated parameters forms a basis for establishing the accuracy of test predictions, covering the full range of in-vessel core degradation phenomena expected in light water reactor severe accident transients. The emphasis is on integral experiments, where interactions amongst key phenomena as well as the phenomena themselves are explored; however separate-effects experiments are also considered especially where these extend the parameter ranges to cover those expected in postulated LWR severe accident transients. As well as covering PWR and BWR designs of Western origin, the scope of the review has been extended to Eastern European (VVER) types. Similarly, the coverage of phenomena has been extended, starting as before from the initial heat-up but now proceeding through the in-core stage to include introduction of melt into the lower plenum and further to core coolability and retention to the lower plenum, with possible external cooling. Items of a purely thermal hydraulic nature involving no core degradation are excluded, having been covered in other validation matrix studies. Concerning fission product behaviour, the effect of core degradation on fission product release is considered, but not its detailed mechanisms; fission product transport is also outside the scope and has been covered in other validation matrix studies.

The report initially provides brief overviews of the main LWR severe accident sequences and of the dominant phenomena involved. The experimental database is then summarised, with test conditions, phenomena covered and parameter ranges being presented in concise standard tabular formats to aid comparison amongst the different experimental series. These data are then cross-referenced against a condensed set of the phenomena and test condition headings presented earlier, judging the results against a set of selection criteria and identifying key tests of particular value. Areas where data are still required are identified. Finally, the main conclusions and recommendations are listed.

The main body of the report is supplemented by an appendix which summarises the experiments listing the most important references for data and evaluation reports for each test and/or relevant series, indicating the availability of the data for further analysis, while in addition evaluating the strengths and weaknesses of the experiments in providing data for code validation. Overall, the report is designed to help code developers in choosing tests to help formulate and validate new models, by summarising the relevant data in one place in a

convenient form, and to aid reviewers and users of codes to judge whether validation of a particular programme is sufficient for given plant applications, by checking that the relevant phenomena and parameter ranges have been covered.

Two categories of key tests are defined, in merit order:

- Category 1 experiments are amongst the best qualified for code validation in their field. ISPs normally fall into this category. Data are well documented and boundary conditions are well defined (these conditions may be relaxed if there are specific unique features). Category 1 tests are strongly recommended for the validation of system codes (depending on their specific objectives);
- Category 2 experiments are well qualified for code validation, and could be used to increase the degree of confidence in a code's suitability for a given application. The experiment may not be unique, but valuable in the sense of parameter range.

In general, no key test assignments are made for separate effects experiments, since they are unlikely to be used directly for system code validation. Exceptions are made in the case of bundle ballooning and fuel coolant interaction (FCI) experiments as these have some integral characteristics.

Twelve tests of the core degradation integral experiments and one reactor accident were selected as Category 1: CORA-13, CORA-28, CORA-33, CORA-W2, Phebus B9+, PBF SFD-1.4, ACRR ST-1, ACRR DF-4, LOFT LP-FP-2, Phebus FPT1, ACRR MP-1&2, and TMI-2.

Twenty-one tests of the core degradation integral experiments were selected as Category 2: CORA-2, CORA-5, CORA-12, CORA-15, CORA-17, CORA-31, CORA-30, Phebus SFD C3+, Phebus SFD AIC, NRU FLHT-5, ACRR-DF-2, Phebus FPT0, Phebus FPT4 (provisional), Sandia XR1-2, SCARABEE BF1, ACRR DC-1, CODEX-AIT1, CODEX-AIT2, QUENCH-01, QUENCH-03, and QUENCH-04.

Of the bundle separate effects experiments four tests were selected: REBEKA-6 and NRU MT-4 for category 1 and for category 2 Phebus 218 and MRBT B6.

Of the fuel-coolant interaction experiments seven tests were selected: FARO L-14, FARO L-28, and KROTOS K-44 for category 1 and for category 2 FARO L-11, FARO L-31, FARO L-33, and KROTOS K-58.

Concerning the late phase, the reactor situation is best covered by the following separate effects test: BALI, RASPLAV Salt, SIMECO, BENSON Rig and the CYBL facility.

Based on the completeness of the experimental data base necessary for code validation, and reflecting the degree of understanding of phenomena, it is considered that the following parameters or processes are not fully covered or understood only in a limited way:

- Effects of high burn-up, MOX, quenching at high temperature, and air ingress on core degradation;
- Transition from early to late phase, crust failure with subsequent slumping of melt into the lower plenum and quenching;
- Thermal loads to RPV by phase separation in molten pool including metallic layers and their consequences on vessel failure.

Continual updating of the matrix is considered worthwhile on a regular basis to monitor the adequacy and completeness of the experimental database for the code validation. This is particularly important regarding the late phase, which is currently less well covered than the early phase.

CONTENTS LIST

Empty page

LIST OF TABLES

Empty page

LIST OF FIGURES

Empty page

ABBREVIATIONS

ACRR	Annular Core Research Reactor
ADS	Automatic Depressurisation System
AECL	Atomic Energy of Canada Limited
AEA	AEA Technology
AEKI	Atomenergia Kutatóintézet
AIC	Ag-In-Cd (Control Rod Absorber Material for PWR)
AIT	Air Ingress Test
ATWS	Anticipated Transient Without Scram
B&W	Babcock and Wilcox
BCD	Battelle Columbus Division
BOP	Balance Of Plant
BMWi	German Federal Ministry for Economics and Technology
BWR	Boiling Water Reactor
CANDU	Canadian Deuterium-Uranium Reactor
CDF	Core Damage Frequency
CE	Combustion Engineering
CEA	Commissariat à l'Energie Atomique
CEC	see EC
CEN	Centre d'Etudes Nucléaires
CFM	Central Fuel Module
CHF	Critical Heat Flux
CODEX	COre Degradation EXperiment
CSARP	Co-operative Severe Accident Research Program
CPU	Central Processor Unit
CRD	Control Rod Drive
CRNL	Chalk River Nuclear Laboratories
CSD	see SFD
CSN	Consejo de Seguridad Nuclear
CSNI	Committee on the Safety of Nuclear Installations
DF	Debris Formation
DNB	Departure from Nucleate Boiling
DOE	Department of Energy
EC	European Commission
ECC	Emergency Core Coolant
ECCS	Emergency Core Coolant System
ECN	Energieonderzoek Centrum Nederland (see NRG)
ENEA	Energia Nucleare ed Energia Alternative
EPRI	Electric Power Research Institute
EU	European Union
FAI	Fauske and Associates
FLHT	Full Length High Temperature
FORTUM	Fortum Engineering Ltd (formely IVO)
FP	Fission Product
FzK	Forschungszentrum Karlsruhe (formerly KfK)
GE	General Electric
GRS	Gesellschaft für Anlagen und Reaktorsicherheit
HPIS	High Pressure Injection System

HTS	High Temperature Shield
IDCOR	Industry Degraded Core Rulemaking Program
IKE	Institut für Kernenergetik und Energiesysteme
ILCL	Intact Loop Cold Leg
INEL	Idaho National Engineering Laboratory (now INEEL)
IPE	Individual Plant Evaluation
IPSN	Institut de Protection et de Sureté Nucléaire
ISP	International Standard Problem
IST	International Standard Temperature
IVO	Imatran Voima Oy (see FORTUM)
JAERI	Japan Atomic Energy Research Institute
KAERI	Korea Atomic Energy Research Institute
KfK	see FzK
KI	Kurchatov Institute
LOCA	Loss of Coolant Accident
LOSP	Loss of Off-Site Power
LOFT	Loss of Fluid Tests
LP	LOFT Project
LPIS	Low Pressure Injection System
LWR	Light Water Reactor
NEA	Nuclear Energy Agency
NPP	Nuclear Power Plant
NRG	Nuclear Research and Consultancy Group (formerly ECN and KEMA)
NRU	National Reactor Universal
NSRR	Nuclear Safety Research Reactor
NUPEC	Nuclear Power Engineering Centre
ODE	Ordinary Differential Equations
OECD	Organisation for Economic Co-operation and Development
PBF	Power Burst Facility
PCMI	Pellet Clad Mechanical Interaction
PCS	Primary Coolant System
PIE	Post Irradiation Examination
PNS	Projekt Nukleare Sicherheit
PORV	Power Operated Relief Valve
PRA	Probabilistic Risk Assessment
PSA	Probabilistic Safety Assessment
PTE	Post Test Examination
PWG	Principal Working Group
PWR	Pressurised Water Reactor
QA	Quality Assurance
RBMK	Light Water Cooled, Graphite Moderated Channel Type Reactor*
RCA	Re-inforced Concerted Action
RCS	Reactor Coolant System
RIA	Reactivity Initiated Accident
RPV	Reactor Pressure Vessel
SASA	Severe Accident Assessment Branch
SFD	Severe Fuel Damage (in French: CSD)
SLCS	Standby Liquid Control System
SNL	Sandia National Laboratory
SOAR	State of the Art Report

ST	Scoping Test / Source Term
STCP	Source Term Code Package
TH	Thermal hydraulic
TMI-2	Three Mile Island Unit 2
TMLB'	Transient with loss of secondary system steam relief valves and of on and off-site power (NUREG-1150 notation)
TUH	Technische Universität Hannover
TUM	Technische Universität München
UCLA	University of California Los Angeles
UCSB	University of California Santa Barbara
UPM	Universidad Politécnica de Madrid
UKAEA	United Kingdom Atomic Energy Authority
USNRC	United States Nuclear Regulatory Commission
VTT	Valtion Teknillinen Tutkimuskeskus (Technical Research Centre of Finland)
VVER	see WWER
WWER	Water Moderated, Water Cooled Energy Reactor*

* taken from IAEA specific publications of the Extrabudgetary Programme on the safety of WWER and RBMK NPPs

Empty Page

GLOSSARY

Severe Accident:	A reactor core accident which is more severe than a design basis accident and results in substantial damage to the core.
Core Uncovery:	The water mixture level in the reactor vessel falls below the top of the active fuel.
Core Damage:	The fuel assemblies are disfigured by mechanical fracturing, or by liquefaction due to material interactions or by melting.
Core Melt:	The reactor core overheats and this leads to substantial melting or liquefaction of the core material.
Degraded Core:	An advanced state of core damage in which the original fuel bundle geometry has been substantially lost.
Early Phase:	Refers to the initial stages of core damage, including clad oxidation and the melting and relocation of mainly metallic material. A mainly rod-like geometry is maintained.
Late Phase:	Refers to the stages of core degradation involving substantial melting and relocation of fuel materials including s, including the transfer of materials to the lower vessel plenum and the containment if that occurs. The core may lose its rod-like geometry and include debris/rubble bed and melt pool regions.

Empty page

2. ACCIDENT SEQUENCES FOR LWRs

The objective of this chapter is to define in a general way the initial and boundary conditions of the reactor core and the core degradation processes during the course of a severe accident. The scope is limited to the Light Water moderated Reactors (LWRs), this means that for example neither the degradation of Canadian Deuterium-Uranium (CANDU) reactor pressure tubes nor degradation of the graphite moderated RBMKs are considered herein. Also detailed characterization of plant sequences including accurate quantification of possible parameter ranges, to establish a data base for the identification of gaps in the experimental data base, is beyond the objectives of this report.

This chapter is based on the description of accident sequence phenomena and boundary conditions in "Primary System Fission Product Release and Transport-State of the Art Report to the CSNI" [2.1] which provides also a brief collection of plant transient data to be expected in severe accident sequences, along with the corresponding EC report [2.2]. Also taken into account are the recently published status reports on VVER specific features [2.3], on Molten Material Relocation [2.4], on Core Quench [2.5], [2.6], on Molten Fuel Coolant Interaction [2.7], [2.8]and the Proceedings of the Workshop on In-Vessel Core Retention and Coolability [2.9], and the Rasplav Application Report [2.10].

2.1 Plant Types

The plant types considered in this chapter are those with reactors that are uranium dioxide (UO_2) fuelled, and light water moderated and cooled. This includes light water reactors (LWRs), i.e. pressurized water reactors (PWRs and VVERs) and boiling water reactors (BWRs) of U.S. and European origin that have been designed, built, and operated by Organization for Economic Cooperation and Development (OECD) member countries. Advanced design plants are not explicitly discussed in this report, although advanced light water reactors (ALWRs), including passive plants, are expected to have RCS accident boundary conditions similar to low-pressure sequences for existing LWRs.

The sizes of Western PWRs range from the single loop 510-MW(t) Zorita plant in Spain to large four-loop 4270-MW(t) units, such as the Chooz B1 and B2 plants in France. Despite such differences, which are mainly reflected in the fission product and core material inventories, there are no substantial differences in the basic nuclear and thermal-hydraulic parameters such as system pressure (~ 16 MPa), inlet temperature (~ 565 K), fluid temperature rise (30 - 35 K) or power density in the core (25 - 40 kW/kg uranium). The core material inventories of a typical 3600-MW(t) PWR are 100000 kg urania fuel, 26000 kg Zircaloy cladding, 2800 kg absorber material (Ag, In, Cd) and 4000 kg stainless steel structure material [2.11]. There are several PWRs with burnable neutron poison rods with gadolinium or control rods with boron carbide. Depending on the accident sequence, large amounts of boric acid (up to 40000 kg) can be injected by means of the emergency core cooling system (ECCS).

Despite the sometimes significantly different RCS designs or control systems, the arrangements of the fuel rods, spacer grids, control rods and guide tubes are nearly identical. This means that local processes are similar for all Western PWRs discussed in this report.

The sizes of Eastern PWRs range from six-loop 1300-MW(t) VVER-440 plant to large four-loop 3000-MW(t) VVER-1000. Despite such differences, which are mainly reflected in the fission product and core material inventories, there are no substantial differences in the basic nuclear and thermal-hydraulic parameters such as system pressure (12 - 16 MPa), inlet temperature (540 - 561 K), fluid temperature rise (~ 30 K) or power density in the core (~37 kW/kg uranium). The main difference from Western reactors cores is the triangular grid which results in a more densely packed core, and in the case of VVER-440 the six-edge fuel assembly canister (Zr2.5%Nb) and absorber elements (boron steel 2 % B, 20 % CR, 16 % Ni) with movable fuel assemblies. With these canisters they are more BWR-like than PWR-like. The VVER-440 reactors have valves in the hot and cold legs to isolate the loops in case of leakage from steam generator tubes. The second important difference from Western reactors is the use of horizontal steam generators, this results in less effective natural convection in the loop. The core material inventories of the VVER-1000 are 80098 kg urania fuel, 22630 kg Zr1%Nb cladding, 272 kg boron carbide (B_4C) as absorber material and 4342 kg stainless steel structural material for the Russian fuel type [2.12] and 91755 kg urania fuel, 24766 kg Zircaloy (including 1092 kg spacer grids), 206 kg boron carbide in upper part of control rods and 327 kg Ag-In-Cd Alloy in lower part for the Westinghouse fuel type (Temelin NPP, Czech Republic) [2.3]. There are several PWRs with burnable neutron poison rods with gadolinium or control rods with boron carbide. Depending on the accident sequence, large amounts of boric acid (up to 90 m^3 of water with 40 g of H_3BO_3/kg of water concentration) can be injected by means of the emergency core cooling system (ECCS).

The thermal power of BWRs range from the small 183-MW(t) Dodewaard plant in the Netherlands (now shut down) to the large 3840-MW(t) Grundremmingen B&G plants in Germany. The basic nuclear and thermal parameters are system pressure (~ 7.1 MPa), which determines the steam outlet temperature (~ 560 K), feed water temperature (455 - 490 K) and specific power (20 - 30 kW/kg uranium). The core material inventories of a typical 3800 MW(t) BWR are 155000 kg urania fuel, 76000 kg Zircaloy cladding and channel boxes, 1200 kg absorber material (B_4C) and 15000 kg stainless steel structural material. Under Accident Transients Without Scram (ATWS) conditions or as an accident management action, large quantities of borax and boric acid (on the order of 4000 kg) might be injected by means of the standby liquid control system (SLCS).

As with PWRs, there are very different BWR system designs with regard to the pressure suppression system or the containment configuration. On the other hand, the arrangement of both the fuel rods in the channel boxes and the control blades are very similar for the various types of BWRs. In BWR cores, the control blades consist of small-diameter stainless steel tubes filled with boron carbide which are positioned between the boxes. Regarding the core geometry, differences only exist in the distribution of fuel rods and water holes within a fuel element, which might affect the relocation and blockage processes.

The similarities of PWR and BWR core designs imply that the most variant conditions are the power density due to fission and decay heat, and the fluid state, which depend on plant status, initiating event and accident progression. These conditions are discussed below.

2.2 Plant Status and Initiating Event

The plant may be in different conditions:

- reactor operation
- hot or cold standby
- shutdown cycle.

Most severe accident risk analyses reflect the reactor operation [2.13], [2.14], [2.15]. Although there are differences among the plants analyzed, the dominant sequences tend to be the same; differences appear mainly in their expected frequencies and uncertainties. The dominant accident groups, each one including similar sequences, for PWRs and for BWRs are:

- Loss of offsite power (LOSP) or station black out
- Transients with scram function (TMLB')
- Transients with failure of scram function (ATWS)
- Small break loss of coolant accidents (SB-LOCA)
- Steam generator tube rupture (SGTR)
- Steam generator header cover leakage (only VVER)
- Interfacing loss of coolant accidents or V-Sequence
- Intermediate break loss of coolant accidents
- Large break loss of coolant accidents (LB-LOCA).

The core damage frequencies (CDFs) leading to core melt range up to 3.10^{-4}. They provide insight to the reader on the relative likelihood of various sequence types and indicate weaknesses in the safety systems or guide cost-benefit analyses. Independent of the likelihood of a specific sequence, the severe accident computer codes should be able to cope with each physically reasonable accident progression.

In the following, the different accident sequences starting from normal operation are briefly described.

2.2.1 PWR Accident Sequences

Station blackout sequences are initiated by a loss of offsite power (LOSP). With safety systems functioning normally, the LOSP would result in reactor trip, emergency diesel actuation, and decay heat removal via the secondary side. However, in station blackout sequences, the concurrent failure of the emergency diesels involves the loss of the injection which precludes the cooling to the reactor coolant pump seals. This might result in a component failure and create a small LOCA. The additional failure of the auxiliary feedwater (TMLB') causes a pressure increase with the opening of the pressurizer relief valves. Inventory will be lost through the relief valves as they open and close in cycles or as they might erroneously stay open. Due to the lack of AC power, the safety injection systems are inoperable and core damage will result.

Transient sequences at power can be initiated by a number of events that result in a reactor trip. Additional failure leading to loss of decay heat removal would be required to cause core damage. Transients tend to lead to similar RCS condition (e.g. high pressure) as station blackouts.

Within the class of LOCAs in PWRs, various sequences are evaluated, including those resulting from large, intermediate, and small breaks with failure of the emergency core cooling systems (ECCSs), from the beginning or after the start of sump water recirculation. Only passive accumulators are assumed to be operational. These sequences can lead to core degradation at different times, depending on the location and size of the break, plant condition and failure modes.

Small LOCAs are associated with RCS ruptures with blowdown rates equivalent to double-ended circumferential breaks in pipes <5 cm in diameter. The RCS pressure tends to remain higher than secondary side pressure, and a reactor trip occurs. As the break size is insufficient to provide core cooling, even with high pressure injection, decay heat removal through the secondary side or through primary feed and bleed is necessary. Moreover, long-term cooling must be provided for. The failure to accomplish high-pressure injection or the decay heat removal function will lead to core damage.

Intermediate LOCAs are associated with RCS ruptures and flow through open valves with blowdown rates equivalent to double-ended circumferential breaks between 5 and 15 cm in diameter. The RCS pressure remains stable, but lower than secondary side pressure.

Large LOCAs are beyond that size but the associated severe accident phenomenology is similar to that of intermediate breaks. These breaks cause a rapid coolant blowdown, lasting seconds to minutes. The rapid depressurization causes the reactor shutdown, which is later maintained by injecting borated water. The core reflooding and decay heat removal functions must be assured, which requires the correct actuation and operation of the low-pressure systems and systems for the containment cooling function. If such safety functions are not accomplished, core damage will occur.

SGTR and interfacing LOCA sequences will generally have RCS conditions that are bounded by the sequences previously discussed.

Concerning VVER there are no new initial events leading to core melt, except the leakage or rupture of steam generator collector, which generally results in larger break sizes than steam generator tube ruptures. The accident progression in VVERs in general is similar to that in PWRs. However the differences due to material and geometry can result in differences in the accident sequence and the timing of the event.

2.2.2 BWR Accident Sequences

A BWR station blackout begins with a turbine trip followed by the loss of all AC power. The reactor is shutdown, and can be depressurized if battery power remains available. In the case the reactor is not depressurized, the removal of decay power may be accomplished with high-pressure injection systems operating with turbine-driven pumps, but only if station DC power is available. If such systems become depleted before AC power is restored, core damage occurs (long term station black out) [2.16]. If the high pressure injection system is inoperable from the beginning, core damage occurs much earlier (short term station black out).

Transients, including anticipated transient without scram (ATWS), require the intervention of operators to depressurize the system, to scram the reactor manually, or to actuate manually the secondary shutdown system, i.e. the standby liquid control system (SLCS), if it is not

automatically initiated. Several BWR ATWS sequences could be considered, involving various combinations of failure to shutdown the reactor by manual scram or by the secondary shutdown system. If shutdown is achieved by the secondary shutdown system, but the vessel is not manually depressurized, then the high-pressure injection system may take decay heat out to the suppression pool. If the suppression pool is not cooled, the pool will become saturated. Pool saturation or impurities in the pool produce failure of the high-pressure system, and core damage results. If shutdown is not achieved and if a relief valve remains stuck open, then the outcome of the process will depend on the extent to which the core is cooled with the low pressure injection system and the recirculation system.

LOCAs tend to be lower frequency in BWRs due to the lower system pressure, the presence of internal recirculation pumps in some designs, and due to larger redundancies in the ECCSs, active and sometimes passive, plus the possibility of automatic or manual depressurization.

2.2.3 Stand-by and shut down conditions

Accidents in PWRs and BWRs starting from hot or cold standby conditions are in principle similar to those initiated during normal reactor operation. They are different with regard to timing of the accident progression and heat-up rates but they do not create new failure modes.

A different failure mode might occur if the accident is initiated during a shutdown cycle of a reactor [2.17], [2.18]. In this period, the RCS is often open to the containment atmosphere and minimal safety systems are functional. Sometimes even the vessel head is dismantled. This means that, in the case of failure of the decay heat removal system, boildown occurs. This boiling process might be very slow, and might be accompanied by air ingression. Studies [2.19], [2.20] have shown that these shutdown cycle accidents contribute significantly to the overall core meltdown risk.

Starting from the different initiating events, the accident progression will be briefly discussed in the following section.

2.3 Degraded Core Accident Progression

A severe accident sequence involves a large number of phenomena that can be extended over long periods of time. The importance of any particular phenomenon will change as the accident progresses. The in-vessel sequences may be divided into four time intervals [2.20]:

Dominant Phenomena	Time Interval
Thermal hydraulic and Neutronic Transient	Initiation of accident until superheat in core
Core Uncovery and Heat-up	Superheat in core until core temperature exceeds 1500 K
Oxidation, Melting, Relocation and Slumping in Core Region	Core temperature exceeding 1500 K until core slump
Lower Plenum Heat-up and Vessel Failure	Formation of molten pool in lower plenum until vessel failure

The first and partly the second time interval are dominated by thermal-hydraulics and are very plant and sequence dependent. It is already covered by the "CSNI Code Validation Matrix of Thermo-hydraulic Codes for LWR LOCA and Transients" [2.21] and "Separate Effects Test

Matrix for Thermal-hydraulic Code Validation" [2.22]. Therefore the accident progression during the third and fourth intervals will be discussed herein.

Accidents that lead to core damage can result from a number of different types of event sequences as described earlier. However, all of these core damage accidents have certain common chemical and physical phenomena which are briefly described in their approximate order of occurrence in a degraded core accident. More detailed information on these phenomena can be found in [2.23], [2.24] [2.25] and [2.26].

The time from accident initiation up to core uncovery varies from very short, less than 10 min in case of LB-LOCA, to very long, about 6 to 10 h in case of long-term LOSP or TMLB'. Also the system pressure varies from low, about 0.3 MPa in case of LB-LOCA, to high 7 - 15 MPa during transients without depressurization.

After the core is uncovered, heat transfer from the fuel to the steam is low compared with decay heat, and the fuel temperature increases. At this time, the mixture level is established in the lower core region or, in case of BWR and actuation of Automatic Depressurization System (ADS), below the core. The low mixture level results in very low steam generation and steam flow into the core. The high temperature leads to oxidation of the Zircaloy fuel cladding and hydrogen generation and can also lead to clad ballooning and rupture.

Clad rupture is the cause of first fission product release. While the effect of clad ballooning and rupture on other core degradation phenomena is somewhat uncertain, it may reduce natural circulation flows between the core and upper plenum, causing reduced heat transfer and therefore more rapid heat-up of the core [2.27].

Zircaloy (Zr1%Nb in the case of VVER) cladding oxidation by steam causes acceleration of the core heat-up rate. Heat-up rate due to decay heat alone is in the range of 0.4 to 1.0 K/s, depending on the location in the core and the particular accident sequence, and can increase to well above 1 K/s as the local temperature increases above ~1300 K due to rapid oxidation of Zircaloy and the strongly exothermic nature of the reaction. In accidents with low decay heat (shut down cycle) the heat-up rate is lower than 0.2 K/s. In this case, an oxidation excursion will not occur, because the threshold temperature for a runaway reaction is not reached. Substantial oxidation of the cladding material may nevertheless still occur. Oxidation of Zircaloy increases the melting temperature, and high oxygen content in molten Zircaloy limits UO_2 dissolution [2.28], [2.29].

The core melt and initial relocation portion of accident progression encompasses low-temperature material interaction, metallic and U-Zr-O type melt formation and relocation. This part of the core degradation with no loss of rod-like geometry is named the "early phase of core degradation".

Core melt progression is initiated as a result of dissolution or eutectic reactions of core materials at temperatures well below the melting temperatures of the fuel and its cladding. These reactions involve control rods, burnable poison rods, clad, and structural materials forming relatively low temperature liquid phases [2.30]. PWR control rod material (Ag-In-Cd) is molten at ~1100 K [2.31], and the molten Ag-In-Cd alloy will chemically dissolve Zircaloy. However, due to chemical compatibility of Ag-In-Cd with its stainless steel clad, control rod failure would not be expected to occur until about 1500 K for low-pressure sequences and 1700 K for high pressure sequences [2.32]. At low pressure the stainless steel

clad fails before reaching its melting point due to internal pressure, deformation, and contact with the Zircaloy guide tube. In BWRs, VVERs and some PWRs with boron carbide (B_4C) as absorber, the major low-temperature reaction is between boron carbide (B_4C) and stainless steel at about 1500 K [2.30]. That is about the same temperature as the failure temperature of Ag-In-Cd control rods.

Metallic melts generated by these low-temperature interactions are able to dissolve other structures as BWR or VVER channel boxes and fuel rod cladding. They flow downwards in the core until they reach cooler regions where the melts tend to solidify, forming partial blockages in the flow channels between fuel rods, particularly in PWRs. Due to lower steaming rates and potentially higher temperatures in the lower part of the core, metallic melt can drain out of the core in BWRs [2.24]. The metallic blockages can restrict flow and cause accelerated heat-up of the core. UO_2 fuel can be liquefied at temperatures well below (up to 300 K or even more) its melting point (3100 K) by dissolution in molten Zircaloy (melting point 2030 to 2250 K, depending upon oxygen content) or other metallic material as iron [2.28], [2.29]. At higher temperatures, fuel liquefaction can occur due to the interaction between UO_2 and ZrO_2. The mainly ceramic melt $(U,Zr)O_2$ can lead to a blockage at a higher elevation in the core than the metallic blockage due to its higher freezing temperature (up to ~2800 K) [2.23].

As a result of diversion of steam around the blockage and the low thermal conductivity of the ceramic material, heat transfer from the ceramic blockage is slow, and a molten pool can form within a ceramic crust. This loss of rod-like geometry, which can also result from rod slumping with a solid debris formation, corresponds to the onset of the "late phase of core degradation". This has been observed to some extent in integral experiments, such as the recent Phebus FPT0 test [2.33], that were run to lower damage levels and to a significant extent in the Three Mile Island Unit-2 (TMI-2) accident. Lower melting point structural and other materials resistant to oxidation (e.g. nickel and silver) have been observed in the $(U,Zr)O_2$ ceramic melt.

The oxidation potential within molten pools has been estimated from measurements of the chemical forms (metals compared with oxides) within the melt [2.23]. These observations indicate that the oxygen potential is fairly high. Hydrogen-to-steam partial pressure ratios of the order of 0.01 to 1 form the range predicted for core wide averaged gas flow in LWR degraded core accidents.

A steam-starved environment can cause higher hydrogen-to-steam partial pressure ratios, which can result in reducing conditions. However, steam starvation over large volumes of the core is inconsistent with experience, i.e. the noncoherent nature of core melt progression and the large amounts of water that would still be present at this stage of most accidents in PWRs. Most BWR scenarios have lower steaming rates which cause more frequent steam starvation.

Crust failure and melt relocation to the lower plenum are late-phase core damage progression phenomena for which the uncertainties are greater than for the early phase phenomena [2.34]. The general understanding of the late-phase phenomena is based on examination of the damaged TMI-2 core, because large-scale experiments have not been run at high enough temperatures and for long enough time periods for the phenomena to occur fully. The TMI-2 accident progression suggests that, if the accident is unmitigated, the molten material will relocate into the lower region of the reactor vessel, either as a result of crust failure or but more unlikely of pool overflow from over the top of the crust. Approximately 20 tons of ceramic melt relocated into the lower plenum in the TMI-2 accident. The relocation to the

lower plenum is likely to be rate-limited due to the localized nature of the breach in the ceramic crust and the presence of structures in the core as well as core support structures that intercept and redirect the melt streams. This rate-limited relocation is expected to increase the steam generation and to some extent the oxidation and in turn hydrogen generation [2.30].

The so called TMI-2 scenario of melt relocation is typical for accident progression with high water inventory and water level in the lower core part. In scenarios with very low water inventory and water level below the lower core support plate, total core slumping due to failure of the core support plate is more likely to occur in PWRs than in BWRs. In BWRs the core support structure consists of many guide tubes which are supported by the RPV lower head. This makes a local failure more likely and results in a rate-limited relocation as in the TMI-2 scenario.

In general, the core slumping or core relocation into the lower plenum is characterised by a low degree of physical understanding and might never be described deterministically for all possible kinds of scenario. Therefore conservative assumptions regarding melt superheat, relocation rate, melt fragmentation etc. should be used for different scenarios to cover a sufficiently wide range of consequences regarding steaming rate, pressure build-up, chemical reaction, debris bed or cake formation etc. Due to the fact that the RPV wall is cold and wetted in general, jet impingement can be excluded as a failure mechanism of the RPV [2.35], [2.36]. Therefore short-term effects of melt relocation are mainly the re-pressurisation of the RCS, which is strongly coupled with the relocation scenario. On the other hand the long term effect depends more on the physico-chemical melt behaviour and the boundary condition of the melt in the lower plenum.

The long-term behaviour of the core material in the lower plenum is important for the estimation of RPV failure and the consequences for the thermal loads to the containment. If sufficient water is available in the lower plenum and the accumulated melt mass limited as in TMI-2, then a water-filled gap between the crusted melt and the RPV wall might protect the wall from thermal loads. Also effective ex-vessel cooling of medium-size LWRs can remove the decay heat and protect the RPV against failure. Small penetrations are unlikely to fail, as long as the RPV wall remains at low temperature due to refreezing of the melt in the tubes.

The main uncertainties for the estimation of RPV failure besides the gap and ex-vessel cooling are the corium melt mass accumulated in the lower plenum, the heat flux distribution for inhomogeneous melt due to melt separation or metallic melt accumulation on top of the ceramic melt pool, the melting of structure material in the lower plenum and finally the local or global failure mode of the RPV wall.

The TMI-2 examination showed that the peripheral fuel assemblies remained intact after the relocation of the central core region into the lower plenum and molten pool formation. It can be expected that even after the vessel failure large mass of core components remains in the reactor vessel. Following the lower head damage air can enter the primary system and the character of the degradation process can be changed compared to steam atmosphere conditions. The interaction of air with Zr alloys and UO_2 pellets can strongly affect the evolution of severe accident scenarios through heat generation, increased core degradation and fission product release. The interaction of air with fission products can influence the radiological source term due to the volatilisation of ruthenium oxide. The Zr oxidation in air produces for 85% more heat than in steam. The UO_2 pellets can be further oxidised and this results in a lower melting point.

Natural circulation has been identified as an important phenomenon in PWRs, particularly when the RCS pressure is high. Three potential natural circulation flow paths exist: in-vessel circulation; hot leg counter current flow, including flow into the steam generator tubes; and flow through the coolant loops [2.30]. The two main effects of natural circulation are enhancing heat transfer from the core region to other structures in the RCS and enhancing gas flow in the core, which might keep core temperatures low and delay melt progression. The changed temperature distribution in the core may affect the way the core degrades, and the coherency of any melt progression.

As noted, variations can exist within a sequence depending upon the status of plant systems and operator actions to manage the accident. The accident management strategy for a core damage accident while the core is still in the reactor vessel would consist of two main actions: (1) water makeup into the reactor vessel to reflood the partially damaged core and terminate the accident and (2) RCS depressurization to allow low-pressure makeup and to avoid high pressure melt ejection, should the core melt through the reactor vessel lower head.

Several of the integrated core damage progression tests have been reflooded, resulting in production of significant amounts of steam, with further oxidation and hydrogen generation as observed in some CORA tests and in LOFT LP-FP-2. This renewed heatup is important regarding accident management, as the additional hydrogen might threaten containment integrity and increased fission product release would increase the source term. The increasing fuel temperatures, being counter-intuitive, might confuse the operators into taking inappropriate action. Moreover, reflooding can produce a debris bed of fragmented fuel particles that lose their cladding restraint due to oxygen embrittlement. It is estimated that about one-third of the total hydrogen generated in the TMI-2 accident was produced during reflood from the B-loop transient [2.37].

Given these considerations, reflooding of degrading core has been investigated extensively both experimentally through integral and separate-effects tests, and by modelling. These efforts are summarised in [2.5] and [2.6]. It has been established that for quenching below 1870 K cracking of the protective oxide shell on the Zircaloy cladding, through thermal shock and phase change of the oxide, can expose new metallic surfaces which can oxidise at an increased rate. However this appears insufficient to trigger a new oxidation excursion. Renewed excursion is observed for quenching above 2070 K, where this mechanism does not apply; the reason is not fully established but oxidation of relocating Zr-rich melt may be a strong contributing factor. The continuing QUENCH experimental programme at FZ Karlsruhe aims to resolve the issue.

During the period of in-vessel melt progression before reactor vessel lower head failure, a significant fraction of the fission products released from fuel will reduce the decay heat in the core region and it will deposit on RCS surfaces either by aerosol or vapour deposition. In an accident that involves an open flow path (two holes in the system), air can be drawn through the vessel through natural convection ("chimney effect"), potentially oxidizing the remaining metallic materials if the temperature is sufficiently high and increasing the fission product release, particularly ruthenium [2.17], [2.18]. Design features of the plant, such as the possibility to flood the reactor cavity, can reduce the extent of this effect, but increase the possibility of ex-vessel steam explosions.

Recently there has been significant interest and activity in the area of risk during shutdown conditions. This is due to several factors, including a number of refuelling outage incidents that have occurred at U.S. plants in the last several years: the Vogtle loss of AC power incident [2.19], [2.38] in 1990; recent probabilistic risk assessment (PRA) work suggests that shutdown conditions contribute significantly to the total risk of core damage [2.19] and that the characteristics of plant conditions during shutdown may be less forgiving than during power operation. This less forgiving nature is due to reduced technical specifications, higher dependence on operator action, and the potential for the RCS and containment to be open.

The conditions in the RCS during shutdown are different from the conditions for accidents at power. Radioactive decay has significantly reduced the fission product activity in the core, particularly for volatiles, compared with immediately after shutdown. Therefore, decay heat levels are lower, leading to lower fuel heat-up rates in the order of 0.1 K/s. Rapid temperature escalation at 1500 K is less likely because the thick oxide layer formed on the clad outer surface tends to reduce the oxidation reaction rate. The important safety issue in the intact circuit case is whether the system can repressurise sufficiently that gravity-driven water make-up could be prevented. On the other hand, if the RCS is open to containment, this means that the RCS is likely to be exposed to air. This might lead to more rapid temperature escalation due to the higher exothermal reaction energy but not to hydrogen generation.

Based on these scenarios the physical and chemical phenomena will be briefly described in a more general sense in the following chapter.

References

[2.1] Wright A L et al., "Primary System Fission Product Release and Transport: A State-of-the-Art Report to CSNI", NUREG/CR-6193, NEA/CSNI/R(94)2, June 1994.

[2.2] Hocke K-D, Adroguer B, Shepherd I and Schatz A, "Fission Product Release : State-of-theArt Review", EUR 16499 EN, 1995.

[2.3] Hózer Z, Trambauer K and Duspiva J, "Status Report on VVER-Specific Features Regarding Core Degradation", NEA/CSNI/R(98)20, September 1998.

[2.4] Bandini G, Gauntt R O, Okkonen T, Suh K Y, Shepherd I and Linnemann T, "Molten Material Relocation to the Lower Plenum: A Status Report, September 1998", NEA/CSNI/R(97)34, September 1998.

[2.5] Haste T J, Adroguer B, Aksan N, Allison C M, Hagen S, Hofmann P and Noack V, "Degraded Core Quench: A Status Report, August 1996", NEA/CSNI/R(96)14, OCDE/GD(97)5, August 1996.

[2.6] Haste T J and Trambauer K, "Degraded Core Quench: Summary of Progress 1996-1999", NEA/CSNI/R(99)23, February2000.

[2.7] CSNI, 'Technical Opinion Paper on Fuel-Coolant Interaction", NEA/CSNI/R(99)24, November 1999.

[2.8] Magallon D et al., "MFCI Project Final Report", European Commission report INV-MFCI(99)-P007, 1999.

[2.9] Trambauer K et al, "OECD Workshop on In-Vessel Core Debris Retention and Coolability, Garching, 3-6 March 1998: Summary and Conclusions", NEA/CSNI/R(98)21, January 1999.

[2.10] Tuomisto H, Strizhov V, Sehgal B R, Behbahani A, Gonzalez R, Sanderson B, Trambauer K, "Application of the OECD Rasplav Project Results to Evaluations at Prototopic Accident Conditions" Draft 3. April 2000.

[2.11] Bowsher B R, "Fission Product Chemistry and Aerosol Behaviour in the Primary Circuit of a Pressurized Water Reactor Under Severe Accident Conditions", Progr. Nucl. Energy 20 (3), 199 (1987).

[2.12] Preliminary Passport for Temelin NPP, Internal Report, CEZ-ORGREZ Brno, (in Czech), 1989.

[2.13] U.S. Nuclear Regulatory Commission, "Severe Accident Risks: An Assessment for Five U.S. Nuclear Power Plants", NUREG-1150, Final Summary Report, December 1990.

[2.14] "German Risk Study Nuclear Power Plants, Phase B", Gesellschaft für Reaktorsicherheit mbH, GRS-72, Köln, June 1989.

[2.15] "SWR Sicherheitsanalyse" Gesellschaft für Anlagen- und Reaktorsicherheit (GRS) mbH, GRS-102, Köln, June 1993.

[2.16] Hodge S A, Clevelend J C, Kress T S and Petek M, "Identification and Assessment of BWR In-Vessel Severe Accident Mitigation Strategies", NUREG/CR-5869, October 1992.

[2.17] Powers D A, Kmetyk L N and Schmidt R C, "A Review of the Technical Issues of Air Ingression During Severe Reactor Accidents", NUREG/CR-6218, September 1994.

[2.18] Shepherd I et al., "Oxidation Phenomena in Severe Accidents (OPSA) Final Report", EUR 19528 EN, 2000.

[2.19] U.S. Nuclear Regulatory Commission, "Evaluation of Shutdown and Low Power Risks", SECY-91-283, 9 September 1991.

[2.20] Jenks R P et al., "SCDAP/RELAP5 Independent Peer Review", Los Alamos, NM, LA-12481, January 1993.

[2.21] Aksan N et al., "CSNI Code Validation Matrix of Thermo-Hydraulic Codes for LWR LOCA and Transients", CSNI Report 132, Paris, March 1987.

[2.22] Aksan N, D'auria F, Glaeser H, Pochard R, Richards C and Sjoberg A, "OECD/NEA-CSNI Separate Effects Test Matrix for Thermal-Hydraulic Code Validation, Vols. 1 & 2", OCDE/GD(94)82 & 83, September 1993.

[2.23] Hobbins R R et al., "Review of Experimental Results on Light Water Reactor Core Melt Progression", Nucl. Technol. 95, September 1991.

[2.24] Wright R W et al., "Core Degradation and Fission Product Release, The Phebus Fission Product Project", Elsevier Science Publishers, Essex, England, 1992.

[2.25] Allison C et al., "Severe Core Damage and Associated Fission Product Release", Prog. Nucl. Energy 20 (2), 1987.

[2.26] Shepherd I et al., "Investigation of Core Degradation (COBE) Final Report", EUR 18982 EN, 1999.

[2.27] Bayless P et al., "Feedwater Transient and Small Break Loss of Coolant Accident Analyses for the Bellafonte Nuclear Plant", NUREG/CR-4741, March 1987.

[2.28] Adroguer B et al., "Analysis of the Fuel Cladding Chemical Interaction in PHEBUS SFD Tests Using ICARE2 Code", p. 137 in Proceedings of IAEA Meeting on Behaviour of Core Materials and Fission Product Release in Accident Conditions in LWRs, Aix-en-Provence, France, March 1992, International Atomic Energy Agency, IAEA-TEC DOC-706, June 1993.

[2.29] Adroguer B et al, "Corium Interactions and Thermochemistry (CIT Project) Final Report, European Commission report INV-CIT(99)-P040, IPSN/DRS/SEMAR 99/123, December 1999.

[2.30] Kinnersly S R et al., "In-Vessel Core Degradation in LWR Severe Accidents: A State-of-the-Art Report to CSNI", NEA/CSNI/R(91)12, November 1991.

[2.31] Bowsher B R et al., "Silver-Indium-Cadmium Control Rod Behaviour During a Severe Reactor Accident", UK Atomic Energy Authority report AEEW-R 1991, United Kingdom, 1986.

[2.32] Petti D A, "Silver-Indium-Cadmium Control Rod Behaviour in Severe Reactor Accidents", Nucl. Technol. 84 128, 1989.

[2.33] Hanniet-Girault N And Repetto G, "Phebus FPT0 Final Report", IPSN/DRS/SEA report SEA 1/99, IP/99/423, February 1999.

[2.34] Linnemann Th, Koch M K and Unger H, "Review of the TMI-2 Accident and Late Phase SFD Code Modelling with View on Material Movement to the Lower Head", Ruhr University of Bochum Report RUB E-193, INV-COBE(98)-D008, February 1998.

[2.35] Sehgal B R et al., "Melt-Vessel Interactions (MVI) Final Report", European Commission, INV-MVI/FI4S-CT95-0007, January 2000

[2.36] Krieg R et al., "Reactor Pressure Vessel under Severe Accident Loading (RPVSA) Final Report", FZKA 6358, European Commission, INV-RPVSA/FI4S-CT95-0002

[2.37] Ruan P et al., "Thermal Interactions During the Three Mile Island Unit 2 2-B Coolant Pump Transient", Nucl. Technol. 87, August 1989.

[2.38] U.S. Nuclear Regulatory Commission, "Loss of Vital AC Power and the Residual Heat Removal System During Mid-Loop Operations at Vogtle Unit 1 on March 20, 1990", NUREG-1410, June 1990.

3 IDENTIFICATION OF PHENOMENA AND DEGREE OF PHYSICAL UNDERSTANDING

The quantification of uncertainties of specific processes depends on the knowledge about the involved phenomena, their physical or chemical modelling and the analytical approach or numerical simulation. Since the models employed in diverse computer codes are different, general statements regarding uncertainties must be oriented on the specific phenomena listed below.

The identification and description of phenomena is based on the In-Vessel Core Degradation Code Validation Matrix [3.1], and the Status Report on VVER-Specific Features Regarding Core Degradation [3.2] and extended to the late phase of core degradation including in-vessel core debris retention phenomena.

The definition of the different accident stages also follows the validation report [3.1]:

Severe Accident	A reactor core accident which is more severe than a design basis accident and results in substantial damage to the core;
Core Uncovery	The swell level in the reactor vessel falls below the top of the active fuel;
Core Damage	The fuel assemblies are disfigured by mechanical fracturing, or by liquefaction due to material interactions or by melting;
Core Melt	The reactor core overheats and this leads to substantial melting or liquefaction of the core material;
Degraded Core	An advanced state of core damage in which the original fuel bundle geometry has been substantially lost;
Early Phase	Refers to the initial stages of core damage, including clad oxidation and the melting and relocation of mainly metallic material. A mainly rod-like geometry is maintained;
Late Phase	Refers to the stages of core degradation involving substantial melting and relocation of fuel materials including ceramics, including the transfer of materials to the lower vessel plenum and the containment if that occurs. The core may lose its rod-like geometry and include debris/rubble bed and melt pool regions.

The evaluation of the degree of physical understanding is based on individual experience regarding the uncertainties of available experiments as well as model verification and code validation against experiments and evaluation of recent reports [3.3], [3.4], [3.5] under consideration of its significance and consequence on the accident progression. Three categories have been considered for the classification of the degree of physical understanding:

High	The phenomenon is well understood. The processes are adequately modelled and well verified in general.
Medium	The phenomenon is on the whole understood, uncertainties remain for unexplored parameter rages or extrapolation to reactor scale. The main processes are described by adequate models but the verification is not complete by the limited data base.
Low	The phenomenon is only partly understood. The models are rudimentary. The model verification is insufficient.

Phenomenon	Description	Understanding
I Fission and decay heat	Fission and decay heat determine the specific heat source in the fuel which is an important parameter for the heat-up rate as long as chemical reactions are not dominant.	
I.1 Burn-up	Burn-up is proportional to generated power and operating time. It determines inventories of fission products, activation products and actinides and subsequently the decay heat.	Given as boundary condition
I.2 Decay time	Decay time is the time after reactor shutdown. Post-decay heat decrease with time which results in lower heat-up rate.	Given as boundary condition
I.3 Recriticality	Recriticality occurs if the whole or a part of the reactor becomes critical after shutdown with the consequence that the heat source is dominated by fission.	High for intact geometry, **Low** for damaged core region
I.3.1 Boron dilution	Recriticality is possible if an insufficiently borated water slug enters the core region.	High, except mixing in lower plenum
I.3.2 Absorber-fuel separation	Absorber material fails at lower temperatures than fuel rods. After its relocation to lower core regions or below, recriticality is possible due to reflooding.	High.
II. Fluid state	The fluid is on one hand the dominant heat sink in water reactors. On the other hand its oxygen potential might lead to exothermic chemical reactions.	
II.1 System pressure	System pressure determines fluid conditions, heat transfer and fuel rod behaviour	Depends on accident sequence
II.2 Core uncovery	Fast core uncovery is possible by main coolant pump trip if the RCS is highly voided or by fast depressurization with failure of emergency core cooling, which results in a swell level below the core, low steam flow and uniform core heat-up. Slow core uncovery or boil-down takes place if the system is slowly depressurized or the system pressure is kept constant, with decreasing coolant inventory, which results in steep axial temperature gradients above the dryout zone.	Depends on accident sequence
II.3 Core reflood	Core reflood occurs if sufficient water is injected into the core from above or/and from below. The core can be reflooded totally or partially depending on the injection rate. If the injection is interrupted, subsequently the core uncovers again. At high core temperature core reflood is accompanied by serious core damage or degradation.	High during early phase, **Low** for degraded core and rubble bed
II.4 Gas composition	The sources of non-condensable gases are metal oxidation, hydro-accumulator injection, or air ingress. They affect heat transfer and fission product release and transport.	Determined by accident sequence
II.5 Geometry effects	The shape of structures determines the coolant flow path and might change during the accident.	

Phenomenon	Description	Understanding
II.5.1 Blockage	Partial or even total blockage obstructs the coolant flow and might result in local steam starvation. It results from ballooning, mechanical obstruction and debris bed formation	High in core region, **Low** in core support structure.
II.5.2 Bypass	Flow bypass can be established due to structural failure of core baffle (PWR), canister wall (BWR) or shroud (VVER). The bypass flow becomes important in conjunction with flow blockages in the core due to this amplification.	*Medium* in core region, **Low** for structures
II.5.3 Failure of structures	The failure of structures might change the flow path geometry by creating openings e.g. in canister wall (BWR) or obstacles. The degradation of the fuel rod structure or even failure of core support structures by thermal load or jet ablation with material relocation results in debris regions with less porosity and permeability as well as voided zones with higher porosity and permeability. These processes alter the flow conditions and heat transfer to the fluid significantly.	**Low**
III. Initial core damage	The initial core damage covers the behaviour of fuel rods, absorber and structural components during the early phase of core degradation including heat transfer, mechanical behaviour, melting and relocation.	
III.1 In-vessel heat transfer	The in-vessel heat transfer describes the interaction between core and coolant. Three regimes are possible: boil-off, dry core and quenching.	
III.1.1 Boiloff	Boiloff is a steady evaporation of coolant with increasing core uncovery. When part of the core is uncovered, the heat transfer regime locally switches from nucleate boiling to single convection with the vapour phase (dry out), which causes a significant increase of the wall temperature.	High for intact or damaged core
III.1.2 Dry core	The core becomes totally dry if the swell level falls below the lower core support plate. At constant pressure the evaporation rate mainly depends on the radiative heat transfer but also on the heat which is transferred by axial conduction and by the relocation of materials in the lower head. This results in low steam flow which limits the oxidation at higher temperatures (T > 1500 K).	High for intact or damaged core, *medium* for degraded core or core debris
III.1.3 Quenching	If sufficient water is injected into the core due to reflood from bottom or/and the top, then the heat transfer from the core to the coolant strongly increases and with it the steam generation. The high steam availability and shattering of oxide layers due to thermal shock can result in strong oxidation and subsequently in high hydrogen generation and increased core damage. When the rod or debris surface temperature drops below the rewetting temperature (Leidenfrost point), the heat transfer regime changes from film boiling to nucleate boiling (return to nucleate boiling conditions) and the local surface temperature tends rapidly to the saturation value leading to wall quenching.	*Medium* for intact or damaged core, **Low** for degraded core or core debris

Phenomenon	Description	Understanding
III.2 Fuel rod mechanical behaviour	While the fuel maintains rod-like geometry the following main phenomena occur: fuel/cladding contact, clad ballooning, flowering, embrittlement, irradiated fuel effects, fuel and non-fuel dissolution, oxide shell failure.	
III.2.1 Fuel-cladding contact	High system pressure yields to fuel/clad contact during heat-up, which enables UO_2/zirconium eutectic interactions to take place.	High
III.2.2 Ballooning	At low system pressure, ductile (metallic) clad creeps at elevated temperatures which can result in flow blockage. At a certain strain the clad fails locally, which enables oxidation of the inner clad surface in the vicinity of the rupture.	High
III.2.3 Flowering	Embrittled (oxidized) clad splits axially under high azimuthal thermal stress caused by rapid oxidation.	*Medium*
III.2.4 Embrittlement	Embrittled clad shatters due to thermal stress caused by rapid cool-down during quenching and can result in debris formation.	**Low**
III.2.5 Irradiated fuel effects	Irradiated fuel releases fission products when it is dissolved by liquid zirconium. It may also swell into a foamy mass, due to expansion of fission gas in the fuel matrix.	**Low**
III.2.6 Non-fuel dissolution	The early liquefaction of core components due to chemical interactions takes place at temperatures several hundred degrees below their melting points. These interactions are possible between stainless steel or Inconel and zirconium, stainless steel and boron carbide, zirconium and silver-indium-cadmium alloy.	High
III.2.7 Fuel dissolution	Zirconium and zirconium-bearing eutectics react slowly in the solid state, but much more rapidly in the liquid state, with solid UO_2 to form U/Zr/O eutectics which have melting temperatures up to 1000 K below that of the ceramic fuel itself.	High
III.2.8 Oxide shell failure	Depending on the degree of oxidation the clad fails at higher temperature which enables liquefied fuel to relocate.	*Medium*
III.2.9 Absorber assembly behaviour	Light water reactors use the following three kinds of absorber material: Ag-In-Cd alloy (AIC), B_4C, boron steel.	
III.2.9.1 Silver-indium-cadmium	At elevated temperatures the alloy melts and cadmium evaporates and pressurizes the absorber rod which yields in clad deformation. The clad and guide tube fails due to the stainless steel - zirconium interaction which enables the absorber melt to spread into the rod assembly and causes further damage due to AIC - zirconium interaction.	*Medium*
III.2.9.2 Boron carbide	The control rod degradation starts with chemical reactions between B_4C and stainless steel cladding and liquefaction at elevated temperatures which causes clad failure and spreading of absorber melt. This may attack the canister walls (BWR) or rod assembly (PWR).	*Medium*

Phenomenon	Description	Understanding
III.2.9.3 Boron steel	In the VVER-440 the molten part of boron steel control assemblies interacts with the Zr2.5%Nb shroud of the fuel assemblies.	*Medium*
III.2.10 Structures	This section considers spacer grids, shrouds or canister walls and lower core supports	
III.2.10.1 Spacer grid	Grids are made wholly of Inconel or stainless steel, or made mainly of zirconium but with Inconel springs. The Inconel or stainless steel dissolves zirconium cladding at elevated temperatures, perforating the fuel rod and leading to the release of gaseous fission products. The amount of liquid phases formed may be considerable, and may significantly attack and dissolve UO_2 fuel after destruction of the cladding.	*Medium*
III.2.10.2 Canister wall	Canister walls are subject to interaction with absorber melt which causes liquefaction and subsequently attacks to the fuel rods. Their failure enables cross-flow between the rod assemblies and blockage in colder regions.	*Medium*
III.2.10.3 Lower core support	These structures can be ablated by melt jets or form blockages by accumulation of debris or freezing of melt and subsequently fail by thermal loads.	**Low**
IV. Oxidation and hydrogen	Oxidation of metallic components changes the material composition of the core and leads to additional heat generation and hydrogen production.	
IV.1 Material composition		
IV.1.1 Zirconium	Oxidation of zirconium in steam is highly exothermic and leads to temperature escalation at elevated temperatures contributing substantially to core heat-up and hydrogen generation, provided that the steam supply is sufficient	High
IV.1.2 Stainless steel	The oxidation of steel is less exothermic and the surface area generally much smaller than that of the cladding and therefore less significant than zirconium oxidation.	High
IV.1.3 Fuel	If the UO_2 fuel is exposed to steam or air at high temperatures, it can oxidize to hyperstoichiometric forms. High pressures promote higher degrees of oxidation. Fuel oxidation can result in enhanced fission product release and degradation.	*Medium*
IV.1.4 Boron carbide	Oxidation of boron carbide in steam is exothermic and produces reaction products such as boric oxide, carbon monoxide and methane. The boric oxide affects fission product transport.	*Medium*
IV.2 Fluid composition		
IV.2.1 Steam	The steam availability depends on reactor type and accident progression. The steam partial pressure is reduced by the generated hydrogen. Blockage formation enforces local steam starvation.	High, depends on accident sequence

Phenomenon	Description	Understanding
IV.2.2 Hydrogen	Hydrogen is generated due to metal oxidation by steam. It enhances natural convection and heat transfer but reduces steam condensation. It can be absorbed by zirconium to some extent.	*Medium*
IV.2.3 Air	The oxidation by air is more exothermic than that by steam but without hydrogen generation. Nitriding of zirconium may occur particularly if the oxygen content of the air is exhausted. Fuel oxidation by air results in hyperstoichiometric urania and higher release rates for numerous fission products.	*Medium*
IV.3 Hydriding	Metallic (β) zirconium can absorb considerable amounts of hydrogen at intermediate temperatures accompanied by exothermic reaction. The kinetics depends on fluid conditions and oxide shell thickness.	**Low**
IV.4 Pre-oxidation	Oxide layers can delay interaction (liquefaction) with other materials and the oxidation excursion, they lower heat-up rates and peak temperatures.	High
IV.5 Loss of protective shell	On quenching by water, the oxide shell on the outside of the cladding above can shatter through thermal shock, exposing unreacted zirconium underneath.	**Low**
IV.6 Relocated material	Metal-rich relocating melts and refrozen crust may continue to oxidize and contribute to heat-up and hydrogen production.	
IV.6.1 Molten film	Metal-rich relocating melt continues to oxidize on its surface in steam, provided the temperature is high enough. Increased ceramic fractions lead to reduced oxidation rates.	**Low**
IV.6.2 Crust	Metal-rich crust continues to oxidize on its surface in steam, provided the temperature is high enough. Increased ceramic fractions lead to reduced oxidation rates.	*Medium*
V. Fission product release	The release of fission products and other materials from the core is strongly coupled with the core behaviour and feeds back to the degradation process. It is not further discussed in this paper/report.	High for volatile, *medium* for less volatile fission products, **Low** for melt pool & crust
VI. Core degradation and melt progression	In the late phase of core degradation the heat-up and material interactions lead to relocation of core materials, formation of debris beds and of molten pools.	
VI.1 Limited material relocation	Liquefied or shattered material relocates generally downwards once it loses its integrity.	
VI.1.1 Candling	Candling is a gravity-driven downward flow of melt along structure surfaces in the form of droplets or rivulets. The candling process ceases by freezing or by reaching an obstacle.	*Medium*

Phenomenon	Description	Understanding
VI.1.2 Spreading	Spreading or radial movement of melt is caused by a driving pressure difference, either after rupture of cladding or hydrostatic head, if the downward flow is hindered.	**Low**
VI.1.3 Particulate debris	Particulate debris induced by thermal stress or thermal shock falls downward and may contribute to the formation of a debris bed and blockage.	**Low**
VI.1.4 Flow dragging	If the drag force is high enough due to high fluid velocity particulate debris or melt droplets are carried by the flow upwards and through the coolant system.	**Low**
VI.2 Blockage formation	Mechanical obstruction, thermal gradient and/or metallic crust can stop material relocations and result in blockage formation.	
VI.2.1 Mechanical obstruction	Mechanical obstructions or obstacles are generally grid spacers, lower core support structures or structures at the lower end of channel box as well as previously formed clad balloons.	*Medium* for core region, **Low** for lower part
VI.2.2 Thermal gradient	Relocating melt freezes if the clad temperature is lower than the liquidus temperature of the melt. Steep thermal gradients generally exist above the water level and at the lower end of the core.	High
VI.2.3 Metallic Crust	As the process of solidification of relocating metallic melt continues, a crust will form local blockages and act as a crucible for melt arriving later. The crust might melt again and relocate further.	*Medium*
VI.3 Debris bed formation	The accumulation of solid particles and/or melts is called debris bed formation	
VI.3.1 Fuel melting	If the fuel rod temperature reaches the solidus temperature of UO_2, ceramic melting begins. The solidus temperature is lowered by ZrO_2 and metallic remnants like Zr and Fe. The melting process is also influenced by oxygen content and high burn-up.	*Medium*
VI.3.2 Fuel rod collapse	If the cladding is fragile due to complete oxidation, or the fuel is decladded or has lost its support from beneath, it might break into pieces and form particulate debris. This process may be initiated by thermal shock due to reflood.	**Low**
VI.3.3 Particulate debris	The particulate debris generally consists of pieces or fragments of oxidized cladding and/or fuel pellets. It can be coolable or it can heat up and build or contribute to a melt pool.	**Low**
VI.3.4 Melt pool	A ceramic melt pool is formed by accumulation of fuel melt and/or oxidized cladding from rods or particulate debris. Melting of the upper core support or upper plenum structures may contribute to the melt pool.	**Low**
VI.4 Debris bed	The debris bed can be characterized by external heat transfer, debris bed thermal hydraulics and melt formation.	

Phenomenon	Description	Understanding
VI.4.1 External heat transfer	Depending on the surrounding fluid state or structure, the debris is cooled by conduction, convective heat transfer (one or two-phase) to the coolant and radiation to the surroundings.	*Medium*
VI.4.2 Debris thermal hydraulics	The heat-up or cooling of the debris depends on the external heat transfer and the debris porosity. If the debris bed is embedded in water and critical heat flux and porosity are not limiting, the debris does not heat up or will be quenched. If the convective heat transfer from the debris to the coolant is less than the heat generation, the debris will dry out and may melt. In this case, the debris porosity decreases and melt will fill in the pores following gravity as well as surface tension forces.	**Low**
VI.4.3 Melt formation	With high heat generation or increasing debris bed size, the debris overheats and melts partially or totally and may form a melt pool if the melt is collected by a crucible-like crust.	*Medium*
VI.5 Molten pool		
VI.5.1 Pool thermal hydraulics	Natural circulation exists in melt pools with heat sinks on its boundary. Heat is transferred from the melt pool to the boundary by conduction and convection. Degassing and precipitation might enhance the heat transfer. Besides the numerical simulation of a fully three-dimensional multi-component flow, the heat transfer from the pool to the boundary may be described by correlations as a function of the Rayleigh number (Ra), depending on the size, shape, heat source and thermophysical properties (Ra $=10^{15}$ - 10^{16}). Slip or no-slip conditions on the upper pool surface have some effect.	*Medium*
VI.5.2 Crust behaviour	Depending on the internal heat generation, heat conductivity, heat transfer conditions on both sides of the crust, and the surrounding temperature distribution, the heat flux from the melt to the crust will vary with location, and with it the crust thickness too. The stress in the crust depends on the local support, pressure difference across the crust, hydrostatic head of the melt pool, additional loads from overlying debris and thermal strain. If the crust fails locally, cracks may be formed, or total crust failure with slumping occurs.	**Low**

Phenomenon	Description	Understanding
VI.5.3 Heat transfer to surroundings	There are three distinctive configurations: (1) At very high local temperatures, or accumulation of material with low melting point, melt is in direct contact with steam or hydrogen, and radiative heat transfer to the surrounding structure will dominate the external heat transfer. (2) The surface temperature is below the melt temperature and a stable crust exists. Single or two-phase heat transfer regimes are possible, depending on the temperature; radiative heat transfer might be important. (3) The crust is covered by particulate dry or wet debris. The external heat transfer depends on the heat transfer and conditions in the debris bed. If water overlies the molten pool, unstable film boiling takes place, with or without crust formation and possible remelting.	*Medium*
VI.5.4 Slumping	Slumping is the massive melt relocation following total crust failure. The melt delivery depends on the driving forces and melt accumulation above crust failure. The melt jet interacts with the fluid, with possibly oxidation, melt fragmentation and extensive vapour generation in contact with water, which might result in steam explosions. The melt jet can also interact with structures, such as fuel assemblies, core surroundings, core support plate and lower internals. The core slumping process is a fundamental precursor for the debris/molten pool behaviour in the lower plenum.	**Low**
VII. Core debris in lower plenum	The last phase of in-vessel core degradation before vessel failure is related to the behaviour of particulate debris and molten pool in the lower plenum.	
VII.1 Particulate debris	Particulate debris in the lower plenum behaves similarly to that in the core region. It might be below or/and above a molten pool.	
VII.1.1 Debris bed formation	The debris bed is formed by relocation of particulate debris from the core region or by relocation of melt with fragmentation and solidification and its accumulation in the lower plenum. The relocation is either continuous or spontaneous.	**Low**
VII.1.2 Debris bed heat transfer	The heat-up or cooling of the debris depends on the external heat transfer and the debris porosity and permeability. If the debris bed is surrounded by water and critical heat flux and permeability are not limiting, the debris does not heat-up or will be quenched. If the convective heat transfer from the debris to the coolant is less than the heat generation, the debris will dry out and may melt. In this case, the debris porosity decreases and melt will fill in the pores following gravity as well as surface tension forces. Besides that the coolant flow pattern is affected by boundary effects and counter current flow.	*Medium*

Phenomenon	Description	Understanding
VII.2 Pool behaviour	A molten pool in the lower plenum behaves in principle similarly to that in the core region but its size might be much larger due to the crucible like pressure vessel wall. It might be below or/and above of a debris bed.	
VII.2.1 Pool formation	The molten pool is formed by molten debris or by relocation of melt from the core region without significant fragmentation and its accumulation in the lower plenum. The relocation is either continuous or spontaneous. Molten structure material might contribute to the melt pool.	**Low**
VII.2.2 Thermal hydraulics	Natural circulation exists in melt pools with heat sinks on its boundary. Heat is transferred from the melt pool to the boundary by conduction and convection. Degassing and precipitation might enhance the heat transfer. Besides the numerical simulation of a fully three-dimensional multi-component flow, the heat transfer from the pool to the boundary may be described by correlations as a function of the Rayleigh number (Ra), depending on the size, shape, heat source and thermophysical properties (Ra =10^{15} - 10^{16}). Slip or no-slip conditions on the upper pool surface have some effect. If a metallic layer is formed on the top of the melt, the heat flux will be concentrated by this layer (focusing effect).	*Medium*
VII.2.3 Stratification	Immiscible liquid phases might segregate and result in stratification. It depends on physical and chemical properties as well as thermal and flow conditions and affects slightly the heat source distribution and significantly the heat flux distribution to the boundary in case that the heat conductivity varies a lot.	**Low**
VII.2.4 Solidification	Solidification occurs if the melt temperature drops below the liquidus temperature. Non-eutectic mixtures result in concentration differences of liquid phase and solidified phase. The formation of a mushy zone is unlikely under reactor-typical conditions.	*Medium*
VII.3 Crust behaviour		
VII.3.1 Thermal behaviour	Depending on the internal heat generation, heat conductivity, heat transfer conditions on both sides of the crust, and the surrounding temperature distribution, the heat flux from the melt to the crust will vary with location, and with it the crust thickness.	*Medium*
VII.3.2 Mechanical behaviour	The stress in the upper crust depends on pressure difference across the crust, additional loads from overlying debris and thermal strain. Cracks may be formed if the crust fails locally. Deformation of the supporting vessel wall affects the lower crust behaviour. If the lower crust (or crucible) has a high load bearing capacity, local support allows gap formation between crust and wall.	**Low**
VII.4 In-vessel heat transfer	The conditions for the upper crust are similar to those in the core region, the lower and side crust conditions are different.	

Phenomenon	Description	Understanding
VII.4.1 Upper crust condition	There are three distinctive configurations: (1) At very high local temperatures, or accumulation of material with low melting point, melt is in direct contact with steam or hydrogen, and radiative heat transfer to the surrounding structure will dominate the external heat transfer. The upper heat losses decrease considerably if the environmental temperature approaches the melt temperature. (2) The surface temperature is below the melt temperature and a stable crust exists. Single or two-phase heat transfer regimes are possible, depending on the temperature; radiative heat transfer might be important. (3) The crust is covered by particulate dry or wet debris. The external heat transfer depends on the heat transfer and conditions in the debris bed. If water overlies the molten pool, unstable film boiling takes place, with or without crust formation and possible re-melting.	*Medium*
VII.4.2 Lower crust condition	There are three distinctive configurations too: (1) There is no thermal resistance, except heat conduction, if the surface temperature is higher than the melting temperatures of crust and/or wall. (2) The heat transfer depends on contact resistance, radiative and conductive heat transfer across the gap if a stable crust exists and the wall surface temperature is below its melting temperature (3) The heat transfer depends on single or two-phase flow if the wall surface temperature is below its melting temperature and coolant is able to enter the gap. Particulate debris between crust and wall acts as a thermal insulation and protects the wall.	High for configurations 1 and 2, **Low** for configuration 3
VII.5 Ex-vessel heat transfer	The ex-vessel heat transfer determines the temperature of the vessel wall and consequently the time to failure under thermal loads. It depends strongly on the design of vessel support, insulation and reactor pit (cavity) as well as the availability of water.	
VII.5.1 Dry cavity	The heat transfer coefficients are generally low and dominated by thermal radiation at elevated temperature. The temperature drop across the vessel wall is small and vessel failure has to be expected if large quantities of core debris has relocated into the lower plenum without internal cooling.	High
VII.5.2 Wet cavity	The heat transfer coefficients are generally high if sufficient water flow is not hindered by thermal insulation or steam binding. For heat flux densities lower than critical heat flux (DNB) the temperature drop across the vessel wall is large and vessel integrity might be conserved, even if large quantities of core debris has relocated into the lower plenum without internal cooling.	*Medium*
VII.6 Vessel wall behaviour	The vessel wall is an important barrier if it remains intact. The accident mitigation depends on the containment integrity if it fails.	

Phenomenon	Description	Understanding
VII.6.1 Elastic deformation	At low wall temperature only elastic deformation under thermal and mechanical loads is significant. In case of late cavity flooding pressurized thermal shock has to be considered.	High
VII.6.2 Plastic deformation	At elevated temperature plastic deformation under thermal and mechanical loads is significant. The stress is shifted to cooler wall portions.	*Medium*
VII.6.3 Vessel failure	At high temperature the creep velocity increases considerably with stress and the unzipping of the vessel occurs in short time.	**Low**
VII.6.4 Thermal ablation	Thermal ablation is possible due to jet impingement during melt relocation on a dry surface or by thermal attack by intensive contact with ceramic crust or metallic melt.	*Medium*

References

[3.1] Haste T J, Adroguer B, Gauntt R O, Martinez J A, Ott L J, Sugimoto J and Trambauer K, "In-Vessel Core Degradation Code Validation Matrix", NEA/CSNI/R(95)21, OCDE/GD(96)14, Paris, 1996.

[3.2] Hózer Z, Trambauer K and Duspiva J, "Status Report on VVER-Specific Features Regarding Core Degradation", NEA/CSNI/R(98)20, September 1998.

[3.3] Bandini G, Gauntt R O, Okkonen T, Suh K Y, Shepherd I and Linnemann T, "Molten Material Relocation to the Lower Plenum: A Status Report, September 1998", NEA/CSNI/R(97)34, September 1998.

[3.4] "In-Vessel Core Debris Retention and Coolability, Workshop Proceedings, March 1998, Garching near Munich", NEA/CSNI/R(98)18, Paris, February 1999.

[3.5] Richard P et al., "In-Vessel Corium Retention Strategies (IVCRS) Final Report", E.C. / CEA Cadarache report N.T. SERSI/LEFS/99-5046, February 2000.

4. EXPERIMENTAL DATABASE

This chapter provides a summary of the experimental database on which the validation matrices are founded. In order to facilitate comparison of the main features and data available from the different experimental facilities, a standard format has been adopted [4.1] using tables as far as possible.

In the first section, integral facilities are considered, starting with early phase experiments, then moving to late phase experiments, the TMI-2 accident, and concluding with miscellaneous items. For each facility, the following information is given:

- a summary of the objectives, facility description, test description and physical processes quantified, in narrative format;
- a schematic diagram of the test facility; and
- a set of three tables, respectively summarising:
  - general information about the facility;
  - the main experimental conditions, starting with geometrical and physical details, followed by boundary conditions, then giving information on the length and termination of the tests; and
  - the main phenomena exhibited, starting with the early phase (low temperature) then moving to the late phase (high temperature).

In the second section, similar data are provided for separate-effects facilities. For these, some modifications were required to the standard format, to provide the most appropriate information for each of the separate phenomena considered. The general layout for the experiments associated with each phenomenon is as follows:

- a summary of the objectives, facility description, test description and processes quantified (if these are similar for a number of facilities, a single account is given to cover them all); and
- a single table summarising geometrical information and boundary conditions, followed by the ranges of the main experimental parameters covered, such as temperature and time.

The information given necessarily varies amongst the separate-effects tables, to characterise best the experiments being summarised.

This chapter is supplemented by an Appendix which gives greater detail on the various experiments than is provided in the present chapter. In particular, lists of data and evaluation reports are provided, along with information on the availability of the data, and discussion of the strengths and weaknesses of individual experiments and of the series in general. The evaluations are taken into account in selecting key tests in the validation matrices themselves, while the references form the starting point for analysts who wish to use the data for detailed code assessment.

4.1 Integral Facilities

4.1.1 NIELS

4.1.1.1 Objectives

The objectives of the NIELS series carried out at KfK (now FZK) Karlsruhe in the period 1982 to 1986 were to investigate PWR fuel rod and small bundle behaviour. The test parameters studied and varied were initial heat-up rate, maximum cladding temperature and the influence of neighbouring fuel rods on temperature escalation and damage progression.

4.1.1.2 Facility Description

The NIELS out-of-reactor facility is illustrated schematically in Figure 4.1.1, with general information given in Table 4.1.1.1. The NIELS facility was constructed to perform single rod and small bundle experiments. The single rods and the bundle, composed of a 3x3 array of fuel simulators, were surrounded by an Al_2O_3 or Zircaloy shroud, respectively which was insulated with a ZrO_2 fibre ceramic wrap. The fuel rod simulator was made of a central tungsten heater of 6 mm diameter, which is surrounded by annular UO_2 pellets and the normal PWR Zircaloy cladding of 10.75 mm outer diameter and a wall thickness of 0.72 mm. The maximum length was 0.4 m. A steam flow of 1 g/s was inlet to the bundle. The system pressure was about 0.1 MPa. Temperatures were measured by thermocouples and pyrometers. Blockage formation and material distribution were determined by destructive post-test examinations. Aerosol compositions were identified by filter probes.

4.1.1.3 Test Description

Each test is conducted in four phases: pre-heating in argon; start of electrical heating and of steam injection; increase of power, leading to oxidation excursion or faster heat-up and to relocation of absorber material (only ABS series) and U/Zr/O melt; and cooling in argon with power switched off. The transient phase typically lasts 1200 to 5000 s with heat-up rates from 0.5 to 2.5 K/s and maximum temperatures up to about 2500 K (see Table 4.1.1.2).

4.1.1.4 Processes Quantified

The main phenomena covered in the NIELS series are shown in Table 4.1.1.3. The variation of heat-up rates, maximum temperatures and material combinations provided first insights into the importance of chemical interactions, melt formation, relocation and blockage.

Non-prototypic features such as the temperature dependence of axial power distribution and the very small bundle size must be accounted for in interpreting the test results.

4.1.2 CORA

4.1.2.1 Objectives

The objectives of the CORA series carried out at Forschungszentrum Karlsruhe (FZKA, previously KfK), between 1987 and 1993 were to investigate early-phase core degradation in

light water reactors (PWR, BWR and VVER designs). In particular, the series of 19 tests covered absorber behaviour, quench, the effect of heat-up rates, varying steam supply and initial pre-oxidation.

4.1.2.2 Facility Description

The CORA out-of-reactor facility is illustrated schematically in Figure 4.1.2, with general information given in Table 4.1.2.1. A fuel rod bundle of representative PWR, BWR or VVER design of overall length 2 m (heated length 1 m) is surrounded by a permanently-installed high temperature shield. Decay heat is simulated by electrical heating with tungsten rods installed within the alternately-positioned heated rods. Coolant (superheated steam and argon) is injected laterally at the bottom of the heated section; quench is simulated by raising a water-filled cylinder around the rods. On-line measurements are made of temperatures, pressures, rod powers, hydrogen production etc.; these are supplemented by video recordings of the melt progression. The division of fluid flow between the main and bypass channels is not however qualified experimentally. Comprehensive destructive post-test examinations determine such quantities as blockage formation and material distribution.

4.1.2.3 Test Description

Each test is conducted in four phases: pre-heating in argon to about 600 K, initiation of electrical heating and of steam injection; raising of electric power to give an initial heat-up of 0.2-1.0 K/s, leading generally to an oxidation excursion, with relocation of control rod material and U/Zr/O melt and blockage formation (peak temperatures ~2200 K); cooling in argon or quench by water, with power switched off. The transient phase typically lasts 1500-9000 s. The range of experimental conditions is surveyed in Table 4.1.2.2.

4.1.2.4 Processes Quantified

The main phenomena covered in the CORA series are shown in Table 4.1.2.3. The orderly variation of parameters, such as rod internal pressure, presence and nature of absorber material, heat-up rate, quench or slow cooling, means that by comparison amongst the tests the relative influence of phenomena such as clad ballooning, non-fuel eutectic interactions (absorber, grid, cladding), steam starvation, pre-oxidation effects etc. on melt formation, relocation and blockage, and on hydrogen production, may readily be deduced. Non-prototypic features such as the temperature dependence of the axial power distribution, the artificial axial stability afforded by the tungsten heaters, and the varying bypass flow, must be accounted for in interpreting the test results.

4.1.3 PHEBUS SFD

4.1.3.1 Objectives

Between 1986 and 1989, six Severe Fuel Damage (SFD) tests were conducted in the PHEBUS reactor at Cadarache, France. The objective of this programme was to investigate the early phase of core degradation using fresh fuel rods of representative 17x17 PWR design. In particular were investigated: Cladding oxidation with related H_2 generation and clad damage, chemical interactions between non-fuel materials (spacer grids, AIC control rod) and between

fuel and cladding, melt relocation and core blockage, fuel rod oxidation and fragmentation under rapid cooling. Onset of solid debris bed formation was also observed.

4.1.3.2 Facility Description

The test train is located in a SFD loop crossing the central part of the PHEBUS driver core which supply the nuclear power (Figure 4.1.3). The fuel rods were 1.3 m long with a central 0.8 m long fissile zone. The rods were held in place by two Inconel or Zircaloy spacer grids. The test bundle is surrounded by an insulating zirconia shroud with an inner octagonal Zircaloy liner. The outer pressure tube is cooled by an independent pressurised cooling circuit (see Figure 4.1.3)

On-line measurements are made of temperatures (fuel centreline, cladding, shroud and coolant), coolant flow rates, pressures and hydrogen production. An important effort has been done to determine the power evolution and the axial power profile during the tests for intact and degraded geometries (measurement of the driver nuclear power, measurements and calculations of the coupling factor between the driver core and the bundle in various geometries, gross gamma scanning).

Post Test Examinations (PTE) of axial and radial sectioning of the bundle determined such quantities as clad oxidation, chemical interactions, blockage formation and material distribution.

General information on the PHEBUS-SFD programme is given Table 4.1.3.1.

4.1.3.3 Test Description

In general, PHEBUS-SFD test sequences include the following phases:

- Pre-transient phase to reach nominal conditions for the driver reactor circuit and the cooling circuit of the pressure tube. Then, initial conditions are reached in the SFD circuit feed by steam or helium;
- Heat up phase of the transient raising the nuclear power and driving the gas injection (steam, helium or hydrogen) as foreseen in the test protocol;
- Final power shutdown and bundle cooldown in a gaseous atmosphere (either steam or helium);
- Post-test destructive examinations of the bundle.

The heat-up phase can last up to 14000 s. The range of experimental conditions is presented in Table 4.1.3.2.

4.1.4.4 Processes Quantified

The main phenomena covered in the PHEBUS SFD programme are shown in Table 4.1.3.3. The piloting of both the gas flow injection and the nuclear power enabled different SFD conditions to be reached in order to favour, for each test, a limited number of degradation phenomena such as cladding oxidation and related H_2 production, non-fuel material interactions (absorber, grid, cladding), fuel-dissolution by solid and molten Zircaloy and resulting clad

failure, metallic and ceramic melts relocation, early AIC control rod degradation and oxidation and shattering of embrittled rod cladding during a rapid cooling.

Due to the limited number of tests and the choice of test objectives focusing on selected degradation phenomena the scope of the early phase of core degradation was not totally covered. In particular phenomena such as clad ballooning, oxidation of Zr-rich melts, fuel dissolution under oxidizing conditions and quenching were not investigated. On the other hand the tests are easy to analyze and valuable for code validation.

Non-prototypic features are common to small bundle tests such as unprototypical radial and axial power profiles. Unplanned design constraints induced uncertainties in the radial heat losses through the insulating porous zirconia shroud which have complicated the post-test analyses.

4.1.4 PBF-SFD

4.1.4.1 Objectives

Between 1982 and 1985, four severe fuel damage (SFD) tests were conducted in the Power Burst Facility (PBF) at the Idaho National Engineering Laboratory (INEL). These four in-pile experiments were the first tests performed as part of an internationally sponsored light water reactor SFD research programme initiated by the U.S. Nuclear Regulatory Commission (NRC).

- The specific objectives of the PBF-SFD series of tests were to:
- investigate fuel rod damage following severe cladding oxidation, melt relocation, and fuel rod fragmentation;
- measure the release rates, transport, deposition of fission products;
- determine the magnitude and timing of hydrogen generation;
- determine the behaviour of irradiated fuel rods compared with fresh fuel rods and to evaluate the effects of control rods.

4.1.4.2 Facility Description

The PBF reactor consists of a driver core and a central flux trap contained in an open tank reactor vessel. An independent pressurized water coolant loop can provide a wide range of thermal-hydraulic conditions within the flux trap test space.

An in-pile tube fits in the central flux trap region to contain the test train assembly.

The PBF-SFD test trains were designed and built by the Pacific Northwest Laboratory (PNL) and assembled at the INEL. An elevation view of the test train within the in-pile tube is shown in Figure 4.1.4.

The fuel rods were 0.9 m long and representative of a 17x17 PWR design. The rods were arranged in a 6x6 square lattice, without the four corner rods. The rods were held in place by Inconel grid spacers. The test bundles were contained in an insulating zirconia shroud, sandwiched between inner and outer Zircaloy walls (see Figure 4.1.4)

The rods were cooled by a measured coolant flow (water/argon) into the bundle, which was boiled away by fission heat to produce steam. An independent flow cooled the outer shroud.

The test train was instrumented to measure fuel and control rod cladding and centreline temperatures, coolant temperatures, shroud temperatures, fuel and control rod internal pressure, and coolant flow rates and pressures. In addition, a fission product and hydrogen measurement system was also included. Post Test Examination (PTE) included gross gamma scanning, neutron tomography, and destructive sectioning.

General information on the PBF-SFD test series is given in Table 4.1.4.1.

4.1.4.3 Test Description

In general, the PBF-SFD test sequence of operations include the following phases:

- power calibration measurements;
- high power operation for fuel conditioning and long-lived fission product inventory generation;
- shutdown;
- low power operation to build up a short-lived fission product inventory;
- a coolant boildown;
- the high temperature transient;
- power shutdown and test assembly cooldown;
- bundle storage;
- post-test bundle examination.

The range of experimental conditions for the four PBF-SFD tests is presented in Table 4.1.4.2.

4.1.4.4 Processes Quantified

The main phenomena exhibited in the PBF-SFD experiments are summarized in Table 4.1.4.3.

With reduced makeup flow to the test assembly, fission power ramp and the additional heat generated from metal/steam reactions, test section temperatures rose rapidly resulting in clad failure; Zircaloy melting; fuel liquefaction; materials interaction; melt relocation; and the release of hydrogen, aerosols, and fission products.

The PBF-SFD tests were the first in-pile fuel damage tests, and they provided most of the early understanding of degraded core phenomena. The tests are mainly relevant for early phase melt progression phenomena.

The tests had substantial uncertainties in the steam boil-off rate and some unplanned features in some tests (for instance, breach of the shroud wall), which have complicated the post-test analyses.

4.1.5 NRU-FLHT

4.1.5.1 Objectives

Between 1985 and 1987, four full-length high temperature (FLHT) tests of the Coolant Boilaway and Damage Progression (CBDP) Program were conducted by PNL in the NRU reactor at Atomic Energy of Canada Ltd. (AECL) Chalk River using highly instrumented and insulated assemblies of 12 full-length (3.7 m) light water reactor (LWR) fuel rods.
The objectives of the CBDP Programme were to:

- obtain data for evaluating the effects of coolant boilaway and core damage progression in an LWR; and
- investigate integral severe accident phenomena along a full-length bundle.

4.1.5.2 Facility Description

The FLHT test hardware consists of the following four components plus the NRU reactor: test train assembly, steam closure cave (SCC), effluent control module (ECM), and a data acquisition and control system (DACS). The general arrangement of these components during a test in the NRU reactor is shown in Figure 4.1.5. Figure 4.1.5 also illustrates the general FLHT test section, cross-section, and a detailed test section axial schematic.

During a boilaway transient, two coolant systems are used. The test train external coolant system continuously circulates subcooled, pressurized water around a closed loop piping system. The water cools the external surfaces of the test train assembly. The second system is a once-through circuit that supplies subcooled, pressurized water from a storage tank to the fuel bundle inlet region. This water then flows up among the fuel rods, the upper plenum, through the closure, SCC, ECM, and finally into a storage tank.

General information on the FLHT test series is given in Table 4.1.5.1.

4.1.5.3 Test Description

The FLHT test operations include up to five phases:

- pretest installations and checkout with reactor at zero power;
- commissioning and calibration with reactor at zero power;
- preconditioning operation (FLHT-4 and -5 only) with reactor at full power;
- coolant boilaway/severe damage transient with reactor at constant 5% of full power;
- post-test examinations.

The planned operation of the boilaway includes bringing the reactor to low power (~5% of full power) with 1 kg/s bypass flow and 0.13 kg/s bundle coolant flow. After calorimetry and stabilization at 23 kW or 30 kW bundle nuclear power, the plenum section is drained and heated, and the assembly inlet flow is reduced to 9.4 g/s to arrive at a steady-state dryout front position ~0.7 m below the top of the fuel column. The bundle calorimetry and plenum

drain/heat-up operations are pre-transient operations that are conducted before the boilaway transient.

The coolant boilaway is started by making a rapid reduction in the bundle inlet flow to ~1.3 g/s. The hold time from the first attainment of cladding melt temperatures (2100 K) to the termination of the experiment varies from test to test.

The range of experimental conditions for the four FLHT tests is presented in Table 4.1.5.2.

4.1.5.4 Processes Quantified

The main phenomena exhibited in the FLHT experiments are summarized in Table 4.1.5.3.
The four FLHT tests have contributed data on SFD behaviour due to a dynamically changing coolant level with full length fuel and a constant fission power level, although most of the bundle degradation occurred with a constant water level from make-up flow. All the tests have resulted in extensive and severe fuel rod damage, with the severity and extent of the damage increasing with each subsequent test. Fuel foaming was observed in tests 4 and 5.

The relatively large radial heat losses from the test section are non-prototypic and may affect the melt relocation, refreezing, and remelting.

4.1.6 ACRR-ST

The ACRR-ST experiments were performed for the U.S. Nuclear Regulatory Commission between 1986 and 1989 for the purpose of generating fission product release information to improve modelling and predictive capabilities necessary for making regulatory decisions concerning reactor safety issues for severe accidents.

4.1.6.1 Objectives

The objectives of the ST programme were to characterize fission product release from irradiated LWR fuels by using in-pile fission heating methods. The emphasis was on characterizing release from the fuel as a function of oxidizing or reducing conditions and fuel damage state; however, the program scope was reduced to investigate release behaviour only under reducing conditions.

4.1.6.2 Facility Description

The ST tests were carried out in the ACRR (Annular Core Research Reactor), a pool type reactor with a dry central irradiation cavity capable of driving experiments with fissionable material under steady state, pulse or programmed power transient mode. The ST tests made use of BR-3 irradiated fuel situated in a recirculating flow loop which were fission heated by neutrons from the ACRR driver core (BR-3 was a small PWR research reactor in Belgium, decommissioned in 1988). Fission product release rates were measured as the test fuel temperature was gradually heated by the driver core. General information on the ACRR-ST experiments is given in Table 4.1.6.1.

4.1.6.3 Test Description

The ST test bundle of four BR-3 rods was situated in a ZrO_2-lined flow channel within a zirconia fibre insulated pressure vessel. The four-rod fuel bundle was fission heated by neutrons provided by the ACRR driver core to temperatures in the vicinity of 2500 K. A schematic of the ST test section is given in Figure 4.1.6. As the test fuel temperature was increased, the release fission products were measured by sampler bottles, filters, and thermal gradient aerosol deposition tubes. The range of experimental conditions for the 2 ACRR-ST tests is given in Table 4.1.6.2.

4.1.6.4 Processes Quantified

The main focus of the ST experiments was to measure fission product release rates from degrading fuel, but there was also important information obtained relative to fuel damage behaviour. Most important was the extreme degree of fuel foaming and swelling that occurred as the Zircaloy cladding became molten and penetrated the cracks in the fuel pellets. The main processes quantified in the ACRR-ST experiments are summarized in Table 4.1.6.3.

4.1.7 ACRR-DF

The ACRR-DF (Damaged Fuel) experiments, like the ST experiments, were also in-pile tests that made use of the ACRR central irradiation cavity to fission heat a fuelled test bundle. The focus of the DF tests however was primarily related to investigating fuel damage and melt progression processes. The tests were conducted in the period 1982 and 1989.

4.1.7.1 Objectives

The objectives of the DF tests were to obtain quantified information on fuel damage processes as a function of the particular severe accident conditions. The severe fuel damage processes investigated included fuel heat-up in flowing steam, clad heating by oxidation with steam, hydrogen generation, fuel pellet attack by molten cladding material, metallic melt relocation and blockage formation, and the nature of the degradation of the fuel rod geometry.

4.1.7.2 Facility Description

The DF test bundles were fabricated of from 9 to 14 half metre long fresh UO_2 fuel rods. A schematic of a typical DF test bundle is shown in Figure 4.1.7. The rod bundle was contained within a flow channel made from low density zirconia fibre. The insulated assembly was housed within a steel pressure vessel and situated in the central irradiation cavity of the ACRR. Steam was fed into the bottom of the fuel bundle as the fuel rods were fission heated by the ACRR driver core. Fuel temperatures were measured with W/Re and Pt/Rh thermocouples, hydrogen generation was measured in the tests, and an end-on view of the damage process was provided by a video recording system.

General information on the ACRR-DF experiments is given in Table 4.1.7.1.

4.1.7.3 Test Description

A typical DF test would begin with a preheating period without steam addition, followed by a slow fission heated initiation period with steam being fed into the test bundle. The initial heat-up rate was typically on the order of 1 to 2 K/s. As the bundle temperatures increased, the ACRR driver core power would be increased to maintain the desired 1 or 2 K/s heating rate. When the bundle temperatures increased above about 1700 K, a localized temperature escalation due to rapid Zircaloy oxidation would typically be seen. This escalation would exhibit a heat-up rate on the order of 10 to 20 K/s. Clad melting followed rapidly with melt relocation and blockage formation. Test termination would follow soon after melt relocation had been detected. Following completion of the experiment, the test bundle would be stabilized with epoxy and examined both by radiography and by destructive metallurgical examination. The range of experimental conditions for the 4 ACRR-DF tests is given in Table 4.1.7.2.

4.1.7.4 Processes Quantified

The processes quantified in the DF experiments include cladding oxidation behaviour, hydrogen generation, fuel pellet erosion by molten cladding, blockage formation by relocating molten metallic and metallo-ceramic materials, and the degree of degradation of the fuel rods. As with most in-pile tests, all of the DF tests had some unplanned features which complicated post test analysis (for example, test DF-1 experienced condensation of steam within the test section, which later revaporized, causing uncertainties in the knowledge of the steam flow rate for the test). The main processes quantified in the ACRR-DF experiments are summarized in Table 4.1.7.3.

4.1.8 LOFT LP-FP

4.1.8.1 Objectives

The Loss of Fluid Test Facility (LOFT) was first conceived by the USAEC in 1962. Following the completion of the facility in 1976, a series of thermal hydraulic-type tests was carried out under the sponsorship of the USNRC, to study large and small break accidents. The TMI-2 accident strongly stimulated additional research, especially on processes occurring in severely damaged cores. As a consequence, the OECD/NEA called for a new cooperative LOFT Project, which started in 1983. The technical programme was agreed to include 8 experiments. The first 6 were devoted to thermal hydraulic issues, and the remaining 2 included damage to the fuel and releases of fission products. These last two tests were named the LP-FP series, and their specific objectives were:

- Perform integral tests to study PWR core behaviour during LOCA-type sequences with delayed operation of the ECCS;
- Make tests as prototypic as possible, simulating actual sequences in a PWR scale model, and including all phases expected during the accident: reactor scram, fuel heat-up, fuel damage, and recovery by ECC initiation;
- Attain fuel temperatures high enough to produce fuel damage and fission product inventory release. Objectives for the second test were more ambitious: it should attain temperatures above 2100 K, and produce substantial fuel damage and meltdown.

4.1.8.2 Facility Description

The LOFT facility was essentially a small PWR with a thermal output of 50 MW. The active nuclear height was 1.7 m, which is half that used in commercial plants. The facility was designed to model a Westinghouse plant, with 4 loops, on a volumetric scale of approximately 1/50 (the vertical scale for the fuel being 1/2.2). The standard configuration of the LOFT system provides for the simulation of a large LOCA. The single intact loop, comprising circulating pumps, steam generator, pressurizer and connecting pipe work, represents the 3 intact loops of a commercial plant. The broken loop is fitted with two quick opening valves which provide flow path for escaping coolant equivalent to the two exposed ends of a broken pipe. The fluid escaping through the quick opening valves is conducted to the burst suppression tank which simulates the containment of a full-sized plant. LOFT was provided also with a scaled version of the ECCS. The standard LOFT configuration was changed for the second LP-FP test. The broken loop was removed and a blowdown line was connected to the hot leg, and discharged into a suppression vessel. The blowdown line was to simulate the discharge through a break in the LPIS.

The standard central assembly of the LOFT core consisted of a 15x15 array of Zircaloy-clad fuel pins with dimensions corresponding to those in common commercial use. The core and particularly the central assembly was highly instrumented with nuclear flux detectors and thermocouples of various types. Figure 4.1.8 shows the central fuel assemblies (CFM) used in the LP-FP series. The CFMs were surrounded by four standard assemblies in a cruciform pattern, with special triangular arrays to fill in the corners.

In the case of the FP-01 test, the assembly included an inner 11x11 array surrounded by a thin Zircaloy flow shroud. To ensure higher temperatures in the CFM, twenty-two special fuel pins within the shroud were enriched to 6% U^{235} (instead of the standard 4%). Twenty of the high enrichment pins were pressurized as in normal commercial reactor fuel, but the remaining two were unpressurized so that they would remain intact during the experiment, and they would be examined afterwards.

The objectives of the FP-02 test would inevitably lead to very severe fuel damage, and it was obviously necessary to restrict the high temperatures to the interior of the assembly. The design was based on an 11x11 array of test fuel pins surrounded by a 25.4 mm thick heat-resisting shroud. The shroud consisted of zirconia tiles within a Zircaloy cladding. The assembly contained 100 pressurized fuel rods (enriched to 9.744% U_{235}) and 21 Zircaloy guide tubes, 11 of which contained stainless steel clad control rods (see Figure 4.1.8). Further general information about the series is given in Table 4.1.8.1.

4.1.8.3 Test Description

<u>LP-FP-1</u>

The pre-irradiation phase in the LOFT reactor attained a mean burnup of 1417 MWd/tU. This means that the mix of fission products was somewhat untypical of that likely to exist in a commercial reactor. The reactor was scrammed one minute before opening the blowdown valves, to delay the onset of high temperatures. It was planned to initiate the ECCS when the standard fuel pins of the periphery of the CFM reached a temperature limit. However, the test was manually aborted due to a erroneous indication. During the second attempt to run the test a

spurious cold water injection occurred, which delayed the heat-up. As a result, only 8 of the 20 pressurized fuel pins failed, thus reducing the fission product release.

LP-FP-2
The pre-irradiation phase allowed the fuel to attain a mean burnup of approximately 420 MWd/tU. The test was initiated by scramming the control rods, and turning off the reactor coolant pumps. The LPIS line discharge was opened, and the fuel temperatures rose and passed 2100 K at 25 min. The experiment was terminated 4.5 min afterwards by initiating the ECCS. This quenched the fuel surfaces, but the central molten region took several hundred seconds to cool.

The conditions for both tests are summarised in Table 4.1.8.2.

4.1.8.4 Processes Quantified

The main phenomena exhibited are summarized in Table 4.1.8.3. Only limited fuel clad swelling, rupture, and fission product release and transport were quantified in test LP-FP-01. The LP-FP-02 test attained much higher temperatures. It was an integral test, in which many processes involved in early and late phase PWR core degradation were present.

4.1.9 PHEBUS FP (Bundle aspect only)

The Phebus FP programme is led by the Institut de Protection de Sûreté Nucléaire (IPSN) of the French Commissariat à l'Energie Atomique (CEA) and the Commission of the European Communities (CEC) with international participation from USNRC, COG, NUPEC, JAERI, KAERI, HSK and PSI.

4.1.9.1 Objectives

The objective is to investigate the main phenomena governing degradation of fuel as well as Fission Product (FP) release, transport and behaviour in the containment during a beyond design basis accident occurring in a Light Water Reactor. The scope involves release of FPs from degraded irradiated fuel as well as FP/aerosol physics and chemistry both in the primary circuit and in the containment building. The bundle aspect involves the late phase of core degradation up to the fuel melting with the related FP release (volatiles and non-volatiles). These tests will enable investigation of specific phenomena not observed in the previous PHEBUS SFD programme: simultaneous Zr oxidation escalation-melting-interaction with UO_2 in an oxidising environment, effect of control rod materials (Ag-In-Cd or B_4C), chemical interactions at high temperature, solid debris bed evolution up to molten pool formation, and UO_2 oxidation by steam and air.

The first three tests of the programme, FPT0, FPT1 and FPT4, were performed in December 1993, July 1996 and July 1999 respectively in the Phebus reactor at Cadarache, France. The current test matrix involves 6 tests (Table 4.1.9.2).

4.1.9.2 Facility Description

The test train is located in a loop crossing the central part of the Phebus driver core which supplies the nuclear power (Figure 4.1.9). In tests FPT0, FPT1, FPT2 and FPT3 the fuel rods

are 1.13 m long with a 1 m long fissile zone, are held in place by two Zircaloy spacer grids and are arranged in a 5x5 square lattice without the four corner rods. The absorber rod in the centre of the bundle contains Ag-In-Cd in the first three of these tests and B_4C in FPT3. Only the first test FPT0 was performed using trace-irradiated fuel. For the rest of the matrix, irradiated fuel rods (~ 23 GWd/tU to 33 GWd/tU) are used. The last test FPT5 should investigate the effects of air ingress on an irradiated fuel bundle without a control rod.

The test bundle is surrounded by an insulating zirconia shroud with an inner circular ZrO_2 or ThO_2 layer, an external ZrO_2 layer and a pressure tube of Inconel coated on the internal face by flame-sprayed dense ZrO_2. These three annular structures are separated by two gaps under cold conditions. The outer pressure tube is cooled by an independent pressurised cooling circuit. The rods are cooled by a measured gaseous flow of steam imposed at the entrance.

The FPT4 test uses a debris bed configuration (0.36 m height) with two parts : passive (0.12 m height) and active UO_2 including ZrO_2 fragments (0.24 m height).

Measurements in the bundle involve mainly temperatures: fuel centreline and cladding (for fresh fuel rods), control rod, stiffeners, shroud and coolant. After failure of the rod TCs, the bundle temperature is controlled by shroud TCs located inside and on the outer surface of the external ZrO_2 insulating layer. Two ultrasonic thermometers should enable improved control of bundle temperatures at different levels. These tests are foreseen with 18 rods with intermediate burn-up (no TCs) and 2 fresh fuel rods to enable the implementing of some rod TCs allowing a direct measurement of fuel temperature. Coolant flow rates, hydrogen production and FP are measured in the circuit. In particular, an On Line Aerosol Monitor (OLAM) device enables the detection of major events of the core degradation. The measurement system for the power of the driver core and fission chambers located around the bundle can also detect significant core material relocation events.

Measurements in the debris bed FPT4 test involve mainly temperatures in the fuel, shroud and coolant. After failure of the fuel TCs, the temperature is controlled by shroud TCs located inside and on the outer surface of the external ZrO_2 insulating layer. Several ultrasonic thermometers installed in this test should enable control of the debris bed temperature at different levels.

Gamma-scanning examinations of some FPs and activation products of bundle structures enable the mean axial profiles of fuel and control rod mixtures to be measured. In addition, a large set of tomographies are performed enabling a rapid and precise overview of the bundle degradation and of the final axial distribution of bundle materials on the basis of their densities. Final destructive examinations enable cross and axial cuttings for more detailed quantification of the bundle degradation.

General information on the Phebus FP programme is given in Table 4.1.9.1.

4.1.9.3 Test Description

The test sequence of operations for the tests FPT0, FPT1 and FPT2 are similar:

- Pre-test bundle examinations,
- Irradiation phase for producing short-lived FPs. This phase lasted 9 days with a bundle power around 230 kW for FPT0, and about 7 days with a power ranging from 180 to 230 kW for FPT1,
- Shutdown,
- Preparation phase for the transient (34 hours for FPT0) with measurement of the coupling factor between the experimental bundle and the driver core,
- Pre-transient phase with different temperature plateaux for thermal calibration of the bundle,
- Transient phase with nuclear power increase,
- Final coolant phase with a shutdown and a moderate steam cooling,
- Post-test bundle examinations.

The test sequence of operations for FPT4 is quite different:

- Pre-test bundle examinations,
- Measurement of the coupling factor between the experimental debris bed and the driver core by a calorimetric method,
- Pre-transient phase with different temperature plateaux for thermal calibration of the debris bed,
- Transient phase with nuclear power increase (successive power plateaux),
- Final coolant phase with a shutdown and a moderate steam cooling,
- Post-test bundle examinations.

The range of experimental conditions for the first three tests is presented in Table 4.1.9.2.

4.1.9.4 Processes Quantified

The Phebus FP Programme is underway. The first three tests FPT0, FPT1 and FPT4 have been performed at the cut-off date of this report.

The heat-up phase of FPT0 was characterised by a sharp clad oxidation escalation (10K/s) with peak temperatures as high as 2700 K. After oxidation, the further power increase and gas flow rate reduction enabled fuel temperatures greater than 2300 K to be achieved. Different large fuel relocation events were identified on-line by various measurements, in particular by the OLAM device. The radiography and the 52 tomograms of the final state of the bundle showed a severe core degradation far beyond any previous experiment.

The fuel degradation during the heat-up phase following the oxidation runaway was characterised by a step by step slumping down of the fuel located in between the two spacer grids, involving almost all the inner rods and part of the outer ones. This happened at a

temperature of about 2500 K, far below the urania melting point. The relocation led to the formation of a molten pool on the lower grid. A final relocation of the molten material below the lower grid was observed just at the end of the experiment.

It is clear that FPT0 degradation results concern the transition from the early phase to the late phase of core degradation. In addition FP release and aerosol production were found to be significantly affected by the core material interactions and core degradation events which appear to be at least as important as the fuel temperature itself.

The second test, FPT1, with irradiated fuel was performed with similar bundle conditions regarding the temperature and the atmosphere evolution. A similar degradation pattern was observed, with early fuel slumping down. Fuel swelling of irradiated fuel (243 GWd/tU) was observed. The mass in the molten pool was lower than in FPT0, due to earlier termination of the experiment. Non-destructive post test examinations (more than 400 tomograms) allowed a 3D reconstruction of the damaged fuel bundle. Destructive post-test examinations are still in progress.

The third test FPT4 has only very recently been conducted, early indications are that a large molten pool formed below the debris mid plane, with a large cavity at bed mid-height and probably a vault on top of the bed. Further data will emerge in due course.

Main phenomena exhibited in FPT0, FPT1 and FPT4 (provisional) and foreseen to be studied in FPT2 and FPT3 are summarised in Table 4.1.9.3. It must be pointed out that this table is indicative of the current status of the programme.

4.1.10 ACRR-MP

The ACRR-MP tests were a series of two in-pile tests focused on investigating "late phase" melt progression processes. For this reason, the MP tests examined a degraded fuel geometry instead of fuel rods. The original test matrix of 6 tests was reduced to the two tests described here. The tests were carried out in the years 1989 to 1992.

4.1.10.1 Objectives

The objectives of the MP tests were to investigate late phase melt progression processes after the fuel rod geometry of the reactor core has degraded to a rubble bed geometry, as occurred in the TMI-2 accident. These melt progression processes include the melting dynamics of fuel debris (UO_2/ZrO_2), the growth and formation of a molten fuel pool, the migration of molten fuel materials through the fuel rubble and through intact rod geometry, and the role of metallic and ceramic crusts in the retention of molten fuel material.

4.1.10.2 Facility Description

A schematic of the MP test section is shown in Figure 4.1.10. The MP test design was that of a fuel debris bed of UO_2 and ZrO_2 (~3 kg) situated above an intact fuel rod array of 32 fresh Zircaloy-clad fuel rods. A metallic preformed "crust", made to represent the Zr-rich metallic blockage that forms when the fuel rod cladding melts and relocates, was situated at the top of the 32-rod array, just below the debris bed. The entire assembly was contained within a fully dense ThO_2 crucible which was insulated with zirconia fibre and contained within a steel

vessel. The assembly had no provision for steam flow and the gas environment was He. The fuel debris was fission heated by the ACRR driver core. Temperatures were measured in the fuel debris and lower rod array with W/Re and Pt/Rh thermocouples. General information on the ACRR-MP experiments is given in Table 4.1.10.1.

4.1.10.3 Test Description

Tests MP-1 and MP-2 were quite similar (almost identical in fact) in their construction, and differ primarily in the extent of melt progression that occurred in each test. The MP tests were conducted by fission heating the fuel debris in a stair-stepped fashion, allowing a thermal equilibrium to take place after each temperature boost of about 500 K. Peak temperatures attained in both tests exceeded 3200 K and test MP-2 attained a maximum of about 3400 K. Both tests generated molten pools of fuel material, but the MP-2 test extended the melt progression so that the ceramic fuel melt failed the lower metallic crust, and entered the intact fuel rod region. After cooldown of the experiments, the test sections were stabilized with epoxy, examined radiographically and sectioned for metallurgical examination. The range of experimental conditions for the 2 ACRR-MP tests is given in Table 4.1.10.2.

4.1.10.4 Processes Quantified

The MP tests provided information on ceramic melt formation and flow through porous fuel debris, on material interactions between ceramic fuel melt and adjacent metallic crusts, and on the migration of the ceramic melt into the intact fuel rod region. A large amount of the information from the MP tests derives from the metallurgical examination. The main processes quantified in the ACRR-MP experiments are summarized in Table 4.1.10.3.

4.1.11 SANDIA XR

The XR (Ex-Reactor) tests, conducted at Sandia National Laboratories in the period 1993-96 for the U.S. Nuclear Regulatory Commission, are out-of-pile experiments focused on core melt progression behaviour in boiling water reactors, with an emphasis on behaviour of relocating metallic melts. Two preliminary experiments and one large-scale experiment were performed.

4.1.11.1 Objectives

The Ex-Reactor (XR) tests investigate the behaviour of melting and relocating metallic core materials (stainless steel control blades and Zircaloy fuel canister and fuel rod cladding materials) in the lower core and core plate region. The objectives of the tests are to determine under what conditions the draining metallic melt forms stable lower core blockages, which are assumed to lead to a TMI-like in-core molten pool formation, and under what conditions such metallic blockages do not form. In the latter case, a continuous drainage of core materials into the lower vessel head is presumed to occur, as opposed to the TMI-like in-core melt pool formation. The two differing melt progression scenarios lead to important differences in the timing and mode of pressure vessel breach, hence it is important to characterize this core melt progression branch point.

4.1.11.2 Facility Description

The Ex-Reactor test facility includes a large test vessel which may be inerted with argon to prevent unwanted oxidation of the test section Zircaloy components at high temperatures, and a large (225 kW) high frequency (3 kHz) power supply for use in the preparation of high temperature metallic melts used in the conduct of the tests. The test facility includes a data acquisition system for collecting thermocouple data and a real-time X-ray imaging system for use in characterizing the behaviour of the draining metallic melts and the blockage formation process. The metallic melts are prepared by a unique inductively-heated radiant cavity wire melting furnace. The metallic feed material is introduced to the furnace as wire stock, and is quickly melted as it enters the furnace. The melting rate may be adjusted to simulate the reactor accident conditions by adjustment of the wire feeding rate. Figure 4.1.11 illustrates the arrangement of the Ex-Reactor test facility, including a cross-section of the test package. General information on the XR experiments is given in Table 4.1.11.1.

4.1.11.3 Test Description

The XR tests simulate the conditions in the lower ½ to 1 metre of the BWR core after the core water level has dropped below the core plate, and just as the stainless steel control blades are beginning to melt. Lower core structures are represented in the XR test section using prototypic materials and include fuel rods, fuel canister walls, control blade, fuel canister nose piece and support piece, lower core plate and control rod drive tube. The structures of the test section are represented in full scale, in some cases using actual BWR core components. Prototypic temperatures are imposed on the test section, and metallic melt is delivered to the top of the test section, simulating the melting and draining of the upper core metallic materials into the lower core region. The volume of melt introduced to the test section is scaled to represent the full height of core above the lower ½ to 1 metre. The range of experimental conditions for the XR tests is given in Table 4.1.11.2.

In the conduct of the XR experiments, the thermal conditions in the lower part of the dry BWR core, corresponding to that of a Short Term Station Blackout accident at the time of incipient metallic core component melting, are imposed on the test section. Metallic melt is introduced to the top of the test bundle, simulating the draining of metallic core materials from the upper core regions into the lower metre of the core. The melt consists of first, an alloy of stainless steel and boron carbide, representing the melting and draining of the control blade materials, and following this, a melt consisting of Zircaloy is added, representing the later-melting Zircaloy fuel rod cladding and channel box materials. In total, about 12 kg of molten control blade material and 65 kg of molten Zircaloy are added to the test section over a period of about ½ hour.

During the melt introduction period, the test section temperatures are monitored, providing thermal signatures of the spatial pathways taken by the draining melts. In addition, real-time X-radiography provides visual indications of the melt draining and blockage formation behaviour.

4.1.11.4 Processes Quantified

The information gained in these tests provides for an understanding of the initial structural damage caused by the draining metallic melts and the nature of the initially forming blockages, if any. While in the course of a BWR "dry core" transient, robust lower core metallic

blockages may form, it is also possible that the chemical aggressiveness of the molten materials together with the high enthalpy content of the Zircaloy melt would combine to destroy the lower core structures, including the lower core plate. In that event, drainage, and not core blockage, would be indicated. Current models of these processes are unable to predict with certainty which of these two radically different melt progression pathways is more likely, and these tests help to provide the experimental evidence necessary for resolving these uncertainties. The main processes quantified in the XR experiments are summarized in Table 4.1.11.3.

4.1.12 TMI-2

4.1.12.1 Introduction

The Three Mile Island Unit 2 (TMI-2) PWR underwent a prolonged LOCA on March 28, 1979, that resulted in severe damage to the reactor core. As a consequence of the TMI-2 accident, the nuclear community embarked on a thorough review of the causes and consequences of severe core damage accidents. The OECD has sponsored an ambitious international cooperation programme to evaluate and understand the TMI-2 accident. This was a three-tier programme which included a computer code benchmark exercise (1989), post-irradiation examination of samples from various parts of the core (1990), and the recently concluded TMI-2 Vessel Inspection Programme (1993). The TMI-2 analysis programme has allowed reasonable estimation of what happened during the accident, and has provided very valuable data. Though not a planned experiment, where boundary conditions are well defined and dedicated data gathering systems are used, the TMI-2 accident provides the only severe accident data base for an integrated, full scale, PWR, available for benchmarking computer codes and for comparing with results obtained in small-scale experimental facilities.

4.1.12.2 Reactor Description

TMI-2 was a 2720 MW(th) PWR of Babcox and Wilcox design and manufacture. Its primary system consisted of reactor vessel, two loops, with one once-through steam generator in each loop, and two circulating pumps in each loop, electrically-heated pressurizer, and piping (see Figure 4.1.12). General information is summarised in Table 4.1.12.1.

4.1.12.3 Accident Description

The accident was initiated by a transient that produced failure of the main feedwater, while the auxiliary feedwater system had been put out of operation. Reactor scram followed, and an increase in the RCS pressure. The PORV in the pressurizer opened and remained stuck open, which produced a continuous loss of coolant. Safety injection was manually isolated early in the transient, because the operators believed wrongly that the system was "solid". The accident was similar to sequences of station blackout and small break that have been postulated in accident analysis.

For the analysis exercise, the accident was divided into four phases. Phase 1 covers the time from accident initiation (0 min) to shutdown of the last reactor coolant pump (100 min) due to cavitation. Phase 2 (100 to 174 min) covers initial core uncovery, and the heat-up and melting of the reactor core. At the start of Phase 3 (174 to 200 min), the core level was recovered. A short flow transient from restart of the 2B RC pump occurred, that was terminated after less

than a minute by pump cavitation, rewet the degraded core, and reheat-up of the core followed. During Phase 4 the HPI was initiated, the core level recovered, but heat-up and melting of the molten consolidated region continued, and relocation of core material to the lower plenum occurred at 226 min. The lower plenum debris was quenched, after some damage to the lower head, and forced flow was resumed in the RCS at 15.5 hours.

The accident conditions are summarised in Table 4.1.12.2, and a schematic diagram of the end state of the damaged core is shown in Figure 4.1.12.

4.1.12.4 Processes Quantified

The main phenomena encountered in the TMI-2 accident are summarized in Table 4.1.12.3. Almost all phenomena of interest in in-vessel severe accident research, excepting vessel lower head failure, occurred in this accident. It should be noted the natural circulation phenomena observed in this B&W plant with once-through steam generators could be markedly different to those observed, for example, in a Westinghouse plant with U-tube steam generators, therefore the thermal hydraulic behaviour should not be assumed to be typical of all cases.

4.1.13 SCARABEE BF1

4.1.13.1 Objectives

The SCARABEE BF test series was performed by IPSN/CEA in the SCARABEE reactor at Cadarache, France, in the period 1985 to 1989. It was aimed at studying in the framework of fast reactor safety analysis the behaviour of a volumetrically heated molten fuel pool resulting from a sub-assembly melting at full power. The first test BF1, with pure molten UO_2, has a rather fundamental character interesting also for other accident situations, including PWR severe accident conditions, characterized by the existence of a molten pool. This configuration is of interest for studying the heat flux distribution at the boundary of the pool and the corresponding heat transfer coefficient.

The two other tests, performed at higher powers (pure UO_2 boiling and molten UO_2 plus boiling steel) are less prototypic of PWR conditions and are not presented in this report.

4.1.13.2 Facility Description

The test train is located in a loop crossing the central part of the SCARABEE driver core which supplies the nuclear power. Test BF1 started with a pre-fabricated solid debris bed of UO_2 pellets (~ 5 kg of UO_2) in a 0.06 m diameter Stainless Steel (SS) crucible cooled by a surrounding sodium flow. This device enabled the study of heat transfer from the pool for different total nuclear powers imposed. Figure 4.1.13 gives the scheme of the test section and the instrumentation.

On-line measurements were made of temperatures in the debris bed (3 W/Re TC and two tungsten ultrasonic TC giving temperatures on 4 different vertical sections for each). Other TCs measured, at different elevations, the SS wall temperature (inner and outer surface) and the temperature of the external cooling fluid. Nuclear power inside the SS crucible is well-characterized, with neutronic calculations and heat balance in the external cooling circuit.

Post Test Examinations (PTE) based on gamma scanning, neutronographic examinations and radial and axial cuttings have been done to give a final picture of the refrozen pool inside the crucible (mass distribution and crust thickness on the crucible wall). General information on the SCARABEE BF test series is given in Table 4.1.13.1

4.1.13.3 Test Description

- Pre-transient phase to reach nominal conditions for the driver reactor circuit and the cooling circuit of the SS crucible. Then initial conditions are reached in the solid debris bed;
- Melting phase up to 30 kW in the test section during the first plateau;
- Heat-up phase of the transient raising the nuclear power by steps and performing five additional stabilized power plateaux.

The melting and heat-up phases last 3600 s. For further experimental data see Table 4.1.13.2.

4.1.13.4 Processes quantified

Two power plateaux are of particular interest. The first one (30 kW) which includes the transition from a solid pack of compact fuel pellets (no cladding) to a molten pool. During this first plateau the temperature of the molten pool was measured (two ultrasonic thermocouples). One of them indicated at the end of the plateau (1000 s long) a temperature of about 120 K greater than the UO_2 melting temperature, which allowed the determination of a heat transfer coefficient. The last plateau is also of interest because it corresponds to the largest pool with the highest temperature and the post mortem examinations give information on this state such as the crust thickness profile on the SS crucible walls and UO_2 distribution.

Radial heat fluxes profiles and upward flux through the pool surface are deduced from temperature measurements in the wall crucible and in the external cooling circuit. These fluxes profiles are characteristic of heat transfer by natural convection in a pool (laminar regime during the first plateau, turbulent regime during the final plateau). The crust thickness was derived from on-line measurements and post-test examinations. The contact resistance between the crust and the crucible wall was characterized. Valuable information on the characteristics of heat losses through the top of the pool, in case of an upper temperature near the melting point, was also derived, and heat transfer coefficients were established for laminar and turbulent flow regimes. For further experimental data see Table 4.1.13.3.

4.1.14 ACRR-DC

The ACRR-DC (Dry Capsule) experiments DC-1 and DC-2 were in-pile tests performed in the ACRR at Sandia National Laboratories in the early 1980s. The tests were debris bed tests involving UO_2 fuel rubble, and therefore, bear some similarities to the MP tests. They focused on melting dynamics of fuel debris and on the effect of metallic content in the ceramic fuel debris.

4.1.14.1 Objectives

The objectives of the DC tests were to characterize heat transfer in dry high temperature fuel debris geometry and to investigate the melting dynamics within the bed as fuel melting temperatures were attained. DC-2 additionally investigated the effect of metal content (stainless steel) on these processes.

4.1.14.2 Facility Description

A schematic diagram of the DC test package is shown in Figure 4.1.14. A fuel debris bed of about 2 kg of powdered and granular UO_2 fuel material was contained within ThO_2-lined tungsten crucible. The debris region was insulated radially, and actively cooled on the top and bottom. The test bed was instrumented with ultrasonic thermometers. General information on the DC tests are given in Table 4.1.14.1.

4.1.14.3 Test Description

The conduct of the DC tests was similar to that of the MP tests in that a stair-stepped fission heating history was used which allowed for periods of thermal equilibrium to occur between successive increases in temperature. Peak temperatures in the DC-1 test, which involved only pure UO_2, exceeded 3400 K, generating a large molten region. The DC-2 test, which included stainless steel, reached only 2600 K before test termination. Following test completion, the packages were examined metallurgically. The range of experimental conditions for the 2 DC tests is given in Table 4.1.14.2.

4.1.14.4 Processes Quantified

The DC tests were aimed at gaining measured information to allow evaluation of models for predicting thermal conductivity in high temperature fuel debris beds and on observing the melting and pool growth phenomena. Thermal records of the heating profiles were recorded and the metallurgical examinations were thorough. The main processes quantified in the DC tests are summarized in Table 4.1.14.3.

4.1.15 CODEX

4.1.15.1 Objectives

The objectives of the CODEX series being carried out at AEKI, Budapest from 1995 onwards are to investigate early-phase core degradation in light water reactors (Western LWR and VVER designs). The series of 5 main tests to date has investigated the effects of quench in VVER geometry, and the effect of air ingress on pre-oxidised Western LWR bundles.

4.1.15.2 Facility Description

The CODEX out-of-reactor facility is illustrated schematically in Figure 4.1.15, with general information given in Table 4.1.15.1. A fuel rod bundle of representative Western LWR or VVER-440 design of overall cladded length 1.15 m (heated length 0.6 m) is surrounded by a permanently-installed high temperature shield. Decay heat (with compensation for heat losses) is simulated by electrical heating with tungsten heaters installed within all but the central rod

(9-rod square array for PWR/BWR, 7-rod hexagonal array for VVER). Coolant (superheated steam, argon or argon/oxygen mixture) is injected laterally at the bottom of the heated section, while cold air or a fast, cold argon flow (for rapid cooling) can be injected into the bottom of the heated section. In the tests not involving air ingress, quench can be effected by injection of water into the bottom of the bundle. On-line measurements are made of temperatures (thermocouples and pyrometers), pressures, rod powers, hydrogen production etc.; in the last air ingress test these were supplemented by video recording of the melt progression near the top of the heated section. In the air ingress tests there are on-line measurements of the aerosol rate and size distribution. Destructive post-test examinations determine such quantities as blockage formation and material distribution, while in the air ingress tests the aerosol composition is determined by analysis of impactor and filter data.

4.1.15.3 Test Description

Each test was started by pre-heating the bundle in hot argon to about 800-900 K. In the VVER tests the bundle was then ramped initially at 0.5-0.6 K/s in steam until the desired maximum temperature of up to ~2300 K was reached (in some cases following an oxidation excursion), then cooled in warm argon or quenched by water, with power switched off. In the air ingress tests the bundle was pre-oxidised in an argon/25%oxygen mixture or steam before the transient phase in air was entered. The air ingress tests were terminated from the desired maximum temperature (2200-2300 K) by rapid cooling in a high flow of argon at room temperature, again with power switched off. An extensive commissioning test (a series of ramp and hold periods in argon) was carried out using the first air ingress bundle (these data are useful for model qualification rather than code validation). The range of experimental conditions is surveyed in Table 4.1.15.2.

4.1.15.4 Processes Quantified

The main phenomena covered in the CODEX series are shown in Table 4.1.15.3. The VVER tests investigate behaviour without quench, and with quench from two different temperatures and with different amounts of oxidation at the onset of reflood. The AIT tests cover the effects of air ingress at similar temperatures but with different levels of bundle pre-oxidation. The aerosol measurements enable the detection of fuel volatilisation, which may occur through oxidation of UO_2 exposed to air.

4.1.16 QUENCH

4.1.16.1 Objectives

The general objective of the QUENCH programme at Forschungszentrum Karlsruhe (FZKA, previously KfK) is to provide an extensive experimental database on quench of an overheated LWR core while in a mainly rod-like state, giving improved understanding of the effects of water addition at different stages of the rod degradation. More detailed aims are the determination of a failure criterion for oxidised cladding and of the hydrogen source term. The bundle experiments summarised here are supplemented by an extensive series of single-rod quench experiments and by measurements of hydrogen absorption and release by Zircaloy cladding. The main parameters so far considered are heat-up rate, degree of cladding pre-oxidation, flooding rate and temperature at the onset of quenching.

4.1.16.2 Facility Description

The QUENCH out-of-reactor bundle facility is illustrated schematically in Figure 4.1.16, with general information given in Table 4.1.16.1. A fuel rod bundle of representative Western LWR design of overall length 2.5 m (heated length 1 m) is surrounded by a permanently-installed high temperature shield. The fuel rod simulators contain sintered zirconia pellets. Decay heat is simulated by electrical heating with tungsten rods installed in all but the central rod of the 21-rod array. Superheated steam with argon as a carrier gas is injected at the bottom of the test section; the quench water (or cold steam) for cooling enters through a separate line at the bottom. On-line measurements are made of temperatures, pressures, rod powers, hydrogen production etc. The hydrogen produced is measured by two independent means (mass spectrometer and Caldos device). Comprehensive destructive post-test examinations determine such quantities as extent of oxidation, crack patterns in oxide films, blockage formation and material distribution.

4.1.16.3 Test Description

The test sequence consists of the following main phases: an initial heatup in steam/argon to about 1000 K until the bundle is stabilised; a second heatup and pre-oxidation phase (if required, typically at 1400-1600 K); a transient phase during which an uncontrolled oxidation excursion may occur; and finally a quench phase induced by reflooding the bundle from the bottom, or by injection of cold steam (top injection is being considered for future tests). Reflood with water is in two phases; in the first water is injected at a high rate to fill the lower plenum rapidly; in the second the desired injection rate for the bundle section is employed. Additional calibration phases may be used; this was particularly the case during commissioning. The range of experimental conditions is surveyed in Table 4.1.16.2.

4.1.16.4 Processes Quantified

The main phenomena covered in the QUENCH bundle series are shown in Table 4.1.16.3. Particular attention is paid to the consistency and accuracy of the hydrogen source term measurements.

4.1.17 FARO

The FARO programme is led by the Institute for Systems, Informatics and Safety (ISIS) of the Joint Research Centre of the European Commission, Ispra site, Italy (JRC-Ispra), with participation from US-NRC. The programme consists of tests performed in two separate facilities: FARO and KROTOS. In the following sections the scope and work performed to date in FARO is described.

4.1.17.1 Objectives

The FARO test programme has been designed to improve understanding on molten core/ coolant/structure interaction by performing experiments at large scale in realistic conditions in order to reduce the uncertainties on the reactor system response to melt progression and relocation. In the FARO facility, the penetration and quenching of molten corium into the water of the lower plenum or reactor cavity and its subsequent settling on the bottom structures are simulated. The conditions are realistic for the melt composition (UO_2-ZrO_2-Zr), for the water

depth (up to 2 m) and for the system pressure and temperature (up to 5.0 MPa, 536 K). Melt quantities up to 200 kg and 3300 K are used.

The first full size test of the programme was performed in December 1993 with 150 Kg of UO_2-ZrO_2-Zr melt poured into a saturated water pool at 5 MPa system pressure. A total of 12 tests have been performed in various conditions. In addition, two experiments have been performed related to testing the performance of ex-vessel core catcher based on core melt spreading and cooling concept.

4.1.17.2 Facility Description

The FARO plant is located within the containment shield of the former ECO (Experience Critique Orgel) reactor in building 42 of JRC-Ispra. A typical experimental arrangement for melt/water interaction tests is shown in Figure 4.1.17a. The interaction vessel for FCI (designed for 10 MPa, 573 K) is connected to the UO_2-ZrO_2 melting furnace (Figure 4.1.17b) via the release channel and isolated from it during interaction by the valve SO2. The main characteristics are summarised in Table 4.17.1.

4.1.17.3 Test Description

The corium is melted in the FARO furnace by direct heating using three power supplies form 3000V/2A to 60V/15000A. The melt is then delivered to a release vessel to let time for isolating the furnace form the interaction vessel, measuring the initial temperature by using tungsten ultrasonic sensors (Ispra development) and insuring a controlled release of the melt to the water. The melt is released into the water by gravity whatever the system pressure. The test vessel is connected downstream to a condenser via a steam/water separator and exhaust valves. The purpose of this unit is to vent and condense the excess of steam produced during the melt quenching. Alternatively to the FCI vessel, a test section for spreading experiments is installed. The main boundary conditions are summarised in Table 4.17.2.

The principal quantities measured are the temperature of the melt, the pressures and temperatures both in the freeboard volume and in the water, and the temperatures in the debris catcher bottom plate. Visualisation of the processes is provided by a series of video cameras with rate up 1000 f/s.

4.1.17.4 Main Findings

No spontaneous steam explosion has occurred in any of the tests. In long pours, continuous break-up and constant quenching rate has been observed for all the time of the jet. Debris beds of mean particle size above 3 mm have been produced. In some cases, the debris consisted of a conglomerate ("cake") in contact with the bottom plate and overlaying fragments (loose debris). The addition of metallic phases in a stoichiometric oxidic corium enhances melt break-up and steam production. Significant hydrogen production as been noticed when quenching initially oxidic melts. A steam explosion has been obtained by applying an external trigger in unconstrained conditions (3-D reactor-like), showing limiting damage to the internals and no structural damage to the vessel. The spreading tests showed that crust formation, against bulk freezing, is the limiting process to the spreading of core melts with small solidus-liquidus range. The main phenomena observed for each test are summarised in Table 4.17.3.

4.1.18 KROTOS

The FARO programme is led by the Institute for Systems, Informatics and Safety (ISIS) of the Joint Research Centre of the European Commission, Ispra site, Italy (JRC-Ispra), with participation from US-NRC. The programme consists of tests performed in two separate facilities: FARO and KROTOS. In the following sections the scope and work performed to date in KROTOS is described. KROTOS is strictly more of a separate-effects test series, but is included here in the integral section because of its close links with FARO, and because of the detailed information that is now available at the conclusion of the programme.

4.1.18.1 Objectives

The main objective of the KROTOS tests is to investigate steam explosions and, in particular, different stages of it: pre-mixing, triggering, propagation and expansion which determine the energetics and structural loading. Typically, these experiments are designed to help directly modelling efforts of the separate phases of energetic steam explosions by maintaining well-defined test geometry and conditions. KROTOS tests have been performed with various simulant materials, such as tin and alumina, or with a prototypic corium mixture (80 wt% UO_2 + 20 wt% ZrO_2) with masses ranging from 1.5 kg to 6 kg.

4.1.18.2 Facility Description

The KROTOS test facility consists of a radiation furnace, a release tube and the test section. The furnace includes a cylindrical tungsten heater element which encloses the crucible containing the melt material. A series of concentric tungsten, molybdenum and steel radiation shields are placed around the heater element. The crucible is held in place by means of a pneumatically operated release hook. The furnace is designed to operate from vacuum up to 1.0 MPa overpressure. The 3-phase electric power supply has a maximum power of 200 kW. Depending on the crucible design and melt composition, melt masses in the range of about 1 to 6 kg can be produced. Maximum achievable temperatures are 3300 K. The melt temperature is controlled by an optical bi-chromatic pyrometer measuring the wall temperature of the crucible. Main characteristics are summarised in Table 4.18.1.

The lower part of the KROTOS facility consists of a pressure vessel and test section (see Figure 4.18.1), both made of stainless steel. Both have view ports for visualisation purposes. The pressure vessel is designed for 4.0 MPa at 493 K. It is a cylindrical vessel of 0.57 m inner diameter and 2.0 m in height (volume: ~0.35 m^3) with a flanged flat upper head plate. The test section consists of a strong stainless steel tube of inner diameter 200 mm and outer diameter 240 mm. The water level is variable up to about 1.3 m. The bottom of the test section is closed with a plain closing plate or with plate housing a trigger device. The trigger device consists either of a gas chamber (volume of 29.5 cm^3) which can be charged to a pressure of up to 20 MPa (nitrogen) and is closed by a 0.25 mm thick steel membrane or an explosive charge. Its purpose is to produce a well-defined pressure pulse that is capable initiating a steam explosion.

4.1.18.3 Test Description

The crucible containing the melt is released from the furnace and falls by gravity through a ~5.2 m long release tube. Half-way down the tube, a fast isolation valve separates the furnace from the test section below. The crucible strikes a retainer ring at the end of the tube where a

conical-shaped spike pierces the bottom of the crucible and penetrates into the melt allowing the melt to pour out through the openings in the puncher. The injection diameter of the melt jet is defined by guiding it through a funnel of high temperature refractory material with an exit diameter of 30 mm. The jet pours into the water-filled test section, and triggering applied as required. The main boundary conditions are summarised in table 4.18.2.

4.1.18.4 Main Findings

The main findings of KROTOS tests to date can be divided in two categories: direct observations of the test outcomes and implications of these observations. Since the KROTOS tests do not alone address scaling to an actual reactor geometry, care has to be taken to apply the findings directly to such a case. The main phenomena observed are summarised in Table 4.18.3.

The main finding is that no steam spontaneous explosions have been obtained with corium melts poured into highly subcooled or near-saturated water pools under a range of different initial conditions. However, under certain thermodynamic initial conditions the mixture of melt and water can be artificially triggered, but energy released and generated structural load are relatively small. On the other hand, independent of water subcooling, alumina melt pour can produce a coarse mixture with water that readily produces a strong steam explosion either spontaneously or by means of external trigger. The energy yield of these explosions is significant and can lead to structural damage.

The beneficial results from the reactor safety perspective of having demonstrated a low propensity for producing an energetic steam explosion with corium melts is still overshadowed by the lack of a clear explanation why another type of high temperature oxidic material can produce an highly energetic explosion. Until this difference is well-understood and can be reproduced by models, the strong influence of melt composition means that steps are still needed to close the steam explosion issue . However, it is believed that the KROTOS facility will produce the key data to bring the issue resolution closer in the near future.

4.2 Separate Effects Facilities

4.2.1 Clad Ballooning

The phenomenon of ballooning in Zircaloy-clad fuel rods has been extensively investigated in design-basis LOCA studies, where the major concern was the impediment to the ECCS caused by extensive flow blockage. It was comprehensively reviewed in the corresponding SOAR [4.2], which noted that most of the database consisted of single rod tests performed out-of-reactor. These served to elucidate the controlling factors, however the strains obtained could not be taken as representative of those occurring in large arrays, since the effect of the neighbours, mechanical and thermal hydraulic, are not present. The current survey, which treats ballooning as a separate effect, concentrates on providing significant examples from the more recent bundle tests, including some which were performed after the SOAR [4.2] was completed. In general, for unrecovered accidents, the tests in which ballooning occurs during heat-up in single phase steam, rather than in reflood conditions, are most relevant for the present case. Details of the extensive single rod programmes are given in [4.2]. Since the

bundle experiments are carried out under broadly similar conditions, one section only is provided to cover the most important tests for consideration in the present circumstances. These tests are summarised in Table 4.2.1.

4.2.1.1 Objectives

The objectives of ballooning experiments are to measure the amount of cladding strain and coolant channel blockage which occurs when cladding deforms at high temperatures (over 1000 K) under the influence of a net outwards pressure during simulated loss-of-coolant accident conditions.

4.2.1.2 Facility Description

In a typical test section, a bundle of pressurised rods (typically 25 to 49) is positioned inside a shroud which provides mechanical restraint and which may be heated to minimise the radial temperature differences. A guard ring of unpressurised rods may serve similar purposes. In nuclear heated tests, the rods are filled with UO_2 fuel pellets and the assembly is loaded into a reactor to be driven by fission power. In an electrically heated test, the rods contain internal resistance heaters which may be fabricated to impose an axial power profile typical of that experienced in-reactor. The rods are filled with helium at such a pressure that ballooning occurs in the desired temperature range (high a-phase of Zircaloy, 1000-1150 K, to give maximum blockage). Instrumentation includes cladding and sometimes fuel centreline thermocouples, fluid thermocouples, internal rod pressure and system pressure gauges and coolant flowmeters. The internal pressure gauges enable measurement of the burst times and hence the burst temperatures. Cladding strains and flow blockages are determined as a function of axial position in the bundle by destructive post-test examination involving sectioning the deformed bundle. The amount of clad oxidation may also be measured.

4.2.1.3 Test Description

In electrically heated tests, the bundle is heated in flowing steam at decay heat powers (which give heat-up rates of typically 7 K/s), until ballooning and clad rupture occurs. There may be a simulated refill/reflood phase before or after the clad deformation. A similar procedure may be followed in-reactor, alternatively a full LOCA transient may be simulated, with blowdown, refill and reflood phases included. If there is no reflood phase, the power is switched off at the end of the transient phase and the bundle is allowed to cool to room temperature.

4.2.1.4 Processes Quantified

Clad strain and bundle blockage are determined as a function of the pressure difference (which determines the cladding stress), temperature, and metallurgical state of the cladding if required (including the extent of oxidation).

4.2.2 Materials Interactions

The following three sections outline separate-effects experiments in the areas of metal oxidation, structural materials interactions (not involving fuel) and metal/ceramic interactions (including fuel interactions). Since the methods and objectives in each section are similar, only an overview of the general area is given, not of the individual experiments. In each

section, a single table is given to summarise the main results quoted. The sections follow the temperature order in which the reactions tend to occur in a typical severe accident.

4.2.2.1 Material Oxidation

The processes considered here are the oxidation of Zircaloy, Zr1%Nb, stainless steel and boron carbide in steam, and Zircaloy in air. Zircaloy is used for fuel rod cladding and spacer grids in modern PWR and BWR plants, and for control rod guide tubes in PWRs; its oxidation is highly exothermic and commonly leads to a runaway "oxidation temperature excursion" above ~1473 K in steam and at as low as 1173 K in air. The same remarks apply to Zr1%Nb which is used for fuel rod cladding in VVERs. Stainless steel was used for cladding in some early LWR designs, and is now used for example for PWR control rod guide tubes and in BWR control blade assemblies. The oxidation energy is about one-tenth of that of the Zircaloy/steam reaction. Boron carbide is used as an absorber in BWRs, VVERs and in some PWR designs. The oxidation of Zircaloy and stainless steel in steam has been extensively reviewed in the literature, especially in the SOAR on fuel rod behaviour in design-basis LOCA's [4.1], therefore a full listing of their measurements is not given here; instead the information given is restricted to experiments highlighted in the SOAR on in-vessel core degradation [4.3], plus one more recent series which extends the range of pressures for which data are available. The material oxidation experiments are summarised in Table 4.2.2.1.

4.2.2.1.1 Objectives

The objectives are to measure the reaction rates of the materials over a range of temperatures and to quantify them, usually in the form of correlations (which are usually parabolic with time). Some specialised tests deal with oxidation in impure atmospheres (e.g. for steam with an excess of the reaction product hydrogen present), and in the presence of pre-oxidation and in the presence of cladding deformation; these are not presented here but are summarised in [4.2].

4.2.2.1.2 Facility Description

A variety of facilities is used, employing heating methods such as electrical resistance heating (direct or indirect), induction, or more recently laser heating. Temperature control is usually achieved by coupling the power supply with temperature measurements; fast-acting systems are needed particularly for high temperature oxidation of Zircaloy and Zr1%Nb where the reaction heat is large. Superheated steam (for steam oxidation experiments) is generated externally and passed over the specimen, which for metals is generally of tubular or cylindrical form; in boron carbide experiments a variety of specimen configurations has been used (powder, pellets, coupons etc.) and there is some evidence that the reaction rate depends on the form of the specimen. Temperatures themselves are measured with thermocouples or pyrometers, sometimes the hydrogen production is monitored. Weight gain, oxide layer thickness and (for Zircaloy) the oxygen-stabilised a-layer thickness are measured post-test following sectioning, etching and polishing of the specimen. Eddy current probes can provide an initial non-destructive indication of oxide layer thickness.

4.2.2.1.3 Test Description

The specimen is heated rapidly (sometimes in an inert atmosphere) to the test temperature, allowed to react for the desired time, and allowed to cool (again sometimes in an inert atmosphere).

4.2.2.1.4 Processes Quantified

The oxidation rate is quantified in terms of temperature and time; separate relationships may be given for the weight gain or loss (for boron carbide where the reaction products are mostly or completely gaseous or aerosol), oxide thickness and (for the Zr-bearing alloys), the oxygen-stabilised a-layer. The correlations are most usually of Arrhenius temperature dependence and power-law (e.g. parabolic) time dependence. Different correlations may apply in different temperature regions.

4.2.2.2 Structural Material Interactions

This section covers interactions between pairs of materials commonly used for cladding, spacer grids, absorber rods or assemblies, etc. Usually the materials form eutectics which have melting points below those of the respective components, leading to early liquefaction and component failure. Pre-oxidation, causing the formation of an oxide barrier between the components, delays the onset of the reaction. These experiments considered are summarised in Table 4.2.2.2.

4.2.2.2.1 Objectives

The objectives are to measure the reaction rates of the material couples over a range of temperatures and times.

4.2.2.2.2 Facility Description

A crucible geometry is usually employed; the crucible is made of the higher melting point material and contains a specimen of the other material, which may be pre-oxidised (the pre-oxidation delays the start of the eutectic reaction). The whole assembly is heated in a furnace (electric/infrared) in an inert atmosphere to avoid unwanted oxidation. Temperatures are measured on-line; reacted layer thicknesses are determined post-test following sectioning as for oxidation measurements.

4.2.2.2.3 Test Description

The specimen is heated to the test temperature, allowed to react for the desired period, and allowed to cool.

4.2.2.2.4 Processes Quantified

The reaction rates are quantified in terms of the reaction layer thicknesses as functions of time and temperature; the forms of the correlations are usually as for oxidation reactions. Where there is pre-oxidation, the time taken for the oxide layer to disappear is quantified in terms of its thickness and temperature.

4.2.2.3 Metal/Ceramic Interactions

This section covers mainly the reactions between UO_2 fuel and Zircaloy cladding, and the dissolution of zirconium dioxide by liquid Zircaloy. Recent studies have considered simultaneous dissolution of UO_2 and ZrO_2 by molten Zircaloy, and also the breach of ZrO_2 shells by Zr-rich melt contained inside, which in a severe accident can lead to large-scale relocation of U-bearing melt with loss of rod-like geometry. The experiments considered are summarised in Table 4.2.2.3.

4.2.2.3.1 Objectives

The objectives are principally to measure the reaction rates of the material couples over a range of temperatures and times. Breach criteria experiments explore the range of conditions (temperature, oxide thickness) in which the oxide shells are vulnerable to rupture.

4.2.2.3.2 Facility Description

A crucible geometry is usually employed; the crucible is made of the higher melting point material and contains a specimen of the other material. More rarely, the more prototypic rod-like geometry is employed. The atmosphere may be inert (argon) or oxidising (steam, or an argon/steam mixture). Electric, radiant or inductive heating is used to achieve the required temperatures. The temperatures are measured on-line; reacted layer thicknesses are determined post-test following sectioning as for oxidation measurements.

4.2.2.3.3 Test Description

The specimen is heated to the test temperature, allowed to react for the desired period, and allowed to cool.

4.2.2.3.4 Processes Quantified

The reaction rates are quantified in terms of the reaction layer thicknesses as functions of time and temperature; the forms of the correlations are usually as for oxidation reactions.

4.2.3 Reflood

The following two sections outline separate-effects single rod oxidised Zircaloy quench test programmes carried out at the Japanese Atomic Energy Research Institute (JAERI) and Forschungszentrum Karlsruhe (FZK). The test series address safety issues relevant to accident management measures which involve water injection into a degrading core. The main features are summarised in Table 4.2.3.

4.2.3.1 JAERI

4.2.3.1.1 Objectives

NSRR reflooding tests have been conducted using the Nuclear Safety Research Reactor (NSRR) of the Japan Atomic Energy Research Institute (JAERI) in order to investigate the fuel

failure behaviour and failure conditions due to quenching by delayed reflooding after a loss of coolant accident.

Specific objectives of this test series were to:

- investigate the conditions of fuel fracture by quenching as parameters of oxide layer thickness on cladding tube and of cladding temperature before quenching;
- investigate the characteristics of cladding fracturing by quenching; and
- investigate the effect of steam generated during reflooding on fuel quenching behaviour.

4.2.3.1.2 Facility Description

The NSRR is an annular core pulse reactor (ACPR) which has an experimental cavity in the core centre. Using this reactor, rapid heating of a test fuel rod by single pulse operation and relatively slow heating by the controlled pulse power operation are available.

A test fuel rod is irradiated and heated within an experimental capsule which has an adiabatic test section. At the bottom of the test section, an electro-magnetic valve is installed as water inlet in order to simulate delayed reflooding.

4.2.3.1.3 Test Description

In each test, a test fuel rod was quenched by water injected into the test section after heating by the irradiation. The environment of the test fuel rod during heating was steam or helium gas. Temperature was measured at 6 points on the cladding surface by thermocouples during heating and quenching.

Tests were conducted in the cladding temperature range 1000 to 1800°C. Oxidation of the cladding tube was below 40% of the cladding thickness.

After each test, post-test examination of each test fuel rod was carried out. The oxide layer thickness and microstructure of the cladding tube were measured.

4.2.3.1.4 Processes Quantified

Some test fuel rods were broken into two parts or into a few pieces by quenching in the test. A condition of cladding fracturing by quenching was investigated as parameters of cladding temperature and oxide layer thickness. The boundary of cladding fracturing by quenching is planned to be clarified using other general parameters.

4.2.3.2 Fz Karlsruhe

4.2.3.2.1 Objectives

An extensive programme of single-rod quench tests is being carried out on pre-oxidised Zircaloy single rod specimens at Fz Karlsruhe (formerly KfK), in support of the QUENCH test series (section 4.1.16). To date, the experimental series have covered specimens pre-oxidised either in argon/25% oxygen or argon/steam (separate series), then quenched by water or cooled rapidly by cold steam injection. An accompanying experimental programme studies the uptake

and release of hydrogen by metallic Zircaloy. Both quench and hydrogen experimental programmes are continuing, accompanied by detailed modelling support from the Russian Academy of Sciences (IBRAE).

The main objectives are:

- provision of an extensive experimental database for the development of detailed mechanistic models for quench of a degraded core in a rod-like geometry;
- investigation of the physico-chemical behaviour of the overheated fuel elements under different flooding conditions; and
- examination of the behaviour of the cladding - cracking of the oxide layer results in oxidation of the new metallic surfaces and additional hydrogen production.

The main experimental parameters quantified are the extent of pre-oxidation and the temperature of the tube before cooldown.

4.2.3.2.2 Facility Description

The tube specimen of length 100 to 150 mm (either open or closed end), which may be filled with zirconia pellets, is suspended by a thin rod inside a quartz tube. The quartz tube is surrounded by an induction heating coil. Water quenching of the heated specimen is carried out by raising a water-filled cylinder in a similar manner to that in the CORA facility (q.v., section 4.1.2); a valve prevents evaporation of the quench water before the quench phase. In an alternative configuration, cold steam is injected at the bottom of the facility in the cooldown phase.

4.2.3.2.3 Test Description

The specimen is pre-oxidised in an argon/oxygen (20 vol.% O_2) or an argon/steam mixture to the desired extent (up to 50% of the cladding wall thickness) at 1400°C in the QUENCH apparatus, raised or lowered to the test temperature (1000 to 1600°C) by heating inductively in argon, then quenched by raising the quench cylinder at 3 to 30 mm/s or cooled rapidly by injection of steam at up to 2 g/s at 150°C. The temperature of the specimen and the hydrogen production are continuously recorded. Video recording of the quench process is supplemented by post-test metallographic and scanning electron microscope examination to establish the physico-chemical condition of the specimen, e.g. to determine how much cracking of the oxide film has taken place. The hydrogen uptake of the specimen is determined in the LAVA facility.

4.2.3.2.4 Processes Quantified

Correlation of the generated hydrogen with the physico-chemical state of the specimen before and after the test, with the test conditions, provides information concerning the dominant mechanisms occurring during the quench of oxidised Zircaloy. Investigation of the cracking (fragmentation) of oxide films on quench, which leads to the exposure of fresh Zircaloy metal surfaces, renewed rapid metal oxidation, temperature increase and strong hydrogen production, is of particular interest. Comparing the results of quenching specimens pre-oxidised in argon/oxygen and argon/steam gives insights into hydrogen absorption/release phenomena and their effects in quenching. Comparing results of water-quenched and steam-cooled tests

provides information on the influence of thermal hydraulic conditions; in addition the thermal hydraulic conditions in the steam-cooled tests are more precisely defined.

4.2.4 Melt Pool Thermal Hydraulics

This section describes the major separate-effects facilities on melt pool thermal hydraulics. The objectives are the estimation of flow characteristics, heat transfer on the pool boundaries and crust formation.

4.2.4.1 Technische Universität Hannover

4.2.4.1.1 Objectives

The objectives of the reactor safety research projects RS 48 and RS 166, supported by the Bundesministerium für Forschung und Technologie, were to determine the heat transfer between melt and reactor pressure vessel as well as between melt and the concrete of the basement. The results can be applied to the conditions of a melt pool in the core region too.

4.2.4.1.2 Facility Description

The temperature distribution in the simulant material for the melt was measured by holographic interferometry. Therefore the experiments were limited to two-dimensional convection in slab geometries. The slabs were rectangular or semicircular with different sizes and different liquid level heights. In one test series, penetration of melt jet was simulated. The test fluid was water. Uniform internal heating was provided by electric current from the side glass walls throughout the liquid.

The facility and parameter ranges covered are summarised in Table 4.2.4.

4.2.4.1.3 Test Description

Starting from isothermal conditions for fluid, and temperature controlled walls, internal heating induces non-stationary interference figures with the development of the temperature field.

4.2.4.1.4 Processes Quantified

Stationary and transient temperature fields were recorded by means of holographic interferometry to derive the heat flux distribution. The Nusselt number as a function of Rayleigh numbers was varied by different geometrical sizes and internal heat sources in the range from 1.0e+6 to 1.0e+9.

4.2.4.2 Ohio State University (1)

4.2.4.2.1 Objectives

The objectives of the test series, sponsored by the United States Nuclear Regulatory Commission, were to measure the heat transfer coefficient of internal heated layers at high Rayleigh numbers to provide the basis for building models for more complicated molten core geometries.

4.2.4.2.2 Facility Description

The experimental apparatus consisted of a horizontal fluid layer bounded from above by a plate of constant temperature and from below a plate with zero heat flux. The layer thickness of the square test cell was varied by changing spacers between the horizontal plates. The electrodes were placed on two sides of the test cells. Specific quantities of silver nitrate were dissolved in demineralized water.

The facility and parameter ranges covered are summarised in Table 4.2.4.

4.2.4.2.3 Test Description

Starting from isothermal conditions, specific amounts of internal heat were induced by electric current with control of temperature and heat flux on the upper and lower plates. Typically after 6 - 8 h stationary conditions were established.

4.2.4.2.4 Processes Quantified

Energy balances from power input and power extraction on the top plate as well as temperature measurements by thermocouples, the Nusselt number was derived for different Rayleigh numbers up to 1.0e+12 by variation of power input and layer height.

4.2.4.3 Ohio State University (2)

4.2.4.3.1 Objectives

The objectives of these experiments, supported by the United States Nuclear Regulatory Commission, were to measure steady state heat transfer coefficients in a volumetric heated fluid in a scaled configuration analogous to core melt in the bottom of the reactor vessel.

4.2.4.3.2 Facility Description

The experimental apparatus consisted of a right circular cylinder mounted on a spherical segment with a total polar angle of 60° (the calotte) and a horizontal circular plate with variable height above the calotte to vary the aspect rations. The thermal boundary conditions maintained were zero heat flux on the lower surface and side wall and constant temperature on the upper surface. The aqueous copper sulphate solution was heated by 60 Hz alternating current passing through the fluid from the lower to the upper boundaries.

The facility and parameter ranges covered are summarised in Table 4.2.4.

4.2.4.3.3 Test Description

Starting from isothermal conditions specific internal heat was induced. A period of 8 - 48 h, depending on the Rayleigh number and the maximum depth of the fluid, was needed to reach steady state heat transfer data derived from thermocouple readings with an accuracy of $\pm$ 0.03 K.

4.2.4.3.4 Processes Quantified

For various aspect ratios (L/D = 0.1 to 0.7) the average Nusselt number at the upper surface, given by the temperature difference between the lower an upper bound, was correlated with the Rayleigh number, derived from the internal heat generation, in the range of 1.0e+7 to 10e+14. For high aspect ratios the Nusselt number approaches that for horizontal layer. With lower aspect values the Nusselt number has a much lower power law dependence on the Rayleigh number.

4.2.4.4 AEA Technology (AEAT)

4.2.4.4.1 Objectives

Various test series, funded by the UK Health and Safety Executive, were performed at Culham Laboratory with the objectives of investigating the effect of precipitation and growth of dendrites on heat and momentum transfer in the boundary layer between a multi-component melt pool and crust.

4.2.4.4.2 Facility Description

The experiments were performed in a well-insulated rectangular tank with a square cross-section. The base of the tank was either insulated or electrically heated, while the top was cooled by circulating refrigerant. The heating and cooling power was limited to 2.5 kW. Pure water was used for control experiments and sodium sulphate or sodium nitrate solution for the others.

The facility and parameter ranges covered are summarised in Table 4.2.4.

4.2.4.4.3 Test Description

The temperature of the cooling plate was maintained above the eutectic (minimum freezing) temperature but well below the saturation temperature. The power of the heater plate was varied to establish different boundary layer structures. Typical time to reach steady state conditions was 1 hour. Longer times are needed if a stably stratified layer forms beneath the top plate.

4.2.4.4.4 Processes Quantified

Beside integral values such as heating power and upper and top plate temperatures, the refractive index and temperature in the boundary layer were measured. Derived values are Nusselt number as a function of Reynolds number in the range from 1.0e+7 to 1.0e+10, boundary layer thickness and concentration profile across the boundary layer.

Due to the precipitation of the denser component:

- a stably stratified layer is created near the downward facing cold boundary if the Reynolds number is - untypically for plant applications - very low.
- A stratified layer at the upward facing cold boundary might become unstable (not verified in this test series).

4.2.4.5 COPO I

4.2.4.5.1 Objectives

The experimental facility COPO, located in the Hydraulic Laboratory of Fortum Power and Heat (formerly, Imatran Voima Oy, IVO), was constructed to measure the heat flux distribution at the boundaries of a large volumetrically heated pool at higher Rayleigh numbers relevant to molten corium pool inside the lower head of a RPV. The results are relevant for molten pools in the core region too. The facility is modelled as part of a VVER-440 lower head.

4.2.4.5.2 Facility Description

The experimental approach is based on using a two-dimensional "slice" of the Loviisa lower head, including a portion of the cylindrical vessel wall, at linear scale 1:2. Uniform "Joule" heating is provided by electrodes on the insulated flats. The side and bottom walls consist of 57 separate cooling units which allow local heat flux measurements. Water is used as coolant. Pool depths of 0.8 and 0.6 m were realised.

The facility and parameter ranges covered are summarised in Table 4.2.4.

4.2.4.5.3 Test Description

Separate cooling units are grouped to five adjustable coolant circuits which allows to obtain nearly isothermal boundary conditions. After sufficiently isothermal and stationary conditions had been reached, fluid and boundary temperatures and heat fluxes were measured.

4.2.4.5.4 Processes Quantified

The temperature field, power input and heat flux distribution have been measured. Averaged Nusselt number as function of internal Rayleigh number (2.0e+14 - 2.0e+15) as well as relative Nusselt number as function of local position have been derived from the measurements.

4.2.4.6 COPO II

4.2.4.6.1 Objectives

The experimental facility COPO II, located in the Hydraulic Laboratory of Fortum Power and Heat (formerly Imatran Voima Oy, IVO), was constructed to measure the heat flux distribution at the boundaries of a large volumetrically-heated pool with crust formation at higher Rayleigh numbers relevant to molten corium pool inside the lower head of a RPV. Two versions of the facility exist: one modelling a VVER-440 lower head and another one with a Western PWR (e.g. AP600) geometry.

4.2.4.6.2 Facility Description

The experimental approach is based on using a two-dimensional slice of the lower head at linear scale 1:2. Uniform "Joule" heating is provided by electrodes on the insulated flats. The top and bottom walls consist of numerous separate elements which allow local heat flux measurements. Liquid nitrogen is used as the coolant of the boundaries, which ensures crust (ice) formation at the inner surface of the boundaries.

Also stratified pool experiments have been carried out, in which the fluid volume was divided into a volumetrically heated lower part (simulating the oxidic part of a corium pool) and a nonheated upper part (simulating a metallic layer). The two layers were separated a by a thin aluminium plate.

The facility and parameter ranges covered are summarised in Table 4.2.4.

4.2.4.6.3 Test Description

After reaching sufficiently stationary conditions, fluid and boundary temperatures and the heat fluxes were measured.

4.2.4.6.4 Processes Quantified

The temperature field, power input and heat flux distribution have been measured. Averaged Nusselt number as function of internal Rayleigh number (4.0e+14 - 4.0e+15) as well as relative Nusselt number as function of local position have been derived from the measurements.

4.2.4.7 ACOPO

4.2.4.7.1 Objectives

The ACOPO refers to Axisymmetry COPO, and it is a descendant of the original COPO experiment. It was constructed during/for the licensing review of AP600, with the purpose of obtaining detailed experimental data under reactor-prototypic geometry and Rayleigh numbers (1.0e+16 to 1.0e+17).

4.2.4.7.2 Test Facility

The facility models in 1/2 scale the corium liquid pool in the vessel lower head in hemispheric geometry. The simulant material is preheated externally and cooled at the spherical and top boundaries with 15 separate controlled cooling units.

The facility and parameter ranges covered are summarised in Table 4.2.4.

4.2.4.7.3 Test Description

The test is a transient cool-down of pre-heated simulant material (water).

4.2.4.7.4 Processes Quantified

Measured are the pool temperature of the fluid, the temperature distribution on the boundaries and the heat flux to the boundaries in 15 separate segments. Because of the large scale, quasi-static conditions prevail, and a complete cooldown yields a complete trajectory in Nu-Ra space, that is the coorelation sought for each local position of the boundary.

4.2.4.8 University of California, Los Angeles (UCLA)

4.2.4.8.1 Objectives

The objectives of this test series, jointly sponsored by the US Department of Energy (DOE) and Electric Power Research Institute (EPRI), was to measure the heat flux distribution of a volumetrically heated pool as function of Rayleigh number in a spherical geometry. Further characteristics are pool depth and the conditions on the pool surface: free or rigid, adiabatic or cooled.

4.2.4.8.2 Facility Description

The apparatus consist of a rectangular, water-filled tank, in which a glass bell jar is partly submerged. The bell jar contains the test fluid (R-113) which is volumetrically heated by microwaves, guided by a copper tube from the magnetron. An air-cooled plexi-glass slice can be imposed as a rigid wall condition on the top pool surface in the bell jar.

The facility and parameter ranges covered are summarised in Table 4.2.4.

4.2.4.8.3 Test Description

After filling of the test liquid into the bell jar and a calibration phase for the imposed power the tank was filled with water, which was maintained at a constant temperature by cooling. Nearly steady-state temperatures were reached after one hour, the entire test run was carried out for about six hours.

4.2.4.8.4 Processes Quantified

The temperature distributions in the pool and on the inner and outer surface of the bell jar as well as the total heat generation in the test fluid have been measured. Derived values are the Nusselt number as function of Rayleigh number in the range from 1.0e+11 to 1.0e+14 and the local heat transfer coefficient along the hemispherical wall for the three different boundary conditions on the top surface.

4.2.4.9 BALI

4.2.4.9.1 Objectives

The objectives of the BALI experiment, operated by Service de Thermohydraulique des Réacteurs (STR) from Centre d'Etudes Nucléaires (CEN) Grenoble, are to investigate the thermal hydraulics - i.e. the temperature and velocity distributions and boundary layer behaviour - of a homogenous volumetrically heated liquid pool with variable viscosity as well as the effects of solidification (crust formation) or ablation, focusing effect due to a metal layer on the top of the pool, and gas release of sacrificial material at the pool boundaries for the simulation of ex-vessel MCCI.

4.2.4.9.2 Facility Description

The test section is a 100° sector slab with uniform "Joule" heating, provided by electrodes supported by the glass flats. The lower boundary, cooled by cryogenic fluid, carries a porous

wall which allows even gas injection. A frozen ice layer may be obtained by decreasing the temperature of the coolant.

The facility and parameter ranges covered are summarised in Table 4.2.4.

4.2.4.9.3 Test Description

Different flow patterns can be established by varying the heat input, temperature of the coolant, pool height, with and without top cooling, and gas injection. The test fluid is a water/salt solution with addition of glycerine to vary the viscosity.

4.2.4.9.4 Processes Quantified

Measured quantities are temperature (thermocouples), velocities (LDA System) and void fraction (gamma absorption system) of the test fluid as well as the heat flux to the semicircle boundary.

4.2.4.10 RASPLAV AW200

4.2.4.10.1 Objectives

The objectives of the test series with corium performed by the Russian Research Centre "Kurchatov Institute" RRC-KI and supported by OECD countries, are to investigate melt pool thermal hydraulics as well as crust formation and ablation under plant specific conditions, i.e. with reactor-typical materials. The test series are supported by specific separate-effects tests and an experimental programme to generate a thermophysical data base for the high temperature range.

4.2.4.10.2 Test Facility

The facility consists of the test section placed in a containment with an argon environment. The experimental section has a semicircular slab loaded with U-Zr-O mixture, heated by conduction from the side walls. The high temperature resistant side walls are heated inductively and protected by tungsten sheaths. The lower boundary reflect a slice of lower head. It is made of stainless steel and water cooled. The top boundary is insulated.

The facility and parameter ranges covered are summarised in Table 4.2.4.

4.2.4.10.3 Test Description

The test section is loaded with sintered, brick-shaped UO_2-ZrO_2-Zr briquettes with additives of mixed-oxides (i.e. La_2O_3, FeO). The U/Zr ratio varies between 1.2 and 1.6, the oxidation extent between 22 and 100 %, and the carbon content between 0.01 and 0.3 %. After heat-up, thermal steady state conditions (2700 - 3100 K) are maintained as long as possible to maximise the melt volume.

4.2.4.10.4 Processes Quantified

On-line measurements are of (1) the temperatures of the corium (thermocouple and pyrometer), of the steel wall, of the side wall and further safety relevant components, (2) electrical power,

(3) local heat flux through the steel wall, and (4) heat-up of the coolant to close the energy balance. In the fourth test melt was sampled from different locations during steady-state conditions. Extensive post-test examinations are carried out to determine melt volume, concentration distribution etc.

4.2.4.11 RASPLAV Salt

4.2.4.11.1 Objectives

The objectives of the salt test series performed by the Russian Research Centre "Kurchatov Institute" RRC-KI and supported by OECD countries, are to investigate melt pool thermal hydraulics as well as crust formation and ablation under plant specific conditions with simulant materials. The test series are supported by material properties measurements thermophysical data base of the used salt mixtures in the high temperature range.

4.2.4.11.2 Test Facility

The facility models the corium liquid pool in the vessel lower head in plane slice geometry. Eutectic and non-eutectic salts with different Prandtl numbers are used. The salt is heated by conduction from the side walls or directly by electric resistance. The lower boundary is cooled by forced convection. The top boundary is either adiabatic or isothermal. The simulation of an overlying metal layer (focusing effect) is possible.

The facility and parameter ranges covered are summarised in Table 4.2.4.

4.2.4.11.3 Test Description

One test series is composed of several thermal steady-state regimes at different salt temperatures, power levels or boundary conditions.

4.2.4.11.4 Processes Quantified

Electrical power, average salt temperature, the temperature of the side walls, of the boundaries, and of the coolant are measured continuously. During the steady-state regime the temperature field in the salt and the crust thickness are measured.

4.2.4.12 SIMECO

4.2.4.12.1 Objectives

The objectives of the test series performed by the Royal Institute of Technology, Sweden, are to investigate ordinary and stratified melt pool thermal hydraulics, crust formation, and crust ablation under plant specific conditions with salt as simulant materials. The test series are supported by material properties measurements for a thermophysical data base of the salt used mixtures in the high temperature range.

4.2.4.12.2 Test Facility

The facility models in 1/10 scale the corium liquid pool in the vessel lower head in plane slice geometry with a semicircular section and a vertical section. The simulant material is heated

internally by electric resistance wire. The side walls are insulated. The lower and top boundary are cooled by two water cooling loops. Eutectic and non-eutectic salt mixtures are employed for oxide melt simulation and crust formation. For the simulation of an overlaying metal layer (focusing effect) appropriate molten metals are used.

The facility and parameter ranges covered are summarised in Table 4.2.4.

4.2.4.12.3 Test Description

The test is composed of transient heat-up and thermal steady state regimes at different salt temperatures, power levels or boundary conditions.

4.2.4.12.4 Processes Quantified

Electrical power input and the heat losses to the coolant are measured as well as melt pool temperature, the temperature distribution on the side walls and of the boundaries and the local heat flux to the lower boundary.

4.2.5 Gap Thermal Hydraulics

This section describes the major separate-effects facilities on the thermal hydraulics of a gap between the melt pool and the RPV-wall. The chapter considers also gap thermal hydraulics between a core catcher and the RPV-wall. The objectives are the estimation of flow characteristics and heat transfer on the gap boundaries.

4.2.5.1 CHFG experiments

4.2.5.1.1 Objectives

As part of the SONATA-IV (Simulation Of Naturally Arrested Thermal Attack In-Vessel) program at KAERI (Korea Atomic Energy Research Institute) is conducting experiments on critical heat flux (CHF) or dry-out in hemispherical narrow gaps. The objectives are to investigate the cooling mechanism and to develop an empirical correlation applicable to this geometry.

4.2.5.1.2 Facility Description

The experimental facility consists of an electric heater inside of a hemispherical copper shell, an insulated, stainless steel pressure vessel representing the lower plenum in 1/8 scale, a heat exchanger, a coolant control system and a coolant injection tank. An electrical rod heater is put inside a hemispherical copper shell, which provides the maximum average heat flux of 500 kW/m^2 at the outer surface. Five units of the pressure vessel have been manufactured to provide variable gap sizes of 0.5, 1.0, 2.0, 5.0, 10.0 mm between the copper shell and pressure vessel itself. Water and Freon R-113 have been used as cooling fluids. The liquid level is maintained in the pressure vessel to cover the copper shell completely. 66 thermocouples are embedded in the copper shell to measure temperature and local heat flux.

The facility and parameter ranges covered are summarised in Table 4.2.5.

4.2.5.1.3 Test Description

Starting from low power conditions, the power is increased stepwise after reaching quasi steady state temperature readings (15 min to more than 60 min at high power). When all temperature readings increase monotonically, the power is switched off.

4.2.5.1.4 Processes Quantified

Stationary and transient temperature fields and local heat flux were recorded by the data acquisition system. Dry-out occurs due to CCFL (Counter Current Flow Limit) at the upper part of the gap rather due to CHF.

4.2.5.2 BENSON test rig

4.2.5.2.1 Objectives

The objectives of the test series, performed by Siemens (KWU) and sponsored by the German Ministry of Education, Science, Research and Technology (BMBF), were to estimate the limits of heat removal by gap cooling at relevant system parameters, similar to those in TMI-2.

4.2.5.2.2 Facility Description

The test section, installed in the BENSON test rig, is mainly constituted by an electrically-heated spherical section, that serves as a mock-up of the core melt surrounded by a crust under the same geometrical conditions as in TMI-2. The mock-up of the pressure vessel is located below the heated section with a defined gap. Water was used as the coolant. The liquid level was variable from 0.5 m up to a value which corresponds to 10 K sub-cooling. 60 thermocouples are embedded in the heated section and 18 in the cooled section.

The facility and parameter ranges covered are summarised in Table 4.2.5.

4.2.5.2.3 Test Description

In order to determine the maximum possible heat removal rate, the power is gradually increased, with the remaining parameters held constant. If a boiling crisis occurs, detected by sudden increase of local temperature, the power is shut down.

4.2.5.2.4 Processes Quantified

Besides the temperatures, average heat flux, and total pressure, pressure difference between the centre and the periphery of the gap are measured. Under specific conditions regular oscillations were recorded with an amplitude corresponding to the static pressure head across the gap.

4.2.5.3 CTF

4.2.5.3.1 Objectives

The objectives of these experiments, performed by Russian Research Centre - Kurchatov Institut (RRC-KI) and supported by the United States Nuclear Regulatory Commission, were to measure the maximum power which can be removed by gap cooling under different conditions.

4.2.5.3.2 Facility Description

The Coolability Test Facility (CTF) is a part of the thermo-hydraulic KC (???) test facility. It is a electrically heated vertical or inclined flat channel with variable gap width or heated length. One or two side walls can be heated. The unheated wall allows visual observations. In case of high pressure, the facility is placed into a tight vessel.

The facility and parameter ranges covered are summarised in Table 4.2.5.

4.2.5.3.3 Test Description

Starting from low power, the power was increased stepwise to establish quasi-steady-state conditions (oscillating local temperatures with constant amplitude). Continuous temperature increase at constant power indicates dry-out.

4.2.5.3.4 Processes Quantified

Numerous temperatures of wall and fluid, local void fractions, total pressure, local pressure drop at different locations and total power input were measured. The averaged heat flux was estimated.

4.2.5.4 CORCOM

4.2.5.4.1 Objectives

The objectives of the CORCOM (Cooling Of Relocated COrium Material) test series, performed by Technical University of Munich, Institute A for Thermodynamics and sponsored by the German Ministry of Education, Science, Research and Technology (BMBF), were to simulate thermal-hydraulics of debris-wall interactions comparable to those observed in TMI-2 and to estimate the dry-out of particulate debris with internal heat sources.

4.2.5.4.2 Facility Description

The particle bed consists of steel spheres and is located in a rectangular glass trough with inclined bottom to represent a part of the debris bed in the TMI-2 lower head and is housed in a high pressure vessel with a steam atmosphere. The debris bed is heated by induction. The glass trough allows visualisation of the flow pattern at the bottom and from the side. Water or Freon R134a is used as coolant. The debris could be flooded from top or from the bottom. A second devise (CORCOM 2) consists of a gap, formed by an electrically heated copper block at the top and a glass plate underneath. The height, length, and inclination of the gap were adjustable. The gap was flooded by one side and closed at the other.

The facility and parameter ranges covered are summarised in Table 4.2.5.

4.2.5.4.3 Test Description

Steady-state experiments started at low power with stepwise increased power after reaching stationary conditions to perform the measurements. In these experiments total dry-out was never observed. In CORCOM 1 transient experiments were performed too. They started with a preheated debris bed with temperatures higher than the Leidenfrost temperature.

4.2.5.4.4 Processes Quantified

Measurements were made of local temperatures and local void fraction in the debris bed, and of the total electric power. Derived values are heat flux and penetration velocity. In CORCOM 2 the local temperatures, local heat fluxes and local void fraction in the gap were measured. In both cases viual observations were possible with high speed camera.

4.2.6 Ex-vessel Thermal Hydraulics

This section describes the major separate-effects facilities on the thermal hydraulics of RPV ex-vessel cooling by flooding of the reactor cavity. The objectives are the estimation of flow characteristics and heat transfer on the outer RPV wall.

4.2.6.1 SULTAN

4.2.6.1.1 Objectives

The purpose of SULTAN, supported by CEA, EdF and Framatome, is to enlarge the data base for critical heat flux (CHF) for conditions typical for ex-vessel cooling and for the modelling and verification of large 3D two phase flow circuits in natural convection.

4.2.6.1.2 Facility Description

The SULTAN facility was designed as a full-scale analytical forced convection experiment , on a wide range of parameters as mass velocity, pressure, inlet sub-cooling and heat flux. It consists of a highly instrumented vertical or inclined rectangular channel with variable gap width. One (top) side is an electrically heated flat plate (1.5 mm thick).

The facility and parameter ranges covered are summarised in Table 4.2.6.

4.2.6.1.3 Test Description

Starting from a high mass velocity with constant conditions for the other parameters, the mass velocity is gradually decreased to the point where the limit of boiling crisis is obtained, which is indicated by a sharp increase of the temperature of the heated plate. With stationary tests spacial local characteristics of the two phase flow are measured at 25 positions.

4.2.6.1.4 Processes Quantified

Measured are wall and fluid temperatures, absolute and differential pressure, local void fraction and total electrical power. Windows allow the visualisation of the flow with video and high speed films.

4.2.6.2 SBLB facility

4.2.6.2.1 Objectives

The objectives of the test series in the SBLB (Subscale Boundary Layer Boiling) facility, performed by Pennsylvania University and sponsored by the United States Nuclear Regulatory Commission, were to observe the vapour dynamic and the seat venting process in the hemispherical and annular channel as well as to determine the limits of heat removal by ex-vessel cooling.

4.2.6.2.2 Facility Description

The experimental apparatus consists of a water tank with a condensers unit and the test vessel, a 1/15 scaled RPV mock-up, with a thermal insulation structure. The test vessel consists of a hemispherical and a cylindrical part. The thermal insulation consists of a lower octagonal and an upper cylindrical part with one opening on the bottom for water ingress and six openings in the upper cylindrical part to simulate steam venting. The gap between hemisphere and insulation could be varied by changing the height of the insulation. The hemisphere of the test vessel was electrically heated, uniformly or with peaked heat flux distribution. Windows in the water tank allowed visual observations.

The facility and parameter ranges covered are summarised in Table 4.2.6.

4.2.6.2.3 Test Description

After the preheating of the facility, the power is stepwise increased with measurements taken during stationary conditions. If local boiling crisis occurs, detected by sudden increase of local temperature, the power is shut down to protect the facility.

4.2.6.2.4 Processes Quantified

Besides the temperatures, average and local heat flux are measured. Visual observation allows the characterisation of the flow pattern.

4.2.6.3 CYBL

4.2.6.3.1 Objectives

The objectives of the experiments in the CYBL (Cylindrical BoiLing) facility, performed by Sandia National Laboratory, USA and supported by the United States Nuclear Regulatory Commission, were the testing of flooded cavity design.

4.2.6.3.2 Facility Description

The experimental apparatus consists of the test vessel, a 1/1 scaled RPV mock-up, inside a large cylindrical water tank with condenser unit. The test vessel consists of a torispherical and a cylindrical part. The torispherical part of the test vessel was heated, uniformly or with peaked heat flux distribution, by electrical resistance heater or by radiation. Windows in the water tank allowed visual observations.

The facility and parameter ranges covered are summarised in Table 4.2.6.

4.2.6.3.3 Test Description

After pre-heating of the facility, the power was stepwise increased with measurements taken during steady state or quasi steady state conditions.

4.2.6.3.4 Processes Quantified

Besides the temperatures, average and local heat flux are measured. Visual observation allows the characterisation of the flow pattern.

4.2.6.4 ULPU

4.2.6.4.1 Objectives

The objectives of the experiments in the ULPU facility, performed by University of California, Santa Barbara, USA and supported by IVO International Ltd. (today Fortum Engineering Ltd), were the testing of two phase natural convection flow heat transfer behavior of external RPV cooling for the Loviisa NPP. Potential flow instabilities and their possible impact to critical heat flux at the vertical section of the RPV were of particular interest.

4.2.6.4.2 Facility Description

The test section is a full height 1/215 scaled mock-up of the annulus between RPV and reactor cavity including a down-comer for closed circulation loop. The lower part of the riser section, which simulates the lower part of the annulus, is a vertical flow channel with a square cross section. The main heater is attached to the side wall of the section, and it is capable of providing heat fluxes upto 1200 kW/m^2. Above the main heater, the riser continues as a circular vertical channel with heating elements within the channel. Flow restrictions are located at its upper end. A condenser unit is connected to the upper part of the loop to simulate the heat sink by the containment. Most of the flow loop is made of glass, which allows direct visualisation of the flow.

The facility and parameter ranges covered are summarised in Table 4.2.6.

4.2.6.4.3 Test Description

The heating power is stepwise increased, or the exit flow area at the upper end of the riser section decreased, with measurements taken during steady-state conditions, up to the power level or down to the exit flow area when the two-phase natural convection loop breaks down due to the swell level dropping below the exit of the riser section.

4.2.6.4.4 Processes Quantified

Besides temperatures, the power input, mass flow rate, void fractions in the riser section and pressure drop at the exit restriction were measured. The two phase flow patterns were recorded by video.

4.2.7 Gap Formation

This section describes the major facilities exploring the gap formation between the melt pool and the RPV-wall. The experiments involve melt simulation and RPV wall deformation up to rupture for adequate simulation of gap formation and could be also classified as integral or multi effects test facility. They are listed under separate-effects test due to their exploratory character and premature inforamtion.

4.2.7.1 FOREVER

4.2.7.1.1 Objectives

The objectives of the FOREVER (Failure Of REactor Vessel Retention) experiments are to obtain data and to develop validated models on the melt coolability process inside the vessel in the presence of water, in particular on the efficiency of the postulated gap cooling to preclude vessel failure, as well as on the lower head failure due to the creep process in the absence of water inside and/or outside the lower head. The first test series is focused on physical mechanisms which govern the debris-vessel gap formation and vessel creeping. The second series is devoted to gap cooling phenomenology, the third on effects of penetrations on vessel deformation.

4.2.7.1.2 Facility Description

The experimental facility consists of 1/10 scale carbon steel vessel and a internally heated simulate for the corium melt. Auxiliary systems are designed to provide high over-pressure and to allow depressurisation. As simulant material for the corium melt up to 20 dm^3 of binary-oxidic melts with 100-300 K superheat are employed. Its temperature difference between liquidus and solidus is about 50 K, the liquidus temperature ranges from 1300 to 1400 K. The melt is prepared in a Si-C crucible of a 50 kW induction furnace. and then poured into the test section.

The facility and parameter ranges covered are summarised in Table 4.2.7.

4.2.7.1.3 Test Description

The pressure vessel is heated to a designed temperature, then the melt, preheated in the furnace, is poured into the test section and further heated by internal heaters. Then the specified over-pressurisztion is supplied with inert gas.

4.2.7.1.4 Processes Quantified

Thermocouples are used to measure the temperatures of the melt or debris at different locations in the hemispherical pool and to determine the thermal response of the pressure vessel. The vessel deformation and creep are measured by position transducers. Up to 20 linear displacement transducers (LDT) are mounted at five latitude locations of the hemispherical lower head and used to measure the creep behaviour of the three dimensional vessel. Typically three LDTs are deployed at each level. Two of these measure local (vertical / horizontal) displacements, the third an integral displacement.

4.2.7.2 LAVA

4.2.7.2.1 Objectives

As the first phase of the SONATA-IV (Simulation of Naturally Arrested Thermal Attack In Vessel) program, the LAVA (Lower-plenum Arrested Vessel Attack) experiments are being carried out at KAERI. The objectives are to corroborate a gap formation between the debris and the lower head vessel wall and to evaluate the effect of the gap on the cooling characteristics of the lower head vessel using a simulant melt.

4.2.7.2.2 Facility Description

The experiments are performed inside the protection vessel with an inner diameter of 2.4 m and a height of 4.8 m. The experimental facility consists of a thermite melt generator, a melt holder or a melt separator, a test section of the 1/8 linear scale mock-up of the typical reactor vessel lower plenum and a gas supply system for internally pressurizing the LAVA facility. Mixed Al_2O_3/Fe thermite melt or separated Al_2O_3 melt is used as a corium simulant. The test vessel made of commercial carbon steel(SA516-Gr.70) is composed of hemispherical and cylindrical parts with an inner diameter of 0.5 m and thickness of 0.025 m. Temperatures of the thermite melt and the lower head vessel wall are measured by W/Re and K-type thermocouples, respectively. The downward deflection of the lower head vessel is measured by a linear displacement measurement device with the measuring error bound of ± 0.002 mm. The post-test examinations are conducted to check on the existence and the spatial distribution of the gap using an ultrasonic pulse echo method.

The facility and parameter ranges covered are summarised in Table 4.2.7.

4.2.7.2.3 Test Description

The effects of the several major factors having an influence on the coolability of molten material accompanying deformation of the lower head vessel are experimentally evaluated. The internal pressure load on the lower head vessel, the material composition of the corium simulant and the initial conditions of water are selected as the principal experimental parameters. T he experiments are performed under an elevated pressure of about 1.7 MPa considering the low-pressure sequences of the reactor accidents and also the suppression of a conceivable steam explosion. To achieve the necessary internal pressure load onto the lower head vessel wall, the pressure in a lower chamber below the lower head vessel is maintained at 0.1 MPa using a connection path to the atmosphere outside the LAVA vessel depending on the test conditions. The mass of the corium simulant is fixed by 30 kg of Al_2O_3 or 40 kg of Al_2O_3/Fe melt. The initial sub-cooling of water varies from 5.5 K to 55 K.

4.2.7.2.4 Processes Quantified

The results of the gap thickness measurements using the ultrasonic echo pulse method and visual observation for the vessel specimen cut along a centre line address that a gap formed at the interface between the debris crust and the lower head vessel wall with the order of mm. The gap affects the initial heat up of the lower head vessel but has no significant influence during the cool down period in the mixed Al_2O_3/Fe melt tests. On the other hand, the enhanced cooling capacity through the gap is highly distinguished in the pure Al_2O_3 melt tests. That is, steam ventilation via the pores inside the melt layer and as a result additional water ingression into the gap act a key role of a effective cooldown of the lower head vessel in the pure Al_2O_3 melt tests.

Besides temperatures, local heat flux and total power input, mass flow rate and pressure drop were measured. The maximum heat flux (CHF) along the heated surface have been derived for different power distributions and a water level height of 1.2 - 1.8 m above the 0° position of the heater elements.

4.2.8 Fuel Coolant Interaction

This section describes the major separate-effect facilities on the various aspects of fuel-coolant interactions, including premixing and energetics of explosions. The recently completed FARO and KROTOS programmes, for which much detailed information is available, have been included above in the Integral sections 4.1.17 and 4.1.18 respectively, for the reasons indicated there. FCI experimental programmes, including FARO and KROTOS, have recently been summarised in the review of Park et al. [4.4] to which reference could be made if further details are required.

4.2.8.1 WFCI

4.2.8.1.1 Objectives

Nine test series have been performed on University of Wisconsin [4.4] between 1994 and 1999 to obtain well-characterized data for the explosion propagation / escalation phases using simulant fuel compositions and to investigate the effect of particular initial and boundary conditions on the explosion energetics such as mass, temperature, and composition of simulant material, mass; sub-cooling, and surface tension of coolant, as well as effects of triggering and system constraint. The research programme was sponsored by USNRC.

4.2.8.1.2 Test Facility

The facility consists of a furnace made of a ceramic crucible housed in ceramic fibre insulator. The heater was embedded in the insulator. A boron nitride crucible was used for the tests with iron oxide. A transfer vessel was positioned below the furnace to deliver the melt to the test chamber. The test chamber consists of a funnel to collect the displaced water, the slide gate, and the test tube system with a volume of 8.7 dm^3, the trigger device at the bottom of the test tube, and an expansion tube connected with the top of the test tube. A larger test tube with a volume of 34.3 dm^3 was used for the last two experiments. Furnace capability was up to 1500 K for the tin and 2100 K for the iron oxide test series.

4.2.8.1.3 Test Description

Eight test series have been performed with molten tin and one with molten iron oxide. The simulant material was melted and the test loop heated up by the water loop. The molten material was delivered into the transfer vessel and from this into the test tube. After the melt pouring and fuel-coolant mixing the slide gate was closed to isolate the test tube and expansion tube from the funnel. Then the trigger device was initiated if wanted. Once an explosion occurred, the membrane to the expansion tube burst and the dislocation of the piston in conjunction with pressure build-up allowed estimation of the mechanical energy release.

The facility and parameter ranges covered are summarised in Table 4.2.8.

4.2.8.1.4 Processes Quantified

Besides the melt and water temperatures, the piston dislocation and pressure at different positions were recorded. Further thermocouples were used to detect the melt pouring and mixing. A device allowed measurement of the level swell in the funnel above the test section during the fuel-coolant mixing phase.

4.2.8.2 MAGICO-2000

4.2.8.2.1 Objectives

To obtain detailed experimental data on pre-mixing under well-specified conditions so as to provide unambiguous testing of the multi-field aspects of the PM-ALPHA code.

4.2.8.2.2 Test Facility

The facility consists of a furnace made of a perforated graphite block that contains the particles to be released and an open water pool underneath. The furnace can be used for temperatures up to 2300 K. Particulate masses up to ~10 kg can be handled. Both axisymmetric and planar pool geometries can be accommodated. Flash X-ray instrumentation is available.

4.2.8.2.3 Test Description

Particles are allowed to fall, as uniform clouds, into the water pools of various geometries and at different temperatures, while the whole process is visualized both by videocameras as well as by flash X-ray techniques. In this test series cold and hot ZrO_2 particles with 2 and 7 mm diameter have been used.

The facility and parameter ranges covered are summarised in Table 4.2.8.

4.2.8.2.4 Processes Quantified

All visual aspects of the interactions are quantified from the videos and include cloud penetration rates, pool level swell, shape of the interaction zone, etc. Quantitative X-ray radiography is employed to determine the internal features of the interaction zone, such as void and particle volume fraction distributions.

4.2.8.3 SIGMA-2000

4.2.8.3.1 Objectives

The aims are to obtain detailed experimental data on microinteractions (and pressure wave dynamics in two-phase media) under propagation-prototypic local conditions of energetic steam explosions for the validation of the ESPROSE code.

4.2.8.3.2 Test Facility

The facility embodies a hydrodynamic shocktube, equipped with an internal (miniature) melt-generating device to produce and release single drops of melts at desired temperatures up to 2000 K. In this test series single superheated Tin and Iron droplets (mass ~ 1 g) have been investigated under shock waves with 6.8, 20.4 and 27.2 MPa.

The facility and parameter ranges covered are summarized in Table 4.2.8.

4.2.8.3.3 Test Description

The procedure is to generate a melt drop and hit it with a high amplitude, sustained, shock wave, synchronized with the arrival of the drop at the window area. Photographic, high-speed video and flash X-ray equipment are used to record the phenomena observed.

4.2.8.3.4 Processes Quantified

The tests quantify the evolution of the volume and shape of the mixing region and the mass distribution of the fragmented melt within fragmented debris sizes.

References

[4.1] Haste T J, Adroguer B, Gauntt R O, Martinez J A, Ott L J, Sugimoto J and Trambauer K, "In-Vessel Core Degradation Code Validation Matrix", NEA/CSNI/R(95)21, OCDE/GD(96)14, Paris, 1996.

[4.2] Parsons P D, Hindle E D and Mann C A, "The Deformation, Oxidation and Embrittlement of PWR Fuel Cladding in a Loss-of-Coolant Accident", ND-R-1351(S), CSNI Report 129, September 1986.

[4.3] Kinnersly S R, Lillington J N, Porracchia A, Soda K, Trambauer K, Hofmann P, Waarenpera Y, Bari R, Hunt C And Martinez J, "In-Vessel Core Degradation in LWR Severe Accidents: A State of the Art Report to CSNI, January 1991", NEA/CSNI/R(91)12, November 1991.

[4.4] Park H-S, Chapman R and Corradini M L, "Vapor Explosions in a One-Dimensional Geometry with Simulant Melts", NUREG/CR-6623, October 1999.

Empty page

Feature	Description	Comments
Location of Facility/ Objectives	KfK Karlsruhe, Germany	Initial investigation of early phase melt progression, including effect of PWR absorber materials.
Number of Tests	23	12 basic single rod tests (ESSI series); 3 additional single rod tests to study the effect of hydrogen (ESA series), 2 3x3 bundle tests with no absorber (ESBU series), 6 3x3 bundle tests including PWR absorber (ABS series).
Duration of Test Series	1982 - 1986	-
Number of Rods/ Heated Length (m)	1 and 9 / 0.4	The rod array is surrounded by an insulating shroud with a Zircaloy liner, itself surrounded by an insulated wall. For the scoping tests ESSI-1, 2 and 3 the heated length was 0.25m.
Heating Method	Electrical	Tungsten resistance heaters used in each fuel rod simulator.
Control Materials	Ag-In-Cd	5 tests (ABS series) with central control rod; 4 tests with a Zircaloy guide tube, 1 test with a stainless steel guide tube.
Spacer Grids	Inconel	2 grids in each bundle test.
Fuel Irradiation (GWD/tU)	None	Depleted UO_2 fuel used.
Fluid Input	Variable steam flow	Some single rod tests explored the effect of different fluid compositions (argon, steam, oxygen). Later bundle tests normally included argon with the steam flow.

Table 4.1.1.1 : NIELS Test Series - General Information

Feature	Description	Comments
System Pressure (MPa)	0.1	-
Fuel Rod Internal Fill Pressure (MPa)	-	-
Initial Heatup Rate (K/s)	0.3 - 4.0	-
Maximum Temperature (K)	<2523	Absorber test with stepwise reduced maximum temperature from 2320 to 1440K.
Final Cooling	slow	-
Notes	-	-

Table 4.1.1.1 : NIELS Test Series - General Information

Test	Number of Rods (Fuel/ Abs)	Spacer Grids (no.)	Fuel Irradiation (GWD/tU)	Fluid	Pressure (MPa) (System/Rod)	Initial Heat-up (K/s)	Max. Tempe-rature (K)	Transient Duration (s)*	Test Termin-ation	Special Condi-tion	Date of Test
ESSI 1	1	-	None	Ar, Stm	0.1	(0.8)	2523	-/800/30/0	S	(a)	1982
ESSI 2	1	-	None	Stm	0.1	4.0	2373	-/380/120/0	S	-	1982
ESSI 3	1	-	None	Stm	0.1	0.5	2073	-/220/0#/0	S	-	1982
ESSI 4	1	-	None	Stm	0.1	0.3	2323	3470/2270/ 1090/0	S	-	1982
ESSI 4/5	1	-	None	Stm, Ar, Vac	0.1	0.5	2243	2480/1390/ 260/0	S	(b)	1982
ESSI 5	1	-	None	Stm	0.1	0.8	2173	1120/770/ 340/0	S	-	1982
ESSI 6	1	-	None	Stm	0.1	1.1	2373	990/560/ 350/0	S	-	1982

Table 4.1.1.2 : NIELS Test Series - Main Experimental Conditions

Key

AIC : Silver Indium Cadmium B_4C : Boron Carbide Incl : Inconel Zry : Zircaloy SS : Stainless Steel

Ar : Argon Stm : Steam Wtr : Water Vac : Vacuum Y : Yes

S : Slow (S < 2 K/s) R : Rapid Q : Quench N : No

* : Transient Duration is total time spent over 1100/1500/2100/2800K respectively, up to when there is no further significant change in core state (here taken as 2100K on final cooldown)

\# : Peak at or close to 2100K used as endtime

(a) : Heat in Ar to 1973K, then steam injection (b) : Successive heat-ups in Ar, Stm, Vac

(c) : Reduced insulation (d) : Reduced insulation, reduced convective cooling

Test	Number of Rods (Fuel/ Abs)	Spacer Grids (no.)	Fuel Irradiation (GWD/tU)	Fluid	Pressure (MPa) (System/Rod)	Initial Heat-up (K/s)	Max. Tempe-rature (K)	Transient Duration (s)*	Test Termin-ation	Special Condi-tion	Date of Test
ESSI 7	1	-	None	Stm	0.1	2.3	2198	630/460/ 220/0	S	-	1982
ESSI 8	1	-	None	Stm	0.1	3.6	2243	600/530/ 440/0	S	-	1982
ESSI 9	1	-	None	Stm	0.1	1.1	2223	-/600/370/0	S	(c)	1982
ESSI 10	1	-	None	Stm	0.1	1.1	2298	530/190/ 120/0	S	(d)	1982
ESSI 11	1	-	None	Stm	0.1	0.8	2173	640/240/ 150/0	S	(d)	1982
ESA 1	1	-	None	Ar, O_2	0.1	0.7	2173	480/100/ 30/0	S	-	1983
ESA 2	1	-	None	Ar, Stm	0.1	0.8	2073	1240/720/ 0/0#	S	-	1983
ESA 3	1	-	None	Ar	0.1	-	-	-	S	-	1984

Table 4.1.1.2 : NIELS Test Series - Main Experimental Conditions

Key

AIC : Silver Indium Cadmium B_4C : Boron Carbide Incl : Inconel Zry : Zircaloy SS : Stainless Steel

Ar : Argon Stm : Steam Wtr : Water Vac : Vacuum Y : Yes

S : Slow (S < 2 K/s) R : Rapid Q : Quench N : No

* : Transient Duration is total time spent over 1100/1500/2100/2800K respectively, up to when there is no further significant change in core state (here taken as 2100K on final cooldown)

\# : Peak at or close to 2100K used as endtime

(a) : Heat in Ar to 1973K, then steam injection (b) : Successive heat-ups in Ar, Stm, Vac

(c) : Reduced insulation (d) : Reduced insulation, reduced convective cooling

Test	Number of Rods (Fuel/ Abs)	Spacer Grids (no.)	Fuel Irradiation (GWD/tU)	Fluid	Pressure (MPa) (System/Rod)	Initial Heat -up (K/s)	Max. Tempe-rature (K)	Transient Duration (s)*	Test Termin -ation	Special Condi-tion	Date of Test
ESBU 1	9	Incl(2)	None	Ar, Stm	0.1	2.0	2523	1200/940/ 100/0	S	-	1983
ESBU 2A	9	Incl(2)	None	Ar, Stm	0.1	0.5	2448	3600/1660/ 820/0	S	-	1984
ABS 1	8/ 1(AIC)	Incl(2)	None	Ar, Stm	0.1	0.5	2320	-	S	-	1984
ABS 2	8/ 1(AIC)	Incl(2)	None	Ar, Stm	0.1	0.5	2120	-	S	-	1984
ABS 3	8/ 1(AIC)	Incl(2)	None	Ar, Stm	0.1	0.5	1670	-	S	-	1984
ABS 4	8/ 1(AIC)	Incl(2)	None	Ar, Stm	0.1	0.5	1440	-	S	-	1984
ABS 6	8/ 1(AIC)	Incl(2)	None	Ar, Stm	0.1	0.5	1670	-	S	SS-guide T	1985

Table 4.1.1.2 : NIELS Test Series - Main Experimental Conditions

Key

AIC : Silver Indium Cadmium B_4C : Boron Carbide Incl : Inconel Zry : Zircaloy SS : Stainless Steel

Ar : Argon Stm : Steam Wtr : Water Vac : Vacuum Y : Yes

S : Slow (S < 2 K/s) R : Rapid Q : Quench N : No

* : Transient Duration is total time spent over 1100/1500/2100/2800K respectively, up to when there is no further significant change in core state (here taken as 2100K on final cooldown)

\# : Peak at or close to 2100K used as endtime

(a) : Heat in Ar to 1973K, then steam injection (b) : Successive heat-ups in Ar, Stm, Vac

(c) : Reduced insulation (d) : Reduced insulation, reduced convective cooling

Test	Thermal Response	Clad Ballo-oning	Clad Oxida tion, H_2 Release	Material Interactions and Melting			Partic-ulate Debris	Bloc-kage	Late Phase		FP and Aerosol Release
				Abso-rber	Spacer Grid	Fuel			Crust	Melt Pool	
ESSI 1	Y*	N	L	N	N	D	N	N	N	N	N
ESSI 2	Y*	N	I	N	N	D	N	N	N	N	N
ESSI 3	Y*	N	H	N	N	N	N	N	N	N	N
ESSI 4	Y*	N	H*	N	N	N	N	N	N	N	N
ESSI 4/5	Y*	N	H*	N	N	N	N	N	N	N	N
ESSI 5	Y*	N	I	N	N	(D)	N	N	N	N	N
ESSI 6	Y*	N	I	N	N	D	N	N	N	N	N
ESSI 7	Y*	N	L	N	N	D*	N	N	N	N	N
ESSI 8	Y*	N	L	N	N	D*	N	N	N	N	N
ESSI 9	Y*	N	I	N	N	D	N	N	N	N	N
ESSI 10	Y*	N	I	N	N	D	N	N	N	N	N
ESSI 11	Y*	N	L	N	N	D	N	N	N	N	N

Table 4.1.1.3 : Main Phenomena Exhibited in the NIELS Experiments

Key

* : Main phenomena - : Not Measured U : Unknown Y : Yes N : No or None

AIC : Silver Indium Cadmium B_4C : Boron Carbide Incl : Inconel Zry : Zircaloy

S,D,C : Solid/solid interaction with Zry, Dissolution by Zry, Ceramic melt, for fuel

L,I,H : Low, Intermediate, High (0-33-66-100% for blockage, with 0% the initial bundle state) V,LV : Volatile (Cs,I_2), Low Volatile (Ba,Sr), for FP Release

Met/Cer/Rem : Metallic, Ceramic, Remelt for crust Frmn/Slmp : Formation, Slump for melt pool

Test	Thermal Response	Clad Ballo-oning	Clad Oxida tion, H_2 Release	Material Interactions and Melting			Partic-ulate Debris	Bloc-kage	Late Phase		FP and Aerosol Release
				Abso-rber	Spacer Grid	Fuel			Crust	Melt Pool	
ESA 1	Y*	N	Y(Ox) N(H_2)	N	N	D*	N	N	N	N	N
ESA 2	Y*	N	Y	N	N	N	N	N	N	N	N
ESA 3	Y*	N	N	N	N		N	N	N	N	N
ESBU 1	Y*	N	I	N	N	D*	N	H?	N	N	N
ESBU 2A	Y*	N	H	N	N	D	N	H	N	N	N
ABS 1	Y	N	H	AIC*	Incl	D*	N	H	N	N	N
ABS 2	Y	N	H	AIC*	Incl	D	N	I	N	N	N
ABS 3	Y	N	I	AIC*	Incl	N	N	L	N	N	N
ABS 4	Y	N	L	N	N	N	N	N	N	N	N
ABS 6	Y	N	I	AIC*	Incl	N	N	N	N	N	N

Table 4.1.1.3 : Main Phenomena Exhibited in the NIELS Experiments

Key

* : Main phenomena - : Not Measured U : Unknown Y : Yes N : No or None

AIC : Silver Indium Cadmium B_4C : Boron Carbide Incl : Inconel Zry : Zircaloy

S,D,C : Solid/solid interaction with Zry, Dissolution by Zry, Ceramic melt, for fuel

L,I,H : Low, Intermediate, High (0-33-66-100% for blockage, with 0% the initial bundle state) V,LV : Volatile (Cs,I_2), Low Volatile (Ba,Sr), for FP Release

Met/Cer/Rem : Metallic, Ceramic, Remelt for crust Frmn/Slmp : Formation, Slump for melt pool

Feature	Description	Comments
Location of Facility/ Objectives	FZ Karlsruhe, Germany	Investigation of early phase melt progression in PWR , BWR and VVER for unrecovered and quenched transients.
Number of Tests	19	Also 2 scoping tests (B and C) with alumina pellets.
Duration of Test Series	06Aug87 - 21Apr93	Post-test examinations and reporting continued to 1998.
Number of Rods/ Heated Length (m)	25 to 59 / 1.0 (PWR/BWR); 19 / 1.0 (VVER)	The rod array is surrounded by an insulating shroud with a Zircaloy liner, itself surrounded by a permanently-installed high temperature shield. PWR and BWR tests use a square lattice, VVER tests a hexagonal lattice.
Heating Method	Electrical	Tungsten resistance heaters are used. Heated rods alternate with unheated rods on a square lattice for PWR/BWR tests. For VVER tests the central rod and outer ring of 12 rods are heated, the middle ring of 6 rods is unheated.
Control Materials	Ag-In-Cd / B_4C	PWR control rod guide tubes were of Zircaloy.
Spacer Grids	Inconel and Zircaloy (PWR/BWR); stainless steel (VVER)	3 grids used in each test, either 3 Zircaloy, or top & bottom grid Zircaloy with central grid Inconel for PWR/BWR tests, or 3 stainless steel for VVER tests.
Fuel Irradiation (GWD/tU)	None	Depleted UO_2 fuel used.
Fluid Input	Variable steam flow - trace to 12 g/s	Argon used in addition to the steam flow (typical mass ratio 4:3 in the heat-up phase). In most tests, there was coolant bypass, owing largely to the presence of viewing windows.

Table 4.1.2.1 : CORA Test Series - General Information

Feature	Description	Comments
System Pressure (MPa)	0.2 to 1.0	-
Fuel Rod Internal Fill Pressure (MPa)	0.2 to 6.0	Internal pressure insensitive to temperature increase, due to presence of large external cold volumes in pressure transducers.
Initial Heatup Rate (K/s)	0.2 to 1.0	-
Maximum Temperature (K)	<2300 to 2500	-
Final Cooling	Variable - slow, or water quench	Three tests with water quench, remainder with slow cooldown in argon.
Notes	ISP	CORA-13 (PWR) was used for OECD/CSNI ISP-31; CORA-W2 (VVER) was used for ISP-36. The VVER tests used materials of VVER-1000 type, e.g. cladding and shroud liner were of Zr1%Nb alloy.

Table 4.1.2.1 : CORA Test Series - General Information

Test	Number of Rods (Fuel/ Abs)	Spacer Grids (no.)	Fuel Irradiation (GWD/tU)	Fluid	Pressure (MPa) (System/ Rod)	Initial Heat-up (K/s)	Max. Tempe-rature (K)	Transient Duration (s)*	Test Termin -ation	Special Condi-tion	Date of Test
2	25	Incl(1) Zry(2)	None	Ar, Stm	0.2/0.7	1.0	2300	950/700/ 400/0	S(Ar)	Bypass	06Aug87
3	25	Incl(1) Zry(2)	None	Ar, Stm	0.2/0.5	1.0	2700	1750/1400/ 1000/0	S(Ar)	Bypass	03Dec87
5	24/ 1(AIC)	Incl(1) Zry(2)	None	Ar, Stm	0.2/0.4	1.0	2300	1350/950/ 800/0	S(Ar)	Bypass	26Feb88
12	23/ 2(AIC)	Zry(3)	None	Ar, Stm	0.2/0.3	1.0	2300	1500/1150/ 600/0	Q(Wtr)	Bypass	09Jun88
16	18/ blade	Zry(3)	None	Ar, Stm	0.2/0.6	1.0	2300	1550/1100/ 800/0	S(Ar)	Bypass	24Nov88
15	23/ 2(AIC)	Incl(1) Zry(2)	None	Ar, Stm	0.2/6.0	1.0	2300	1200/950/ 450/0	S(Ar)	Bypass	02Mar89
17	18/ blade	Zry(3)	None	Ar, Stm	0.2/0.5	1.0	2300	1400/1000/ 750/0	Q(Wtr)	Bypass	29Jun89

Table 4.1.2.2 : CORA Test Series - Main Experimental Conditions

Key

AIC	: Silver Indium Cadmium	B_4C	: Boron Carbide	Incl	: Inconel	Zry	: Zircaloy	SS	: Stainless Steel
Ar	: Argon	Stm	: Steam	Wtr	: Water	Y	: Yes	hex	: hexagonal grid
S	: Slow (S < 2 K/s)	R	: Rapid	Q	: Quench	N	: No		(otherwise square)

blade : BWR control blade simulator consisting of Zircaloy channel box walls and a control blade simulator (stainless steel plus typically 9 B_4C-loaded rodlets)

* : Transient Duration is total time spent over 1100/1500/2100/2800K respectively, up to when there is no further significant change in core state (here taken as 2100K on final cooldown)

Test	Number of Rods (Fuel/ Abs)	Spacer Grids (no.)	Fuel Irradiation (GWD/tU)	Fluid	Pressure (MPa) (System/ Rod)	Initial Heat-up (K/s)	Max. Tempe-rature (K)	Transient Duration (s)*	Test Termin -ation	Special Condi-tion	Date of Test
9	23/ 2(AIC)	Incl(1) Zry(2)	None	Ar, Stm	1.0/0.2	1.0	2300	1700/650/ 450/0	S(Ar)	Bypass	09Nov89
7	52/ 5(AIC)	Incl(1) Zry(2)	None	Ar, Stm	0.2/0.5	1.0	<2300	1040/650/ 450/0	S(Ar)	Bypass	22Feb90
18	48/ blade	Zry(3)	None	Ar, Stm	0.2/0.6	1.0	<2300	800/400/ 300/0	S(Ar)	Bypass	21Jun90
13	23/ 2(AIC)	Incl(1) Zry(2)	None	Ar, Stm	0.2/0.4	1.0	2500	1400/1000/ 800/0	Q(Wtr)	Bypass	15Nov90
29	23/ 2(AIC)	Incl(1) Zry(2)	None	Ar, Stm	0.2/0.4	1.0	2300	1600/1150/ 1050/0	S(Ar)	Bypass, Pre-ox ≤ 12 µm	11Apr91
31	18/ blade	Zry(3)	None	Ar, Stm	0.2/0.4	0.3	2300	4600/3850/ 3000/0	S(Ar)	Bypass	25Jul91

Table 4.1.2.2 : CORA Test Series - Main Experimental Conditions

Key

AIC	: Silver Indium Cadmium	B_4C	: Boron Carbide	Incl	: Inconel	Zry	: Zircaloy	SS	: Stainless Steel
Ar	: Argon	Stm	: Steam	Wtr	: Water	Y	: Yes	hex	: hexagonal grid
S	: Slow (S < 2 K/s)	R	: Rapid	Q	: Quench	N	: No		(otherwise square)

blade : BWR control blade simulator consisting of Zircaloy channel box walls and a control blade simulator (stainless steel plus typically 9 B_4C-loaded rodlets)

* : Transient Duration is total time spent over 1100/1500/2100/2800K respectively, up to when there is no further significant change in core state (here taken as 2100K on final cooldown)

Test	Number of Rods (Fuel/ Abs)	Spacer Grids (no.)	Fuel Irradiation (GWD/tU)	Fluid	Pressure (MPa) (System/ Rod)	Initial Heat-up (K/s)	Max. Tempe-rature (K)	Transient Duration (s)*	Test Termin -ation	Special Condi-tion	Date of Test
30	23/ 2(AIC)	Incl(1) Zry(2)	None	Ar, Stm	0.2/0.4	0.2	2300	6800/5400/ 1350/0	S(Ar)	Bypass	30Oct91
28	18/ blade	Zry(3)	None	Ar, Stm	0.2/0.4	1.0	2300	1350/900/ 590/0	S(Ar)	Bypass, Pre-ox ≤ 40 µm	25Feb92
10	23/ 2(AIC)	Incl(1) Zry(2)	None	Ar, Stm	0.2/0.4	1.0	2300	1600/1250/ 950/0	S(Ar)	Bypass	16Jul92
33	18/ blade	Zry(3)	None	Ar, Stm (trace)	0.2/0.5	0.3	2300	4800/4000/ 2550/0	S(Ar)	Bypass	01Oct92
W1	19	SS(3) hex	None	Ar, Stm	0.2/0.35	1.0	2300	2400/1250/ 500/0	S(Ar)	Bypass	18Feb93
W2	18/ 1(B_4C)	SS(3) hex	None	Ar, Stm	0.2/0.3	1.0	2300	2150/1050/ 550/0	S(Ar)	Bypass	21Apr93

Table 4.1.2.2 : CORA Test Series - Main Experimental Conditions

Key

AIC	: Silver Indium Cadmium	B_4C	: Boron Carbide	Incl	: Inconel	Zry	: Zircaloy	SS	: Stainless Steel
Ar	: Argon	Stm	: Steam	Wtr	: Water	Y	: Yes	hex	: hexagonal grid
S	: Slow (S < 2 K/s)	R	: Rapid	Q	: Quench	N	: No		(otherwise square)

blade : BWR control blade simulator consisting of Zircaloy channel box walls and a control blade simulator (stainless steel plus typically 9 B_4C-loaded rodlets)

* : Transient Duration is total time spent over 1100/1500/2100/2800K respectively, up to when there is no further significant change in core state (here taken as 2100K on final cooldown)

Test	Thermal Response	Clad Ballo-oning	Clad Oxida-tion, H_2 Release	Material Interactions and Melting			Partic-ulate Debris	Bloc-kage	Late Phase		FP and Aerosol Release
				Absor-ber	Spacer Grid	Fuel			Crust	Melt Pool	
2	Y*	Y	H	-	Incl*	D*	N	I*	N	N	N
3	Y*	N	H	-	Incl*	D*	N	H*	(Y#)	(Y#)	N
5	Y*	N	H	AIC*	Incl	D*	N	I*	N	N	N
12	Y*	N	H (H in qnch*)	AIC*	Zry	D*	(Y$)	I*	N	N	N
16	Y*	(Y)	I	B_4C*	Zry	D*	N	Y*	N	N	N
15	Y*	Y*	H	AIC*	Incl	D*	N	H*	N	N	N
17	Y*	N	I (H in qnch*)	B_4C*	Zry	D*	(Y$)	Y*	N	N	N
9	Y*	N	I	AIC*	Incl	D*	N	Y*	N	N	N
7	Y*	N	I	AIC*	Incl	D*	N	Y*	N	N	N
18	Y*	N	I	B_4C*	Zry	D*	N	Y*	N	N	N

Table 4.1.2.3 : Main Phenomena Exhibited in the CORA Experiments

Key

* : Main phenomena - : Not Measured U : Unknown Y : Yes N : No or None

AIC : Silver Indium Cadmium B_4C : Boron Carbide Incl : Inconel Zry : Zircaloy SS : Stainless Steel

: Complete blockage of bundle after large-scale dissolution of fuel $: By shattering, during quench

S,D,C : Solid/solid interaction with Zry, Dissolution by Zry, Ceramic melt, for fuel

L,I,H : Low, Intermediate, High (0-33-66-100% for blockage, with 0% the initial bundle state) V,LV : Volatile (Cs,I_2), Low Volatile (Ba,Sr), for FP Release

Met/Cer/Rem : Metallic, Ceramic, Remelt for crust Frmn/Slmp : Formation, Slump for melt pool

Test	Thermal Response	Clad Ballo-oning	Clad Oxida-tion, H_2 Release	Material Interactions and Melting			Partic-ulate Debris	Bloc-kage	Late Phase		FP and Aerosol Release
				Absor-ber	Spacer Grid	Fuel			Crust	Melt Pool	
13	Y*	N	H(H in qnch*)	AIC*	Incl	D*	(Y$)	I*	N	N	N
29	Y*	N	H(incl preox)	AIC*	Incl	D*	N	I*	N	N	N
31	Y*	N	H	B_4C*	Zry	D*	N	I*	N	N	N
30	Y*	N	H	AIC*	Incl	D	N	L	N	N	N
28	Y*	N	H(incl preox*)	B_4C*	Zry	D	N	L	N	N	N
10	Y*	N	I	AIC*	Incl	D*	N	I*	N	N	N
33	Y*	(N)	L	B_4C*	Zry	D*	N	I*	N	N	N
W1	Y*	N	I	N	SS	D*	N	I*	N	N	N
W2	Y*	N	I	B_4C*	SS	D*	N	I*	N	N	N

Table 4.1.2.3 : Main Phenomena Exhibited in the CORA Experiments

Key

* : Main phenomena - : Not Measured U : Unknown Y : Yes N : No or None

AIC : Silver Indium Cadmium B_4C : Boron Carbide Incl : Inconel Zry : Zircaloy SS : Stainless Steel

: Complete blockage of bundle after large-scale dissolution of fuel $: By shattering, during quench

S,D,C : Solid/solid interaction with Zry, Dissolution by Zry, Ceramic melt, for fuel

L,I,H : Low, Intermediate, High (0-33-66-100% for blockage, with 0% the initial bundle state) V,LV : Volatile (Cs,I_2), Low Volatile (Ba,Sr), for FP Release

Met/Cer/Rem : Metallic, Ceramic, Remelt for crust Frmn/Slmp : Formation, Slump for melt pool

Feature	Description	Comments
Location of Facility/ Objectives	IPSN/CEA - Cadarache France, PHEBUS experimental reactor	Investigation of the early phase of core degradation during unrecovered transients.
Number of Tests	6	The 2nd test B9R was performed in two independent parts B9R1 and B9R2.
Duration of Test Series	03Dec86 - 01Jun89	Post test examinations, experimental and analysis reports are finished.
Number of Rods/ Heated Length (m)	Bundle with 21 rods/ 0.80	12.6 mm pitch matrix. The rod array is surrounded by an insulating shroud with an inner octagonal Zircaloy liner.
Heating Method	Fission	Power supplied by neutronic coupling with the PHEBUS driver core to simulate fission product decay heat.
Control Materials	Ag - In - Cd	One central control rod in the last AIC test only. Zircaloy guide tube.
Spacer Grids	Inconel or Zircaloy	Two spacer-grids per test.
Fuel Irradiation (GWd/tU)	None	17 x 17 PWR - type with fresh fuel rods.
Fluid Input	Variable gas injection	Pure steam (0.4 g/s - 4 g/s) or H_2-steam mixture or steam and then helium (0.5 g/s to 0.05 g/s) for helium.

Table 4.1.3.1 : PHEBUS SFD Test Series - General Information

Feature	Description	Comments
System Pressure (MPa)	0.5 to 3.5	-
Fuel Rod Internal Fill Pressure (MPa)	0.1 to 0.7	B9, B9R, B9+, AIC : a fusible seal is located on the upper rod plug to avoid clad ballooning (melting point ~ 1120 K). C3, C3+ : no fusible seal in order to facilitate clad collapse in these high pressure tests.
Initial Heat-up Rate (K/s)	0.2 to 1.7	-
Maximum Temperature (K)	2750 ± 50	Reached in B9+ test.
Final Cooling	Slow except B9R	Slow cooling with helium except a rapid cooling with steam in B9R test.
Notes	ISP	PHEBUS B9+ was used for OECD/CSNI ISP 28

Table 4.1.3.1 : PHEBUS SFD Test Series - General Information

Test	Number of Rods (Fuel/ Abs)	Spacer Grid (no.)	Fuel Irrad-iation (GWD/tU)	Fluid	Pressure (MPa) (System /rod)	Initial Heat-up (K/s)	Max. Tempe-rature (K)	Transient Duration (s)*	Test Termin-ation	Special Condi-tion	Date of Test
B9	21 F	Incl (2)	None	Stm, He	1.9 to 0.5/ 0.7	0.2 up to 1820 K	2150	7000/2600/ 100/0	S(He)	(d)	03Dec86
B9R-1	21 F	Incl (2)	None	Stm, He	2.0 to 0.5/ 0.7	0.2	1800	7400/2800/ 0/0	S(He)	(d)	01Apr88
B9R-2	21 F	Incl (2)	None	He, Stm	0.5/0.7	<0.1 up to 1000 K (a)	2150	3200/800/ 50/0	R(Stm)	(d)	14Apr88
C3	21 F	Incl (2)	None	He(c) H_2, He	3.5/0.1	2.0 (b)	2050	6200/6100/ 0/0	S(He)	Heatup in pure H_2	30Oct87
C3+	21 F	Incl (2)	None	Stm, He	3.5/0.1	1.7	2570	11400/ 6900/ 2800/0	S(He)	-	24Nov88

Table 4.1.3.2 : PHEBUS SFD Test Series - Main Experimental Conditions

Key

AIC	: Silver Indium Cadmium	B_4C	: Boron Carbide	Incl	: Inconel	Zry	: Zircaloy	F	: Fresh fuel rod
Ar	: Argon	Stm	: Steam	Wtr	: Water	Y	: Yes		
S	: Slow (S < 2 K/s)	R	: Rapid	Q	: Quench	N	: No		

* : Transient Duration is total time spent over 1100/1500/2100/2800K respectively, up to when there is no further significant change in core state (here taken as 2100K on final cooldown)

(a) : During pure helium phase

(b) : During a pure hydrogen phase

(c) : Pre-heating helium phase

(d) : Cladding failure imposed when rod plug temperature reached 1120K

Test	Number of Rods (Fuel/ Abs)	Spacer Grid (no.)	Fuel Irrad-iation (GWD/tU)	Fluid	Pressure (MPa) (System /rod)	Initial Heat-up (K/s)	Max. Tempe-rature (K)	Transient Duration (s)*	Test Termin-ation	Special Condi-tion	Date of Test
B9+	21 F	Incl (2)	None	Stm, He	2.0/0.7	0.25	2750	12500/ 11000/ 6000/0	S(He)	(d) He inj. in shroud	26Jan89
AIC	20 F/ 1(AIC)	Zry (2)	None	Stm, He	0.6/0.2	0.3	2100	1500/ 400/ 0/0	S(He)	(d) He inj. in shroud	01Jun89

Table 4.1.3.2 : PHEBUS SFD Test Series - Main Experimental Conditions

Key

AIC	: Silver Indium Cadmium	B_4C	: Boron Carbide	Incl	: Inconel	Zry	: Zircaloy	F	: Fresh fuel rod
Ar	: Argon	Stm	: Steam	Wtr	: Water	Y	: Yes		
S	: Slow (S < 2 K/s)	R	: Rapid	Q	: Quench	N	: No		

* : Transient Duration is total time spent over 1100/1500/2100/2800K respectively, up to when there is no further significant change in core state (here taken as 2100K on final cooldown)

(a) : During pure helium phase

(b) : During a pure hydrogen phase

(c) : Pre-heating helium phase

(d) : Cladding failure imposed when rod plug temperature reached 1120K

Test	Thermal Response	Clad Ballo-ning	Clad Oxida-tion, H_2 release	Material Interactions and Melting			Partic-ulate Debris	Blockage	Late Phase		FP and Aerosol Release
				Absor-ber	Spacer Grid	Fuel			Crust	Melt Pool	
B9	Y*	N	H*	N	Incl	N	N	N	N	N	N
B9R-1	Y*	N	H*	N	Incl	N	N	N	N	N	N
B9R-2	Y*	N (1)	H*, H_2, H*(3)	N	Incl	D (little)	Y* (3)	H*	N	N	N
C3	Y*	N	L(2)	N	Incl*	S*	N	I	N	N	N
C3+	Y*	N	L H_2	N	Incl*	S, D*	Y*	H*	Met	N	N
B9+	Y*	N	H* H_2*	N	Incl*	D*	N	L*	Met/Cer	N	N
AIC	Y*	N	I H_2	AIC*	Zry	N	N	N	N	N	N (4)

Table 4.1.3.3 : Main Phenomena Exhibited in the PHEBUS SFD Experiments

Key

* : Main phenomena - : Not Measured U : Unknown Y : Yes N : No or None

AIC : Silver Indium Cadmium B_4C : Boron Carbide Incl : Inconel Zry : Zircaloy

S,D,C : Solid/solid interaction with Zry, Dissolution by Zry, Ceramic melt, for fuel

L,I,H : Low, Intermediate, High (0-33-66-100% for blockage, with 0% the initial bundle state) V,LV : Volatile (Cs,I_2), Low Volatile (Ba,Sr), for FP Release

Met/Cer/Rem : Metallic, Ceramic, Remelt for crust Frmn/Slmp : Formation, Slump for melt pool

(1) : Flowering (2) : Zry hydriding during a rich hydrogen atmosphere phase (850K<T<1350K)

(3) : During a final rapid cooling (4) : Plugging of a downstream filter by AIC aerosols

Feature	Description	Comments
Location of Facility/ Objectives	Power Burst Facility (PBF) Idaho National Engineering Laboratory (INEL) Idaho Falls, Idaho, USA	The PBF Severe Fuel Damage (SFD) tests were part of an internationally sponsored Light Water Reactor (LWR) SFD research programme initiated by the U.S. Nuclear Regulatory Commission (USNRC). The specific objectives of the PBF-SFD series of tests were to: (1) Investigate fuel rod damage following severe cladding oxidation, melt relocation, and fuel rod fragmentation; (2) Measure the release rates, transport, deposition of fission products; (3) Determine the magnitude and timing of hydrogen generation; (4) Investigate the coolability of test bundles following various types of damage; (5) Determine the behaviour of irradiated fuel rods compared with fresh fuel rods and to evaluate the effects of control rods.
Number of Tests	4	-
Duration of Test Series	29Oct82 - 7Feb85	-
Number of Rods/ Heated Length (m)	28 to 32/ 0.914 to 1.0	Fresh fuel rods were 0.914 m in length, and the irradiated rods were 1.0 m in length.
Heating Method	Fission	Fission power driven by the PBF reactor.
Control Materials	AIC	Silver/Indium/Cadmium control rods were employed in test 1-4 only.
Spacer Grids	Inconel	-
Fuel Irradiation (GWd/tU)	Trace to 38	The ST and 1-1 tests were trace irradiated, test 1-3 and 1-4 contained 26 irradiated (38 GWd/tU) rods and 2 trace irradiated rods.
Fluid Input	0.6 to 16 g/s steam/water	Water addition to bundle during high temperature transient.

Table 4.1.4.1 : PBF-SFD Test Series - General Information

Feature	Description	Comments
System Pressure (MPa)	6.8 to 7.0	-
Fuel Rod Internal Fill Pressure (MPa)	>7.5	Tests ST and 1-1 only.
Initial Heatup Rate (K/s)	0.1 to 2.9	-
Maximum Temperature (K)	>2800	-
Final Cooling	Slow in argon, quench	Two tests were quenched with water, two tests were slow cooled with argon.
Notes	-	-

Table 4.1.4.1 : PBF-SFD Test Series - General Information

Test	Number of Rods (Fuel/ Abs)	Spacer Grids (no.)	Fuel irradiation (GWD/tU)	Fluid	Pressure (MPa) (System/ Rod)	Initial Heat-up (K/s)+	Max. Tempe-rature (K)	Transient Duration (s)*	Test Termin-ation $	Special Condi-tion	Date of Test
ST	32F	Incl (3)	T	Wtr	7/>7.5	0.1-0.15	>2673	7300/4100/ 500/?	Q (Wtr)	N	28Oct82
1-1	32F	Incl (3)	T (.08)	Wtr	6.8/>7.5	0.46/2.9	~2890	2100/1100/ 300/?	R (Ar)	N	8Sept83
1-3	26IR, 2F, 4GT	Incl (3)	38, T	Wtr	6.85/?	0.5/1.9	>2800	1900/1350/ 700-900/?	S (Ar)	N	3Aug84
1-4	26IR,2F, 4GT/ (AIC)	Incl (3)	38, T	Wtr Ar	6.95/?	0.4/1.6	>2800	2900/2000/ 1400/500	S (Ar)	N	7Feb85

Table 4.1.4.2 : PBF-SFD Test Series - Main Experimental Conditions

Key

AIC	: Silver Indium Cadmium	B_4C	: Boron Carbide	Incl	: Inconel	Zry	: Zircaloy
T	: Trace	F	: Fresh	IR	: Irradiated		
Ar	: Argon	Stm	: Steam	Wtr	: Water	Y	: Yes
S	: Slow (S < 2 K/s)	R	: Rapid	Q	: Quench	N	: No

\+ : X/Y where X is heatup rate <1200K and Y is heatup rate >1200K

$: Cooldown procedure after power reduction

* : Transient Duration is total time spent over 1100/1500/2100/2800K respectively, up to when there is no further significant change in core state (here taken as 2100K on final cooldown)

Test	Thermal Response	Clad Ballo-oning	Clad Oxida-tion, H_2 Release	Material Interactions and Melting			Partic-ulate Debris	Bloc-kage	Late Phase		FP and Aerosol Release
				Abso-rber	Spacer Grid	Fuel			Crust	Melt Pool	
ST	Y*	Y	H	N	Incl*	D*	Y	L	N	N	V
1-1	Y*	Y	H	N	Incl*	D*,C	Y	H	Met/Cer	Frmn/Slmp	V
1-3	Y*	Y	H	N	Incl*	D*,C	Y	I	Met/Cer	Frmn/Slmp	V*, LV*
1-4	Y*	Y	H	AIC*	Incl*	D*,C	Y	H	Met/Cer	Frmn/Slmp	V*, LV*

Table 4.1.4.3 : Main Phenomena Exhibited in the PBF-SFD Experiments

Key

* : Main phenomena - : Not Measured U : Unknown Y : Yes N : No or None

AIC : Silver Indium Cadmium B_4C : Boron Carbide Incl : Inconel Zry : Zircaloy $: By shattering, during quench

S,D,C : Solid/solid interaction with Zry, Dissolution by Zry, Ceramic melt, for fuel

L,I,H : Low, Intermediate, High (0-33-66-100% for blockage, with 0% the initial bundle state) V,LV : Volatile (Cs,I_2), Low Volatile (Ba,Sr), for FP Release

Met/Cer/Rem : Metallic, Ceramic, Remelt for crust Frmn/Slmp : Formation, Slump for melt pool

Feature	Description	Comments
Location of Facility/ Objectives	NRU reactor at Chalk River, Ontario, Canada	These tests were performed by the Pacific Northwest Laboratory (PNL) for the U.S. Nuclear Regulatory Commission (NRC) in the NRU reactor at AECL Chalk River as part of the Severe Accident Research Programme. The objectives of the tests were to : (1) Obtain well-characterized data for evaluating the effects of coolant boilaway and core damage progression in an LWR; and (2) Investigate integral severe accident phenomena along a full-length bundle.
Number of Tests	4	Two additional tests were conceptualized, but not performed.
Duration of Test Series	March 85 - May 87	The last conceptualized test (FLHT-6) was constructed, but was cancelled in February 1994.
Number of Rods/ Heated Length (m)	11 or 12 / 3.66	The last 2 tests contained one gamma thermometer (stainless steel tube containing differential thermocouples) or an equivalent "dummy" stainless steel rod.
Heating Method	Fission	Peak fission power was ~0.74 kW/m-rod (driven by the NRU reactor). Each non-irradiated rod contained enriched UO_2 pellets (1.76 to 2.0%)
Control Materials	None	-
Spacer Grids	Inconel and Zircaloy	Eight spacers (each bundle).
Fuel Irradiation (GWD/tU)	None/28	The first 2 tests used no preirradiated rods. The last 2 tests employed 1 irradiated rod (+11 non-irradiated rods).
Fluid Input	Steam, Variable	These were boiloff tests and the makeup "water" flow varied from 0.10 to 1.4 g/s/rod.

Table 4.1.5.1 : NRU-FLHT Test Series - General Information

Feature	Description	Comments
System Pressure (MPa)	1.4	-
Fuel Rod Internal Fill Pressure (MPa)	0.5 to 2.4	-
Internal Heatup Rate (K/s)	0.3 to 2.5	
Maximum Temperature (K)	2300 to 2600	-
Final Cooling	Slow	NRU reactor scrammed, inlet flow shut off, bypass coolant flow maintained.
Notes	-	-

Table 4.1.5.1 : NRU-FLHT Test Series - General Information

Test **	Number of Rods (Fuel/ Abs)	Spacer Grids (no.)	Fuel Irrad-iation (GWD/tU)	Fluid $	Pressure (MPa) (System/ Rod)	Initial Heat-up (K/s)	Max. Tempe-rature (K)	Transient Duration (s) *	Test Termin-ation £	Special Condi-tion	Date of Test
FLHT-1	12	Incl (8)	None	Wtr/ Stm	1.38/ 1.8-2.0	0.3-0.8	2300	3300/600/ 100/0	S	N	Mar85
FLHT-2	12	Incl (8)	None	Wtr/ Stm	1.41/2.4	2.5	2500	1850/1030 /300/0	S	N	Dec85
FLHT-4	10 F, 1 IR 1 gamma	Incl (8)	None 28	Wtr/ Stm	1.40/0.5	1.7	2600	2600/1800 /300/0	S	N	Aug86
FLHT-5	10 F, 1 IR 1 gamma (dummy)	Incl (4) Zry (4)	None 28	Wtr/ Stm	1.40/0.5	2.3	2600	4300/3800 />600/0	S	N	May87

Table 4.1.5.2 : NRU-FLHT Test Series - Main Experimental Conditions

Key

AIC	: Silver Indium Cadmium	B_4C	: Boron Carbide	Incl	: Inconel	Zry	: Zircaloy
F	: Fresh	IR	: Irradiated	gamma	: Gamma thermometer		
Ar	: Argon	Stm	: Steam	Wtr	: Water	Y	: Yes
S	: Slow (S < 2 K/s)	R	: Rapid	Q	: Quench	N	: No

$: Bundle inlet flow during the boilaway transient (0.1g/s/rod except for FLHT-1 (1.4g/s/rod)

£ : NRU reactor scrammed, inlet flow shut off, bypass coolant flow maintained

** : FLHT-3 was conceptualized but not run, and FLHT-6 was conceptualized and built, but the test was cancelled in February 1994

* : Transient Duration is total time spent over 1100/1500/2100/2800K respectively, up to when there is no further significant change in core state (here taken as 2100K on final cooldown)

Test	Thermal Response	Clad Ballo-oning	Clad Oxida-tion, H_2 Release	Material Interactions and Melting			Partic-ulate Debris	Bloc-kage	Late Phase		FP and Aerosol Release
				Abso-rber	Spacer Grid	Fuel			Crust	Melt Pool	
FLHT-1	Y*	Y	L	N	Incl*	D	N	Y	N	N	N
FLHT-2	Y*	Y	I	N	Incl*	D*	N	Y	N	N	N
FLHT-4	Y*	N	H	N	Incl*	D*(F)	N	Y	N	N	V*, LV*
FLHT-5	Y*	N	H	N	Incl*/ Zry	D* F*	N	Y	N	N	V*, LV*

Table 4.1.5.3 : Main Phenomena Exhibited in the NRU-FLHT Experiments

Key

* : Main phenomena - : Not Measured U : Unknown Y : Yes N : No or None

AIC : Silver Indium Cadmium B_4C : Boron Carbide Incl : Inconel Zry : Zircaloy

S,D,C,F : Solid/solid interaction with Zry, Dissolution by Zry, Ceramic melt, Foamed, for fuel

L,I,H : Low, Intermediate, High (0-33-66-100% for blockage, with 0% the initial bundle state) V,LV : Volatile (Cs,I_2), Low Volatile (Ba,Sr), for FP Release

Met/Cer/Rem : Metallic, Ceramic, Remelt for crust Frmn/Slmp : Formation, Slump for melt pool

Feature	Description	Comments
Location of Facility/ Objectives	ACRR-ST Experiment Programme Sandia National Laboratories (SNL) Albuquerque, New Mexico, USA	The ACRR-ST (Annular Core Research Reactor Source Term) experiment programme was part of an internationally sponsored research programme into severe accident behaviour, conducted for the U.S. Nuclear Regulatory Commission (USNRC). The objectives of the ST programme were to investigate fission product release from irradiated LWR fuel in a fission heated environment. The tests focused on fission product release under reducing conditions, but PIE on samples gives information on melt progression behaviour of irradiated fuel rods.
Number of Tests	2	-
Duration of Test Series	1985 to 1989	-
Number of Rods/ Heated Length (m)	4 / 0.3	The ST test bundle was formed from 4 segmented fuel rods. The lower 15 cm segment was fresh UO_2 which served to preheat the inlet gas flow, and the upper 15 cm segment was formed from irradiated BR-3 fuel rods (~47,000 MWd/tonne).
Heating Method	Fission	Fission provided the internal heating source for the fuel rods.
Control Materials	none	-
Spacer Grids	none	-
Fuel Irradiation (GWD/tU)	47	Fresh UO_2 fuel preheated segment and BR-3 irradiated fuel segment. No pre-irradiation.
Fluid Input	Hydrogen, helium	The flow stream was a mixture of hydrogen and helium to provide reducing conditions.

Table 4.1.6.1 : ACRR-ST Test Series - General Information

Feature	Description	Comments
System Pressure (MPa)	0.2 to 2.0	-
Fuel Rod Internal Fill Pressure (MPa)	0.08	Rod internal pressure less than system pressure so that ballooning by internal pressurization did not result.
Initial Heatup Rate (K/s)	1.0 to 1.5	Heatup rate varies over axial extent of bundle - the maximum value is quoted.
Maximum Temperature (K)	~ 2500	-
Final Cooling	slow cool down	-
Notes		-

Table 4.1.6.1 : ACRR-ST Test Series - General Information

Test	Number of Rods (Fuel/ Abs)	Spacer Grids (no.)	Fuel Irradiation (GWD/tU)	Fluid	Pressure (MPa) (System/ Rod)	Initial Heat-up (K/s)	Max. Tempe-rature (K)	Transient Duration (s) *	Test Termin-ation	Special Condi-tion	Date of Test
ST1	4/0	none	47	H_2/Ar	0.2/0.08	1.5	2500	1000/3000/ 1000/0	S	No pre-irradi-ation	28Apr87
ST2	4/0	none	47	H_2/Ar	3/0.08	0.8	2500	1000/3000/ 1000/0	S	No pre-irradi-ation	19Nov87

Table 4.1.6.2 : ACRR-ST Test Series - Main Experimental Conditions

Key

AIC	: Silver Indium Cadmium	B_4C	: Boron Carbide	Incl	: Inconel	Zry	: Zircaloy
Ar	: Argon	Stm	: Steam	Wtr	: Water	Y	: Yes
S	: Slow (S < 2 K/s)	R	: Rapid	Q	: Quench	N	: No

* : Transient Duration is total time spent over 1100/1500/2100/2800K respectively, up to when there is no further significant change in core state (here taken as 2100K on final cooldown)

Test	Thermal Response	Clad Ballo-oning	Clad Oxida-tion, H_2 Release	Material Interactions and Melting			Partic-ulate Debris	Bloc-kage	Late Phase		FP and Aerosol Release
				Abso-rber	Spacer Grid	Fuel			Crust	Melt Pool	
ST1	Y*	N	N	N	N	D*,F*	N	I*	N	N	Y*
ST2	Y*	N	N	N	N	D*,F*	N	I*	N	N	Y*

Table 4.1.6.3 : Main Phenomena Exhibited in the ACRR-ST Experiments

Key

* : Main phenomena - : Not Measured U : Unknown Y : Yes N : No or None

AIC : Silver Indium Cadmium B_4C : Boron Carbide Incl : Inconel Zry : Zircaloy

S,D,C,F : Solid/solid interaction with Zry, Dissolution by Zry, Ceramic melt, for fuel, Foamed, for fuel

L,I,H : Low, Intermediate, High (0-33-66-100% for blockage, with 0% the initial bundle state) V,LV : Volatile (Cs,I_2), Low Volatile (Ba,Sr), for FP Release

Met/Cer/Rem : Metallic, Ceramic, Remelt for crust Frmn/Slmp : Formation, Slump for melt pool

Feature	Description	Comments
Location of Facility/ Objectives	ACRR-DF Experiment Programme Sandia National Laboratories (SNL) Albuquerque, New Mexico, USA	The ACRR-DF (Annular Core Research Reactor Damaged Fuel experiment programme were part of an internationally sponsored research programme into severe accident behaviour, conducted for the U.S. Nuclear Regulatory Commission (USNRC). The objectives of the DF programme were to investigate initial fuel damage processes beginning with intact fuel rods undergoing heatup and progressing through oxidation in steam, hydrogen generation, melting and relocation of the fuel cladding, the formation of blockages, and the degradation of the fuel rod geometry.
Number of Tests	4	-
Duration of Test Series	1983 to 1987	The experiments were performed between 1984 and 1986.
Number of Rods/ Heated Length (m)	9 or 14 / 0.5	The rod array was surrounded by an insulating shroud (low density ZrO_2) within a stainless steel pressure vessel. The fuel rods were Zircaloy-4 clad fresh UO_2. A high density ZrO_2 tube was situated within the insulating region to prevent melt penetration.
Heating Method	Fission	Fission provided the internal heating source for the fuel rods.
Control Materials	Ag-In-Cd / B_4C	PWR control rod (DF-3): stainless steel clad AIC with Zircaloy-4 guide tube; BWR control blade (DF-4): B_4C-filled stainless steel tubes encased in stainless steel sheath.
Spacer Grids	Inconel	1 grid used in tests DF-1,2 and 3. DF-4 used no grid.
Fuel Irradiation (GWD/tU)	None	Fresh UO_2 fuel, enriched to 10% U^{235} used.
Fluid Input	Steam: 0.05 - 0.1 g/s/rod	Steam was injected into the bottom of the test bundle at a controlled rate.

Table 4.1.7.1 : ACRR-DF Test Series - General Information

Feature	Description	Comments
System Pressure (MPa)	0.7 to 2.0	-
Fuel Rod Internal Fill Pressure (MPa)	0.2	Rod internal pressure less than system pressure so that ballooning by internal pressurization did not result.
Initial Heatup Rate (K/s)	0.2 to 2.0	Heatup rate varies over axial extent of bundle - the maximum value is quoted.
Maximum Temperature (K)	~ 2700	-
Final Cooling	slow cool down	-
Notes	-	-

Table 4.1.7.1 : ACRR-DF Test Series - General Information

Test	Number of Rods (Fuel/Abs)	Spacer Grids (no.)	Fuel Irradiation (GWD/tU)	Fluid	Pressure (MPa) (System/ Rod)	Initial Heatup (K/s)	Max. Tempe-rature (K)	Transient Duration (s) *	Test Termin-ation	Special Condi-tion	Date of Test
DF1	9/0	Incl(1)	None	Stm	0.3/0.007	1.00	2700+	1600/400/ 300/200	S	N	15Mar84
DF2	9/0	Incl(1)	None	Stm	1.7/0.1	1.25	2600	1900/1200/ 950/0	S	N	27Oct84
DF3	8/ 1(AIC)	Incl(1)	None	Stm	1.6/0.1	1.20	2400+	950/600/ 250/0	S	N	27Oct85
DF4	14/ 1(SS/B_4C)	none	None	Stm	0.7/0.1	1.20	2720	1600/800/ 500/0	S	N	21Nov86

Table 4.1.7.2 : ACRR-DF Test Series - Main Experimental Conditions

Key

AIC	: Silver Indium Cadmium	B_4C	: Boron Carbide	Incl	: Inconel	Zry	: Zircaloy
Ar	: Argon	Stm	: Steam	Wtr	: Water	Y	: Yes
S	: Slow (S < 2 K/s)	R	: Rapid	Q	: Quench	N	: No

* : Transient Duration is total time spent over 1100/1500/2100/2800K respectively, up to when there is no further significant change in core state (here taken as 2100K on final cooldown)

Test	Thermal Response	Clad Ballo-oning	Clad Oxida-tion, H_2 Release	Material Interactions and Melting			Partic-ulate Debris	Bloc-kage	Late Phase		FP and Aerosol Release
				Abso-rber	SpacerGrid	Fuel			Crust	Melt Pool	
DF1	Y*	N	H	N	Incl	D*	N	I*	Met/Cer	Small (Met/Cer)	N
DF2	Y*	N	H	N	Incl	D*	N	I*	Met/Cer	Small (Met/Cer)	N
DF3	Y*	N	H	AIC*	Incl	D*	N	I*	Met/Cer	Small (Met/Cer)	N
DF4	Y*	N	H	B_4C*	none	D*	N	H*	Met/Cer	Small (Met/Cer)	N

Table 4.1.7.3 : Main Phenomena Exhibited in the ACRR-DF Experiments

Key

* : Main phenomena - : Not Measured U : Unknown Y : Yes N : No or None

AIC : Silver Indium Cadmium B_4C : Boron Carbide Incl : Inconel Zry : Zircaloy

S,D,C : Solid/solid interaction with Zry, Dissolution by Zry, Ceramic melt, for fuel

L,I,H : Low, Intermediate, High (0-33-66-100% for blockage, with 0% the initial bundle state) V,LV : Volatile (Cs,I_2), Low Volatile (Ba,Sr), for FP Release

Met/Cer/Rem : Metallic, Ceramic, Remelt for crust Frmn/Slmp : Formation, Slump for melt pool

Feature	Description	Comments
Location of Facility/ Objectives	LOFT Facility Idaho National Engineering Laboratory (INEL), Idaho Falls, Idaho, USA	The LOFT LP-FP-1 and LP-FP-2 tests were the fission product release and transport tests performed in the Loss-of-Fluid-Test (LOFT) facility. They were the two last experiments performed under the sponsorship of the OECD. LOFT is a 50 MW(th) model of a PWR, complete with core, pressurizer, ECCS, steam generator, pumps, and broken loop simulant.
Number of Tests	2	The FP-1 test simulates a large-LOCA sequence. The FP-2 test simulates a medium-LOCA, V-type sequence.
Duration of Test Series	19Dec84 - 03Jul85	These are the dates the tests were performed respectively. Post-test examinations and reporting continued to 1989.
Number of Rods/ Heated Length (m)	11x11 array / 1.67	The rod array is surrounded by a square Zircaloy flow shroud. In test FP-2, the shroud is itself surrounded by a zirconium oxide high temperature shield. Fuel rod total length was 1.8 m. Active fuel length varied between 1.59 and 1.68 m.
Heating Method	Decay heat	The experimental rod array, called Central Fuel Module or CFM, was placed in the centre of the LOFT core.
Control Materials	Ag-In-Cd	Control rod guide tubes were of Zircaloy.
Spacer Grids	Inconel 718	
Fuel Irradiation (GWD/tU)	0.450-1.400	Fuel pre-irradiation in the LOFT core, during the pre-transient phase, aimed to obtain a fission product inventory and decay heat.
Fluid Input (g/s)	Steam flow: 15 in CFM (FP-2) 23-139 in CFM (FP-1)	Transient started with reactor scram and opening of leakage blowdown valves. Steam flow rate through the CFM was not a test specification.

Table 4.1.8.1 : LOFT LP-FP Test Series - General Information

Feature	Description	Comments
System Pressure (MPa)	15 (Initial pressure) 0.3 (heatup phase FP-1) 1.4 (heatup phase FP-2)	The tests included blowdown, heat-up, and reflood phases
Fuel Rod Internal Fill Pressure (MPa)	0.10 - 2.41	22 prepressurized higher enrichment rods (6%), were used in the FP-1 CFM. All FP-2 rods in the CFM were prepressurized and had 9.744% enrichment.
Initial Heatup Rate (K/s)	2.2 - 50	Heatup rates were typical of the sequences simulated in each test.
Maximum Temperature (K)	2400 - 3000	Unintentional water injection limited the number of failed fuel rods in FP-1 test. Maximum local temperature reached in FP-2 was probably around 3100 K during the reflood phase, as shown by PIE results.
Final Cooling	Water reflood	Substantial fuel damage was caused by reflood in the LP-2 test.
Notes		International cooperation was fostered in this program, especially in a OECD sponsored code comparison exercise for the LP-2 test, which gathered 6 participants.

Table 4.1.8.1 : LOFT LP-FP Test Series - General Information

Test	Number of Rods (Fuel/ Abs)	Spacer Grids (no.)	Fuel Irradiation (GWD/tU)	Fluid	Pressure (MPa) (System/ Rod)	Initial Heat-up (K/s)	Max. Tempe-rature (K)	Transient Duration (s) *	Test Termi-nation	Special Condi-tion	Date of Test
1	100/ 11(AIC) + 10 guides	Incl(5)	1.417	Stm, Water	0.3/ 0.1-2.4	50-60	1200 (meas-ured)	150/0/0/0	Q(Wtr)	Uninten-tional water injection in upper plenum	19Dec84
2	100/ 11(AIC) + 10 guides	Incl(5)	0.448	Stm, Water	1.40/2.41	2.2	3100 (esti-mated)	650/400/ 300/5	Q(Wtr)	Substan-tial fuel damage during reflood	03Jul85

Table 4.1.8.2 : LOFT LP-FP Test Series - Main Experimental Conditions

Key

AIC	: Silver Indium Cadmium	B_4C	: Boron Carbide	Incl	: Inconel	Zry	: Zircaloy
Ar	: Argon	Stm	: Steam	Wtr	: Water	Y	: Yes
S	: Slow (S < 2 K/s)	R	: Rapid	Q	: Quench	N	: No

* : Transient Duration is total time spent over 1100/1500/2100/2800K respectively, up to when there is no further significant change in core state (here taken as 2100K on final cooldown)

Test	Thermal Response	Clad Ballo-oning	Clad Oxida-tion, H_2 Release	Material Interactions and Melting			Partic-ulate Debris	Bloc-kage	Late Phase		FP and Aerosol Release
				Abso-rber	Spacer Grid	Fuel			Crust	Melt Pool	
1	Y*	Y	N	N	N	N	N	N	N	N	V
2	Y	Y	H (H in qnch)*	AIC*	Incl*	D* C*	(Y$)	I* (50%)	N	N	V LV

Table 4.1.8.3 : Main Phenomena Exhibited in the LOFT-LP-FP Experiments

Key

* : Main phenomena - : Not Measured U : Unknown Y : Yes N : No or None

AIC : Silver Indium Cadmium B_4C : Boron Carbide Incl : Inconel Zry : Zircaloy $: By shattering, during quench

S,D,C : Solid/solid interaction with Zry, Dissolution by Zry, Ceramic melt, for fuel

L,I,H : Low, Intermediate, High (0-33-66-100% for blockage, with 0% the initial bundle state) V,LV : Volatile (Cs,I_2), Low Volatile (Ba,Sr), for FP Release

Met/Cer/Rem : Metallic, Ceramic, Remelt for crust Frmn/Slmp : Formation, Slump for melt pool

Feature	Description	Comments
Location of Facility/ Objectives	IPSN/CEA - Cadarache France, PHEBUS experimental reactor	Investigate the late phase of core degradation and the related FP release during unrecovered transients.
Number of Tests	6	The first three tests FPT0, FPT1 and FPT4 have been performed (Dec1993, July 1996 and July 1999).
Duration of Test Series	02 Dec 93 (1st test) 26 July 96 (2nd test) 22 July 99 (3rd test)	Maximum 1 test each 2 or 3 years. Programme in progress.
Number of Rods/ Heated Length (m)	20 1.0	For FPT0, FPT1, FPT2, FPT3 : rods on a 12.6 mm pitch matrix. Initial debris bed configuration in FPT4. Not defined for FPT5.
Mass of fuel (kg)/ Heated Length (m)	5.5 .36	For FPT4 : 2.5 kg of passive UO_2 (0.12 m) and 3.0 kg of active UO_2 (0.24 m) Irradiated UO_2 including ZrO_2 shards (0.75kg).
Heating Method	Fission	Power supplied by neutronic coupling with the PHEBUS driver core to simulate fission product decay heat.
Control Materials	Ag - In - Cd B_4C	One control rod (central rod) in FPT0, FPT1, FPT2, FPT3 (Guide tube in Zircaloy). (B_4C for FPT3). Not defined for the FPT5 test.
Spacer Grids	Zircaloy	Two spacer grids in FPT0, FPT1, FPT2, FPT3.
Fuel Irradiation (GWd/tU)	1st test : fresh fuel Others : 23 to 30 FPT4 : 33	9 days of pre-irradiation in the PHEBUS reactor. BR3 reactor fuel + pre-irradiation in PHEBUS (9 days). EDF fuel for FPT4.
Fluid Input	Variable gas injection	Pure steam (FPT0, FPT1 and FPT2). Steam + H_2 injection in FPT4. Possible He and H_2 injection in FPT3.

Table 4.1.9.1 : PHEBUS FP Test Series - General Information

Feature	Description	Comments
System Pressure (MPa)	0.2	For FPT0, FPT1, FPT2, FPT4, FPT3. Not defined for the FPT5 test .
Fuel Rod Internal Fill Pressure (MPa)	~ 2.4	For FPT0, FPT1, FPT2. Not defined for the FPT3 and FPT5 tests. Not applicable for FPT4 (debris bed).
Initial Heat-up Rate (K/s)	~0.5	For FPT0, FPT1, FPT2, FPT3. Not defined for the FPT5 test.
Maximum Temperature (K)	Fuel melting	For FPT0, a maximum temperature greater than 2800 K has been recorded during oxidation runaway. Subsequent progressive fuel relocation at about 2500K.
Final Cooling	1 to 2 K/s	For FPT0, FPT1, FPT2, FPT3.
Notes	-	FPT4 investigates FP release from a solid debris bed and during its evolution to a molten pool, focusing on low volatile FP and transuranic nucleides. FPT3 will investigate oxidation of B_4C and FP release (with carbon compounds). FPT5 should include UO_2 oxidation by air and no control rod.

Table 4.1.9.1 : PHEBUS FP Test Series - General Information

Test	Number Rods (Fuel/Abs)	Spacer Grid (no.)	Fuel Irradiation (GWD/tU)	Fluid	Pressure (MPa) (System/rod)	Initial Heat-up (K/s)	Maximum Temperature (K)	Transient Duration (s) *	Test Termi-nation	Special Condi-tion	Date of Test
FPT0	20 F, 1 AIC	Zry (2)	T	Stm	0.2/2.8	0.5 (a)	> 2600	11200/7600 6500/2000	S (Stm)	-	02Dec93
FPT1	2 F, 18 IR, 1 AIC	Zry (2)	~ 23	Stm	0.2/2.4	0.5 (a)	> 2600 (d)		S (Stm)	-	26Jul96
FPT2	2 F, 18 IR, 1 AIC	Zry (2)	~ 23	Stm	0.2/~2.5	0.5 (a)	> 2600		S (Stm)		October 2000
FPT4	pre-formed debris bed	N	~ 33	Stm, H_2	0.2/~2.5	-	> 2800		S (Stm)	-	22Jul99
FPT3	Test including B_4C absorber rod (scenario similar to FPT2) : FP release (with carbon compounds)										
FPT5	Air ingress and no control rod : not finalised at the cut-off date										

Table 4.1.9.2 : PHEBUS FP Test Series - Main Experimental Conditions

Key

AIC	: Silver Indium Cadmium	B_4C	: Boron Carbide	Inc	: Inconel	Zry	: Zircaloy	T	: Trace-irradiated
Ar	: Argon	Stm	: Steam	Wtr	: Water	Y	: Yes	IR	: Irradiated fuel
S	: Slow (S < 2 K/s)	R	: Rapid	Q	: Quench	N	: No	H_2	: H_2 injection at bundle inlet

* : Transient Duration is total time spent over 1100/1500/2100/2800K respectively, up to when there is no further significant change in core state (here taken as 2100K on final cooldown)

(a) : Heat-up rate before oxidation escalation

(b) : Information expected at the cut-off date

(c) : To be defined

(d) : According to preliminary analysis

Test	Thermal Response	Clad Ballooning	Clad Oxidation, H_2 release	Material Interactions and Melting			Particulate Debris	Blockage	Late Phase		FP and Aerosol Release
				Absorber	Spacer Grid	Fuel			Crust	Melt Pool	
FPT0	Y*	Y	H* H_2	AIC	Zry	D	U	H	Y	Y	Y* (4) V, AIC Aer
FPT1	Y*	Y	H* H_2	AIC	Zry	D	U	H	Y	Y	Y* (5) V, AIC Aer
FPT2	Y*	Y	I* H_2	AIC	Zry	D*	(3)	(3)	(3)	(3)	Y* (5) V, AIC Aer
FPT4	Y*	N	H_2**	N	N	C* DC	(3)	(3)	(3)	(3)	Y* (6) LV, TU, Aer
FPT3	Y*	Y	I* H_2 (2)	B_4C /SS (3)	Zry	D* (3)	(3)	(3)	(3)	U	Y* (5) V, Cc Aer
FPT5	Bundle objective : FP release from a bundle during an air-ingress transient (still open)										Y* (5)

Table 4.1.9.3 : Main Phenomena Exhibited in the PHEBUS FP Experiments

Key

* : Main phenomena ** : Zr canister oxidation U : Unknown Y : Yes N : No or None

AIC : Silver Indium Cadmium B_4C : Boron Carbide Inc : Inconel Zry : Zircaloy SS : Stainless steel

H_2 : Hydrogen production measured - : Not Measured TU : Transuranic Aer : Aerosol Cc : Carbon compounds

S, D, DC, C : Solid/solid interaction with Zry, Dissolution by Zry, Dissolution by ZrO_2 (for fuel) , Ceramic melt, (for fuel)

Met/Cer/Rem : Metallic, Ceramic, Remelt for crust Frmn/Slmp : Formation, Slump for melt pool

L, I, H : Low, Intermediate, High (0-33-66-100% for blockage, with 0% the initial bundle state) V,LV : Volatile (Cs,I_2), Low Volatile (Ba,Sr), for FP Release

(1) : Information expected at the cut-off date (2) : Including B_4C oxidation

(3) : Expected if the test performed as foreseen (4) : Fresh fuel with 9 days of irradiation

(5) : Intermediate burn-up BR3 fuel (23 to 30 MWd/tU) (6) : EDF fuel burn-up (33 MWd/tU)

Feature	Description	Comments
Location of Facility/ Objectives	ACRR-MP Experiment Programme Sandia National Laboratories (SNL) Albuquerque, New Mexico, USA	The ACRR-MP (Annular Core Research Reactor Melt Progression) experiment programme was part of an internationally sponsored research programme into severe accident behaviour, conducted for the U.S. Nuclear Regulatory Commission (USNRC). The objectives of the MP programme were to investigate late phase melt progression processes in degraded fuel geometry. Specifically, the melting dynamics, molten pool formation and growth, and crust failure and migration through intact structure were investigated.
Number of Tests	2	-
Duration of Test Series	1989 to 1992	-
Debris Bed	~3 kg UO_2/ZrO_2 fuel debris overlying rod stub array	The MP experimental test section consisted of three distinct regions: an upper ceramic debris bed region, an intermediate metallic crust with embedded intact furl rods, and a lower intact rod stub region.
Number of Rods/ Heated Length (m)	32 rods/ ~0.15 m	The lower rod stub region provided a region of intact core structure into which the overlying melt pool/crust region could migrate as the melt progression processes proceeded.
Heating Method	Fission	Fission provided the internal heating source for the debris bed and fuel rods.
Control Materials	Ag, In - MP2	-
Spacer Grids	none	-
Fuel Irradiation (GWD/tU)	none	Fresh UO_2 fuel materials were used in the MP tests.
Fluid Input	none	The ambient environment in the MP tests was helium gas.

Table 4.1.10.1 : ACRR-MP Test Series - General Information

Feature	Description	Comments
System Pressure (MPa)	0.1	-
Fuel Rod Internal Fill Pressure (MPa)	0.1	The fuel rods used in the MP tests were not sealed.
Initial Heatup Rate (K/s)	~0.25	The heating profile in the MP tests was a stair-stepped profile with periods of rapid heating and periods of a steady temperature hold. The average heatup rate is quoted.
Maximum Temperature (K)	~ 3400	-
Final Cooling	slow cooldown	-
Notes	-	-

Table 4.1.10.1 : ACRR-MP Test Series - General Information

Test	Number of Rods (Fuel/ Abs)	Spacer Grids (no.)	Fuel Irradiation (GWD/tU)	Fluid	Pressure (MPa) (System/ Rod)	Initial Heat-up (K/s)	Max. Tempe-rature (K)	Transient Duration (s) *	Test Termin-ation	Special Condi-tion	Date of Test
MP1	32/0	none	0	He	0.1	0.3	3300	6000/4500/ 3500/1000	S	-	13Oct89
MP2	32/0	none	0	He	0.1	0.2	3400	16000/12000 / 10000/5500	S	-	7Nov92

Table 4.1.10.2 : ACRR-MP Test Series - Main Experimental Conditions

Key

AIC	: Silver Indium Cadmium	B_4C	: Boron Carbide	Incl	: Inconel	Zry	: Zircaloy
Ar	: Argon	Stm	: Steam	Wtr	: Water	Y	: Yes
S	: Slow (S < 2 K/s)	R	: Rapid	Q	: Quench	N	: No

* : Transient Duration is total time spent over 1100/1500/2100/2800K respectively, up to when there is no further significant change in core state (here taken as 2100K on final cooldown)

Test	Thermal Response	Clad Ballo-oning	Clad Oxida-tion, H_2 Release	Material Interactions and Melting			Partic-ulate Debris	Bloc-kage	Late Phase		FP and Aerosol Release
				Abso-rber	Spacer Grid	Fuel			Crust	Melt Pool	
MP1	Y*	N	N/A	N (1)	N	C*	Y*	H*	Y*	Y*	N
MP2	Y*	N	N/A	N (2)	N	C*	Y*	H*	Y*	Y*	N

Table 4.1.10.3 : Main Phenomena Exhibited in the ACRR-MP Experiments

Key

* : Main phenomena - : Not Measured U : Unknown Y : Yes N : No or None

AIC : Silver Indium Cadmium B_4C : Boron Carbide Incl : Inconel Zry : Zircaloy

S,D,C : Solid/solid interaction with Zry, Dissolution by Zry, Ceramic melt, for fuel

L,I,H : Low, Intermediate, High (0-33-66-100% for blockage, with 0% the initial bundle state) V,LV : Volatile (Cs,I_2), Low Volatile (Ba,Sr), for FP Release

Met/Cer/Rem : Metallic, Ceramic, Remelt for crust Frmn/Slmp : Formation, Slump for melt pool

(1) : Absorber material in crust, no interaction

(2) : Absorber material in crust, with interaction

Feature	Description	Comments
Location of Facility/ Objectives	Ex-Reactor Test Facility Sandia National Laboratories (SNL) Albuquerque, NM, USA	Investigation of metallic melt drainage and blockage formation behaviour in BWR Short Term Station Blackout Accidents where Vessel Depressurization (Blowdown) has been activated.
Number of Tests	3	Two preliminary tests and one large-scale test were performed.
Duration of Test Series	1993 - 1996	-
Number of Rods/ Heated Length (m)	up to 64 / 1.0	Preliminary tests XR1-1 and XR1-2 did not include fuel rods and instead examined only behaviour of control blade and channel boxes. Test XR2-1 included 64 Zircaloy-4 clad UO_2 fuel rods.
Heating Method	Electrical/Induction	Electrical heating used to heat test periphery. Radiant heating from inductively heated susceptor used to prepare melts and heat portions of the test section.
Control Materials	Stainless steel/B_4C	BWR control blade melt (up to 12 kg) is a central feature of these experiments.
Spacer Grids	None	-
Fuel Irradiation (GWD/tU)	None	Depleted UO_2 fuel used.
Steam Input	None	Argon used to inert test environment since depressurized sequences involve very little steam.

Table 4.1.11.1 : Sandia Ex-Reactor Experiments - General Information

Feature	Description	Comments
System Pressure (MPa)	0.1	-
Fuel Rod Internal Fill Pressure (MPa)	0.1	-
Initial Heatup Rate (K/s)	N/A	Tests examine transient melt flow and blockage behaviour in a heated test section. Sustained heating is not maintained.
Maximum Temperature (K)	1900 K (XR1-1 and 1-2) 2300 K (XR2-1)	Steep axial temperature gradient representing the lower core section. Maximum temperature quoted is the temperature of molten control blade material and Zry.
Final Cooling	slow	Cooldown following melt introduction into test section. Cooldown is over many hours.
Notes	lower core support structure	Fuel canister nose piece and support piece, lower core plate and control rod drive tube are full scale and use prototypic materials.

Table 4.1.11.1 : Sandia Ex-Reactor Experiments - General Information

Test	Number of Rods (Fuel/ Abs)	Spacer Grids (no.)	Fuel Irradiation (GWD/tU)	Fluid	Pressure (MPa) (System/ Rod)	Initial Heat-up (K/s)	Max. Tempe-rature (K)	Transient Duration (s) *	Test Termi-nation	Special Condi-tion	Date of Test
XR1-1	0/ 1(B_4C)	none	None	Ar	0.1/0.1	N/A	1900	N/A	S(Ar)	$	Aug93
XR1-2	0/ 1(B_4C)	none	None	Ar	0.1/0.1	N/A	1900	N/A	S(Ar)	$	Nov93
XR2-1	64/ 1(B_4C)	1 Zr-4	None	Ar	0.1/0.1	N/A	2300	N/A	S(Ar)	$ Pre-ox 20 - 40 µm	12Oct95

Table 4.1.11.2 : Sandia Ex-Reactor Experiments - Main Experimental Conditions

Key

AIC	: Silver Indium Cadmium	B_4C	: Boron Carbide	Incl	: Inconel	Zry	: Zircaloy
Ar	: Argon	Stm	: Steam	Wtr	: Water	Y	: Yes
S	: Slow (S < 2 K/s)	R	: Rapid	Q	: Quench	N	: No

$: Amount of Stainless steel/B_4C/Zry melt and composition

* : Transient Duration is total time spent over 1100/1500/2100/2800K respectively, up to when there is no further significant change in core state (here taken as 2100K on final cooldown)

Test	Thermal Response	Clad Ballo-ning	Clad Oxida-tion, H_2 Release	Materials Interactions and Melting			Partic-ulate Debris	Bloc-kage	Late Phase		FP and Aerosol Release
				Abso-rber	Spacer Grid	Fuel			Crust	Melt Pool	
XR1-1	Y*	N	N/A	B_4C	none	N/A	N	I	N	N	N
XR1-2	Y*	N	N/A	B_4C	none	N/A	N	H	N	N	N
XR2-1	Y*	N	N/A	B_4C	Zr-4	D	N	H	N	N	N

Table 4.1.11.3 : Main Phenomena Exhibited in the Sandia Ex-Reactor Experiments

Key

* : Main phenomena - : Not Measured U : Unknown Y : Yes N : No or None

AIC : Silver Indium Cadmium B_4C : Boron Carbide Incl : Inconel Zry : Zircaloy

S,D,C : Solid/solid interaction with Zry, Dissolution by Zry, Ceramic melt, for fuel

L,I,H : Low, Intermediate, High (0-33-66-100% for blockage, with 0% the initial bundle state) V,LV : Volatile (Cs,I_2), Low Volatile (Ba,Sr), for FP Release

Met/Cer/Rem : Metallic, Ceramic, Remelt for crust Frmn/Slmp : Formation, Slump for melt pool

Feature	Description	Comments
Location of Facility/ Objectives	TMI-2 reactor, Harrisburg, Pa, USA	Production commercial reactor.
Number of Tests	1	Actual sequence in a full-scale reactor: small LOCA-type sequence, with delayed operation of the ECCS, and lack of feedwater to the steam generators.
Duration of Test Series	-	-
Number of Rods/ Heated Length	208x177 / 3.6 m	-
Heating Method	Decay heat	-
Control Materials	Ag-In-Cd Al_2O_3-B_4C	Control rods were clad in stainless steel, burnable poison rods were clad in Zircaloy.
Spacer Grids	Inconel 718	-
Fuel Irradiation (GWD/tU)	0.90 - 6.0	-
Fluid Input	(Steam, Water)	Not a recorded parameter. No data have been found in the analyses performed.

Table 4.1.12.1 : TMI-2 Accident - General Information

Feature	Description	Comments
System Pressure (MPa)	15 (initial pressure) 5 - 15 (heatup phases)	-
Fuel Rod Internal Fill Pressure (MPa)	3.0	-
Initial Heatup Rate (K/s)	0.3	Estimated from analysis performed with the MAAP code.
Maximum Temperature (K)	> 3000	PIE results indicate that fuel melting temperatures were reached during phase 2 of the accident.
Final Cooling	Water reflood	A first water injection took place when one pump was restarted for some time at 174 sec, causing substantial damage. The core was finally cooled after the RCS was depressurized and vented, and the RCS pumps started.
Notes	-	International cooperation was fostered in this programme, especially in a OECD sponsored code comparison exercise, based on a "best estimate TMI-2 accident scenario" which gathered 8 participants. Also, PIE was performed on an international cooperation basis, samples being sent to various laboratories.

Table 4.1.12.1 : TMI-2 Accident - General Information

Test	Number of Rods (Fuel/ Abs)	Spacer Grids (no.)	Fuel Irradiation (GWD/tU)	Fluid	Pressure (MPa) (System/ Rod)	Initial Heat-up (K/s)	Max. Tempe-rature (K)	Transient Duration (s) *	Test Termin -ation	Special Condi-tion	Date of Test
-	177 fuel assem-blies, each (208/ 16(AIC))	8	0.9 - 6.0	Stm, Wtr	5 - 15 during heatup	0.30 (init) 0.65 (after)	> 3000 estim-ated	2700/2300/ 2100/2000 $	Q	19t core reloc-ated to the lower plenum	28Mar79

Table 4.1.12.2 : TMI-2 Accident - Main Conditions

Key

AIC	: Silver Indium Cadmium	B_4C	: Boron Carbide	Incl	: Inconel	Zry	: Zircaloy
Ar	: Argon	Stm	: Steam	Wtr	: Water	Y	: Yes
S	: Slow (S < 2 K/s)	R	: Rapid	Q	: Quench	N	: No

* : Transient Duration is total time spent over 1100/1500/2100/2800K respectively, up to when there is no further significant change in core state (here taken as 2100K on final cooldown)

$: This is an estimation based on results from the analysis performed with the MAAP 3.0 code, by R. Sairanen from VTT, Finland.

Test	Thermal Response	Clad Ballo-oning	Clad Oxida-tion, H_2 Release	Material Interactions and Melting			Partic-ulate Debris	Bloc-kage	Late Phase		FP and Aerosol Release
				Abso-rber	Spacer Grid	Fuel			Crust	Melt Pool	
-	Y	Y	Y*	Y	Y	C*	Y*	Y*	Y*	Y* 45 % of the core mass melted	V

Table 4.1.12.3 : Main Phenomena Exhibited in the TMI-2 Accident

Key

* : Main phenomena - : Not Measured U : Unknown Y : Yes N : No or None

AIC : Silver Indium Cadmium B_4C : Boron Carbide Incl : Inconel Zry : Zircaloy

S,D,C : Solid/solid interaction with Zry, Dissolution by Zry, Ceramic melt, for fuel

L,I,H : Low, Intermediate, High (0-33-66-100% for blockage, with 0% the initial bundle state) V,LV : Volatile (Cs,I_2), Low Volatile (Ba,Sr), for FP Release

Met/Cer/Rem : Metallic, Ceramic, Remelt for crust Frmn/Slmp : Formation, Slump for melt pool

Feature	Description	Comments
Location of Facility/ Objectives	IPSN/CEA - Cadarache France, SCARABEE experimental reactor	Analysis of severe accidents conditions on fast reactor sub-assemblies characterized by molten pools.
Number of Tests	3	The first test BF1 (molten pool) has a rather fundamental character and is of interest for LWR studies on molten pools.
Duration of Test Series	BF1 : April 1985 BF3 : June 1988	-
Initial fuel characteristics	Solid pack of compact UO_2 fuel	BF1 : No cladding. Pack of fuel biscuits. BF2 : Stacking of circular UO_2 biscuits. BF3 : Intact fuel rods (UO_2 - SS clad).
Heating Method	Fission heating	Neutronic coupling with the experimental reactor.
Control Materials	No	-
Spacer Grids	No	-
Fuel Irradiation (GWd/tU)	0	-
Fluid Input	No fluid injection inside the initial debris bed	External cooling of a crucible using a sodium flow.

Table 4.1.13.1 : SCARABEE BF Test Series - General Information

Feature	Description	Comments
System Pressure (MPa)	BF1: 0.45* BF2: 0.05*	Inside the SS crucible.
Initial Heat-up Rate (K/s)	5	Heat-up of a solid UO_2 pellet bed.
Maximum Temperature (K)	3623 K estimated in BF2	-
Final Cooling	-	Slow in order to avoid a thermal shock.
Notes	(*) cover gas pressure above the pools, at the last power plateau	A secondary objective of BF1 was to study with simulants the fission product migration out of a molten pool. For that purpose ~ 4.3 % in mass of simulants was introduced. Analysis of the corresponding results did not allow so far to drawn firm conclusions on this aspect.

Table 4.1.13.1 : SCARABEE BF Test Series - General Information

Test	Fuel Charact-eristic	Spacer Grids (no.)	Fuel Irradiation (GWD/tU)	Fluid	Pressure (MPa) (System)	Initial Heatup (K/s)	Max. Tempe-rature (K)	Transient Duration (s)	Test Termin-ation	Max. Total Power (kW) [Specific Power] (W/g)	Date of Test
BF1	~ 5 kg of fuel pellets (1)	None	0	Only external cooling of the SS crucible (2)	~ 0.45	~ 4 (3)	3230 (4) ~3700 (5)	3000 (6)	Slow cooling	84.4 [5.9 to 17]	April 85

Table 4.1.13.2 : SCARABEE BF1 Test - Main Experimental Conditions

Key

SS : Stainless Steel

(1) : Packed 7 mm diameter UO_2 pellets with a total initial height of 260 mm

(2) : Outside wall T at bottom of crucible : 523 K to 556 K (end)

(3) : During the first plateau just before UO_2 melting

(4) : Temperature measured at the end of first power plateau

(5) : Temperature estimated at the end of last power plateau (6th)

(6) : Transient duration above 3000 K

Test	Thermal Response	UO_2 Debris Melting	Pool Height Evolution	Heat Flux Distribution	Flux Concentration Factor	Debris Dome Formation over the Pool	Wall Erosion of Crucible	Crust Formation on Walls
BF1	Y*	Y*	Y	Y* (1)	Y (2)	Y	Low	Y*

Table 4.1.13.3 : Main Phenomena Exhibited in the SCARABEE BF1 Experiment

Key

* : Main phenomena - : Not Measured U : Unknown Y : Yes N : No or None

Low : < 0.2 mm

(1) : Lateral, bottom, top crucible surfaces

(2) : Ratio of the maximum flux to the average flux

Feature	Description	Comments
Location of Facility/ Objectives	ACRR-DC (Dry Debris Bed Coolability and Melt Dynamics Programme) Sandia National Laboratories (SNL) Albuquerque, New Mexico, USA	The ACRR-DC (Annular Core Research Reactor Dry Capsule) experiment programme was part of an internationally sponsored research programme into severe accident behaviour, conducted for the U.S. Nuclear Regulatory Commission (USNRC). The objectives of the DC programme were to investigate the heatup and melt of dry reactor core debris to determine the thermal conductivity and melting kinetic behaviour of debris beds and dynamics of the formation and thermal characteristics of molten ceramic and/or metallic molten pools.
Number of Tests	2	-
Duration of Test Series	1982 to 1985	-
Debris Bed	DC-1 2.14 kg UO_2 DC-2 1.54 kg UO_2 + 0.51 kg SS	The DC experimental test section consisted of an enriched UO_2 (or UO_2 + Stainless Steel) debris bed contained in a tungsten crucible insulated in the radial direction and actively cooled at the top and bottom surfaces. The test section was enclosed in a steel containment structure and fission heated in the ACRR.
Number of Rods/ Heated Length (m)	none	-
Heating Method	Fission	Fission provided the internal heating source for the debris beds.
Control Materials	SS	Stainless steel incorporated in ST-2.
Spacer Grids	none	-
Fuel Irradiation (GWD/tU)	none	Fresh UO_2 fuel materials were used in the DC tests.
Fluid Input	none	The ambient environment in the DC tests was argon gas.

Table 4.1.14.1 : ACRR-DC Test Series - General Information

Feature	Description	Comments
System Pressure (MPa)	0.034	-
Fuel Rod Internal Fill Pressure (MPa)	N/A	-
Initial Heatup Rate (K/s)	0.1	The heating profile in the DC tests was a stair-stepped profile with periods of rapid heating and periods of a steady temperature hold. The average heatup rate is quoted.
Maximum Temperature (K)	~ 3400 DC-1 2600 DC-2	-
Final Cooling	slow cooldown	-
Notes	-	-

Table 4.1.14.1 : ACRR-DC Test Series - General Information

Test	Number of Rods (Fuel/ Abs)	Spacer Grids (no.)	Fuel Irradiation (GWD/tU)	Fluid	Pressure (MPa) (System/ Rod)	Initial Heat-up (K/s)	Max. Tempe-rature (K)	Transient Duration (s) *	Test Termin -ation	Special Condi-tion	Date of Test
DC1	0/0	none	0	Ar	0.034	0.1	3400	3600	S	N	May83
DC2	0/0	none	0	Ar	0.034	0.1	2600	3600	S	N	May84

Table 4.1.14.2 : ACRR-DC Test Series - Main Experimental Conditions

Key

AIC	: Silver Indium Cadmium	B_4C	: Boron Carbide	Incl	: Inconel	Zry	: Zircaloy
Ar	: Argon	Stm	: Steam	Wtr	: Water	Y	: Yes
S	: Slow (S < 2 K/s)	R	: Rapid	Q	: Quench	N	: No

* : Transient Duration is total time spent over 1100/1500/2100/2800K respectively, up to when there is no further significant change in core state (here taken as 2100K on final cooldown)

Test	Thermal Response	Clad Ballo-oning	Clad Oxida-tion, H_2 Release	Material Interactions and Melting			Partic-ulate Debris	Bloc-kage	Late Phase		FP and Aerosol Release
				Abso-rber	Spacer Grid	Fuel			Crust	Melt Pool	
DC1	Y*	N	N/A	N	N	C*	Y	H*	Y*	Y*	N
DC2	Y*	N	N/A	SS	N	C*, SS	Y	H*	Y*	Y*	N

Table 4.1.14.3 : Main Phenomena Exhibited in the ACRR-DC Experiments

Key

* : Main phenomena - : Not Measured U : Unknown Y : Yes N : No or None

AIC : Silver Indium Cadmium B_4C : Boron Carbide Incl : Inconel Zry : Zircaloy SS : Stainless Steel

S,D,C : Solid/solid interaction with Zry, Dissolution by Zry, Ceramic melt, for fuel

L,I,H : Low, Intermediate, High (0-33-66-100% for blockage, with 0% the initial bundle state) V,LV : Volatile (Cs,I_2), Low Volatile (Ba,Sr), for FP Release

Met/Cer/Rem : Metallic, Ceramic, Remelt for crust Frmn/Slmp : Formation, Slump for melt pool

Feature	Description	Comments
Location of Facility / Objectives	AEKI, Budapest, Hungary	Investigation of early phase melt progression in LWRs for unrecovered and quenched transients, including the effect of air ingress.
Number of Tests	5	Two tests in steam (VVER-440 geometry) and two air ingress tests (Western LWR geometry) have been performed to the end of March 1999. One VVER commissioning test CODEX-1 with alumina pellets was performed initially but data were not recorded so it is not reported here
Duration of Test Series	1995 to date	Programme in progress.
Number of Rods/ Heated Length (m)	9 / 0.6 (PWR), 7 / 0.6 (VVER)	The rod array is surrounded by an insulating shroud with a Zr2%Nb liner, itself surrounded by a permanently-installed high temperature shield. Western PWR-type tests use a square lattice and shroud liner, VVER tests a hexagonal lattice and shroud liner. The high temperature shield is cylindrical.
Heating Method	Electrical	Tungsten resistance heaters are used. All rods are heated apart from the central one.
Control Materials	-	Use of control materials is being considered for future tests.
Spacer Grids	Zircaloy (PWR), stainless steel (VVER)	Two spacer grids (near the top and at the bottom of the heated section in the PWR tests, three grids in the heated section in the VVER tests.
Fuel Irradiation (GWd/tU)	None	Normal UO_2 was used in the VVER tests, and depleted UO_2 was used in the PWR tests, except for the first test CODEX-1 where alumina pellets were used.
Fluid Input	Variable flows of steam, argon, argon/25%oxygen and air	Maximum flows 1.5 g/s steam, 4 g/s hot argon, ~25 g/s cold argon (for fast cooling), 4 g/s hot argon/oxygen, 2.5-4.0 g/s cold air (synthetic – natural).

Table 4.1.15.1 : CODEX Test Series - General Information

Feature	Description	Comments
System Pressure (MPa)	0.15	Maximum value.
Fuel Rod Internal Fill Pressure (MPa)	~ 0.2	The rods are connected together, outside the heated zone, so all have the same internal pressure.
Initial Heat-up Rate (K/s)	0.5 - 0.6	In the first air ingress test AIT1 the air was injected at essentially steady-state (<0.1 K/s), and an oxidation excursion supervened .
Maximum Temperature (K)	2300	This is the highest qualified temperature recorded by thermocouples/pyrometers.
Final Cooling	Variable - by convection to flowing argon, or water quench	One VVER tests with slow cooling in argon (CODEX-2), one VVER test in two steps (3/1 and 3/2) both with water quench, two air ingress tests with fast cooldown in argon (AIT1 and AIT2).
Notes	-	The air ingress experiments incorporate aerosol measurements in the offgas line; number and size distribution on-line, chemical composition off-line.

Table 4.1.15.1 : CODEX Test Series - General Information

Test	Number of Rods (Fuel/ Abs)	Spacer Grid (no.)	Fuel Irrad-iation (GWD/tU)	Fluid	Pressure (MPa) (System /rod)	Initial Heat-up (K/s)	Maximum Tempera-ture (K)	Transient Duration (s) *	Test Termin-ation	Special Condition	Date of Test
2	7	SS(3) hex	None	Ar/Stm	0.21/0.22	0.55	2300	2500/120 0/200/0	S(Ar)	N	29Dec95
3/1	7	SS(3) hex	None	Ar/Stm	0.21/0.22	0.6	1450	730/0/0/0	Q(Wtr)	N	28Nov96
3/2	7	SS(3) hex	None	Ar/Stm	0.21/0.22	0.6	1900	1250/350/ 0/0	Q(Wtr)	pre-ox ~50µm oxide in Stm	29Jan97
AIT1	9	Zry(2)	None	Ar/O_2, Air	0.21/0.22	excursion in Ar/O_2, <0.1 in air	2300 in Ar/O_2 and in air	1250/350/ 0/0	R(Ar)	pre-ox 50-150µm oxide (est.) in Ar/O_2	7May98
AIT2	9	Zry(2)	None	Ar/Stm, Air	0.21/0.22	0.5	(>2200 in air)	1250/350/ 0/0	R(Ar)	pre-ox ~20µm oxide in Stm	28Jan99

Table 4.1.15.2 : CODEX Test Series - Main Experimental Conditions

Key

AIC	: Silver Indium Cadmium	B_4C	: Boron Carbide	Incl	: Inconel	Zry	: Zircaloy	SS	: Stainless Steel
Ar	: Argon	Stm	: Steam	Wtr	: Water	Y	: Yes	hex	: hexagonal grid
S	: Slow (S < 2 K/s)	R	: Rapid	Q	: Quench	N	: No		(otherwise square)

* : Transient Duration is total time spent over 1100/1500/2100/2800K respectively, up to when there is no further significant change in core state (here taken as 2100K on final cooldown)

Test	Thermal Response	Clad Ballo-oning	Clad Oxida-tion, H_2 release	Material Interactions and Melting			Partic-ulate Debris	Bloc-kage	Late Phase		FP and Aerosol Release
				Abso-rber	Spacer-Grid	Fuel			Crust	Melt Pool	
2	Y*	N	H* H_2	-	SS	D	N	I	N	N	-
3/1	Y*	N	I (L in qnch*), H_2	-	SS	L	N	N	N	N	-
3/2	Y*	N	H (L in qnch*), H_2	-	SS	D	N	I	N	N	-
AIT1	Y*	N	H, no H_2, ZrN in air phase	-	Zry	L	N	N	N	N	-
AIT2	Y*	N	H*, (H_2 in preox), ZrN in air phase	-	Zry	D	Y	I	N	N	(U-bearing aerosol in air phase, as UO_2)

Table 4.1.15.3 : Main Phenomena Exhibited in the CODEX Experiments

Key

* : Main phenomena - : Not Measured U : Unknown Y : Yes N : No or None

AIC : Silver Indium Cadmium B_4C : Boron Carbide Incl : Inconel Zry : Zircaloy SS : Stainless Steel

S,D,C : Solid/solid interaction with Zry, Dissolution by Zry, Ceramic melt, for fuel ZrN : zirconium nitride formed

L,I,H : Low, Intermediate, High (0-33-66-100% for blockage, with 0% the initial bundle state) V,LV : Volatile (Cs,I_2), Low Volatile (Ba,Sr), for FP Release

Met/Cer/Rem : Metallic, Ceramic, Remelt for crust Frmn/Slmp : Formation, Slump for melt pool

Feature	Description	Comments
Location of Facility/ Objectives	FZ Karlsruhe, Germany	Investigation of the physico-chemical behaviour of overheated water reactor fuel elements in rod-like geometry under different flooding conditions.
Number of Tests	5	Commissioning and three main tests have been performed to the end of June 1999.
Duration of Test Series	09Oct97 (commissioning tests started) to date	Programme in progress.
Number of Rods/ Heated Length (m)	21 / 1.0	The main rod array is surrounded by an insulating shroud with a Zircaloy liner, itself surrounded by a permanently-installed cylindrical high temperature shield. In addition, a small solid rod is positioned in three of the corners of the rod array (for estimation of pre-oxidation), with a hollow instrumentation tube in the fourth.
Heating Method	Electrical	Tungsten resistance heaters used. All the main rods are heated except for the one in the centre of the square array.
Control Materials	-	Use of PWR and BWR control material is being considered for future tests.
Spacer Grids	Inconel and Zircaloy	5 grids are used in each test (4 in the commissioning test), one of Inconel below the heated section, two of Zircaloy in the heated section, and two of Zircaloy above the heated section (one in the commissioning test).
Fuel Irradiation (GWD/tU)	Not applicable	Sintered zirconia pellets are used.
Fluid Input	Steam flow - trace to 50 g/s (during steam cooling)	Argon used in addition to the steam flow (typical mass ratio 1:1 in the heat-up and pre-oxidation phases).

Table 4.1.16.1 : QUENCH Bundle Test Series - General Information

Feature	Description	Comments
System Pressure (MPa)	0.2	Tests at higher system pressures are being considered for the forward programme, up to the maximum permitted level of 1MPa.
Fuel Rod Internal Fill Pressure (MPa)	0.22	From test 02 onwards a trace of krypton (5%) is used in the argon fill gas to enable detection of cladding breach.
Initial Heatup Rate (K/s)	0.45 to 1.3	-
Maximum Temperature (K)	≤1750 to 2470	These are maximum recorded temperatures. The range of maximum temperature at onset of quench initiation is 1750 to 1970K
Final Cooling	Water quench and injected cold steam	The water enters the inlet of the test section at about 395K, i.e. saturation temperature at 0.2MPa. One test has been performed with rapid cooling by cold steam at 570K, and more such tests are envisaged.
Notes		The bundle tests are supported by extensive programmes of single rod tests (both water quench and steam cooling), and of separate-effects hydrogen absorption/release measurements

Table 4.1.16.1 : QUENCH Bundle Test Series - General Information

Test	Number of Rods (Fuel/ Abs)	Spacer Grids (no.)	Fuel Irradiation (GWD/tU)	Fluid	Pressure (MPa) (System/ Rod)	Initial Heat-up (K/s)	Max. Tempe-rature (K)	Transient Duration (s) *	Test Termin -ation	Special ondi-tion	Date of Test
00	21	Incl(1) Zry(3)	(ZrO_2 pellets)	Ar, Stm	0.2/0.22	1.0	≤1750	18784/265/ 0/0	Q(Wtr)	pre-ox ≤ 500µm oxide	9-16Oct97
01	21	Incl(1) Zry(4)	(ZrO_2 pellets)	Ar, Stm	0.2/0.22	0.5	≤1870	4260/535/ 0/0	Q(Wtr)	pre-ox ≤ 300µm oxide	26Feb98
02	21	Incl(1) Zry(4)	(ZrO_2 pellets)	Ar, Stm	0.2/0.22	0.45-0.9	2470	1470/260/ 120/0	Q(Wtr)	without pre-ox	07Jul98
03	21	Incl(1) Zry(4)	(ZrO_2 pellets)	Ar, Stm	0.2/0.22	0.4-1.3	2470	1200/600/ 150/0	Q(Wtr)	without pre-ox	20Jan99
04	21	Incl(1) Zry(4)	(ZrO_2 pellets)	Ar, Stm	0.2/0.22	0.5-1.5	2350	1200/400/ 15/0	Q(Stm)	without pre-ox	30Jun99

Table 4.1.16.2 : QUENCH Bundle Test Series - Main Experimental Conditions

Key

AIC	: Silver Indium Cadmium	B_4C	: Boron Carbide	Incl	: Inconel	Zry	: Zircaloy
Ar	: Argon	Stm	: Steam	Wtr	: Water	Y	: Yes
S	: Slow (S < 2 K/s)	R	: Rapid	Q	: Quench	N	: No

blade : BWR control blade simulator consisting of Zircaloy channel box walls and a control blade simulator (stainless steel plus typically 9 B_4C-loaded rodlets)

* : Transient Duration is total time spent over 1100/1500/2100/2800K respectively, up to when there is no further significant change in core state (here taken as 2100K on final cooldown)

Test	Thermal Response	Clad Ballo-oning	Clad Oxida-tion, H_2 Release	Material Interactions and Melting			Partic-ulate Debris	Bloc-kage	Late Phase		FP Release
				Abso-rber	Spacer Grid	Fuel			Crust	Melt Pool	
00	Y*	N	H (L in qnch*)	-	N	N	(Y$)	N	N	N	-
01	Y*	N	H (L in qnch*)	-	N	N	N	N	N	N	-
02	Y*	N	H (H in qnch*)	-	Zry	(Y#)	(Y$)	I	N	Y	-
03	Y*	N	H (H in qnch*)	-	Zry	(Y#)	(Y$)	I	N	Y	-
04	Y*	N	H (H in qnch*)	-	N	N	(Y$)	N	N	N	-

Table 4.1.16.3 : Main Phenomena Exhibited in the QUENCH Bundle Test Series

Key

* : Main phenomena - : Not Measured U : Unknown Y : Yes N : No or None

AIC : Silver Indium Cadmium B_4C : Boron Carbide Incl : Inconel Zry : Zircaloy

: Melting of Zry cladding $: By shattering, during quench

S,D,C : Solid/solid interaction with Zry, Dissolution by Zry, Ceramic melt, for fuel

L,I,H : Low, Intermediate, High (0-33-66-100% for blockage, with 0% the initial bundle state) V,LV : Volatile (Cs,I_2), Low Volatile (Ba,Sr), for FP Release

Met/Cer/Rem : Metallic, Ceramic, Remelt for crust Frmn/Slmp : Formation, Slump for melt pool

Feature	Description	Comments
Location of Facility / Objectives	EC-JRC-Ispra, Italy	Investigate core melt/water/structure interactions with large quantities of prototypical UO_2-based corium and core melt spreading
Number of Tests	14	12 FCI tests; 2 spreading tests. All tests performed.
Duration of Test Series	1991-1999	Facility closed mid-1999.
Melt Composition	80wt%UO_2 - 20wt%ZrO_2	77wt%UO_2 - 19wt%ZrO_2 - 4wt%Zr in one test (L-11).
Melt Mass	Up to 200 kg	Maximum proven capacity of the FARO furnace: 300 kg.
Melt Temperature	Up to 3300 K	Melt temperature measured by tungsten ultrasonic sensor developed and manufactured at JRC-Ispra.
Heating Method	Direct electrical heating	3 power supplies from 3000V/2A to 60V/15000A.
Pouring Conditions	Gravity	Jet diameters of 50 and 100 mm in FCI tests; 30 mm in spreading tests.
System Pressure	0.2 to 5.8 MPa	Cover gas mainly steam in saturated water tests, argon in subcooled water tests.
Water Temperature	300 to 540 K	Nearly saturated (in-vessel) and subcooled (ex-vessel) conditions.
Test Section Diameter	0.71 m	In FCI tests L-27 to L-33, the diameter of the housing vessel (FAT) was 1.5 m. The annular gap between the test section and the housing vessel was gas.
Water Depth	0.87 to 2 m	One spreading test in dry conditions (L-26s) and one with a 10 mm water layer on the spreading surface (L-32s).
External Trigger	No	External trigger applied in the last test of the series only (L-33).

Table 4.1.17.1 : FARO LWR Test Series - General Information

Test	Corium Compo -sition	Melt Mass (kg)	Melt Temp. (K)	Release Diameter (mm)	Melt Fall Height in Gas (m)	System Pressure (MPa)	Gas Phase	Water Depth (m)	Water Temper-ature (K)	Water Subcool-ing (K)	Water Mass (kg)	Date of Test
L-06	A	18	2923	100	1.83	5	Stm/Ar	0.87	539	0	120	02Dec91
L-08	A	44	3023	100	1.53	5.8	Stm/Ar	1.00	536	12	255	29Jul92
L-11	B	151	2823	100	1.09	5	Stm/Ar	2.00	535	2	608	02Dec93
L-14	A	125	3123	100	1.04	5	Stm/Ar	2.05	537	0	623	23Jun94
L-19	A	157	3073	100	1.99	5	Stm (1)	1.10	536	1	330	22Jun95
L-20	A	96	3173	100	1.12	2	Stm	1.97	486	0	660	30Jan96
L-24	A	177	3023	100	1.07	0.5	Stm	2.02	425	0	719	05Dec96
L-27	A	129	3023	100	0.73	0.5	Stm	1.47	424	1	536	03Dec97
L-28	A	175	3052	50	0.89	0.5	Stm	1.44	424	1	517	02Apr98
L-29	A	39	3070	50	0.74	0.2	Ar	1.48	297	97	492	02Jul98
L-31	A	92	2990	50	0.77	0.2	Ar	1.45	291	104	481	11Nov98
L-33	A	100 (2)	3070	50	0.77	0.4	Ar	1.60	293	124	625	01Jul99
L-26s	A	160	2950	30	-	0.1	Ar	-	-	-	-	02Jul97
L-32s	A	130	3200	30	-	0.1	Ar	0.01	297	76	6	16Mar99

Table 4.1.17.2 : FARO LWR Test Series - Main Experimental Conditions

Key

A: 80wt% UO_2 - 20wt% ZrO_2, B: 77wt% UO_2 - 19wt% ZrO_2 - 4wt% Zr

Ar: argon Stm: steam

(1): >95wt% steam; <5wt% argon (2): 25 kg of melt pouerd into water at time of trigger

Test	Melt Jet Break-up	Melt Quenching Rate	Debris Bed Formation and Characteristics	Thermal Load on Collecting Structure	Steam Explosion	Hydrogen Production	Ex-vessel Melt Spreading Behaviour
L-06	Yes	Yes	Yes	Yes	No (1)	No	No
L-08	Yes	Yes	Yes	Yes	No	No	No
L-11	Yes	Yes	Yes	Yes	No	Yes	No
L-14	Yes	Yes	Yes	Yes	No	No	No
L-19	Yes	Yes	Yes	Yes	No	Yes (2)	No
L-20	Yes	Yes	Yes	Yes	No	Yes	No
L-24	Yes	Yes	Yes	Yes	No	Yes	No
L-27	Yes	Yes	Yes	Yes	No	Yes	No
L-28	Yes	Yes	Yes	Yes	No	Yes	No
L-29	Yes	Yes	Yes	Yes	No	Yes	No
L-31	Yes	Yes	Yes	Yes	No	Yes	No
L-33	Yes	Yes	Yes	Yes	Yes	Yes	No
L-26s	No	No	Yes	Yes	No	No	Yes
L-32s	No	No	Yes	Yes	No	No	Yes

Table 4.1.17.3 : Main Phenomena Exhibited in the FARO LWR Experiments

Key

(1): Not steam explosion tests, but data showed that spontaneous explosion did not occur in the test conditions

(2): Significant hydrogen production with oxidic melt evidenced and evaluated from tests L-19

Feature	Description	Comments
Location of Facility / Objectives	EC-JRC-Ispra, Italy	Investigate all the phases of steam explosion, assess energetics.
Number of Tests	28	15 alumina and 13 corium.
Duration of Test Series	1991-1999	Prior to 1991, tests with tin were performed
Melt Composition	80w%UO_2 - 20w%ZrO_2 Al_2O_3	Corium Alumina
Melt Mass	Up to 6 kg	Dependent on melt composition, crucible volume max. ~1 litre.
Melt Temperature	Up to 3200 K	Melt temperature measured by bi-colour pyrometer.
Heating Method	Thermal radiation	200 kW three phase with tungsten heater elements.
Pouring conditions	Gravity	Jet diameter of 30 mm, fall height from ~0.4 m-6 m.
System Pressure	0.1 to 0.4 MPa	Cover gas He.
Water Temperature	290-373 K	Nearly saturated and highly subcooled conditions.
Test Section Diameter	0.095 and 0.2 m	First 5 alumina and first 4 corium tests with 0.095 m, rest with 0.2 m dia.
Water Depth	0.88 to 1.1 m	
External Trigger	Yes	Gas or explosive as a driving mechanism

Table 4.1.18.1 : KROTOS Test Series - General Information

Test	Compo-sition	Melt Mass (kg)	Melt Temper-ature (K)	Release Diameter (mm)	System Pressure (MPa)	Gas Phase	Water Depth (m)	Water Temper-ature (K)	Water Subcool-ing (K)	Water Mass (kg)	Ext. Trigger	Date of Test
K-26	A	1.4	2573	30	0.1	He	1.12	333	40	7.2	yes	05Jun91
K-27	A	1.4	2623	30	0.1	He	1.12	361	12	7.2	no	02Oct91
K-28	A	1.4	2673	30	0.1	He	1.12	360	13	7.2	yes	28Nov91
K-29	A	1.5	2573	30	0.1	He	1.08	293	80	7.7	no	03Jun92
K-30	A	1.5	2573	30	0.1	He	1.08	293	80	7.5	no	02Jul92
K-32	C	3.0	3063	30	0.1	He	1.08	351	22	7.1	no	01Sep93
K-33	C	3.2	3063	30	0.1	He	1.08	298	75	7.7	no	21Oct93
K-35	C	3.1	3023	30	0.1	He	1.08	363	10	7.7	yes	21Apr94
K-36	C	3.0	3025	30	0.1	He	1.08	294	79	7.7	yes	02Jun94
K-37	C	3.2	3018	30	0.1	He	1.11	296	77	33.9	yes	02Aug94
K-38	A	1.5	2665	30	0.1	He	1.11	294	79	34.0	no	03Oct94
K-40	A	1.5	3073	30	0.1	He	1.11	290	83	34.6	no	26Feb95
K-41	A	1.4	3073	30	0.1	He	1.11	368	5	33.4	no	13Apr95
K-42	A	1.5	2465	30	0.1	He	1.11	293	80	34.6	no	24May95

Table 4.1.18.2 : KROTOS Test Series - Main Experimental Conditions

Key

A: Al_2O_3 C: 80wt%UO_2 - 20wt%ZrO_2 He: helium

Test	Compo-sition	Melt Mass (kg)	Melt Temper-ature (K)	Release Diameter (mm)	System Pressure (MPa)	Gas Phase	Water Depth (m)	Water Temper-ature (K)	Water Subcool-ing (K)	Water Mass (kg)	Ext. Trigger	Date of Test
K-43	A	1.5	2625	30	0.21	He	1.11	296	100	34.6	no	07Jul95
K-44	A	1.5	2673	30	0.1	He	1.12	363	10	33.2	yes	12Oct95
K-45	C	3.1	3106	30	0.1	He	1.14	369	4	34.0	yes	12Dec95
K-46	C	5.4	3086	30	0.1	He	1.11	290	83	34.0	yes	15Feb96
K-47	C	5.4	3023	30	0.1	He	1.11	291	82	34.0	yes	28Mar96
K-49	A	1.5	2688	30	0.37	He	1.11	294	120	34.0	no	12Jul96
K-50	A	1.7	2473	30	0.1	He	1.11	360	13	33.7	no	29Aug96
K-51	A	1.8	2748	30	0.1	He	1.11	368	5	33.5	no	10Nov96
K-52	C	2.6	3133	30	0.2	He	1.11	290	102	34.0	yes	13Dec96
K-53	C	3.6	3129	30	0.36	He	1.11	290	122	34.0	yes	25Mar97
K-56	C	4.5	3033	30	0.37	He	0.98	290	123	35.1	no	13Nov97
K-57	A	1.4	2670	30	0.1	He	1.03	290	83	36.6	no	12Dec97
K-58	C	4.5	3077	30	0.37	He	0.92	289	125	30.9	yes	03Mar98
K-63	C	4.5	n.a.	30	0.21	He	0.94	295	99	29.6	yes	27Jul99

Table 4.1.18.2 : KROTOS Test Series - Main Experimental Conditions

Key

A: Al_2O_3 C: 80wt%UO_2 - 20wt%ZrO_2 He: helium

Test	Spontaneous Explosion	Triggered Explosion or Interaction	Debris Bed Formation and Characteristics
K-26	No	Yes	Yes
K-27	No	No	Yes
K-28	No	Yes	Yes
K-29	Yes	No	Yes
K-30	Yes	No	Yes
K-32	No	No	Yes
K-33	No	No	Yes
K-35	No	No	Yes
K-36	No	Yes	Yes
K-37	No	No	Yes
K-38	Yes	No	Yes
K-40	Yes	No	Yes
K-41	No	No	Yes
K-42	Yes	No	Yes

Test	Spontaneous Explosion	Triggered Explosion or Interaction	Debris Bed Formation and Characteristics
K-43	Yes	No	Yes
K-44	No	Yes	Yes
K-45	No	No	Yes
K-46	No	Yes	Yes
K-47	No	Yes	Yes
K-49	Yes	No	Yes
K-50	No	No	Yes
K-51	No	No	Yes
K-52	No	Yes	Yes
K-53	No	Yes	Yes
K-56	No	No	Yes
K-57	No	No	Yes
K-58	No	Yes	Yes
K-63	No	Yes	Yes

Table 4.1.18.3 : Main Phenomena Exhibited in the KROTOS Experiments

Insti-tute	Facility	Test No.	Number of Rods (Fuel/ Abs) {unpr.}	Heated Length (m)	Heating Method	Pressure (MPa) (System/ Rod)	Atmos-phere	Initial Heat-up (K/s)	Burst Tempe-rature (K)	Burst Strain Range (%) (mean)	Date
KfK	REBEKA	5	49	3.9	electric	0.45/6.00	stm/2pc	7	1048-1073	39-88(49)	<1983
KfK	REBEKA	6*	49{2$}	3.9	electric	0.45/6.00	stm/2pu	7	1038-1063	32-64(42)	<1984
KfK	REBEKA	7	49	3.9	electric	0.45/6.00	stm/2pu	7	1028-1063	42-87(55)	1984
CEA	PHEBUS	215P	25	0.8	fission	V/4.00	stm	8	1073-1133	20-54(38)	1982
CEA	PHEBUS	215R	25	0.8	fission	V/4.00	stm	8	1073-1133	20-50(38)	1983
CEA	PHEBUS	216	25	0.8	fission	V/3.00	stm	8	1173	20-30	1983
CEA	PHEBUS	218*	25{2$}	0.8	fission	V/3.35	stm	8	1123	14-27(20)	1984
CEA	PHEBUS	219	25	0.8	fission	V/3.00	stm	8	1153	19-46(28)	1984
AECL	NRU	MT3	32{20}	3.66	fission	0.2/3.80	stm/2pu	7	1049-1088	38-94(55)	1981
AECL	NRU	MT4	32{20}	3.66	fission	0.2/4.62	stm	7	1033-1200	53-99(72)	1982
ORNL	MRBT	B3	16	0.915	electric	0.2/11.6	stm	9.5	1020-1052	42-77	1978
ORNL	MRBT	B5	64	0.915	electric	0.2/11.6	stm	9.8	1033-1057	32-95	1980
ORNL	MRBT	B6	64	0.915	electric	0.2/3.2	stm	3.5	1192-1210	21-56	1981

Table 4.2.1: Clad Ballooning Experiments

Key

stm : steam 2pc : 2-phase countercurrent 2pu : 2-phase unidirectional $: instrument tube

V : pressure varies (LOCA simulation) @ : includes irradiated rods

* : REBEKA-6 was selected for ISP-14; PHEBUS 218 was selected for ISP-19

Insti-tute	Facility	Test No.	Number of Rods (Fuel/ Abs) {unpr.}	Heated Length (m)	Heating Method	Pressure (MPa) (System/ Rod)	Atmos-phere	Initial Heat-up (K/s)	Burst Tempe-rature (K)	Burst Strain Range (%) (mean)	Date
JAERI	bundle	13	49	0.85	electric	0.1/4.9	stm	~0.7	1038-1073	(~60)	<1983
JAERI	bundle	17	49	0.85	electric	0.1/4.9	stm	7.6	1048-1118	(~60)	<1983
JAERI	bundle	24	45/4	0.85	electric	0.1/4.9	stm	7.0	1008-1173	(~60)	<1983
INEL	PBF/LOC	3	4@	0.91	fission	2.4-4.9	stm	4-20	1110-1300	20-42	1979
INEL	PBF/LOC	5	4@	0.91	fission	2.4-4.9	stm	0-100	1160-1350	19-48	1979
INEL	PBF/LOC	6	4@	0.91	fission	2.4-4.8	stm	0-100	1066-1098	31-74	1980
AEKI	bundle	6	7	0.15	electric	0.1/5.5	stm	1.2	1143-1173	18-37	1999
AEKI	bundle	8	7	0.15	electric	0.1/2.0	stm	0.6	1073-1173	24-30	1999

Table 4.2.1: Clad Ballooning Experiments

Key

stm : steam 2pc : 2-phase countercurrent 2pu : 2-phase unidirectional $: instrument tube

V : pressure varies (LOCA simulation) @ : includes irradiated rods

* : REBEKA-6 was selected for ISP-14; PHEBUS 218 was selected for ISP-19

Reaction System	Facility/ Institute	Geometry/ Size	Heating Method	Press-ure (MPa)	Atmos-phere	Materials Used	Tempe-rature (K)	Reaction Time (s)	Special Condition	Date
Zry/stm	ANL	wire	cap. disch.	0.1	(water)	Zr Zry-3	1373-2125	*	heating in water	< 1962
Zry/stm	AECL	tube	induc-tion	0.1	steam	Zry-2 Zry-4	1323-2123	up to 7100	-	< 1978
Zry/stm	ORNL	tube	infra-red	0.1/ 3.45-10.34	steam	Zry-4	1173-1773/ 1173-1373	8-2089/ 35-2711	-	< 1979
Zry/stm	KfK	tube	resis-tance	0.1	steam	Zry-4	873-1873	120-90000	-	< 1982
Zry/stm	BMI/ PNL	disc	laser	0.1	steam	Zry-4	1573-2673	-	-	< 1985
Zry/stm	AEA/ SNPDL	tube	resis-tance	0.1	steam	Zry-4	873-1573	60-8000	Variation of Zry-4 types	1986/ 88
Zry/stm	AEA/ RNL	tube	resis-tance	0.1-18.6	steam	Zry-4	1023-1273	240-2500	-	1991/ 92

Table 4.2.2.1: Material Oxidation Experiments

Key

AIC : Silver Indium Cadmium B_4C : Boron Carbide Incl : Inconel Zry : Zircaloy SS : Stainless Steel

qtz : quartz stm : steam vpm : volum parts per million * : reaction times <1s

Reaction System	Facility/ Institute	Geometry/ Size	Heating Method	Press-ure (MPa)	Atmos-phere	Materials Used	Tempe-rature (K)	Reaction Time (s)	Special Condition	Date
Zry/stm	JAERI	tube	resis-tance/ infra-red furnace	0.1	steam, steam/Ar, steam/H_2	Zry-4	1273-1763	120-14400	Effect of steam starvation	< 1989
Zr1%Nb /stm	AEKI	tube	resis-tance	0.1	steam	Zr1%Nb	1173-1473	100-10000	Measurement on of H uptake	1991/ 94
SS/stm	GE/ Ohio	cylinder	resis-tance	0.1	steam	SS 304L	1273-1648	240-7200	Comparison with air oxidation	< 1969
SS/stm	ANL	fuel rod	resis-tance	0.1-1.1	steam	SS 304	1773-1873	600-10800	variation with steam flowrate	1964/ 67
B_4C/stm	UC/ Ohio	0.5g B_4C powder 1 mm deep on Pt disk	electric furnace	0.1	stm/Ar, air/Ar	B_4C surf-ace area 0.44m^2/g	470-1020	to 10hr	continuous weight measurement	1963
B_4C/stm	BMI/ PNWL	borated graphite, 7x13x3 mm parellipipeds	tube furnace	0.1	He / stm (5e3-3e4 vpm)	5wt% B	1100-1200	to 150min	continuous weight measurement	1969

Table 4.2.2.1: Material Oxidation Experiments

Key

AIC : Silver Indium Cadmium B_4C : Boron Carbide Incl : Inconel Zry : Zircaloy SS : Stainless Steel

qtz : quartz stm : steam vpm : volum parts per million * : reaction times <1s

Reaction System	Facility/ Institute	Geometry/ Size	Heating Method	Press-ure (MPa)	Atmos-phere	Materials Used	Tempe-rature (K)	Reaction Time (s)	Special Condition	Date
B_4C/stm	SNL	B_4C coupons 38x1.5x7 mm, and particle bed	reaction tube	0.1	620 torr stm	particle D = 0.8-3.0 mm	1270	to 390min	offgas analysis	1987
B_4C/stm	NKA	B_4C samples, 3x11x15 mm	resis-tance	low (as stm pr)	stm pr 3.19-14.5 mbar	pure B_4C placed on SS slabs	1097-1328	~3-5hr	low pressure	1990
B_4C/stm	JAERI	B_4C and B_4C+graphite pellets, Dxh = 10x10 mm	tubular reaction furnace	0.1	He/0.65% water vapour	B content 30, 40, 50% and pure B_4C (78%)	823-1273	to 9hr	offgas analysis	1992
B_4C/stm	STUK + VTT	(1) ~1g B_4C powder, (2) ~1g B_4C pellets, Dxh = 7.5x13.8 mm	electric heating	0.1	(1) stm/Ar, (2) stm/Ar, and 50%stm 50%H_2	prototypic EdF pellets	(1) 1073 (2) 1273	~1hr	offgas analysis, emphasis on methane formation	1997/ 98

Table 4.2.2.1: Material Oxidation Experiments

Key

AIC : Silver Indium Cadmium B_4C : Boron Carbide Incl : Inconel Zry : Zircaloy SS : Stainless Steel

qtz : quartz stm : steam vpm : volum parts per million * : reaction times <1s

Reaction System	Facility/ Institute	Geometry/ Size	Heating Method	Press-ure (MPa)	Atmos-phere	Materials	Tempe-rature (K)	Reaction Time (s)	Special Condition	Date
AIC/SS	KfK	SS-crucible: D = 6/11 mm AIC: 1.8 g	electric	0.1	Ar	AISI 316 80Ag/15In/ 5Cd	1673-1723	1200	SS melting	< 1990
AIC/Zry	KfK	Zry-crucible: D = 6/11 mm AIC: 1.8 g	electric	0.1	Ar	Zry-4 80Ag/15In/ 5Cd	1273-1473	60-1800	preoxidised Zry (0,10 µm oxide)	< 1990
SS/Zry	KfK	Zry-crucible: D = 6/11 mm SS: 1.5 g	electric	0.1	Ar	AISI 316 Zry-4	1273-1473	60-1800	preoxidised Zry (0, 10-100 µm oxide)	< 1990
SS/Zry	KfK	Zry-crucible: D = 6/11 mm SS: 1.5 g	electric	0.1	Ar	AISI 316 Zry-4	1273-1673	60-18000	preoxidised Zry (0,10,20,50 µm oxide)	1992
SS/ Zr1%Nb	AEKI	quartz tube: Zr: D = 9 mm, h = 4 mm SS: D = 9 mm, h = 4 mm	electric	1.0e-10	Vacu-um	X18H10T Zr1%Nb	1333-1453	30-3000	preoxidised Zr1%Nb (0,3,9,30 µm oxide)	1991/ 94

Table 4.2.2.2: Structural Material Interaction Experiments

Key

AIC : Silver Indium Cadmium B_4C : Boron Carbide Incl : Inconel Zry : Zircaloy SS : Stainless Steel
qtz : quartz irr. : irradiated unirr. : unirradiated

Reaction System	Facility/ Institute	Geometry/ Size	Heating Method	Press-ure (MPa)	Atmos-phere	Materials	Tempe-rature (K)	Reaction Time (s)	Special Condition	Date
Incl/Zry	KfK	Zry-crucible: D = 6/11 mm Incl: 1.5 g	electric	0.1	Ar	Incl 718 Zry-4	1273-1473	60-18000	Preoxidised (0,20,45 µm oxide)	1992
B_4C/SS	KfK	SS-crucible: D = 6/11 mm B_4C: 0.5 g	electric	0.1	Ar	AISI 316 B_4C powder 180-250 µm	1073-1473	6000-1.0e+6	Completely liquified at 1523 K	1989
B_4C/SS	AEKI	SS-crucible: D = 7.6/9.1 mm B_4C: D = 7.6 mm, h = 10 mm	electric	0.1	Ar	X18H10T B_4C pellet	1073-1473	1800-90000	Completely liquified at 1538 K	1991/ 94
B_4C/Zry	KfK	Zry-crucible: D = 6/11 mm B_4C:	electric	0.1	Ar	Zry-4 B_4C powder 180-250 µm	1073-1873	300-1.0e+6	Completely liquified at 1923 K	1989
B_4C/ Zr1%Nb	AEKI	Zr1%Nb-crucible: D = 7,6/9.1 mm B_4C: D = 7.6 mm, h = 10 mm	electric	0.1	Ar	Zr1%Nb B_4C pellet	1473-1873	300-90000	Completely liquified at 1913 K	1991/ 94

Table 4.2.2.2: Structural Material Interaction Experiments

Key

AIC : Silver Indium Cadmium B_4C : Boron Carbide Incl : Inconel Zry : Zircaloy SS : Stainless Steel

qtz : quartz irr. : irradiated unirr. : unirradiated

Reaction System	Facility/ Institute	Geometry/ Size	Heating Method	Press-ure (MPa)	Atmos-phere	Materials	Tempe-rature (K)	Reaction Time (s)	Special Condition	Date
Ag/Zry	JAERI	qtz-crucible: D = 12 mm Zry: D = 10 mm, h = 5 mm Ag: 3 g	electric	0.1	Ar	Zry-4 Ag	1273-1473	30-7200	-	1992
AIC/Zry	JAERI	qtz-crucible: D = 12 mm Zry: D = 10 mm, h = 5 mm AIC: 3 g	electric	0.1	Ar	Zry-4 80Ag/15In/ 5Cd	1273-1473	30-7200	-	1992
SS/Zry	JAERI	Zry-crucible: D = 8/16 mm SS: D = 8 mm, h = 5 mm	Electric infrared	0.1	Ar	SS 304 Zry-4	1273-1573	30-28800	preoxidised Zry (0,10,50 µm oxide)	1995
Incl/Zry	JAERI	Zry-crucible: D = 8.5/16 mm Incl: D = 8.5 mm, h = 5 mm	Electric infrared	0.1	Ar	Incl 718 Zry-4	1248-1523	30-28800	preoxidised Zry (0,10,50 µm oxide)	1995

Table 4.2.2.2: Structural Material Interaction Experiments

Key

AIC : Silver Indium Cadmium B_4C : Boron Carbide Incl : Inconel Zry : Zircaloy SS : Stainless Steel

qtz : quartz irr. : irradiated unirr. : unirradiated

Reaction System	Facility/ Institute	Geometry/ Size	Heating Method	Press-ure (MPa)	Atmos-phere	Materials	Tempe-rature (K)	Reaction Time (s)	Special Condition	Date
B_4C/SS	JAERI	SS-crucible: D = 10/16 mm B_4C pellet: D = 9.9 mm, h = 5 mm B_4C powder:0.5 g	electrici nfrared	0.1	Ar	SS 304 B_4C powder, pellets	1073-1623	30-3.6e+6	-	1995
B_4C/Zry	JAERI	SS-crucible: D = 10/16 mm B_4C pellet: D = 9.9 mm, h = 5 mm	Electric infrared	0.1	Ar	Zry-4 B_4C powder, pellets	1173-1953	30-3.6e+6	-	1995
B_4C+SS/ Zry	JAERI	SS-crucible: D = 10/16 mm B_4C+SS pellet: D = 9.9 mm, h = 5 mm	Electric infrared	0.1	Ar	Zry-4 80wt% SS 304, 20wt% B_4C	1473-1703	30-10800	-	1995

Table 4.2.2.2: Structural Material Interaction Experiments

Key

AIC	: Silver Indium Cadmium	B_4C	: Boron Carbide	Incl	: Inconel	Zry	: Zircaloy	SS	: Stainless Steel
qtz	: quartz	irr.	: irradiated	unirr.	: unirradiated				

Reaction System	Facility/ Institute	Geometry/ Size	Heating Method	Press-ure (MPa)	Atmos-phere	Materials	Tempe-rature (K)	Reaction Time (s)	Special Condition	Date
Zry/UO_2	MONA/ KfK	Fuel rod segment: D = 9.1/10.7 mm L = 150 mm	induct-ive	0.1-4.0	25% O_2 75% Ar	Zry-4 95% TD of UO_2	1173-1673	360-1800	single rod fill gas He	1983
Zry/UO_2	MONA/ KfK	Fuel rod segment: D = 9.1/10.7 mm L = 150 mm	induct-ive	0.1-4.0	Ar	Zry-4 95% TD of UO_2	1273-1973	60-3600	single rod fill gas He	1983
Zry/UO_2	LAVA/ KfK	UO_2-crucible: A = 5.8 cm² Zry: 10 g	induct-ive	0.1-0.3	Ar	Zry-4 95% TD of UO_2	2223-2523	60-7200	Crucible 170 g UO_2	1984
Zry/UO_2	LAVA/ KfK	ZrO_2-crucible: A = 7.6 cm² Zry: 10 g	induct-ive	0.1-0.3	Ar	Zry-4 97.3% ZrO_2 2.7% CaO	2073-2673	60-3600	crucible 75% TD of ZrO_2	1985
Zry+Ag/UO_2	JAERI	UO_2-pellet metal tube	electric	0.1	Ar	50wt% Zry-4 / 50wt% Ag	1473-1703	240-90000	solid UO_2 9 mm dia. pellet	1994
Zry/UO_2	CRNL	Fuel rod segment: D = 15.25/ 14.4 mm, L = 9 mm	radiant energy	0.1	Steam	Zry-4/ CANDU Fuel	2143-2193	80-120	hollow UO_2 9.5 mm dia. pellet	1994 Pro-prie-tary

Table 4.2.2.3: Metal/Ceramic Interaction Experiments

Key

AIC : Silver Indium Cadmium B_4C : Boron Carbide Incl : Inconel Zry : Zircaloy SS : Stainless Steel

UHP : Ultra High Purity irr. : irradiated unirr. : unirradiated

Reaction System	Facility/ Institute	Geometry/ Size	Heating Method	Press-ure (MPa)	Atmos-phere	Materials	Tempe-rature (K)	Reaction Time (s)	Special Condition	Date
Zry/UO_2	CRNL	Fuel rod trefoil segment: D = 15.25/ 14.4 mm, L = 9 mm	radiant energy	0.1	Steam	Zry-4/ CANDU Fuel	2143-2193	80-120	hollow UO_2 9.5 mm dia. pellet	1994 Pro-prie-tary
Zry/UO_2	CRNL	UO_2 crucible: D = 12.1/6.7 mm L = 16.6 mm 13 mm deep	radiant energy	0.1	UHP Ar	O-free Zry and Zry/25% O_2	2273-2473	0-3600	Zry/UO_2 variable ratios	1992/ 93
Zry/UO_2	CRNL	UO_2 crucible: D = 14.4/6.7 mm L = 18.4 mm 15 mm deep	radiant energy	0.1	UHP Ar	O-free Zry and Zry/25% O_2	2473-2773	0-3600	Zry/UO_2 variable ratios	1993/ 94
Zry/UO_2	LBL/ UC	Thoria crucible	induct-ive	0.1	Ar/ 5%H_2	Zry-4	2173-2473	10-200	Diffusion-controlled reaction	< 1988
Zry/UO_2	LBL/ UC	UO_2 crucible	induct-ive	0.1	Ar/ 5%H_2	Zry-4	2223-2473	15-600	Convection-controlled reaction	< 1988
Zry/UO_2	JRC (ITU)	graphite crucible	electric	0.1	Ar	Zry-4/UO_2 irr. and unirr.	2273	25-200	irradiation 53GWd/tU	1997/ 99

Table 4.2.2.3: Metal/Ceramic Interaction Experiments

Key

AIC : Silver Indium Cadmium B_4C : Boron Carbide Incl : Inconel Zry : Zircaloy SS : Stainless Steel

UHP : Ultra High Purity irr. : irradiated unirr. : unirradiated

Reaction System	Facility/ Institute	Geometry/ Size	Heating Method	Press-ure (MPa)	Atmos-phere	Materials	Tempe-rature (K)	Reaction Time (s)	Special Condition	Date
Zr1%Nb/ UO_2	AEKI	Fuel rod segment: D = 7.6/9.1 mm L = 30 mm	induct-ive	4.0	25% O_2 75% Ar	Zr1%Nb VVER fuel	1273-1873	180-7200	single rod	1991/ 94
Zr, Zry+SS, Zry+Ag, Zry+SS+ Ag/UO_2	Skoda-IPSN	UO_2 and ZrO_2 crucibles: D = 4 or 6 mm	electric	0.1	Ar	e.g. 82%Zry/18%Fe, 50%Zry/50%Ag	1573-2273	to ~5000	effect of alloy composition	1997/ 99
FeO/UO_2	JRC-ENEA	UO_2 crucible, FeO pellets of D = 12-14 mm, t = 1 mm	electric induct-ive	0.1	Ar	initial iron oxide was powder, stoichimetric Fe_2O_3 and Fe	1573-2273	to 300	quenched in Ar	1997/ 99
Zry/UO_2	LAVA/ FZKA-AECL	UO_2 crucible, D = 14 mm, t = 5 mm, L = 16.8 mm	tungsten resist-ance	0.1	Ar	UO_2 density 10.0-10.5 g/cm^2, sometimes a yttria disc on crucible base	2373-2573	100-1800	yttria disc gives 1-D dissolution, no disc gives 2-D	1997/ 99

Table 4.2.2.3: Metal/Ceramic Interaction Experiments

Key

AIC : Silver Indium Cadmium B_4C : Boron Carbide Incl : Inconel Zry : Zircaloy SS : Stainless Steel

UHP : Ultra High Purity irr. : irradiated unirr. : unirradiated

Reaction System	Facility/ Institute	Geometry/ Size	Heating Method	Press-ure (MPa)	Atmos-phere	Materials	Tempe-rature (K)	Reaction Time (s)	Special Condition	Date
Zry/ZrO_2	LAVA/ FZKA-AECL	ZrO_2 crucible, (1) D = 27 mm, t = 4.7 mm and (2) D = 14 mm, t = 3.5 mm	electric induct-ive	0.1	Ar	(1) CaO-stabilised ZrO_2 75%TD & Y_2O_3-stabilised ZrO_2 93% TD both used, latter with yttria disc (2) Y_2O_3-stabilised ZrO_2 100% TD	2273-2673	60-7200	yttria disc gives 1-D dissolution, no disc gives 2-D	1997/99
Zry/ZrO_2 +UO_2	LAVA/ FZKA-AECL	UO_2 crucible, D = 14 mm, t = 5 mm, L = 16.8 mm + ZrO_2 rod D = 6.45 mm	tungsten resist-ance	0.1	Ar	CaO-stabilised ZrO_2	2373	108-554	comparison of simultan-eous dissolution rates	1997/99
Zry/ZrO_2	FZKA single rod QUENCH rig	single rod, ZrO_2 pellets, D = 14 mm, l = 50 mm	electric, inductive	0.1	Ar/O_2	Zircaloy-4, ZrO_2	plateau 1673, max. temp. 2073-2573	pre-ox for 2-9min, ramp rates 2-10K/s, until shell failure	investig-ation of oxide shell breach criteria	1999

Table 4.2.2.3: Metal/Ceramic Interaction Experiments

Key

AIC : Silver Indium Cadmium B_4C : Boron Carbide Incl : Inconel Zry : Zircaloy SS : Stainless Steel

UHP : Ultra High Purity irr. : irradiated unirr. : unirradiated

Institute	Facility/ Name	Geometry	Specimen Length (mm)	Heating Method	Pressure (MPa)	Atmos-phere	Quench Temperature (K)	Reflood or Steam Flow	Special Condition	Date
JAERI	-	single rod	370 (fuel 320)	nuclear	0.1 (rod 0.4/0.5)	steam or helium / water quench	1273-2073	70-80 mm/s reflood rate	pre-oxidation up to 40%	<1991
FZKA	QUENCH series 1	single rod, ZrO_2 pellets	150	electric, inductive	0.1	Ar+25%O_2 / water quench	1273/1473 1673/1873	15 mm/s reflood rate	pre-ox in Ar/O_2 <20/~100/~200 /~300µm	1995/97
FZKA	QUENCH series 2	single rod, ZrO_2 pellets	150	electric, inductive	0.1	Ar+25%O_2 / steam cooling	1473/1673/ 1873	1.5-2 g/s steam flow	pre-ox in Ar/O_2 <30/~100/~200 /~300µm	1997
FZKA	QUENCH series 3	single rod, ZrO_2 pellets	150	electric, inductive	0.1	Ar+steam / steam cooling	1373/1473/ 1673/1873	1 g/s steam flow	pre-ox in Ar/steam ~100 - ~350µm stepwise ~30µm	1998

Table 4.2.3: Separate Effects Tests - Reflood

Institute	Facility/ Name	Geometry	Size (cm)	Heating Method	Fluid/ Solids	Tempe-rature (K)	Heat Source (W/cm^3)	Rayleigh Number	Special Condi-tion	Date
TUH	Mayinger	rectangular slab	h x b x s = 5 x 8 x 2	electrical resistance	water	300	< 4.2	1.0e+6 - 1.0e+9	-	1973
TUH	Mayinger	semicircle slab	r x s = 3-28 x 1 h/r = 1-0.25	electrical resistance	water	300	< 0.4	1.0e+7 - 1.0e+10	jet - penet-ration	1973/ 80
OSU	Kulacki	rectangular slab	h x b x s = < 25 x 50 x 50	electrical resistance (60 Hz)	water + $AgNO_3$	300	< 0.04	1.0e+4 - 1.0e+12	-	1975
OSU	Kulacki	cylinder & spherical segment	r = 46 h_{spher} = 12 $h_{cyl} \leq 52$	electrical resistance (60 Hz)	water + $CuSO_4$	300	?	1.0e+8 - 1.0e+14	-	1978
AEAT Culham	Schneider	rectangular tank	h x b x s = 10 x 20 x 20	heat conduction from walls	water + Na_2SO_4/ $NaNO_3$	270/ 290	no internal heat source	1.0e+8 - 1.0e+9	precip-itation of salt crystals	1994
Fortum	COPO I	rectangular & semi-circle slab	h x b x s = 80 x 177 x 10	electrical resistance	water + $ZnSO_4$	340	0.04	1.0e+14 - 1.0e+15	VVER-440 lower head	1993
Fortum	COPO II	rectangular & semi-circle slab	h x b x s = 100 x 200 x 9 & 95 x 178 x 9	electrical resistance	water + $ZnSO_4$	< 350	0.1	1.0e+14 - 1.0e+15	AP600 & VVER-440 lower head	1996

Table 4.2.4: Separate Effects Tests - Melt Pool Thermal Hydraulics

Institute	Facility/ Name	Geometry	Size (cm)	Heating Method	Fluid/ Solids	Tempe-rature (K)	Heat Source (W/cm^3)	Rayleigh Number	Special Condi-tion	Date
UCSB	ACOPO	hemisphere	r = 200	transient cool-down	water	350	preheated	1.0e+16 - 1.0e+17		1997
UCLA	Dhir	hemisphere & vertical section	r = 7.5-22 h/r = 1-0.26	microwave	Freon R-113	300	< 0.006	1.0e+11 - 1.0e+14	free and rigid surface	1994
CEA Gren-oble	BALI	sector of semicircle slab	r x s = 200 x 15 sector: 110°	electrical resistance	water + salt + glycerine	200-300	~ 0.03	1.0e+15 - 1.0e+17	ice crust & metal layer	ongoing
RRC-KI	RASPLAV AW200	semicircle slab	r x s = 40 x 10 h/r = 1	electrical inductive heated side walls	(U,Zr,O)	< 2800	-	1.0e+11 - 1.0e+12	reactor typical material	2000
RRC-KI	RASPLAV Salt	semicircle slab & vertical section	r = 20 s = 11 - 17 h/r < 1.6	side wall & electrical resistance	binary salt $NaF-NaBF_4$ and LiF-NaF-KF	< 1000	< 1	2.0e+11 - 2.0e+13	crust & non-eutectic	2000
RIT	SIMECO	semicircle slab & vertical section	r x s = 26.5 x 9 h/r < 2,35	internally by electric wires	binary salt $NaNO_3$ - KNO_3	< 700	2 - 4	<3.0e+13	crust & non-eutectic & metal layer	ongoing

Table 4.2.4: Separate Effects Tests - Melt Pool Thermal Hydraulics

Institute	Facility/ Name	Geometry	Size & Gap width (mm)	Heating Method	Fluid	Tempe-rature (K)	Heat Flux (kW/m^2)	Pressure (MPa)	Special Condition	Date
KAERI	CHFG	hemisphere 180°	r = 250 s = 0.5 - 10	electrical resistance	water or R113	< 600	< 500	0.1 - 1.0	-	ongoing
Siemens/ KWU	BENSON test rig	spherical section 30°	r = 2000 s = 1.0 - 10	electrical resistance	water	< 750	< 550	1.0 - 12	subcool. < 10 K	1998
RRC-KI	KC/CTF	rectangular vertical or inclined slab	h ≤ 400 b = 200 s = 0.5 - 5.0	electrical resistance	water	< 600	< 1000	0.1 - 8	one and two-sided heated	1997
TU Munich	CORCOM (1)	rectangular inclined slab 10° with debris bed above	l = 480 b = 140 s = 0.5 - 2 h_{dbris} = 140	inductive (3300 Hz)	water or R134a	< 620	< 600 relative to debris cross-sect.	Water: < 10 R134a: 0.8 - 1.8	transient debris bed flooding and quenching	1999
TU Munich	CORCOM (2)	rectangular inclined slab 0 - 25°	l ≤ 480 b = 140 s = 1 - 11	electrical resistance	R134a	< 620	< 750	0.8 - 1.8	-	1999

Table 4.2.5 Separate Effects Tests - Gap Thermal Hydraulics

Institute	Facility/ Name	Geometry	Size (cm)	Heating Method	Fluid	Tempe-rature (K)	Heat Flux (kW/m^2)	Pressure (MPa)	Special Condition	Date
CEA	SULTAN	rectangular vertical or inclined slab	l = 400 b = 15 s = 3 - 15	electrical resistance	water	< 400	< 2000	0.1 - 0.5	forced flow v = 0.01 - 5 m/s	ongoing
Penn State University	SBLB	hemisphere and cylindrical part	r = 15 h_{cyl} = 70 r_{insul} = 23	electrical resistance	water	< 370	< 1200	0.1	insulation of RPV mock-up	1999
SNL	CYBL	torispherical and cylindrical part	r = 185 h_{cyl} = 500	electrical resistance or radiative	water	< 370	< 500	0.1	large scale facility	1993
UCSB	ULPU	upward and downward circular piping	d_{up} = 15.2 d_{down} = 7.6 h = 543	electrical resistance	water	< 370	< 1200	0.1	full height natural convection loop	1994

Table 4.2.6 Separate Effects Tests - External Cooling Thermal Hydraulics

Institute	Facility/ Name	Geometry	Size (cm) Volume (l)	Heating Method	Material RPV / Melt	Tempe-rature (K)	Heat Source (W/cm^3)	Pressure (MPa)	Special Condition	Date
RIT	FOREVER	lower hemisphere upper cylindrical	r = 20 h_{cly} = 40 s_{wall} = 1.5 V_{melt} = 20	electrical resistance	carbon steel / $CaO-B_2O_3$, $CaO-WO_3$	< 1700	< 1	< 4		ongoing
KAERI	LAVA	lower hemisphere upper cylindrical	r = 25 h_{cly} = 80 s_{wall} = 2.5 V_{melt} = 10	thermite melt	carbon steel / Al_2O_3, Al_2O_3/Fe	< 2500	-	< 1.7		ongoing

Table 4.2.7 Separate Effects Tests - Gap Formation

Institute	Facility	Process	Material / Diameter (mm)	Mass (kg)	Max. Tempe-rature (K)	Gas Phase	Pressure (MPa)	Water Subcool-ing (K)	Water Mass (kg)	Ext. Trigger / Shock Wave (MPa)	Date
Uni Wisconsin	WFCI (1)	Explosion propagation and escalation	Sn	0.72 - 4.48	760 - 1250	Ar	0.1	7 - 75	8.6	yes	1999
Uni Wisconsin	WFCI (2)	Explosion propagation and escalation	Fe_2O_3	1.2	1900	Ar	0.1	Top: 15 - 30 Bottom: 15 - 75	8.6/34.3 plus funnel mass	yes	1999
UCSB	MAGICO 2000	Premixing	ZrO_2 Particles d = 2; 7	2.6 - 5.7	300 / 1670 - 2270	Air	0.1	0; 10	160	no	Ongoing
UCSB	SIGMA 2000	Micro-interaction	Sn / Fe Droplets d = 5 - 7	~0.001	1270 - 2070 / 1680 - 1920	Air	0.1	10 / 80	< 10	yes / 6.8; 20.4; 27.2	Ongoing

Table 4.2.8 Separate Effects Tests - Fuel Coolant Interaction

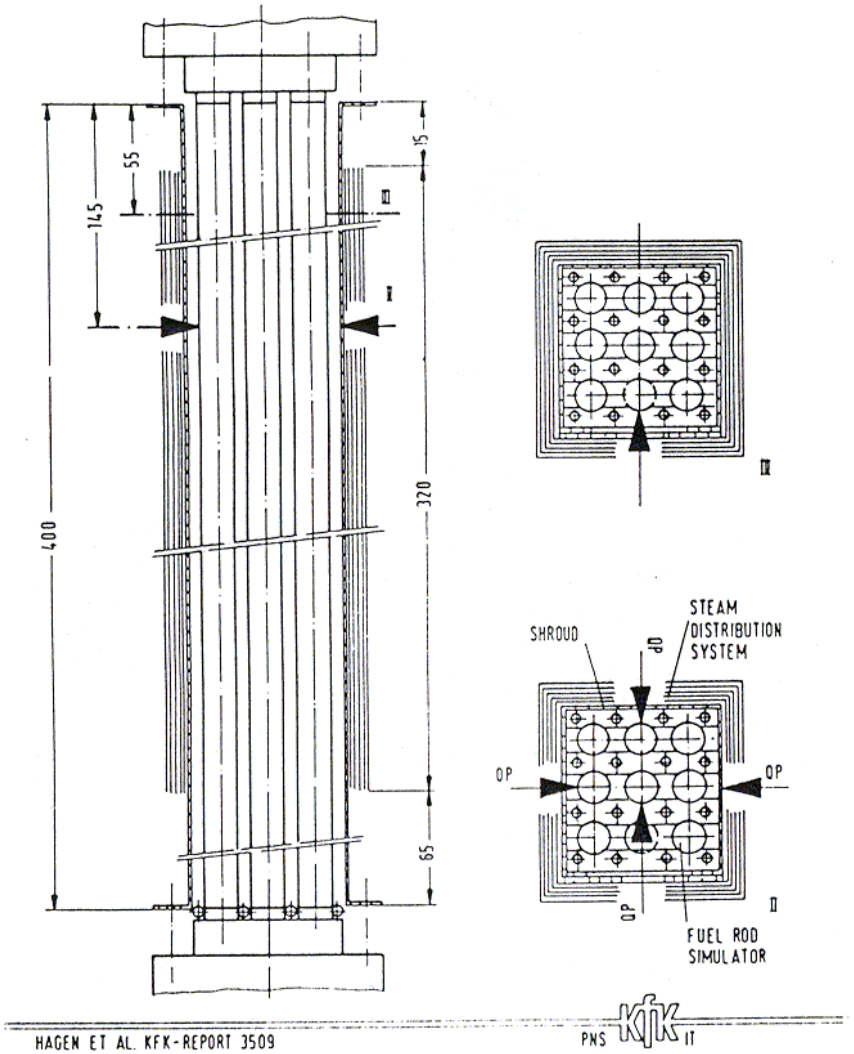

ESBU-2A AXIAL AND RADIAL CROSS SECTIONS AND THE LOCATIONS OF THE TWO-COLOR PYROMETERS

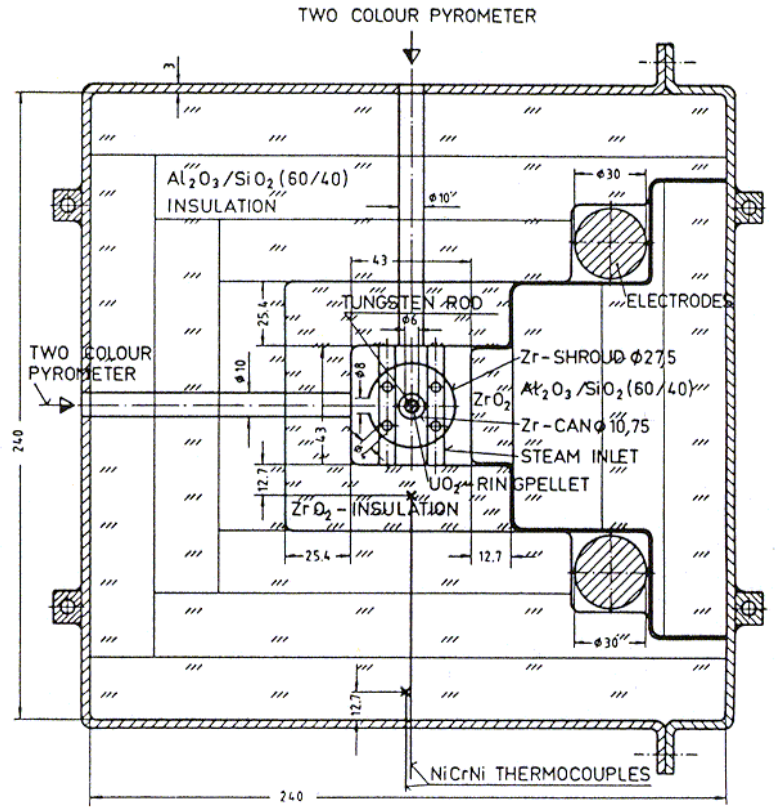

TOPVIEW OF THE EXPERIMENTAL ARRANGEMENT FOR TESTS ESSI-1.2.3

Figure 4.1.1: NIELS Facility Test Trains and Bundle Sections

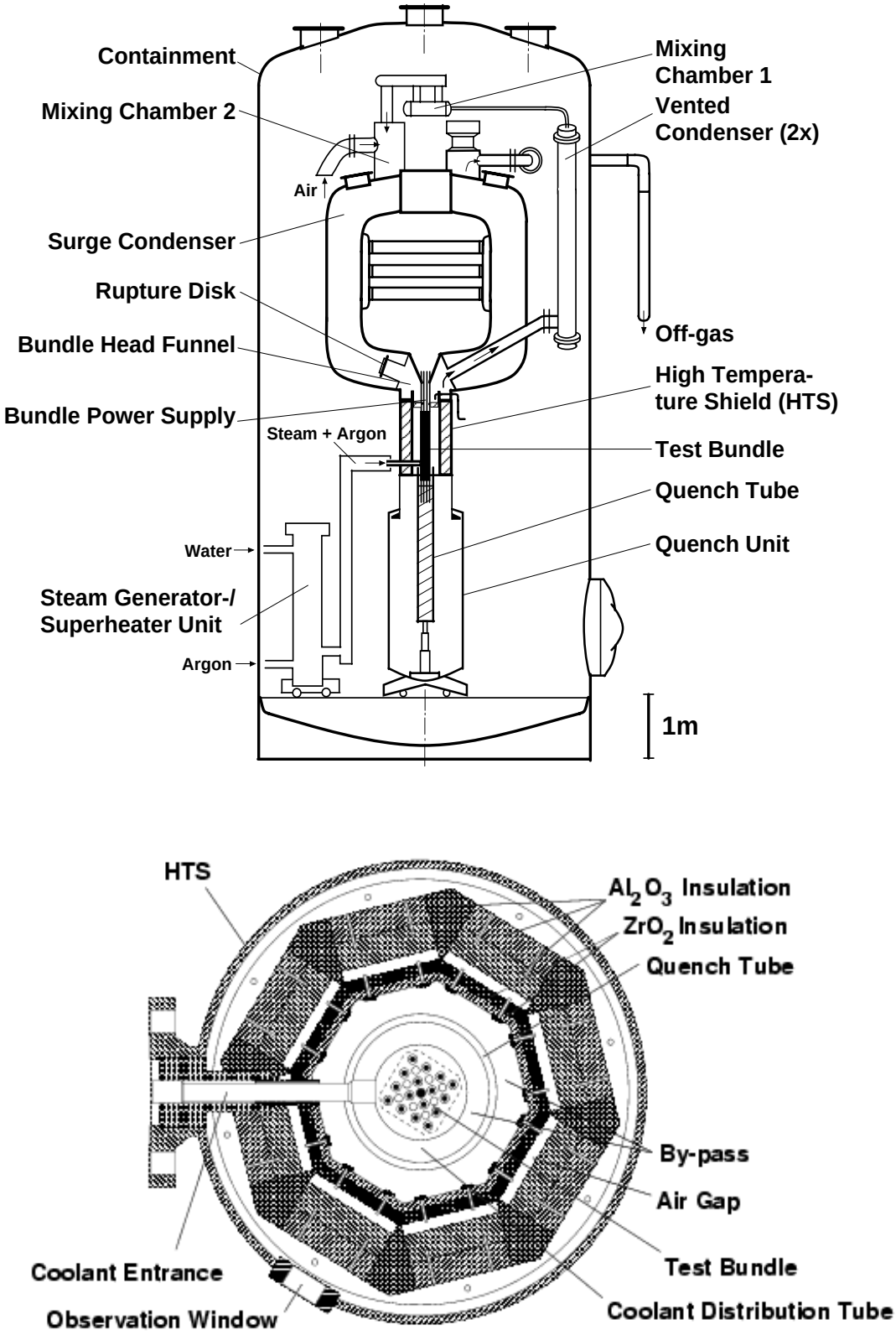

Figure 4.1.2a: CORA Facility and Heat Shield

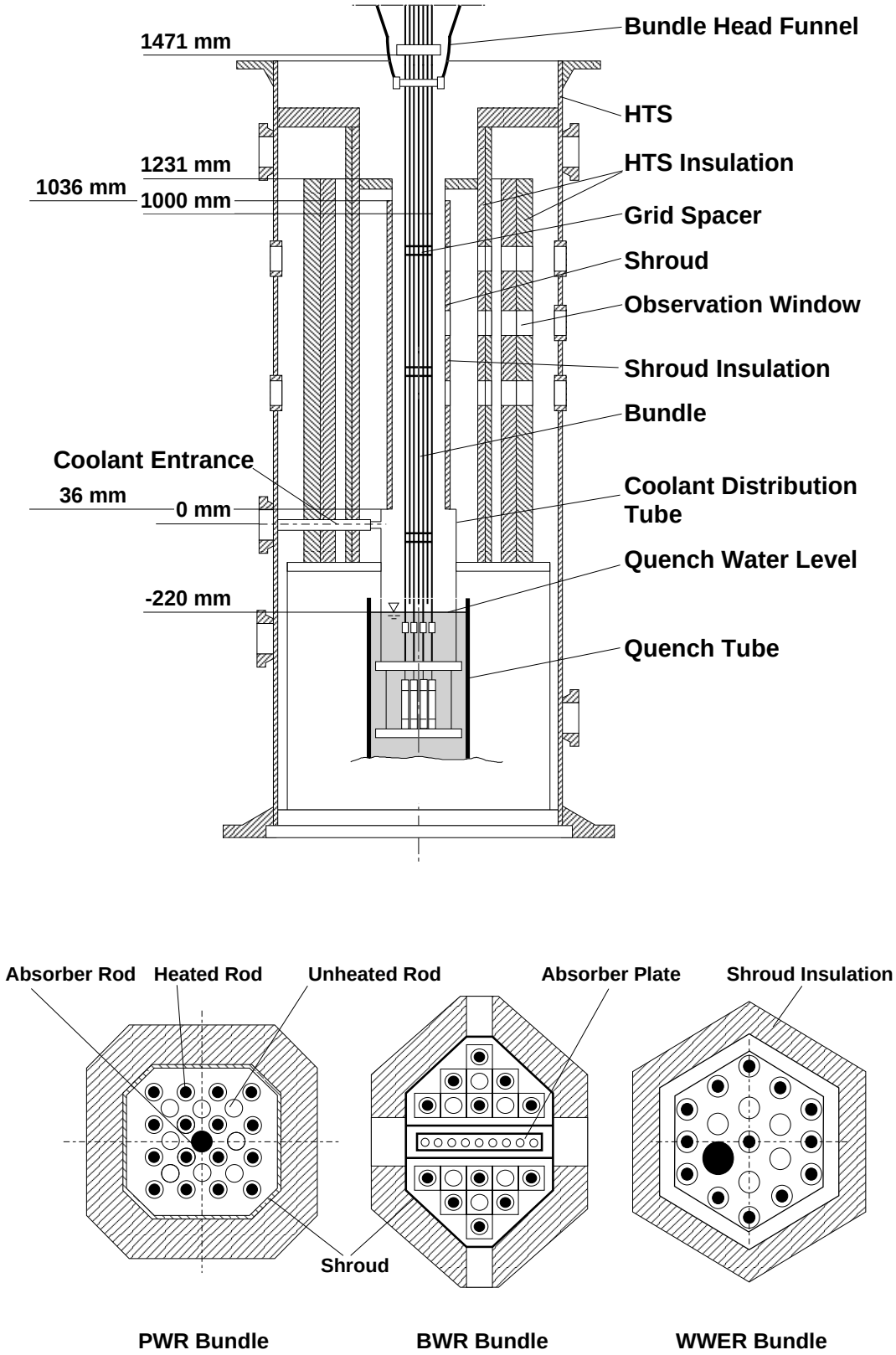

Figure 4.1.2b: CORA Bundle Cross-Sections

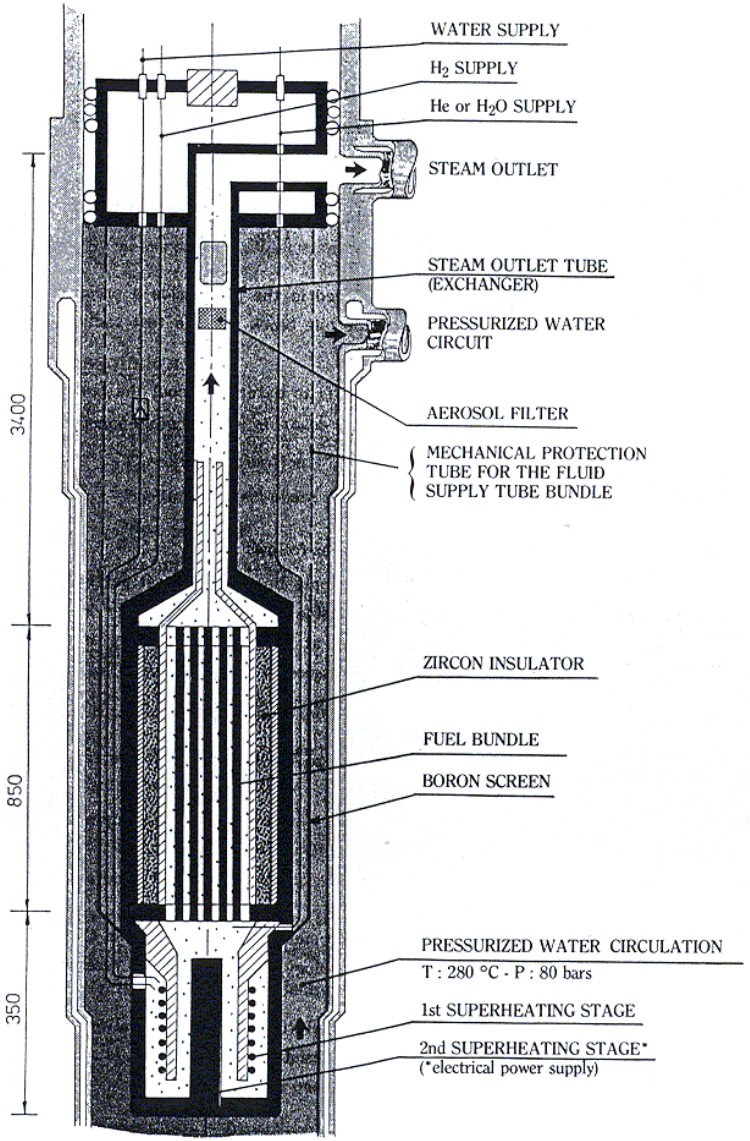

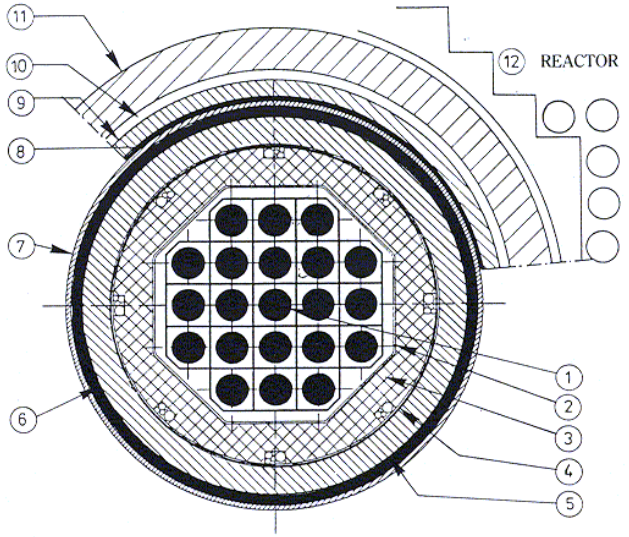

		DESIGNATION (materials)	Int. radius (mm)	Ext. radius (mm)	Thickness (mm)
Test device pressurized water loop	1	21 pin test bundle : UO_2, Zr, H_2O vap, H_2			
	2	Octogonal tube : Zircaloy			0.6
	3	Thermal insulation : porous ZrO_2	47.		
	4	Dense zircon schoop	47.	48.	1.
	5	Test device tube : STAINLESS	48.	56.	8.
	6	Pressurized water : – H_2O, 80 b, 280 °C	56.	9.25	3.25
	7	Screen : boron steel	59.25	60.75	1.5
	8	Pressurized water : – H_2O, 80 b, 280 °C	60.75	62.	1.25
Cell in non-modified pile	9	Inconel pressure tube	62.	67.	
	10	Vacuum	67.	70.	3.
	11	Zircaloy safety tube	70.	82.	12.
Reactor	12	Non modified			

Figure 4.1.3: PHEBUS SFD Test Train and Bundle Section

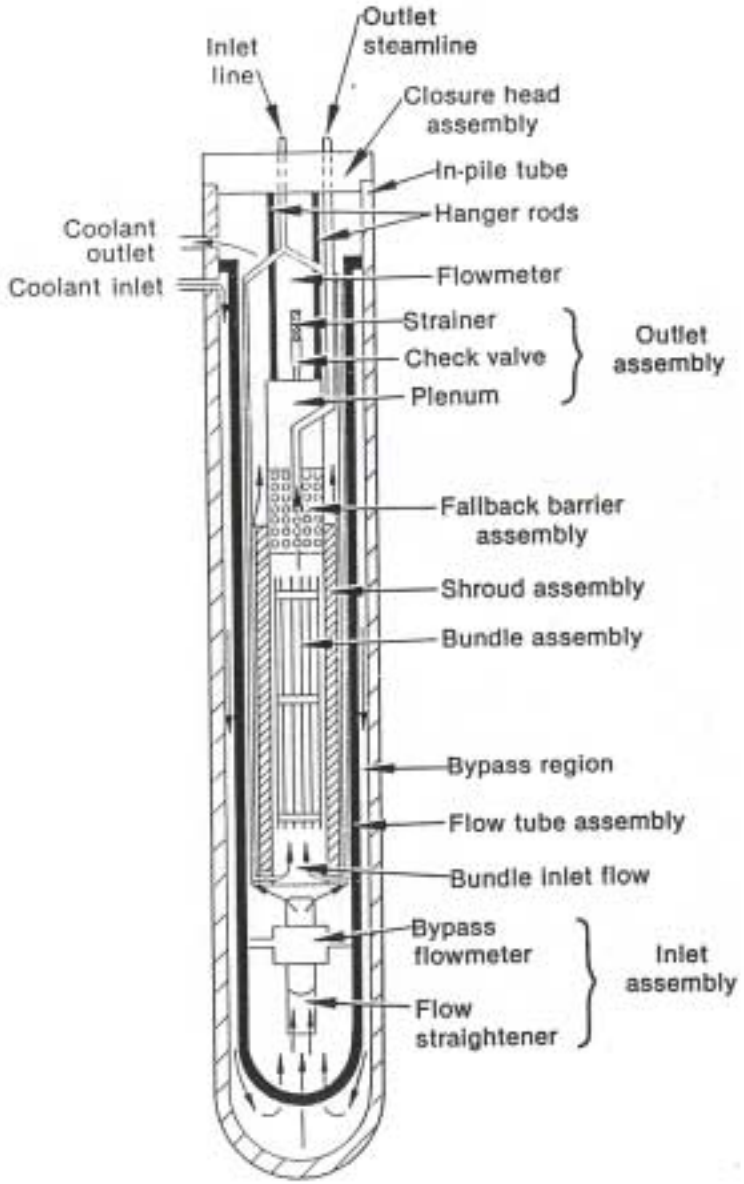

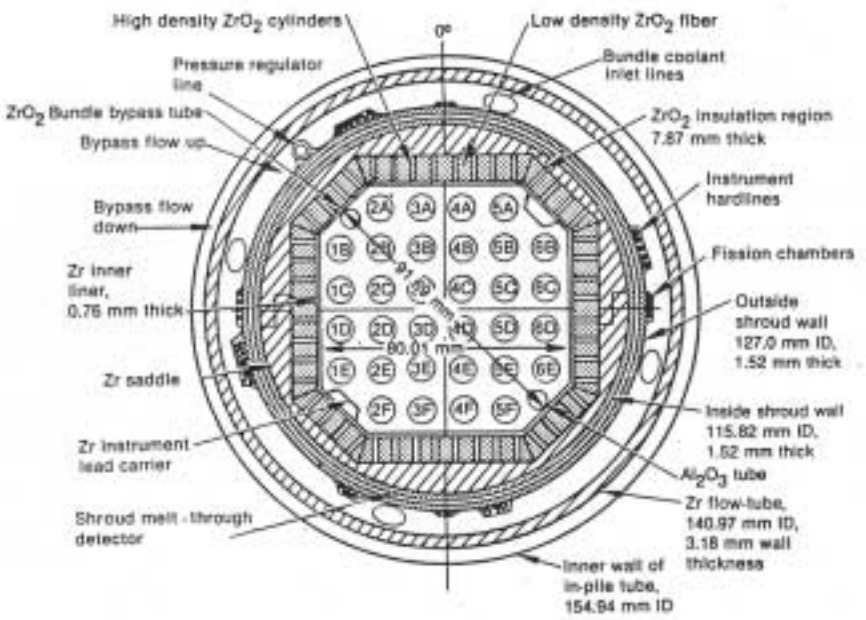

Figure 4.1.4: PBF-SFD Facility Test Train and Bundle Section for the 1.1 Assembly

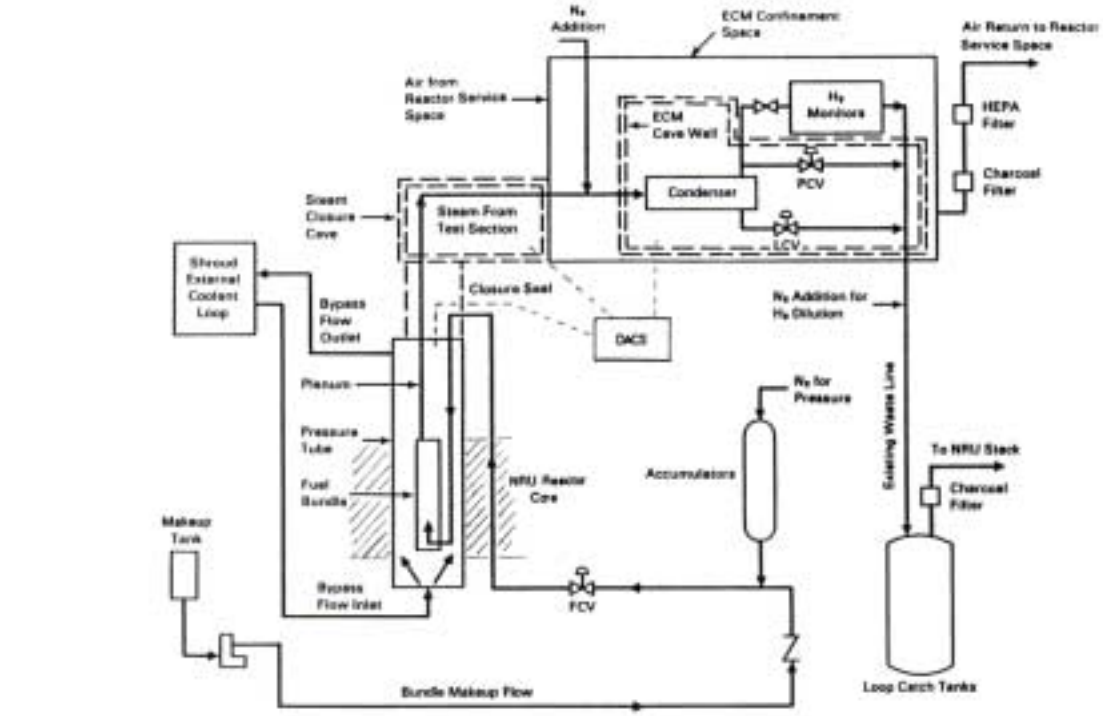

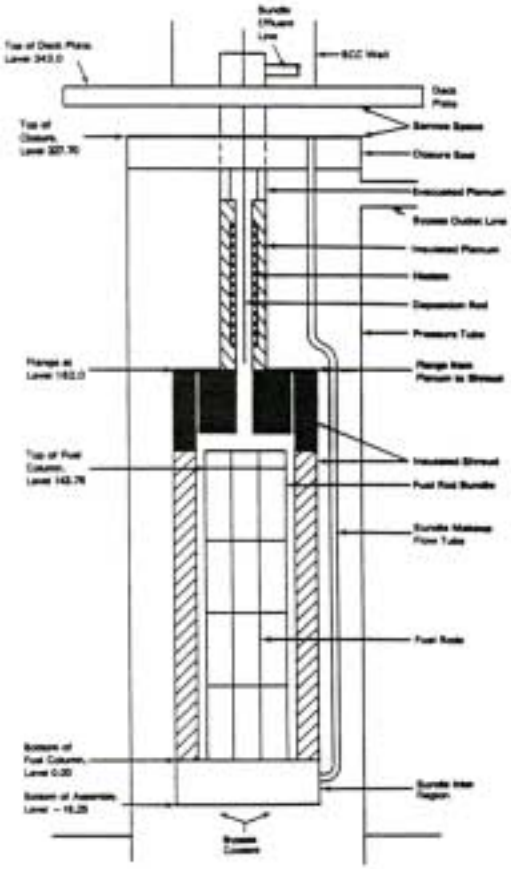

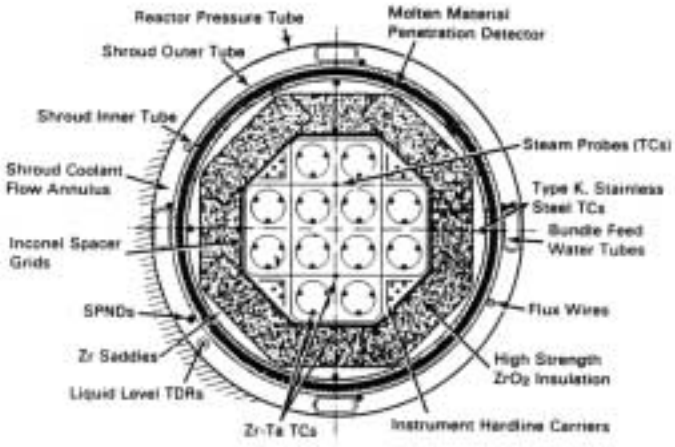

Figure 4.1.5: NRU-FLHT Test Train, Bundle Section and General Hardware Arrangement

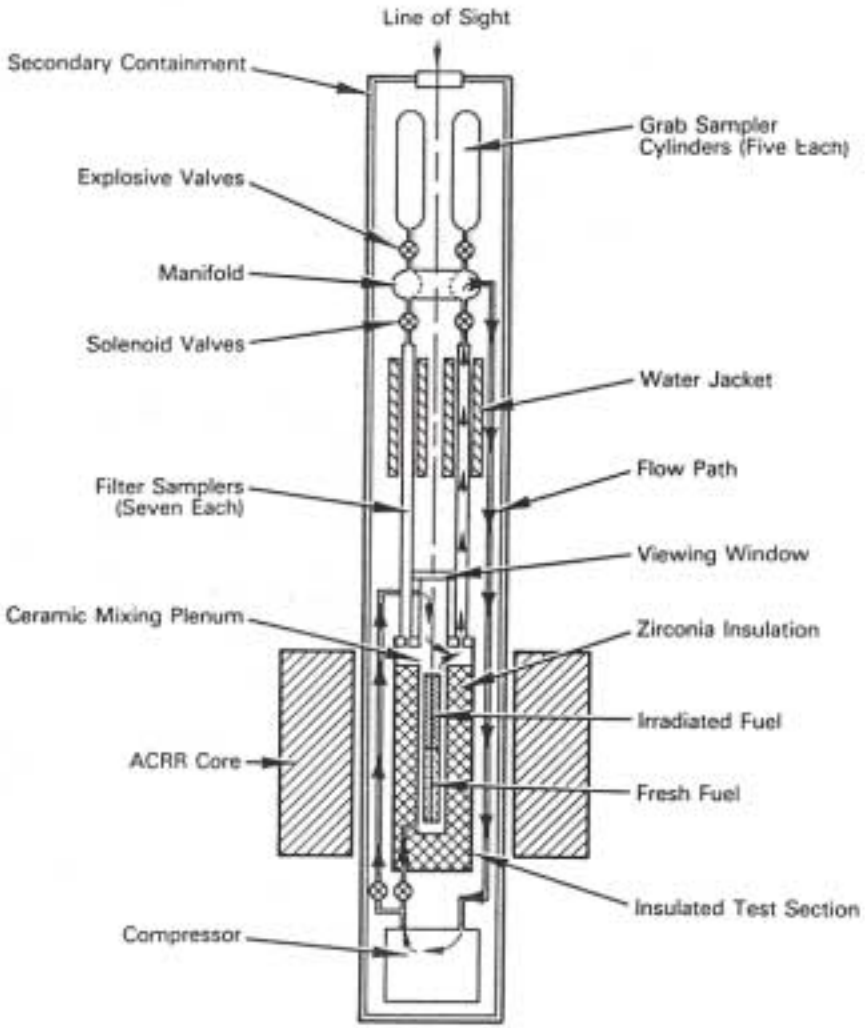

Fig. 1. Schematic of the ST-1 experimental hardware.

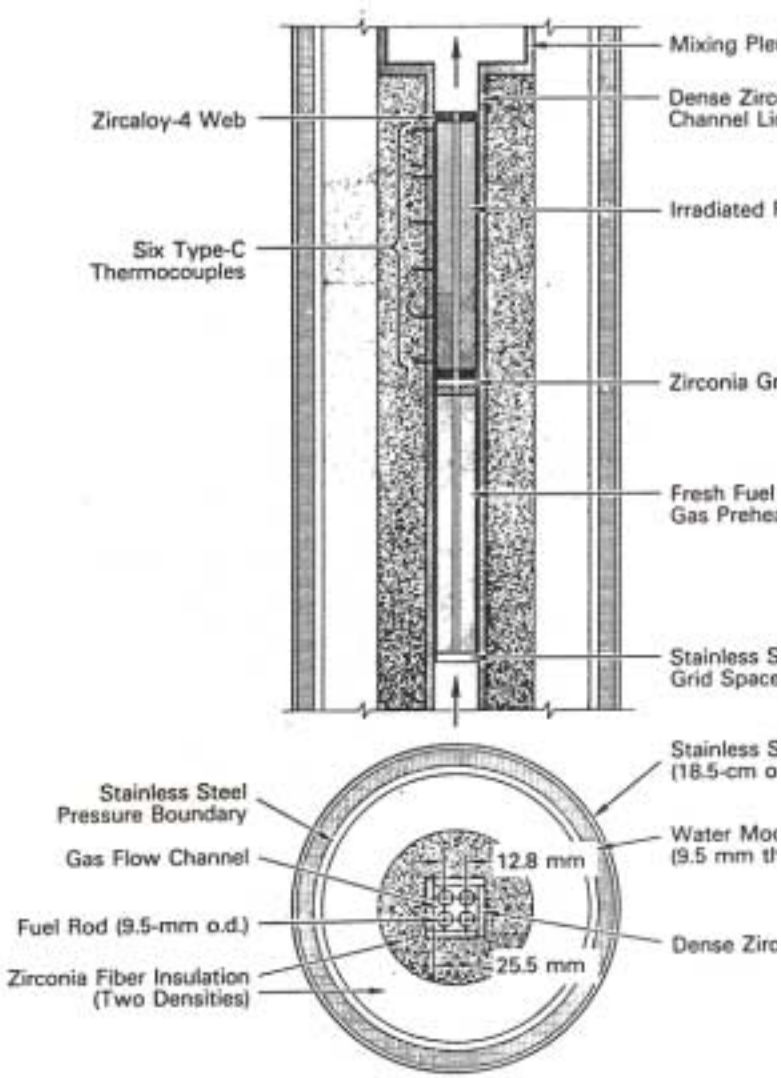

Fig. 2. Cross-sectional views of the ST-1 fueled test section.

Figure 4.1.6: ACRR-ST Test Train and Bundle Section

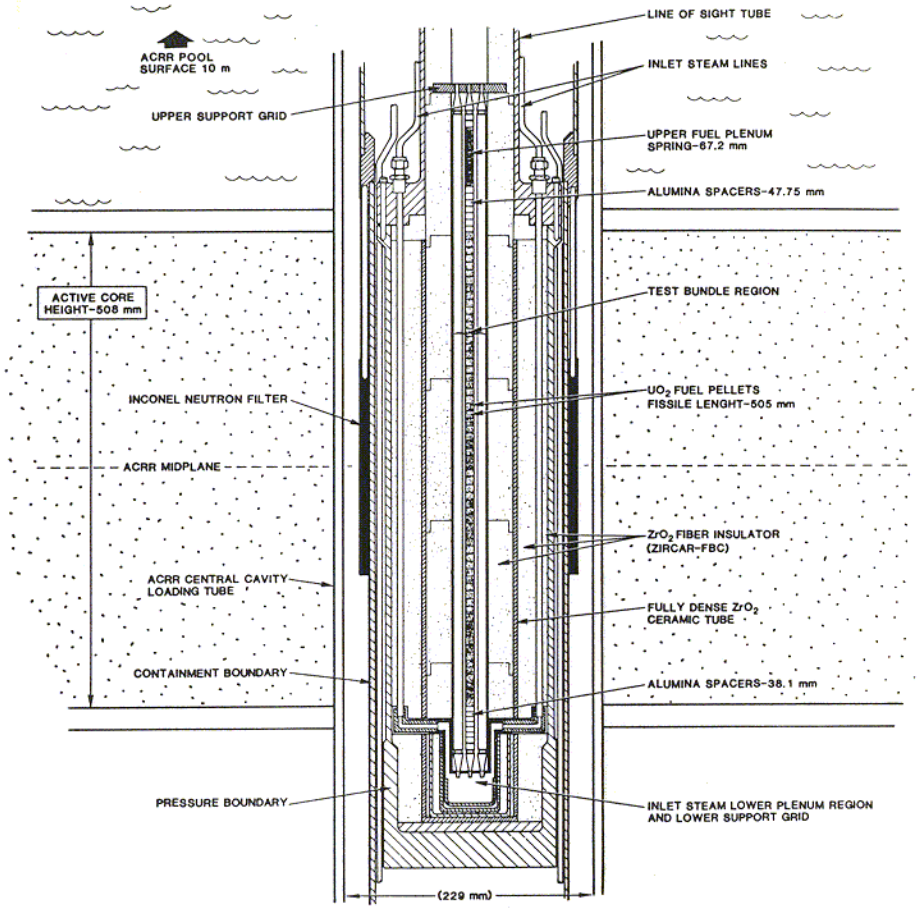

Vertical Cross Section of DF-1 Experiment Test Section

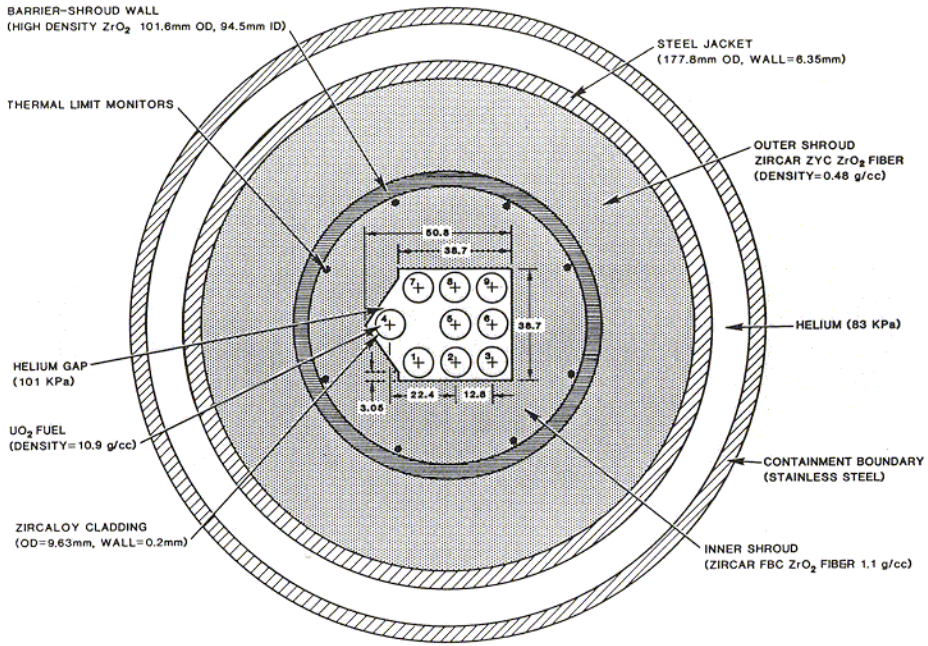

Horizontal Cross Section of DF-1 Experiment Test Section

Figure 4.1.7: ACRR-DF Test Train and Bundle Section

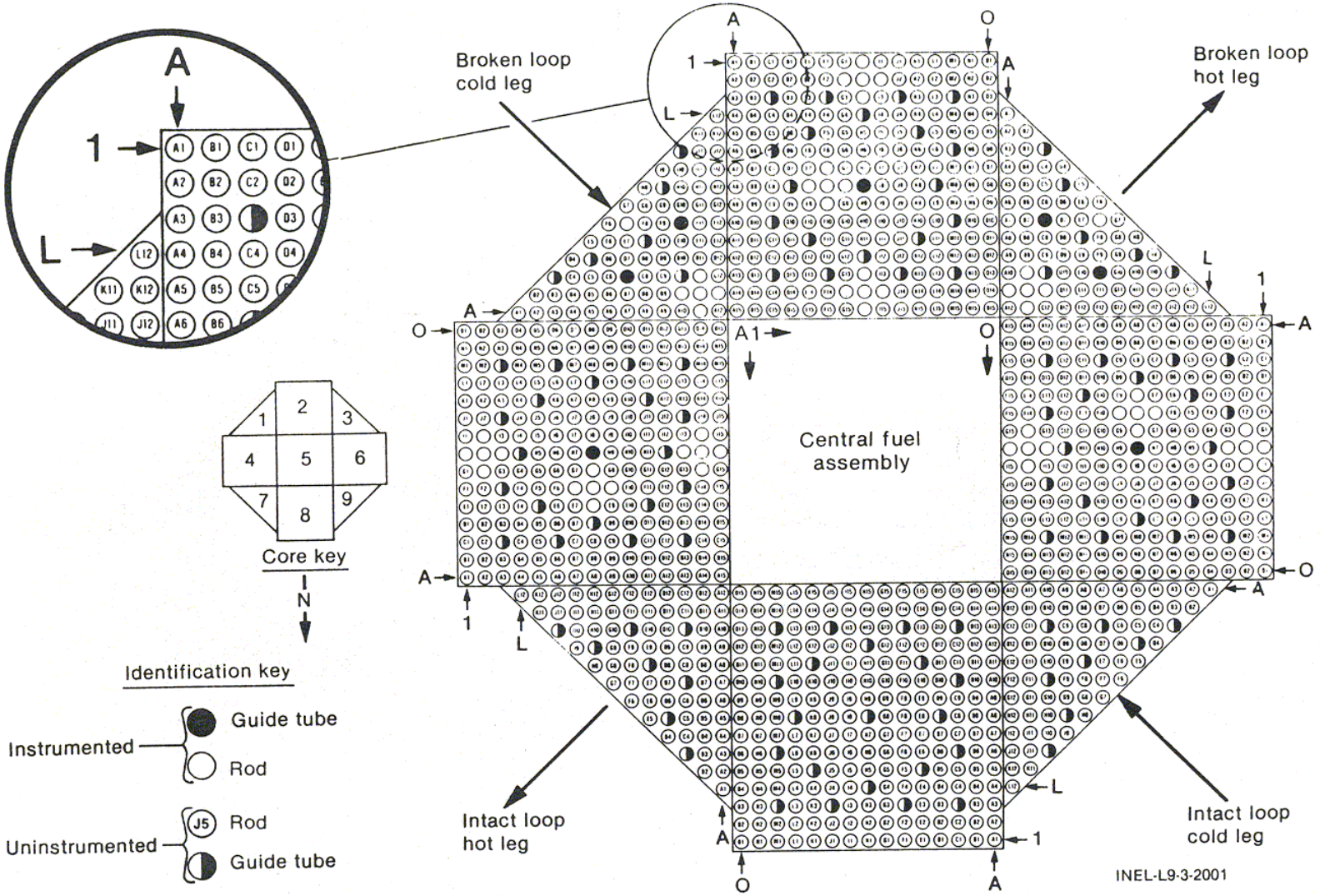

The LOFT core configuration showing the fuel rod and guide tube locations, as well as the locations of the cold and hot legs.

Figure 4.1.8a: LOFT-LP-FP Core Configuration Section

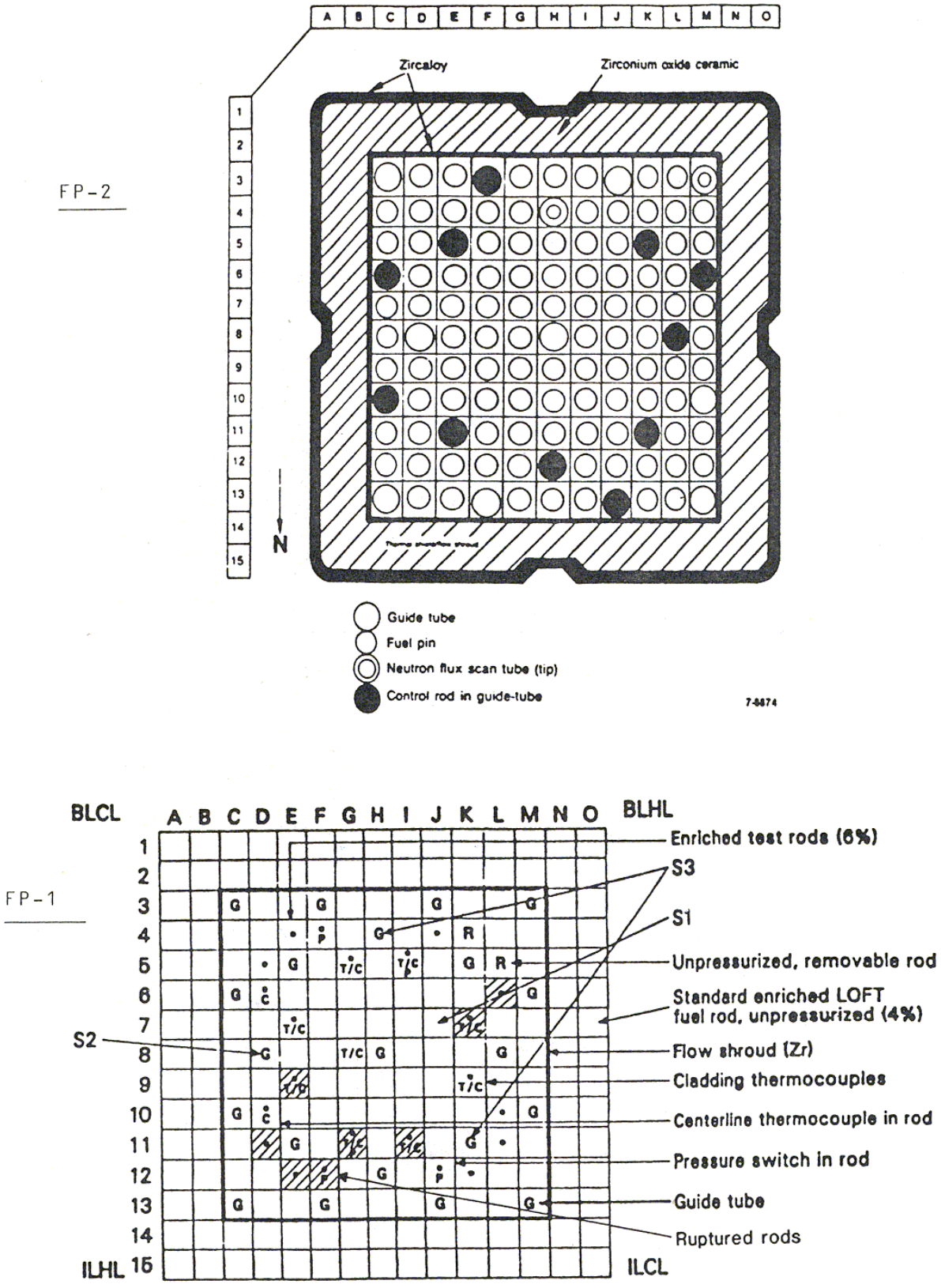

Figure 4.1.8b: LOFT-LP-FP Centre Fuel Module Sections for FP-1 and FP-2

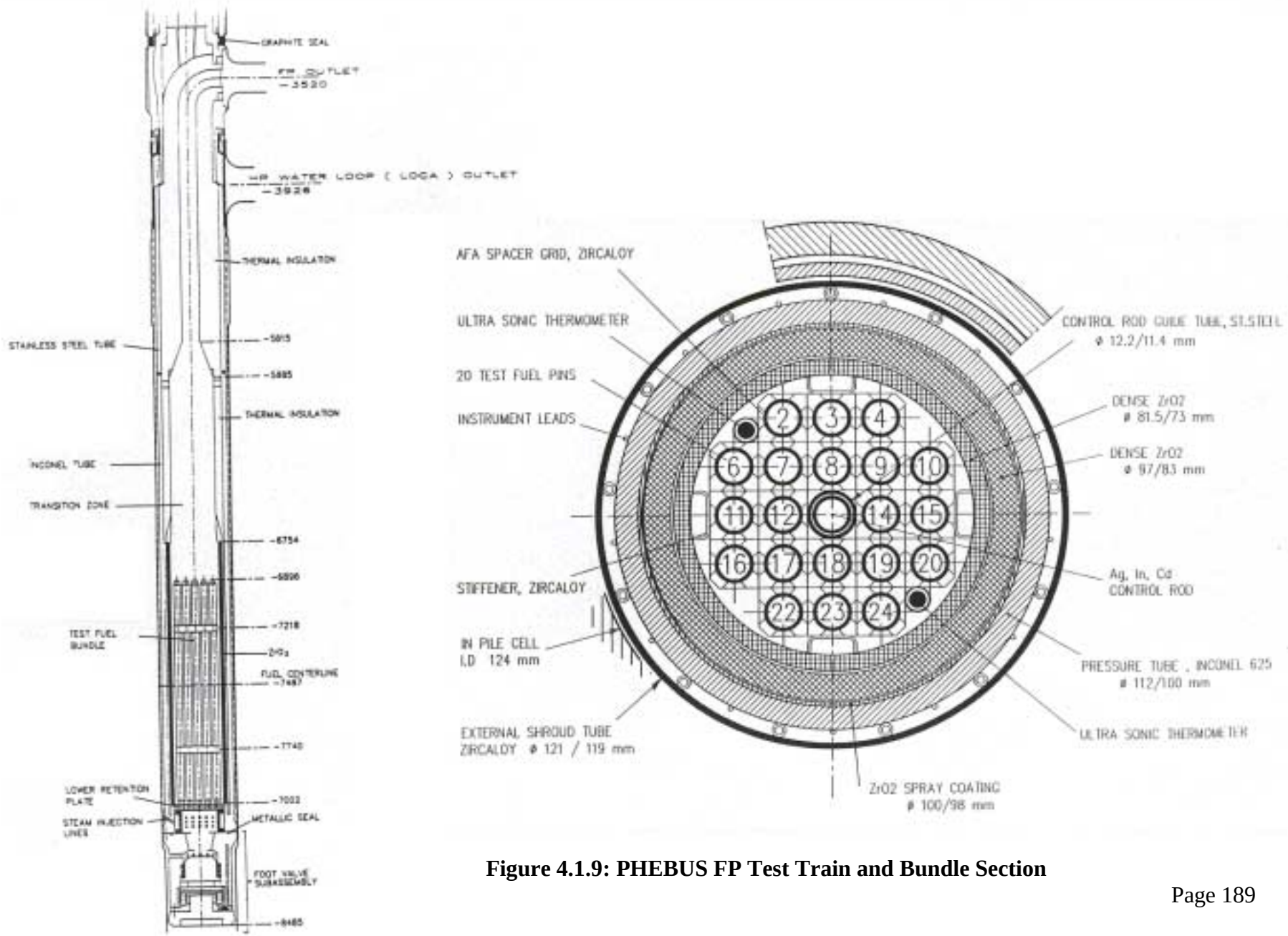

Figure 4.1.9: PHEBUS FP Test Train and Bundle Section

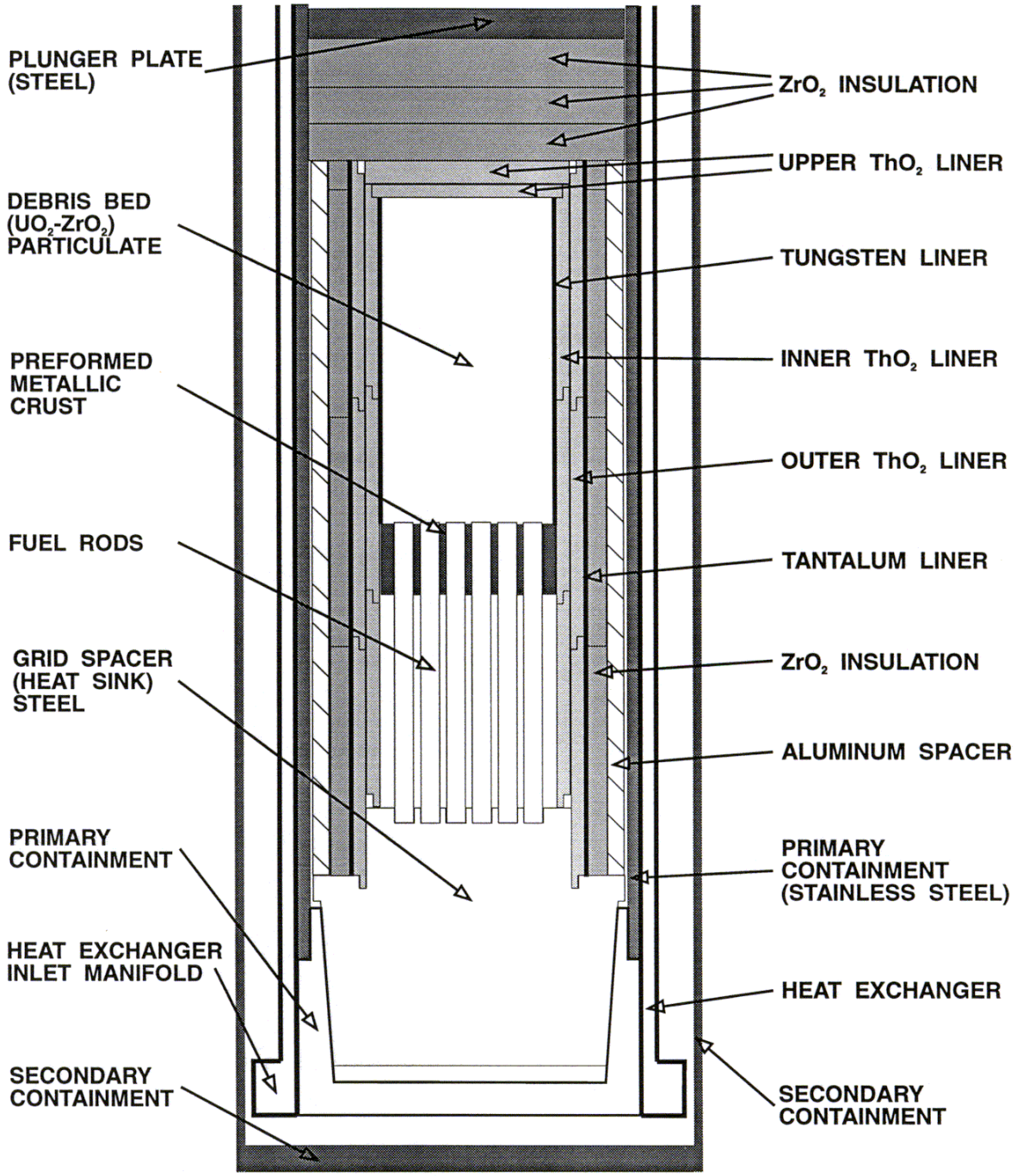

Figure 4.1.10: ACRR-MP Test Train and Bundle Section

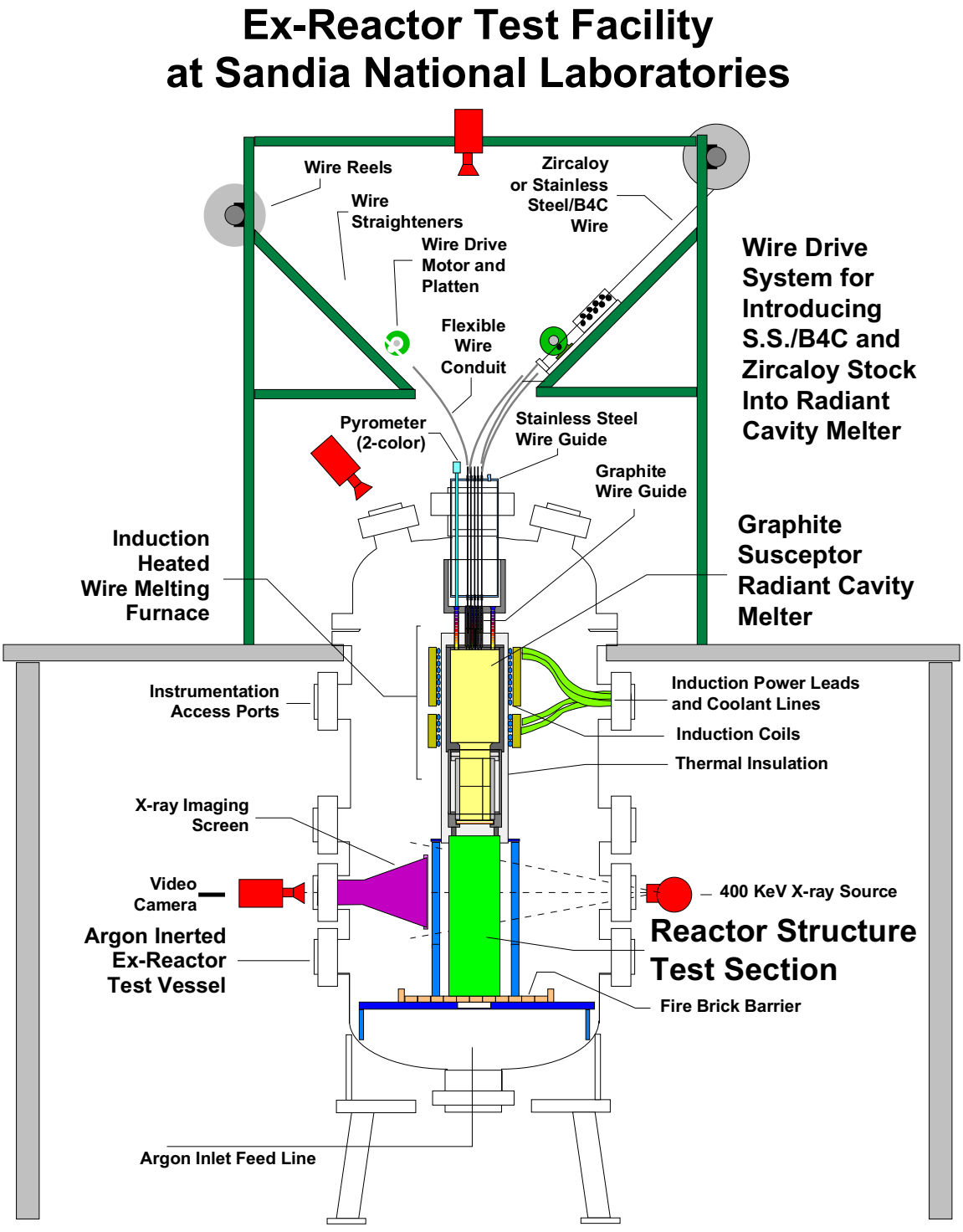

Figure 4.1.11a: SANDIA-XR Ex-Reactor Test Facility - General View

Cross Section of Ex-Reactor Experiment Test Bundle for Examining BWR Metallic Melt Behavior in Lower Core Region

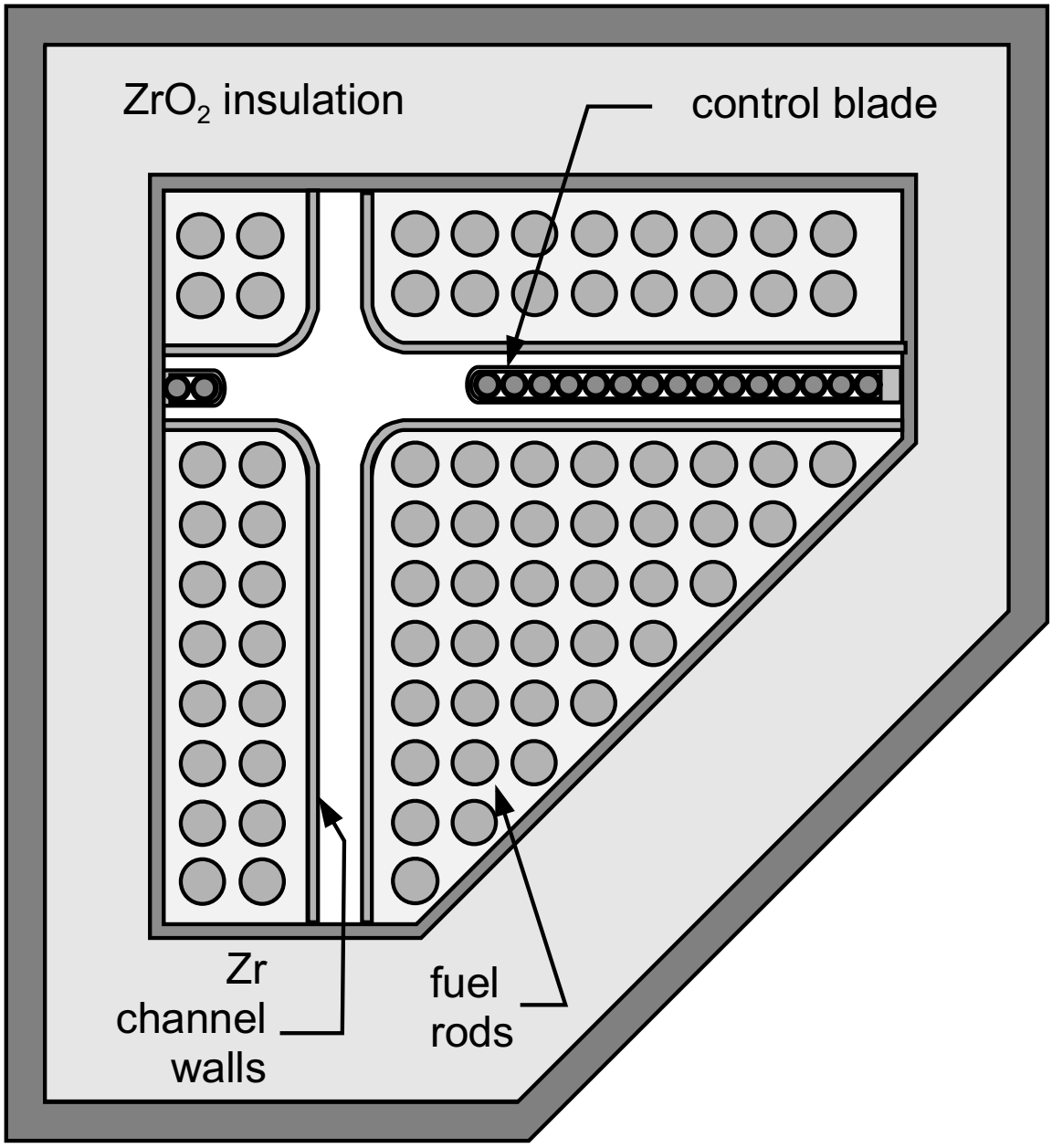

Figure 4.1.11b: SANDIA-XR Ex-Reactor Test Facility - Cross-Section

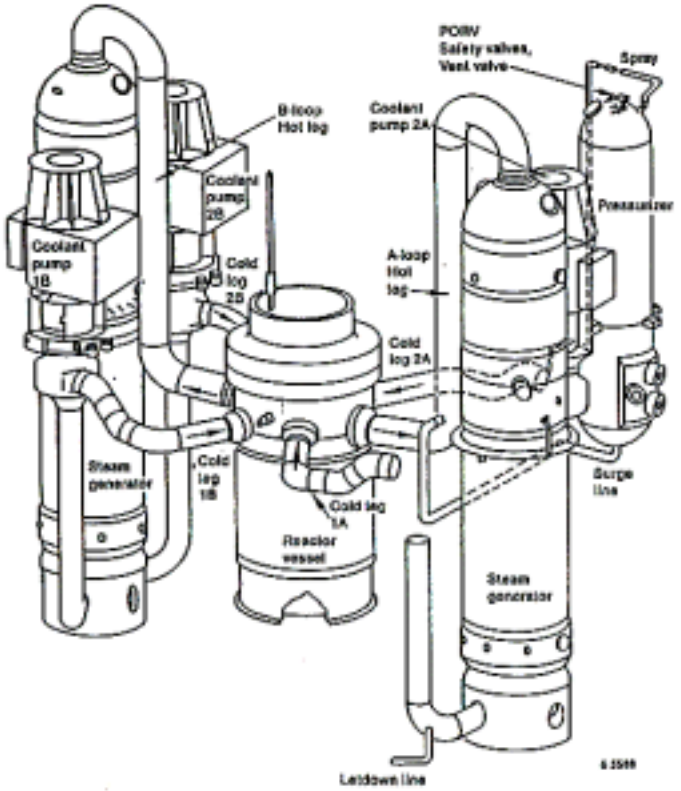

Schematic of the TMI-2 primary system.

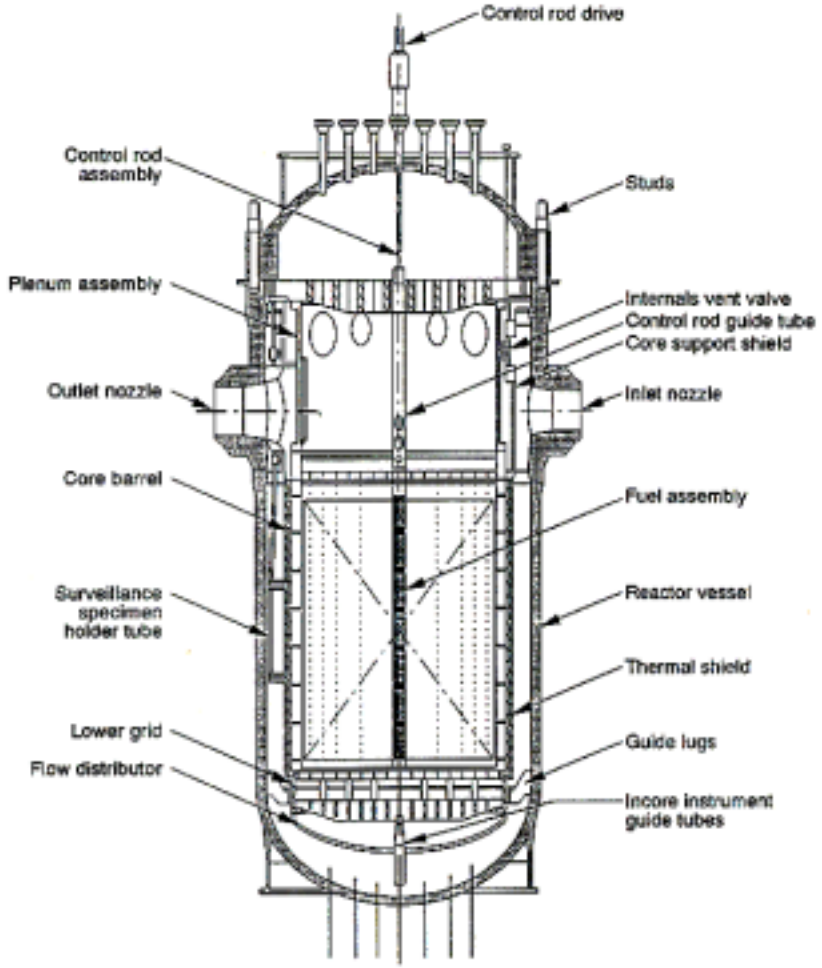

Reactor vessel components.

Figure 4.1.12a: TMI-2 Primary System and Reactor Vessel Component System

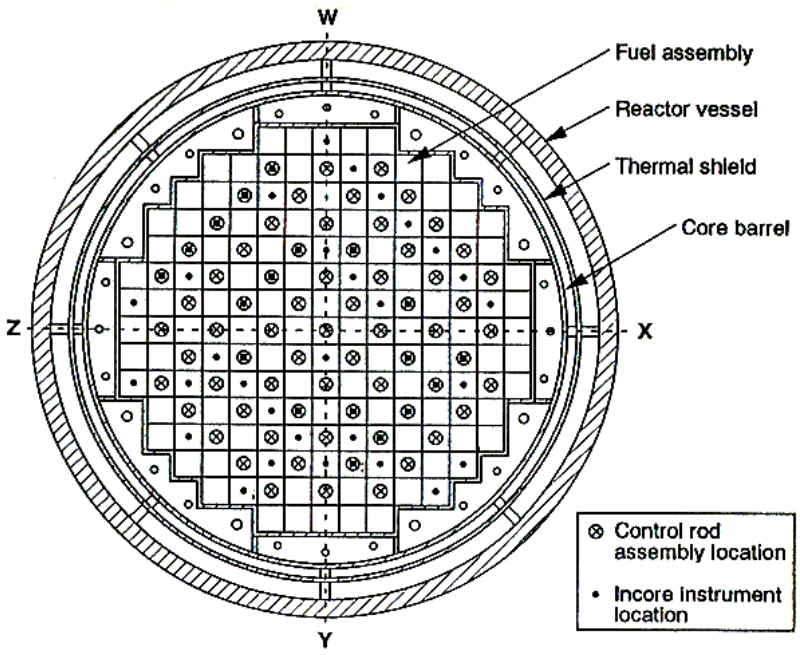

Cross section of the reactor vessel and internals.

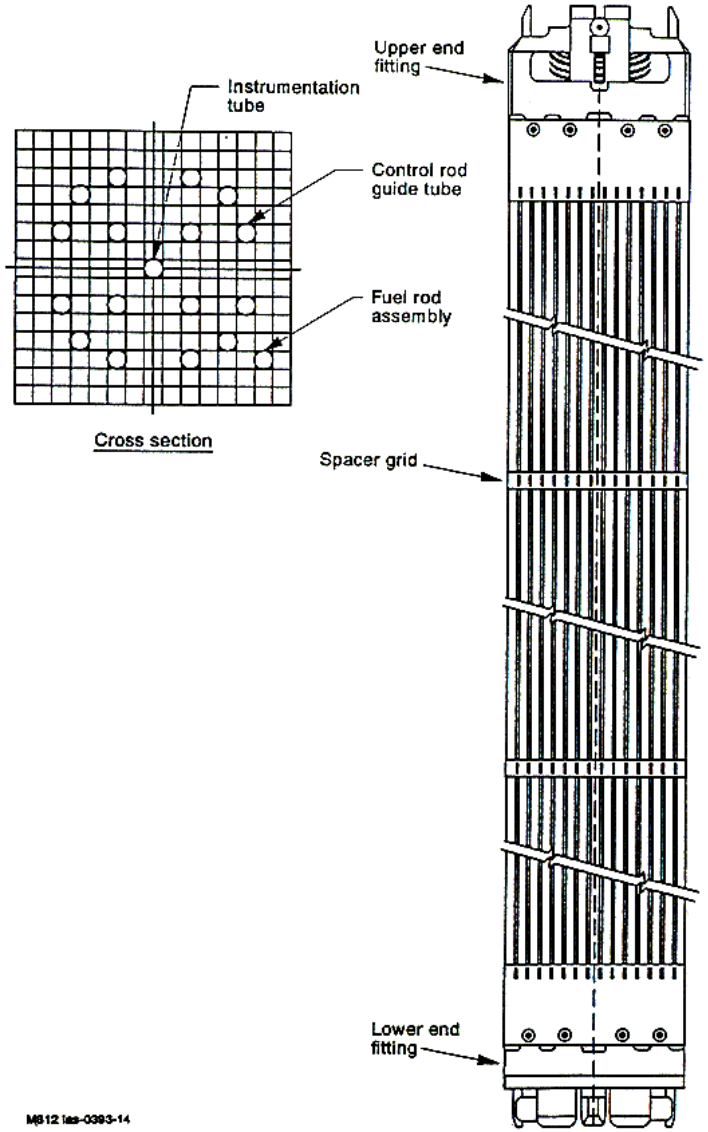

Fuel assembly.

Figure 4.1.12b: TMI-2 Reactor Vessel Internals and Fuel Assembly Sections

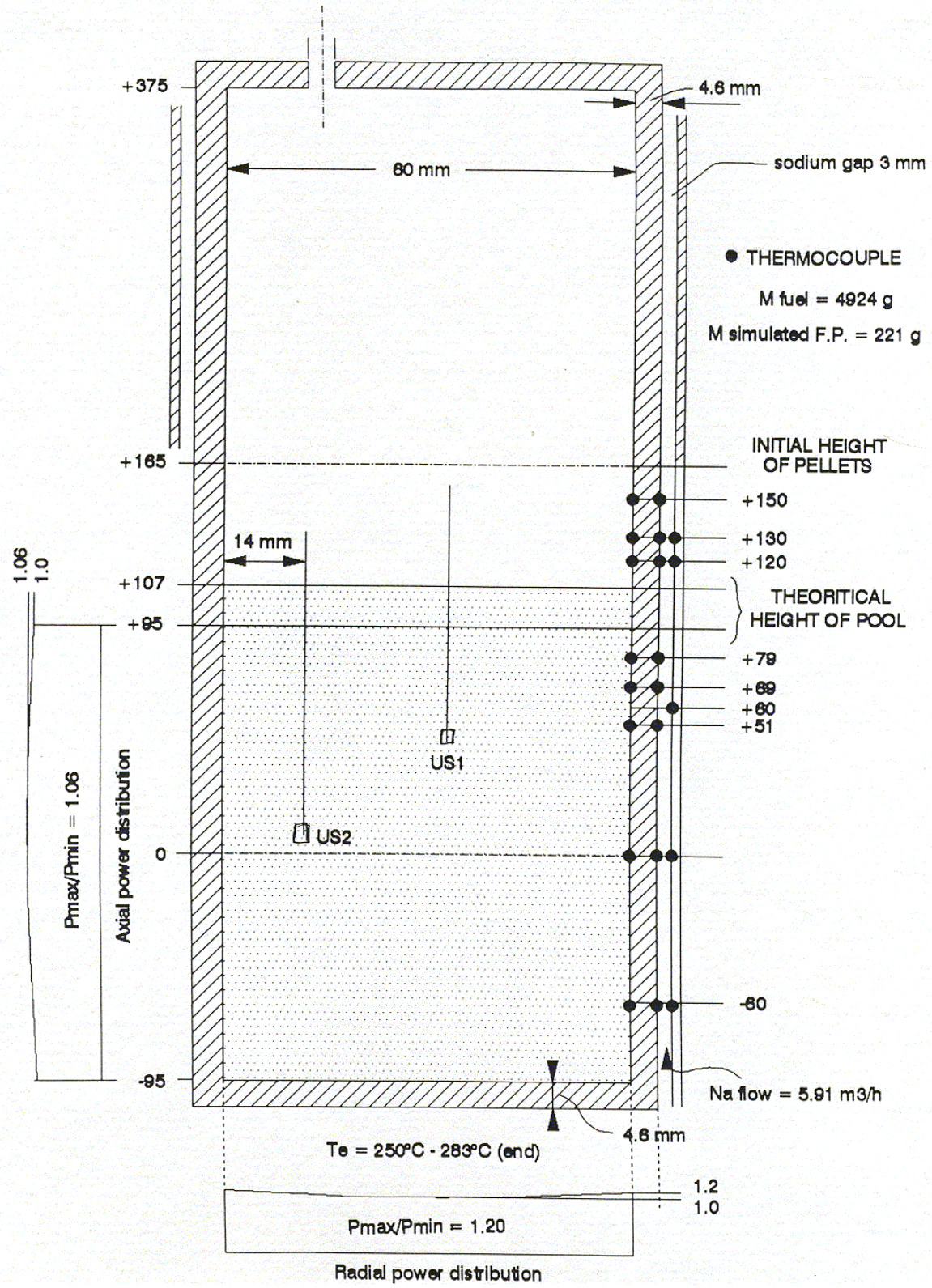

Figure 4.1.13: SCARABEE BF1 Test Train and Instrumentation

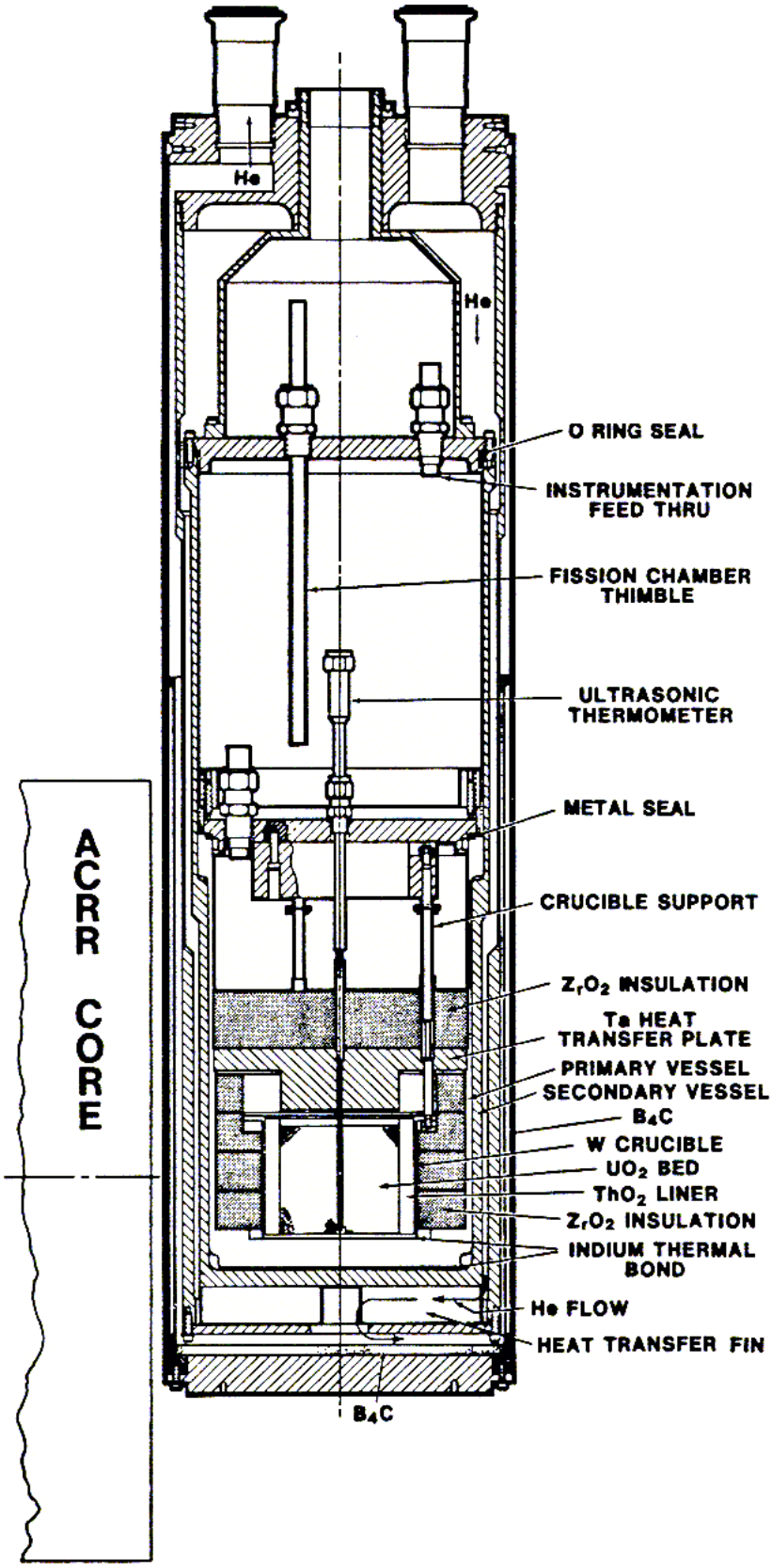

Figure 4.1.14: ACRR-DC Capsule Test Configuration

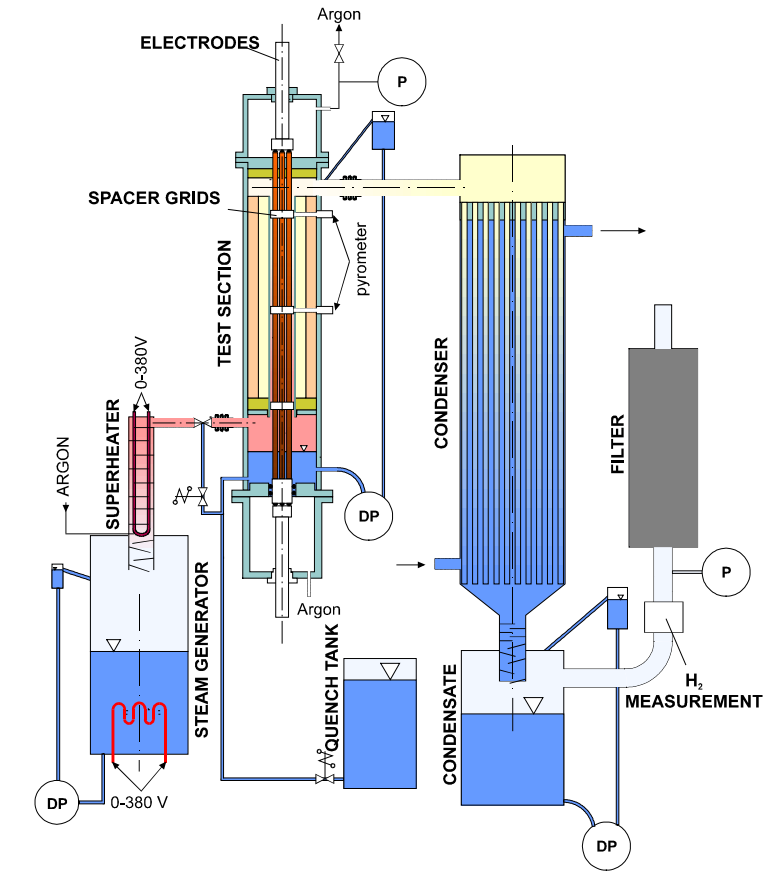

Figure 4.1.15a: General View of the CODEX VVER Facility

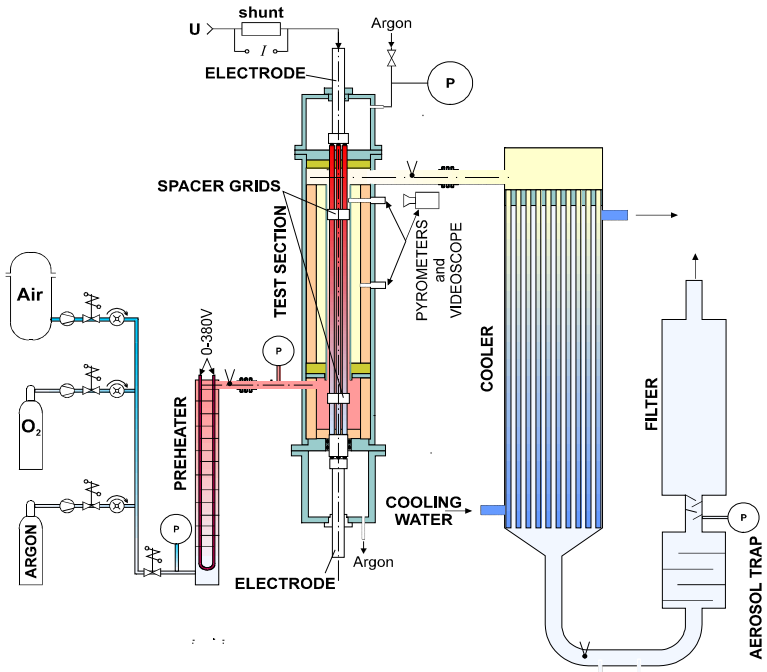

Figure 4.1.15b: General View of the CODEX AIT Facility

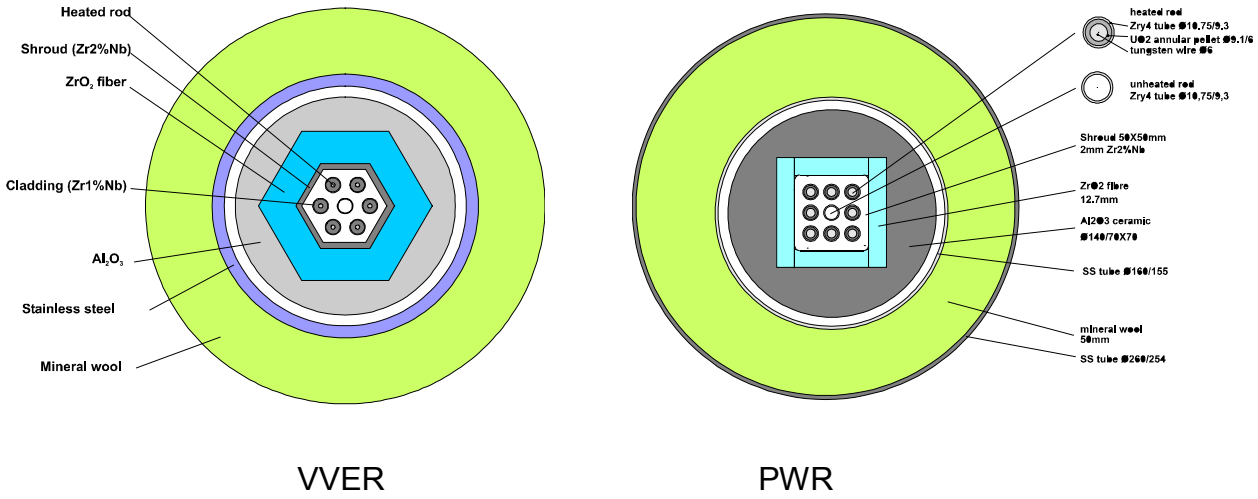

Figure 4.1.15c: CODEX Bundle Cross-Sections

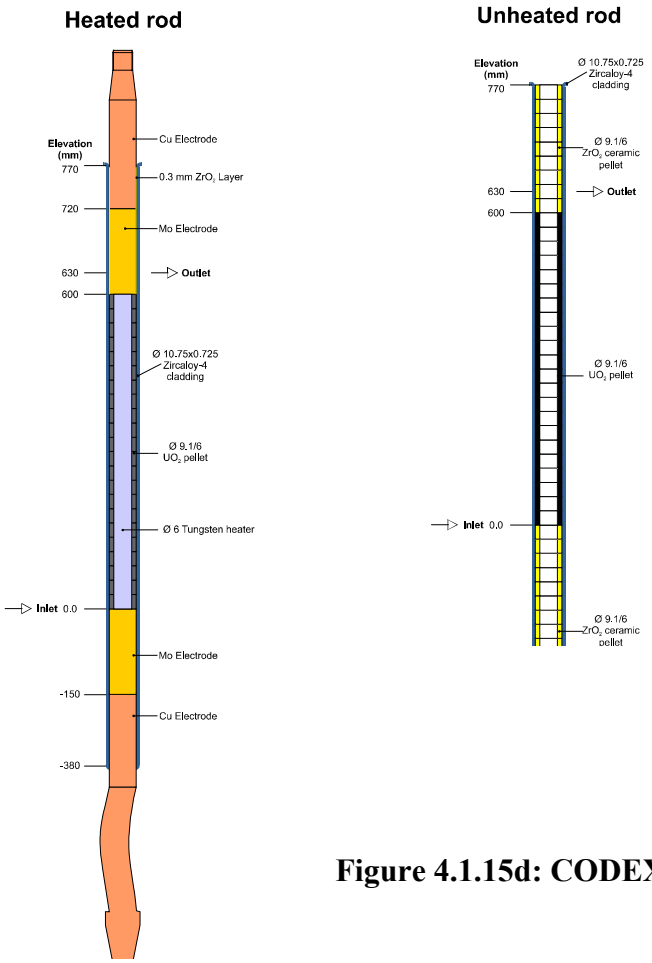

Figure 4.1.15d: CODEX Fuel Rod Simulators

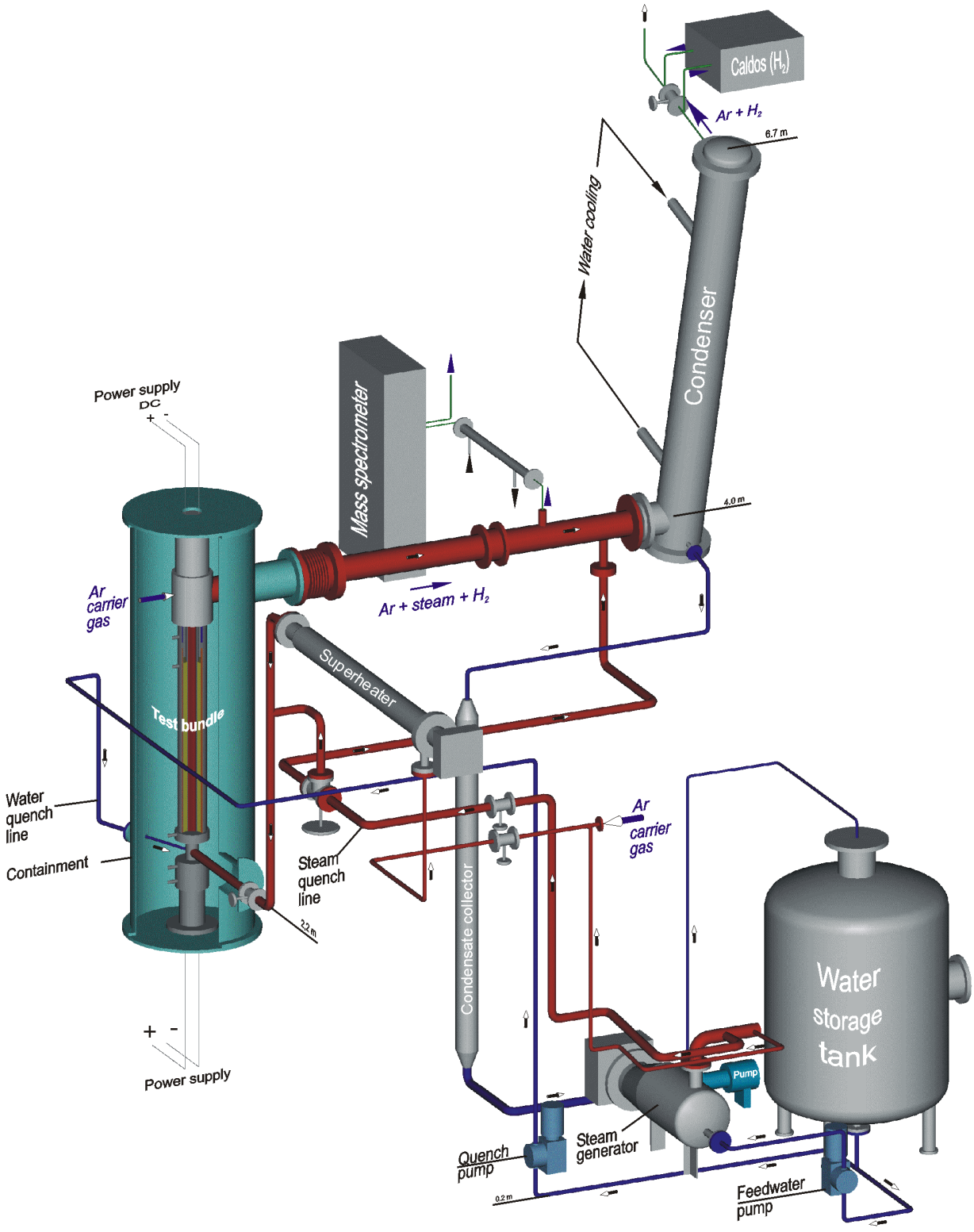

Figure 4.1.16a: FZ Karlsruhe Bundle QUENCH Facility Test Train

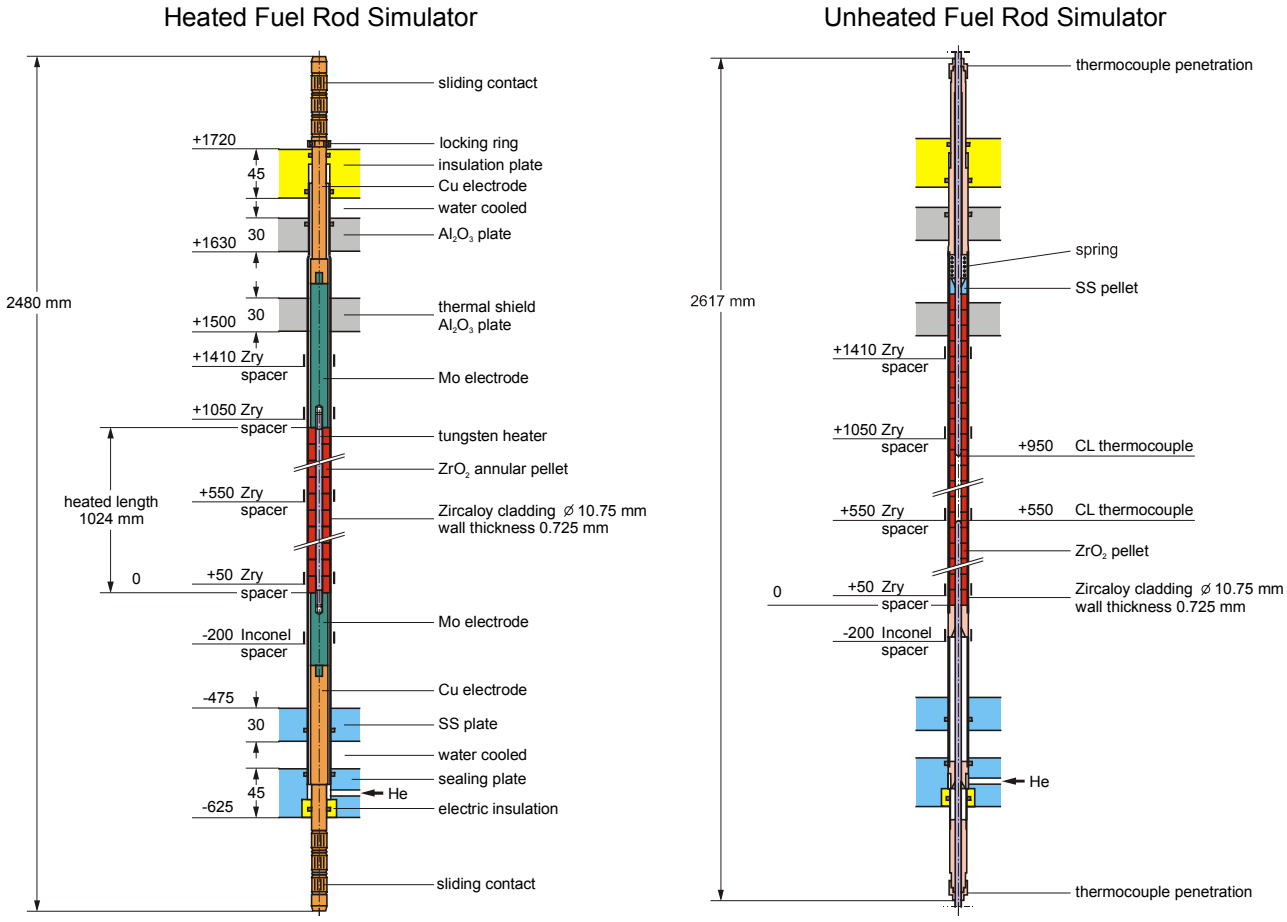

Figure 4.1.16b: FZ Karlsruhe Bundle QUENCH Facility Fuel Rod Simulators

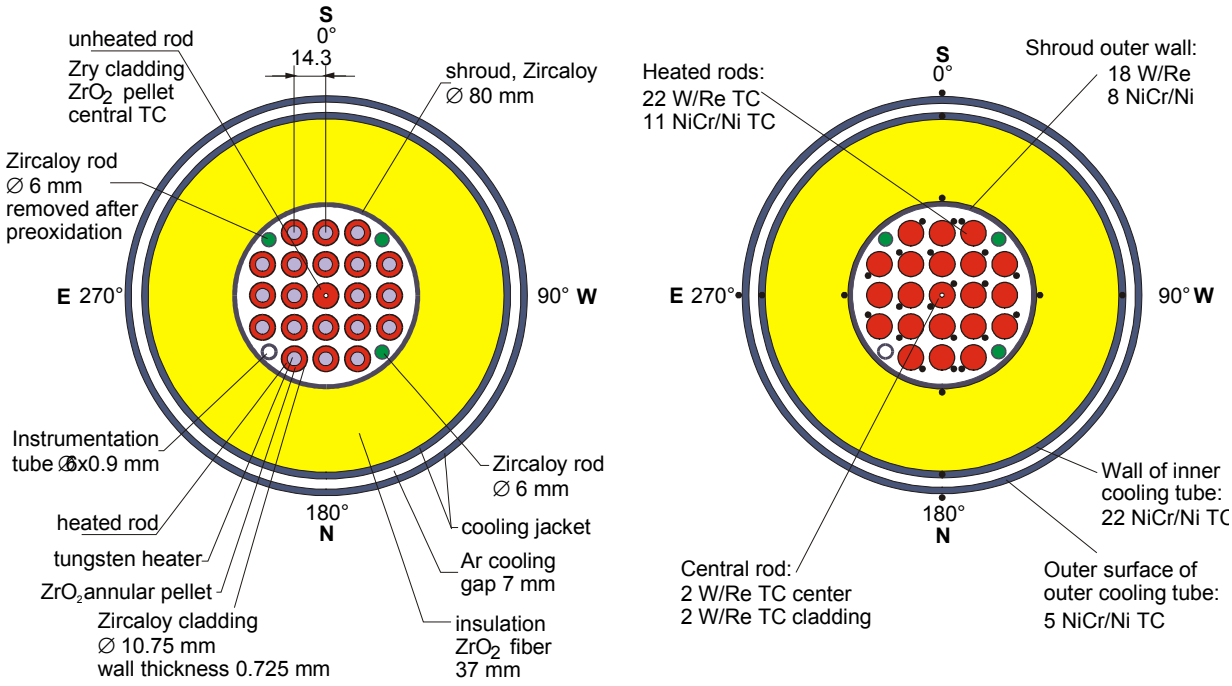

Figure 4.1.16c: FZ Karlsruhe Bundle QUENCH Facility Bundle Cross-Sections

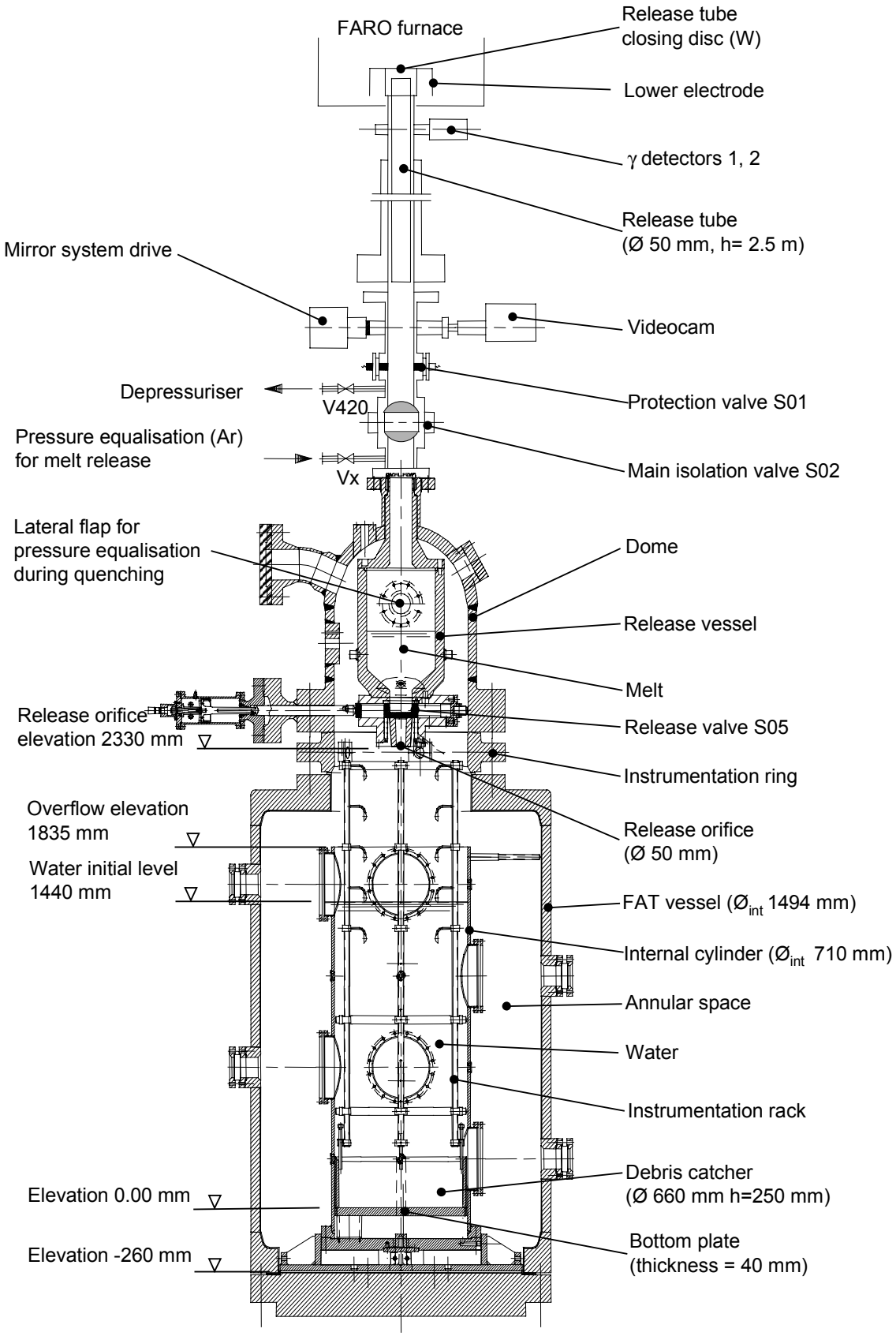

Figure 4.1.17a: Typical FARO Test Arrangement for FCI Test with FAT Vessel

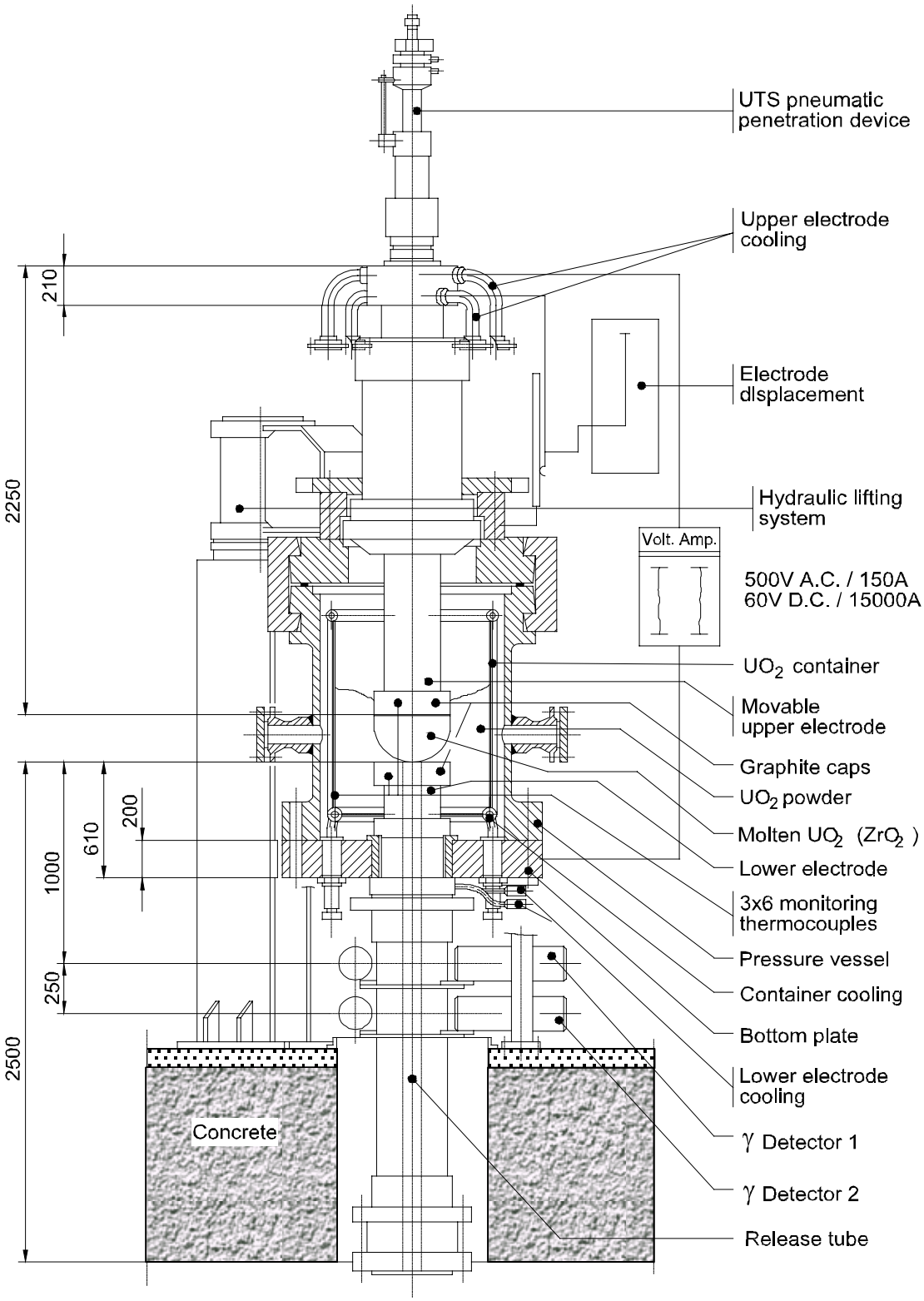

Figure 4.1.17b: FARO Furnace

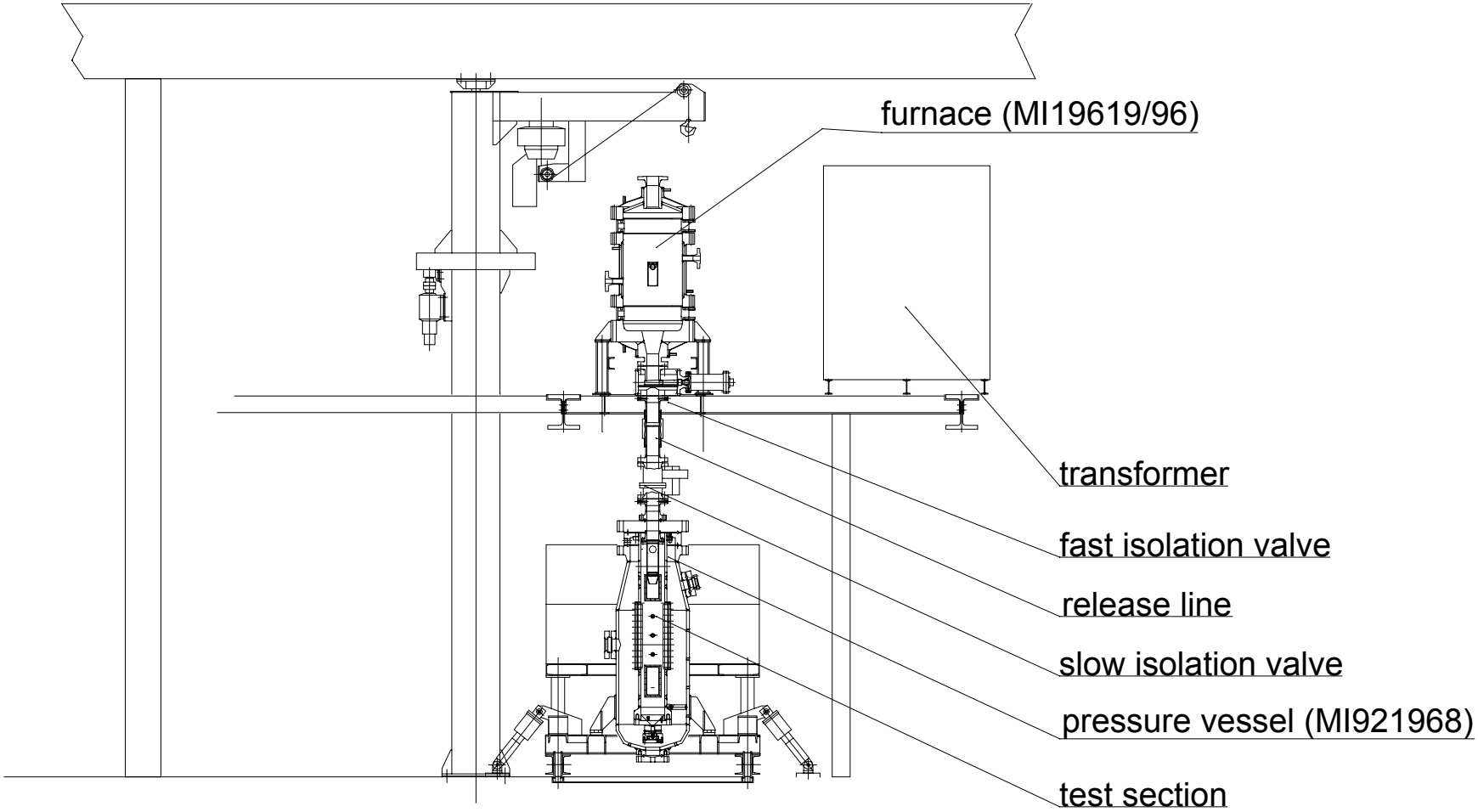

Figure 4.1.18: General View of the KROTOS Facility

Empty page

5. VALIDATION MATRIX

5.1 Matrix Organisation

The objective of the validation matrix table itself is firstly to cross-reference the experiments reviewed against the key experimental features, boundary conditions and phenomena observed, using the same criteria for every experiment (including separate effects tests), secondly to characterise and rank the experiments against an agreed set of selection criteria, and finally to give an overall ranking summarising the value of each experiment for code validation. The choice of selection criteria, and the formatting of the cross-reference table takes into account experience from the Thermal Hydraulic Separate Effects Matrix [5.1]. The sections below summarise the criteria used, present the cross-reference matrix itself in Tables 5.1 to 5.5, justify the selection of the highest ranking tests, and identify qualitatively gaps in the overall database, within the scope of the exercise.

Some simplifications to the organisation have been made with respect to the initial In-Vessel Core Degradation Validation Matrix [5.2]. Most importantly, the categorisation of preferred tests has been reduced from four categories to the top two, as these should be sufficient for code validation in the large majority of cases. This imposes a higher standard on the quality of data/documentation and boundary conditions, therefore the lowest category in each of these has been removed to give two categories remaining in each case. Special treatments apply to late phase separate-effects experiments which do not fit easily into this scheme.

5.2 Selection Criteria

In order to provide ranking of the experiments reviewed, three key features of the experiments and their databases were selected, namely the quality of the data and documentation, the quality of the boundary conditions, and the dominant characteristic (nature and/or purpose of each experiment). Criteria based on these features were applied to each experiment and assignations within the headings were made. Finally, these results were in turn reviewed to give an overall ranking for each experiment. Each of the criteria are outlined below.

5.2.1 Data/Documentation

Two categories of data and associated documentation are defined:

1 : Complete/Full. The information is essentially completely sufficient for analysis of the test;

2 : Incomplete/Preliminary. Not all the data are available, and/or some may be in preliminary form and be liable to change. Nevertheless, enough information is available for a meaningful analysis.

An indication by an asterisk is given regarding whether data are available in electronic form. If data are available in this form, code-to-data comparison is facilitated.

5.2.2 Boundary Conditions

Two categories for the quality of boundary conditions are defined:

1 : Well-defined. All boundary conditions relevant to detailed analysis are known;

2 : Partially-defined. Some judgement and/or sensitivity studies may be needed.

5.2.3 Dominant Characteristics

The dominant characteristic indicates the nature of the test, and the sequence given below bears a relation to how knowledge has progressed in a given area. Thus, understanding proceeds from a qualitative to a quantitative basis. The assignments given are not value judgements per se, but give some indication of the use to which the data have been or could be put.

E : Exploratory. Tests of this kind investigate phenomena which are hitherto poorly understood. The investigation may be of a largely qualitative nature.

P : Parameter Range. In experiments of this nature, phenomena are investigated in a more quantitative manner, to find out how the phenomena are sensitive to changes in boundary conditions.

M : Model Development. The phenomena are investigated in sufficient quantitative detail to enable the formulation of mechanistic models.

U : Unique. There are few or no data available of a similar type. This increases the importance of the data, even though some aspects may be poorly defined.

S : International Standard Problem. The experiment has been selected for an OECD/CSNI International Standard Problem exercise. This implies that the data have been selected as being well-qualified and amongst the best in the field for code analysis, and the data will normally have been analysed by several organisations using a range of computer codes. Detailed reports on the data and on the results of the code analysis (ISP comparison report) are or will be available.

R : Reactor Typical. The data have been obtained under conditions closely or completely prototypic of a severe reactor accident. The test results are easier to transpose to reactor conditions.

Assignments are not made under this heading if inapplicable, if no clear distinction is possible, or if there are insufficient data available to make a valid judgement.

5.2.4 Key Test

The rankings under this heading summarise the results of the previous evaluations. Two categories of key test are defined, in merit order:

1 : Category 1 experiments are amongst the best qualified for code validation in their field. ISPs normally fall into this category. Data are well documented and boundary conditions are well defined (these conditions may be relaxed if there are specific unique features). Category 1 tests are strongly recommended for the validation of system codes (depending on their specific objectives);

2 : Category 2 experiments are well qualified for code validation, and could be used to increase the degree of confidence in a code's suitability for a given application. The experiment may not be unique, but valuable in the sense of parameter range.

In general, no key test assignments are made for separate effects experiments, since they are unlikely to be used directly for system code validation. For example, the results of materials interaction experiments (section 4.2.2) and single rod reflood experiments (section 4.2.3) are generally used to derive correlations or models which are built directly into codes. Exceptions are made in the case of bundle ballooning (section 4.2.1) and fuel coolant interaction (FCI) experiments (section 4.2.8).

In the first of these cases, ballooning is treated as a separate effect in severe accident analysis but was studied as a main objective in design basis analysis. The tests chosen could in principle be used as integral tests for validation of ballooning models in severe accident codes, and are therefore treated the same way in the validation matrix table, see section 5.4.3. The specific ballooning tests listed in the cross-reference table in the same format as in the core degradation integral experiments are judged to be the best from the series reviewed in Chapter 4. Regarding FCI, these tests do not fit easily into the format used for the bundle-like experiments as the boundary conditions and phenomena observed are quite distinct, therefore a separate one is used. Furthermore, some have been treated as integral tests (sections 4.1.17 and 4.1.18). For justification of the treatment and choice of FCI experiments, see section 5.4.4.

The late phase separate-effects experiments described in sections 4.2.4-4.2.8 are of a different nature to the early phase experiments. They cover different processes, and these are modelled in the system codes in a simplified or highly parametric manner. Therefore is questionable if these models can be validated in the same systematic way as for their early phase counterparts. However these experiments are useful for model verification of CFD, structural mechanics and other codes for specific applications. They are summarised in Table 5.5 with cross-reference for specific processes or phenomena. and experiments which represent best conditions in-reactor.

5.3 Cross-Reference Matrix

The resulting cross-reference matrix is presented in Table 5.1 to Table 5.4 according to the categorisation and type of test. The experiments in each table are listed in column order, first by category (if appropriate) and then following the sequencing in Chapter 4. Recent experiments where information is as yet incomplete (currently only PHEBUS FPT4) are identified by italics, indicating a provisional assignment based on our judgement regarding their final status. This is useful in helping to identify further experimental needs.

The row headings give initially the overall ranking ("key test" rating) followed by the secondary criteria on which the overall ranking is based. These are followed in turn by summary identification of the experiment type, main features, boundary conditions and main phenomena observed, using a reduced set of the headings identified in the tables of Chapter 4. The reductions are necessary to make the cross-reference table of a readable and manageable size, while retaining the essential material. The experimental conditions and phenomena observed are extracted from the relevant tables in Chapter 4, while the judgements made regarding selection of tests take into account the additional information (such as availability of documentation) and critiques given in Appendix A. The number of top-ranking tests has been

kept down to that considered necessary for adequate validation of a mechanistic system code such as ATHLET-CD, ICARE2, or SCDAP/RELAP5, as well as for mechanistic models in integral system codes such as ASTEC or MELCOR, within the overall scope laid down for this report, as defined in Chapter 1.

The overall arrangement of the matrix facilitates the addition of new experiments, simply by extending the matrix over additional pages in the same format. The matrix tables conclude with summaries of the abbreviations used.

5.4 Justification of Key Tests

This section provides justification for the category 1 and 2 key test assignations given in Tables 5.1 to 5.4; the reasons may help in deciding which tests to choose, if validation is limited in scope or in the number of analyses which may be performed.

The ordering of the tests given in the following tables does not indicate a ranking within each category.

5.4.1 Category 1 Core Degradation Integral Experiments

For category 1 twelve tests, CORA-13, CORA-28, CORA-33, CORA-W2, PHEBUS B9+, PBF SFD-1.4, ACRR ST-1, ACRR DF-4, LOFT LP-FP-2, PHEBUS FPT1, ACRR MP-1, ACRR MP-2, and the reactor accident TMI-2 were selected. These experiments are listed in Table 5.1.

CORA-13 : This test provides well-qualified, well-documented and extensively analysed data on an electrically heated PWR bundle quenched during early phase melt progression. Detailed data and post-test examination reports are available. It was selected for ISP-31.

CORA-28 : This test gives bounding data on early phase melt progression in a BWR bundle with pre-oxidised cladding and channel box (ZrO_2 thickness up to 40 µm). A detailed data report is available.

CORA-33 : This experiment is a unique source of well-documented data on early phase melt progression under BWR dry core heat-up conditions. A detailed data report is available.

CORA-W2 : This experiment provides the best reference data for early phase core degradation using VVER1000-specific materials including boron carbide absorber in cylindrical geometry. Detailed data and post-test examination reports are available. It was selected for ISP-36.

PHEBUS B9+ : This well-documented and extensively analysed experiment gives well-qualified reference data on early phase bundle degradation in the absence of absorber materials, under nuclear heated conditions. It was selected for ISP-28.

PBF SFD-1.4 : Early phase degradation of a fission heated PWR bundle is studied under a high system pressure (the highest system pressure used in a well-qualified test) with very high temperatures (> 2800 K). The test has been extensively analysed and detailed documentation is available.

ACRR ST-1 : Unique well-documented data are provided on early phase melt progression phenomena associated with irradiated fuel (such as fuel foaming), along with data on fission product release.

ACRR DF-4 : This test provides the reference for early phase melt progression in a fission heated BWR bundle. This test has been extensively analysed and is well-documented.

LOFT LP-FP-2 : This was a large-scale fission product decay-heated PWR test that provides an invaluable link between the smaller-scale tests and the TMI-2 accident. Well-documented core degradation and fission product data are available, and the test has been extensively analysed. The data during reflood, showing renewed heat-up and hydrogen production are also important.

PHEBUS FPT1 : This test provides unique data on the transition from early to late phase core degradation using fuel irradiated to prototypical reactor levels, and the effect of the degradation of such irradiated fuel on fission product release. The experiment has been selected for a future ISP, for which no reference number had been assigned at the time of writing. The data will become freely available in 2001, ready for the start of the ISP.

ACRR MP-1&2 : This pair of tests, which should be considered together for analysis purposes, provide unique information on melting of ceramic debris beds during fission heating, with melt pool and crust formation. The experiments differ in the maximum temperatures, and therefore in the stage, of late phase melt progression reached.

TMI-2 : The TMI-2 accident provides the only full-scale severe core damage data, with all stages of an accident sequence being represented. It has been very extensively documented and analysed. The boundary conditions in many cases are uncertain and the results therefore require considerable interpretation. The chief value of TMI-2 lies in its uniqueness in terms of scale and range of phenomena encountered.

5.4.2 Category 2 Core Degradation Integral Experiments

For category 2 twenty tests, CORA-2, CORA-5, CORA-12, CORA-15, CORA-17, CORA-31, CORA-30, PHEBUS SFD C3+, PHEBUS SFD AIC, NRU FLHT-5, ACRR DF-2, PHEBUS FPT0, Sandia XR1-2, SCARABEE BF1, ACRR DC-1, CODEX-AIT1, CODEX-AIT2, QUENCH-01, QUENCH-03, QUENCH-04, plus one provisional assignment, PHEBUS FPT4, were selected. These experiments are listed in Table 5.2.

CORA general : A main strength of the CORA series is the orderly variation of parameters, so that by comparing tests, the effect of a single parameter may be evaluated. Uncertainties in thermal hydraulic conditions pose a problem common to most tests. Also, a model of the CORA electrical heating element is needed to analyse the experiments. It is therefore recommended that the tests are analysed in groups rather than individually.

CORA-2 : This reference UO_2 test without absorber materials enables the influence of Inconel grid spacer material interactions on early phase core degradation to be studied in isolation. Detailed data reports are available. The large number of viewing ports means that flow bypass was high and detailed account must be taken of this in analysis.

CORA-5 : The influence of PWR absorber materials on early phase core degradation is studied, with an evaluation report available. This test was performed with quartz glass in its viewing ports, therefore bypass flow is negligible.

CORA-12 : This test provides valuable data on quench of a PWR bundle, with an evaluation report on the material behaviour available. It is a useful counterpart test to CORA-13, with reduced hydrogen generation.

CORA-15 : The effect of clad ballooning on PWR early phase melt progression is studied. Documentation so far is however limited.

CORA-17 : The effect of quenching is studied in the presence of BWR absorber materials. With conditions during the heat-up phase being steam-starved, most of the hydrogen (about 90%) is produced during reflood, providing a bounding case for validation of quench models. Documentation so far is however limited.

CORA-31 : The effect of low heat-up rate is studied under BWR conditions, with good documentation being available.

CORA-30 : The effect of low heat-up rate is studied under PWR conditions, documentation is however so far limited. The initial heat-up rate is the lowest investigated in the CORA series, and therefore provided a bounding case.

PHEBUS C3+ : This test enables investigation of the UO_2/Zircaloy reaction within a ZrO_2 shell above 2000 K in the absence of the complicating factors seen in the C3 test, under in-reactor conditions. Detailed data reports are available.

PHEBUS AIC : PWR control rod failure and the spreading/interaction of the absorber material is studied at temperatures low enough to prevent fuel reactions. Thus, PWR absorber effect can be studied in isolation, under in-reactor conditions. Detailed data reports are available.

NRU FLHT-5 : This test gives unique data on early phase melt progression in a PWR bundle under in-reactor conditions with a full-length bundle, which allows the study of freezing and remelting of metallic crusts. The test has reasonably well-controlled boundary conditions. Reasonable documentation is available. However, radial heat losses are very high.

ACRR DF-2 : Well-documented in-reactor data are provided on early phase melt progression in the absence of absorber materials, with medium system pressure.

PHEBUS FPT0 : This test provides unique data on the transition from early to late phase core degradation and the effect of the degradation on fission product release, for fuel with very low burnup (trace-irradiated). It forms a companion to the category 1 test FPT1 which was conducted with prototypically irradiated fuel. An extensive data report is publicly available.

PHEBUS FPT4 : Unique in-reactor data are provided on the transition from debris bed to melt pool geometry, and associated fission product retention and release. The assignment is provisional owing to the fact that at the time of writing the test had been recently completed and much post-test examination and analysis remained to be done. The assignment may be upgraded on future review.

Sandia XR1-2 : Although exploratory in nature, this test provides unique data on the progression of melt through prototypic BWR lower core plate geometry.

SCARABEE BF1 : Unique in-reactor data are provided on high temperature melt pool thermal hydraulics using molten UO_2. Although the test was undertaken as part of a fast reactor programme, the results are applicable to LWR conditions.

ACRR DC-1 : Data are available on the melting of a dry debris bed (fuel/stainless steel) using nuclear heating with very high temperatures (to 3400 K) and melt pool formation being attained; the high temperature aspect is particularly useful. Only hardcopy data are available.

CODEX-AIT1 : This was the first bundle experiment to investigate the effect of air ingress on fuel rod degradation in the early phase. The heatup and degradation in air of the preoxidised bundle was terminated at the point of loss of rod-like geometry, following extensive nitriding of the cladding under oxygen-starved conditions. There is some uncertainty in the thermal hydraulic boundary conditions owing to unmonitored entry of cold air in the heatup phase, and the pre-oxidation in an argon/oxygen mixture is not prototypic.

CODEX-AIT2 : The second bundle experiment to investigate the effect of air ingress on fuel rod degradation in the early phase was terminated following extensive relocation of fuel and oxidised cladding leading to blockage formation. Unique data are provided on UO_2 aerosol formation under such conditions. The pre-oxidation stage, intended to be in steam only, was compromised by leakage of cold air into the test section leading to some uncertainty in heat transfer conditions and oxidation state at the start of air ingress.

QUENCH general : The QUENCH bundle series follows the same philosophy as the CORA series, but investigating reflood of a degrading bundle rather than early phase core degradation generally. Instrumentation was optimised for reflood conditions with special attention paid to measuring the hydrogen release. As for CORA, a model of the electrical heating element used is needed to analyse the experiments, and again it is recommended that the tests are analysed in groups rather than individually, in a way that conditions covering the presence and absence of excess hydrogen production are both studied. The use of zirconia rather than urania pellets is not prototypic. A future QUENCH test with reflood by water has been selected for a new ISP.

QUENCH-01 : The first main bundle quench test covered reflood with water of a preoxidised bundle from a relatively low temperature under conditions which did not lead to a renewed temperature escalation on reflood. It thus serves as a useful reference test.

QUENCH-03 : This experiment covered reflood with water of a non-preoxidised bundle from a higher temperature than that used in QUENCH-01, under conditions which did lead to a renewed temperature escalation on reflood with associated hydrogen production. It thus serves as a counterpart to QUENCH-01. Some uncertainty exists regarding the hydrogen production, with different measuring devices giving inconsistent readings, and so the values quoted finally by the experimenters represent their best judgement.

QUENCH-04 : This was the first QUENCH experiment to employ rapid cooling by steam. It used a non-preoxidised bundle. The test conditions led to a very limited renewed excursion and no significant extra hydrogen production. The use of steam cooling leads to more precise control of the test and in principle to the thermal hydraulic boundary conditions being better defined. However these conditions may not be as prototypic as those with reflood with water. The counterpart preoxidised experiment QUENCH-05 conducted in March 2000 fell outside the review period, but could be considered in future as a convenient test for a paired analysis.

5.4.3 Bundle Separate Effects Experiments

They comprise ballooning experiments in bundle geometry which while addressing the specific issue of clad deformation under design basis conditions, nevertheless have some integral characteristics owing to the interaction of heat conduction, thermal hydraulic, clad oxidation and material deformation effects. Of the four tests selected, REBEKA-6 and NRU MT-4 were assigned category 1, while PHEBUS 218 and MRBT B6 were assigned category 2. These experiments are listed in Table 5.3.

Category 1 Tests

REBEKA-6 : This test is a well-documented and analysed example of a ballooning experiment carried out with a large bundle, with electrical heating. It was selected for ISP-14.

NRU MT-4 : The MT-4 experiment is a well-documented example of a bundle ballooning test carried out under nuclear heating. It is preferred over MT-3 and PHEBUS 218 in the present context as the clad deformation takes place under ramp rather than reflood conditions.

Category 2 Tests

PHEBUS 218 : This ballooning test from the in-reactor PHEBUS LOCA series has the advantages of having been performed in-reactor, and having been the basis of ISP-19. Extensive analysis performed in the framework to some extent balances uncertainty in the thermal hydraulic boundary conditions.

MRBT B6 : This electrically heated ballooning test has the advantage of the use of a very large bundle (64 rods), with clad deformation occurring on a rising temperature ramp (as expected in a severe reactor accident). Data are well-qualified, but cross-bundle temperature gradients are untypical.

5.4.4 Fuel-Coolant Interaction (FCI) Multi Effects Experiments

Three tests, FARO L-14, FARO L-28, and KROTOS K-44, were selected for Category 1:

FARO L-14 : This test provides well-qualified, well-documented first-of-a-kind data on overall quenching of a large pour of molten UO_2-ZrO_2 corium into water in prototypical in-vessel scenario. It was the subject of ISP-39.

FARO L-28 : This test provides well-qualified, well-documented unique data on the quenching behaviour of a long pour of molten UO_2-ZrO_2 corium into water in prototypical moderate pressure in-vessel conditions. The test is particularly well suited to analyse the jet column erosion process. Visualisations are available.

KROTOS K-44 : Baseline test for steam explosion investigation (alumina melt). It provides well-qualified, well-documented data which has been widely used for analysing steam explosion phenomena and validating models.

Four tests, FARO L-11, FARO L-31, FARO L-31, and KROTOS K-58, were selected for Category 2:

FARO L-11 : First-of -kind test showing the effect of the presence of a metallic phase (Zr) on corium melt quenching. There are uncertainties on the initial temperature of the melt and the quantity of hydrogen produced was not measured.

FARO L-31 : This test provides data on overall quenching of molten UO_2-ZrO_2 corium into sub-cooled water (ex-vessel scenario).

FARO L-33 : This test provides first-of-a-kind data on steam explosions involving ~40 kg of molten UO_2-ZrO_2 corium into sub-cooled water in unconstrained geometry.

KROTOS K-58 : Visualisation of corium mixing prior to triggering a propagating event. All data are available and well-documented. There are uncertainties on the effect of windows on energetics.

These FCI experiments are listed in Table 5.4.

5.5 Late Phase Separate Effects Tests

In Chapter 3 the late phase phenomena were identified and described in the last two chapters. The construction of the cross-reference matrix for late phase separate effect tests follows this approach for the aspects of core debris in the lower plenum. The tests which represent best the phenomena under reactor conditions during an unrecovered severe accident are included in this matrix, indicating the phenomena covered.

5.5.1 Melt Pool Thermal-hydraulics

The melt pool thermal hydraulics experiments are used to establish correlations for the heat transfer coefficient from the melt to the wall or to the crust. These correlations are built into the system codes for the calculation of heat transfer and crust thickness considering appropriate phase diagrams for liquefaction and solidification. Therefore it is not useful to validate system codes against thermal hydraulic experiments on molten pools. Nevertheless the benchmarking of system codes models against crust formation experiments is useful for model verification. Beyond that, these experiments can be used for the validation of CFD codes (like TOLBIAC or CONV2D). The reactor situation is best covered by BALI (high Rayleigh number), RASPLAV Salt (crust formation) and SIMECO (two-layer molten pool). Detailed information and data reports of these experiments have to be requested from the operating institutions. The phase separation process is recently investigated in numerous small-scale experiments but not yet described by this validation matrix.

5.5.2 Gap Thermal-hydraulics

Small-scale gap thermal-hydraulics experiments are used to establish correlations for the heat transfer from the debris to the RPV wall and the fluid penetrating the gap in between as well as for the limitation of heat flux. The interpretation and understanding of the gap thermal hydraulics are in a preliminary state. For the verification of specific models the results of the BENSON rig are most useful due to the reactor-typical conditions, even if the maximum heat flux is rather limited. Recent small-scale experiments for debris heat transfer with water and steam flow have been performed (CORCOM). They could be useful for model verification, but they have rather limited heat source density. Up to now there is no system code which is able to simulate adequately the gap thermal hydraulics or quenching of hot debris bed.

5.5.3 Ex-vessel Thermal-hydraulics

The thermal-hydraulic experiments for external cooling of RPV, except SULTAN, were performed to confirm the cooling capability of specific reactor designs. The results could be directly applied or extrapolated to the reactor case. With one experiment (SBLB) the influence of thermal insulation on the cooling capability of a typical reactor design has been investigated. These experiments can be used to verify the thermal hydraulic models under specific conditions. Due to the 1/1 scale the CYBL facility represents best the conditions in a reactor cavity without restriction of water inflow and steam outflow. The SULTAN experiments are more fundamental and were used to establish heat transfer correlations to be implemented in system codes.

5.5.4 Gap Formation

The experiments dealing with gap formation have a more integral character. They combine to some extent in-vessel melt pool thermal hydraulics, crust formation, wall deformation and creeping up to vessel failure. Also injection of water is planned to investigate the potential for gap cooling. The experimental data base is up to now rather sparse. Evaluation of the results has to be left for the future. Also adequate models for gap formation are not yet implemented in system codes.

5.5.5 Fuel Coolant Interaction

Two experimental test series with reactor-typical core melt and conditions are already listed under integral tests (FARO and KROTOS). The tests described in the separate-effects section are devoted to exploration of specific phenomena and do not use real corium. They are useful for model development and model verification in FCI codes. Up to now detailed models for FCI are not yet implemented in system codes which could be validated against these experiments.

5.6 Identification of Remaining Experimental Needs

The defined scope of the validation matrix exercise precludes quantitative identification of the overall adequacy of the database considered in covering the range of conditions likely to be encountered in LWR severe accident sequences. Nevertheless, some qualitative indication of the coverage can be deduced by considering how well populated are the rows of the matrix which cover boundary conditions, phenomena observed etc.

Considering firstly early phase phenomena, it is readily seen that this area has been the subject of much experimental investigation, and that the main phenomena have been well covered on an integral basis. This observation does not necessarily mean, however, that it is possible to formulate mechanistic models with the required degree of fidelity; such judgements are beyond the scope of this report. Turning to the late phase, most of the phenomena have been covered in experiments dealing with defined configurations such as debris beds and melt pools, with the same proviso regarding model development as noted before. Overall, substantial progress has been made since the 1991 SOAR [5.3] and its update [5.4], for example as quoted in the Final Reports of EC Fourth Framework projects [5.5], [5.6], [5.7], [5.8], as summarised in [5.9], in the PHEBUS-2000 Seminar [5.10], and in the Rasplav Application Report [5.11]. It is noted specifically that there are now considerably more data in the late phase area.

Taking this progress into account, and reflecting the degree of understanding of phenomena tabulated in Chapter 3 above, it is considered that the following parameters or processes are not fully covered or understood only in a limited way:

- High burn-up or MOX effects on core degradation;
- Renewed temperature excursion following quenching at high temperatures (>1600°C);
- Effects of air ingress on core degradation;
- Transition from early to late phase core degradation;
- Crust failure mechanism;
- Slumping of melt from the core region into the lower plenum;
- Quenching of melt or hot debris during or after relocation;
- Phase segregation or separation of molten pool;
- Vessel failure under thermal and mechanical loads.

It should be emphasised that this list is limited by the scope of this report. This means, for example, that the feedback of thermal hydraulics phenomena on melt progression, for example that of in-vessel natural circulation in high pressure faults, another area where data may be lacking, cannot be treated here.

New experiments addressing these deficiencies noted above should consider the range of parameters that may occur in severe reactor accidents as far as feasible.

It is noted that at least some of the deficiencies, several of which involve the late phase, will be remedied by successful completion of the remaining tests in the PHEBUS FP programme, of projects in the European Commission 5th Framework programme [5.12] on nuclear fission safety, in the continuing QUENCH bundle experiments at FZ Karlsruhe, and in the proposed OECD-sponsored Masca project which is intended to continue Rasplav.

References

[5.1] Aksan N, D'Auria F, Glaeser H, Pochard R, Richards C and Sjoberg A, "OECD/NEA-CSNI Separate Effects Test Matrix for Thermal-Hydraulic Code Validation, Vols. 1 & 2", OCDE/GD(94)82 & 83, September 1993.

[5.2] Haste T J, Adroguer B, Gauntt R O, Martinez J A, Ott L J, Sugimoto J and Trambauer K, "In-Vessel Core Degradation Code Validation Matrix", NEA/CSNI/R(95)21, OCDE/GD(96)14, Paris, 1996.

[5.3] Kinnersly S R, Lillington J N, Porracchia A, Soda K, Trambauer K, Hofmann P, Waarenpera Y, Bari R, Hunt C and Martinez J, "In-Vessel Core Degradation in LWR Severe Accidents: A State of the Art Report to CSNI, January 1991", NEA/CSNI/R(91)12, November 1991.

[5.4] Haste T J, Adroguer B, Brockmeier U, Hofmann P, Müller K and Pezzilli M, "In-Vessel Core Degradation in Severe Accidents: A State-of-the Art Report, Update January 1991 - June 1995", EUR 16695 EN, 1996.

[5.5] Shepherd I et al., "Investigation of Core Degradation (COBE) Final Report", EUR 18982 EN, 1999.

[5.6] Shepherd I et al., "Oxidation Phenomena in Severe Accidents (OPSA) Final Report", EUR 19528 EN, 2000.

[5.7] Adroguer B et al., "Corium Interactions and Thermochemistry (CIT Project) Final Report“, European Commission report INV-CIT(99)-P040, IPSN/DRS/SEMAR 99/123, December 1999.

[5.8] Magallon D et al., "MFCI Project Final Report", European Commission report INV-MFCI(99)-P007, 1999.

[5.9] G.Van Goethem, A.Zurita, J.Martín Bermejo, P.Lemaître and H.Bischoff, "Main Achievements of FP-4 Research in Reactor Safety", Proceedings of the Fission Safety Symposium (FISA 99 - EU Research in Reactor Safety), EUR 19532 EN, Luxembourg, 29 November - 1 December 1999.

[5.10] IPSN, "Proceedings of the PHEBUS-2000 Seminar, Marseille, France, 20-22 March 2000", to be published, 2000.

[5.11] Tuomisto H, Strizhov V, Sehgal B R, Behbahani A, Gonzalez R, Sanderson B, Trambauer K, "Application of the OECD Rasplav Project Results to Evaluations at Prototopic Accident Conditions" Draft 3. April 2000.

[5.12] Zurita A, van Goethem G and Lemaître P, "Overview of the EC Severe Accident Projects", USNRC Cooperative Severe Accident Research Programme (CSARP) Meeting, Bethesda, Washington, 8-12 May 2000.

Cross-Reference Matrix for Validation of Experiments: Legend to table 5.1, 5.2, 5.3, 5.4.

Key Test	Scale of 1 to 2: most to least suitable for code validation
Selection Criteria	
0.1 Data/Documentation	1 = complete/full; 2 = incomplete/preliminary * = available in electronic form
0.2 Boundary Condition	1 = well defined; 2 = partially defined
0.3 Dominant Characteristic	E = Exploratory; M = Model development; P = Parameter range investigation; R = Reactor typical; S = international Standard problem; U = Unique test
Heat Source	
1.1 Reactor	Y = Yes; n = no (includes fission heat from driver core)
1.2 Heating Method	D = Decay; E = Electrical; F = Fission; M = Micro-wave; W = Wall
1.3 Burn-up	F = Fresh; T = Trace (.lt. 1MWd/kg); M = Medium; H = High (.gt. 40 MWd/kg)
Initial Conditions	
2.1 Heated Length	S = Small (.le. 0.5 m); M = Medium; L = Large (.gt. 1.5 m)
2.2 Fuel Rods	S = Small (.le. 15); M = Medium; L = Large (.gt. 45)
2.3 Spacer Grid Zirconium	Y = Yes; n = no
2.4 Spacer Grid Inconel	Y = Yes; n = no
2.5 Control Assembly AIC	Y = Yes; n = no
2.6 Control Assembly B4C	Y = Yes; n = no
2.7 Core Support Struct.	Y = Yes; n = no
2.8 Initial Fuel Debris	Y = Yes; n = no
2.9 Crust Prefabricated	Y = Yes; n = no
2.10 Preoxidation	n = none; S = Small (.lt. 0.01 mm); M = Medium; L = Large (.gt. 0.05 mm); T = Total
Boundary Conditions	
3.1 Initial Heat-up Rate	L = Low (.le. 0.3 K/s); M = Medium; H = High (.gt. 1 K/s)
3.2 System Pressure	L = Low (.le. 0.5 MPa); M = Medium; H = High (.gt. 3.0 MPa)
3.3 Gas Injection	n = none; A = Air or O2; S = Steam; H = H2; I = Inert
3.4 Steam Starved	Y = global starvation; n = no or only local starvation
3.5 Boil Down	Y = Yes; n = no
3.6 Reflood	n = none; L = at Low temperature; H = at High temperature (.gt. 1800 K); S = rapid cooling by Steam
3.7 Possible Flow Bypass	Y = Yes; n = no
Experimental Conditions	
4.1 Clad Ballooning	Y = Yes; n = no
4.2 Oxidation Excursion	Y = Yes; n = no
4.3 Non Fuel Melt	Y = Yes; n = no
4.4 Fuel Dissolution	Y = Yes; n = no
4.5 Ceramic Melt	Y = Yes; n = no
4.6 Particulate Debris	Y = Yes; n = no Q = from Quench-induced shattering
4.7 Melt Pool	Y = Yes; n = no
4.8 Crust Failure	Y = Yes; n = no
4.9 Structure Ablation	Y = Yes; n = no
4.10 Fission Product Rel.	Y = Yes; n = no; A = fuel Aerosol
	--- indicates not applicable, no clear distinction possible, or insufficient data available to make a valid assignment

Table 5.1: Validation Matrix, Integral Experiments with Key Test Scale = 1 (page 1 of 1)

Test / **Characteristic**	CORA-13	CORA-28	CORA-33	CORA-W2	PHEBUS-B9+	PBF-1-4	ACRR-ST-1	ACRR-DF-4	LOFT LP-FP-2	PHEBUS-FPT1	ACRR-MP-1	ACRR-MP-2	TMI-2
Key Test	1	1	1	1	1	1	1	1	1	1	1	1	1
Data/Documentation	1*	1*	1*	1*	1*	1*	1*	1*	1*	1*	1*	1*	1
Boundary Condition	2	2	2	2	2	2	1	1	2	1	2	1	3
Dominant Characteristic	S	P	U	S	S	R	U	U	R	S	U	U	R
1.1 Reactor	n	n	n	n	n	n	n	n	Y	n	n	n	Y
1.2 Heating Method	E	E	E	E	F	F	F	F	D	F	F	F	FD
1.3 Burn-up	F	F	F	F	F	M	M	F	T	M	F	F	M
2.1 Heated Length	M	M	M	M	M	M	S	S	L	M	S	S	L
2.2 Fuel Rods	M	M	M	M	M	M	S	S	L	M	M	M	L
2.3 Spacer Grid Zirconium	Y	Y	Y	n	n	n	n	n	n	Y	n	n	n
2.4 Spacer Grid Inconel	Y	n	n	Y	Y	Y	n	n	Y	n	n	n	Y
2.5 Control Assembly AIC	Y	n	n	n	n	Y	n	n	Y	Y	n	n	Y
2.6 Control Assembly B_4C	n	Y	Y	Y	n	n	n	Y	n	n	n	n	Y
2.7 Core Support Struct.	N	n	n	n	n	n	n	n	Y	n	n	n	Y
2.8 Initial Fuel Debris	n	n	n	n	n	n	n	n	n	n	Y	Y	n
2.9 Crust Prefabricated	n	n	n	n	n	n	n	n	n	n	Y	Y	n
2.10 Preoxidation	n	M	n	n	n	n	n	n	n	n	T	T	n
3.1 Heat-up Rate	M	M	L	M	L	MH	H	H	H	M	L	L	LM
3.2 System Pressure	L	L	L	L	M	H	L	M	M	L	L	L	H
3.3 Gas Injection	SI	SI	SI	SI	SI	SI	HI	S	S	S	I	I	S
3.4 Steam Starved	n	n	Y	n	Y	n	Y	n	n	n	Y	Y	n
3.5 Boil Down	n	n	n	n	n	Y	n	n	Y	n	n	n	Y
3.6 Reflood	Y	n	n	n	n	n	n	n	Y	n	n	n	Y
3.7 Possible Flow Bypass	Y	Y	Y	Y	n	Y	n	n	Y	n	n	n	n
4.1 Clad Ballooning	n	n	n	n	n	Y	n	n	Y	Y	n	n	Y
4.2 Oxidation Excursion	Y	Y	Y	Y	Y	Y	n	Y	Y	Y	n	n	Y
4.3 Non Fuel Melt	Y	Y	Y	Y	Y	Y	n	Y	Y	Y	n	n	Y
4.4 Fuel Dissolution	Y	Y	Y	Y	Y	Y	Y	Y	Y	Y	n	n	Y
4.5 Ceramic Melt	n	n	n	n	n	Y	n	n	Y	Y	Y	Y	Y
4.6 Particulate Debris	Q	n	n	n	n	Y	n	n	Y	n	Y	Y	Y
4.7 Melt Pool	n	n	n	n	n	Y	n	Y	n	Y	Y	Y	Y
4.8 Crust Failure	n	n	n	n	n	Y	n	n	n	---	n	Y	Y
4.9 Structure Ablation	n	n	n	n	n	n	n	n	n	n	n	n	Y
4.10 Fission Product Rel.	n	n	n	n	n	Y	Y	n	Y	Y	n	n	Y

Table 5.2: Validation Matrix, Integral Experiments with Key Test Scale = 2 (page 1 of 2)

Test / **Characteristic**	CORA-2	CORA-5	CORA-12	CORA-15	CORA-17	CORA-30	CORA-31	PHEBUS-C3+	PHEBUS-AIC	NRU-FLHT-5	ACRR-DF-2
Key Test	2	2	2	2	2	2	2	2	2	2	2
Data/Documentation	1*	2*	2*	2*	2*	2*	1*	1*	1*	2*	1*
Boundary Condition	2	2	2	2	2	2	2	2	1	2	2
Dominant Characteristic	M	M	P	P	P	P	P	P	P	U	E
1.1 Reactor	n	n	n	n	n	n	n	n	n	n	n
1.2 Heating Method	E	E	E	E	E	E	E	F	F	F	F
1.3 Burn-up	F	F	F	F	F	F	F	F	F	FM	F
2.1 Heated Length	M	M	M	M	M	M	M	M	M	L	S
2.2 Fuel Rods	M	M	M	M	M	M	M	M	M	S	S
2.3 Spacer Grid Zirconium	Y	Y	Y	Y	Y	Y	Y	n	Y	Y	n
2.4 Spacer Grid Inconel	Y	Y	n	Y	n	n	Y	Y	n	Y	Y
2.5 Control Assembly AIC	n	Y	Y	Y	n	n	Y	n	Y	n	n
2.6 Control Assembly B_4C	n	n	n	n	Y	Y	n	n	n	n	n
2.7 Core Support Struct.	n	n	n	n	n	n	n	n	n	n	n
2.8 Initial Fuel Debris	n	n	n	n	n	n	n	n	n	n	n
2.9 Crust Prefabricated	n	n	n	n	n	n	n	n	n	n	n
2.10 Preoxidation	n	n	n	n	n	n	n	n	n	n	n
3.1 Heat-up Rate	M	M	M	M	M	L	L	H	M	H	H
3.2 System Pressure	L	L	L	L	L	L	L	H	M	M	M
3.3 Gas Injection	SI	SI	SI	SI	SI	SI	SI	SI	SI	S	S
3.4 Steam Starved	n	n	n	n	n	n	n	Y	n	n	n
3.5 Boil Down	n	n	n	n	n	n	n	n	n	Y	n
3.6 Reflood	n	n	Y	n	Y	n	n	n	n	n	n
3.7 Possible Flow Bypass	Y	n	Y	Y	Y	Y	Y	n	n	n	n
4.1 Clad Ballooning	Y	n	n	Y	n	n	n	n	n	n	n
4.2 Oxidation Excursion	Y	Y	Y	Y	Y	Y	Y	n	Y	Y	Y
4.3 Non Fuel Melt	Y	Y	Y	Y	Y	Y	n	Y	Y	Y	Y
4.4 Fuel Dissolution	Y	Y	Y	Y	Y	Y	Y	Y	n	Y	Y
4.5 Ceramic Melt	n	n	n	n	n	n	n	n	n	n	n
4.6 Particulate Debris	n	n	Q	n	Q	n	n	Y	n	n	n
4.7 Melt Pool	n	n	n	n	n	n	n	n	n	n	Y
4.8 Crust Failure	n	n	n	n	n	n	n	n	n	n	n
4.9 Structure Ablation	n	n	n	n	n	n	n	n	n	n	n
4.10 Fission Product Rel.	n	n	n	n	n	n	n	n	n	Y	n

Table 5.2: Validation Matrix, Integral Experiments with Key Test Scale = 2 (page 2 of 2)

Test / **Characteristic**	PHEBUSFPT0	*PHEBUSFPT4*	SNL-XR1-2	SCARABEEBF	ACRR-DC-1	CODEX-AIT1	CODEX-AIT2	QUENCH-01	QUENCH-03	QUENCH-04
Key Test	2	*2*	2	2	2	2	2	2	2	2
Data/Documentation	1*	*1**	1*	1*	1	2*	2*	1*	2*	1*
Boundary Condition	1	*2*	1	2	1	2	2	1*	1*	1*
Dominant Characteristic	U	*U*	E	U	E	E	U	E	P	E
1.1 Reactor	n	*n*	n	n	n	n	n	n	n	n
1.2 Heating Method	F	*F*	E	F	F	E	E	E	E	E
1.3 Burn-up	T	*M*	---	F	F	F	F	---	---	---
2.1 Heated Length	M	*S*	M	S	S	M	M	M	M	M
2.2 Fuel Rods	M	*n*	---	n	n	S	S	M	M	M
2.3 Spacer Grid Zirconium	Y	*n*	---	n	n	Y	Y	Y	Y	Y
2.4 Spacer Grid Inconel	n	*n*	---	n	n	n	n	Y	Y	Y
2.5 Control Assembly AIC	Y	*n*	---	n	n	n	n	n	n	n
2.6 Control Assembly B_4C	n	*n*	Y	n	n	n	n	n	n	n
2.7 Core Support Struct.	n	*n*	Y	n	n	n	n	n	n	n
2.8 Initial Fuel Debris	n	*Y*	---	Y	Y	n	n	n	n	n
2.9 Crust Prefabricated	n	*n*	---	n	n	n	n	n	n	n
2.10 Preoxidation	n	*T*	---	n	n	M	L	H	n	n
3.1 Heat-up Rate	M	*M*	---	H	L	M	M	M	M	M
3.2 System Pressure	L	*L*	L	L	L	L	L	L	L	L
3.3 Gas Injection	S	*SH*	I	n	I	IA	SA	SI	SI	SI
3.4 Steam Starved	n	*n*	---	Y	Y	n	n	n	n	n
3.5 Boil Down	n	*n*	---	n	n	n	n	n	n	n
3.6 Reflood	n	*n*	---	n	n	n	n	Y	Y	S
3.7 Possible Flow Bypass	n	*Y*	---	n	n	n	n	n	n	n
4.1 Clad Ballooning	Y	---	---	n	n	n	n	n	n	n
4.2 Oxidation Excursion	Y	---	---	n	n	Y	Y	n	Y	Y
4.3 Non Fuel Melt	Y	*n*	Y	n	n	n	Y	n	n	n
4.4 Fuel Dissolution	Y	*n*	---	n	n	n	Y	n	n	n
4.5 Ceramic Melt	Y	*Y*	---	Y	Y	n	n	n	n	n
4.6 Particulate Debris	n	*Y*	---	n	Y	n	n	n	Q	n
4.7 Melt Pool	Y	*Y*	Y	Y	Y	n	n	n	n	n
4.8 Crust Failure	---	---	Y	n	n	n	n	n	n	n
4.9 Structure Ablation	Y	---	Y	n	n	n	n	n	n	n
4.10 Fission Product Rel.	Y	*Y*	---	n	n	n	A	---	---	---

Table 5.3: Validation Matrix, Bundle Separate Effect Experiments with Key Test Scale = 1 and 2

Test / **Characteristic**	REBEKA-6	PHEBUS-218	NRU-MT4	MRBT-B6
Key Test	1	2	1	2
Data/Documentation	1	1	1	1
Boundary Condition	2	3	2	2
Dominant Characteristic	S	S	M	M
1.1 Reactor	n	n	n	n
1.2 Heating Method	E	F	F	E
1.3 Burn-up	F	F	F	F
2.1 Heated Length	L	M	L	M
2.2 Fuel Rods	L	M	M	ML
2.3 Spacer Grid Zirconium	---	---	---	---
2.4 Spacer Grid Inconel	n	---	---	---
2.5 Control Assembly AIC	Y	n	n	n
2.6 Control Assembly B_4C	n	n	n	n
2.7 Core Support Struct.	n	n	n	n
2.8 Initial Fuel Debris	n	n	n	n
2.9 Crust Prefabricated	n	n	n	n
2.10 Preoxidation	n	n	n	n
3.1 Heat-up Rate	H	H	H	H
3.2 System Pressure	L	H	L	---
3.3 Gas Injection	I	S	S	S
3.4 Steam Starved	n	n	n	n
3.5 Boil Down	n	n	n	n
3.6 Reflood	n	n	n	n
3.7 Possible Flow Bypass	n	n	n	n
4.1 Clad Ballooning	Y	Y	Y	Y
4.2 Oxidation Excursion	---	---	---	---
4.3 Non Fuel Melt	---	---	---	---
4.4 Fuel Dissolution	---	---	---	---
4.5 Ceramic Melt	---	---	---	---
4.6 Particulate Debris	---	---	---	---
4.7 Melt Pool	---	---	---	---
4.8 Crust Failure	---	---	---	---
4.9 Structure Ablation	---	---	---	---
4.10 Fission Product Rel.	---	---	---	---

Table 5.4: Validation Matrix, FCI Experiments with Key Test Scale = 1 and 2 (page 1 of 1)

Test / **Characteristic**	FARO-L14	FARO-L28	KROTOS44	FARO-L11	FARO-L31	FARO-L33	KROTOS58
Key Test	1	1	1	2	2	2	2
Data/Documentation	1	1	2	1	1	2	2
Boundary Condition	1	1	1	1	1	1	1
Dominant Characteristic	S	P	P	P	P	P	P
Material Mass, kg	125	175	1.5	151	92	100	4.5
Composition	Cor1	Cor1	Al_2O_3	Cor2	Cor1	Cor1	Cor1
Metal Content	n	n	n	Y	n	n	n
Initial Temperature, K	3123	3052	2673	2823	2990	3070	3077
Initial Debris	Melt	Melt	Melt	Melt	Melt	Melt	Melt
System Pressure, MPa	5.0	0.5	0.10	5.0	0.22	0.40	0.37
Debris Mass / Water Mass	0.20	0.31	0.045	0.25	0.19	>0.16	0.15
Subcooling, K	0	1	80	2	104	124	125
Gas Phase	Stm/Ar	Stm	He	Stm	Ar	Ar	Ar
Trigger	n	n	Y	n	n	Y	Y
Energetic Interaction	n	n	TE	n	n	TE	TE
Hydrogen Generation	n	Y	n.m.	Y	Y	Y	n.m.
Peak Pressure Ratio	1.56	3.40	650	2.02	1.20	26.5	69.7
Debris Formation	Pm	n.a.y.	Ts	Tm	Tm	n.a.y.	Ts

Key:

General	n = no; Y = Yes
Composition	Cor1 = 80wt%UO_2/20wt%ZrO_2; Cor2 = 77wt%UO_2/19wt%ZrO_2/4wt%Zr; Al_2O_3 = aluminium oxide
Gas Phase	Stm = Steam; Ar = Argon; He = Helium
Energetic Interaction	n = none; TE = Triggered Explosion

Total fragmentation (>90%) with small particles, d < 1 mm	Ts
Total fragmentation (>90%) with medium size particles, 1 mm < d < 10 mm	Tm
Total fragmentation (>90%) with large particles, d > 10 mm	Tl
Partial fragmentation with small particles and cake formation	Ps
Partial fragmentation with medium size particles and cake formation	Pm
Partial fragmentation with large particles and cake formation	Pl
Cake formation and little fragmentation (< 10%)	n
Data not measured or not available yet	n.m. / n.a.y.

Table 5.5: Cross reference table for late phase separate effects test

Phenomena	Pool thermal-hydraulics			Gap thermal-hydraulics		Ex-vessel	Gap formation		Fuel coolant interaction	
Test facility	BALI	RASPLAV-Salt	SIMECO	BENSON	CORCOM	CYBL	FOREVER	LAVA	FARO	KROTOS
Debris bed formation									M	S
Debris bed heat transfer					S					
Pool formation										
Pool thermal-hydraulics	L	M	M							
Pool stratification			sim							
Pool solidification		sim	sim							
Crust thermal behavior							I	I		
Crust mechanics							I	I		
Upper crust heat transfer										
Lower crust heat transfer				L	S					
Dry RPV cavity										
Wet RPV cavity						L				
RPV elastic deformation										
RPV plastic deformation							I	I		
Vessel failure							I			
Thermal ablation										

Key:

Scaling of facility: L = large, M = medium, S = small
Material: sim = Simulate material
Status of project: I = Investigation intended

6. CONCLUSIONS AND RECOMMENDATIONS

This report provides the code validation matrix update requested by the CSNI in support of assessment of codes which model the in-vessel stage of core degradation. The matrix can be used for assessing mechanistic codes, as well as mechanistic models contained in integral system codes.

While integral experiments, which cover different phenomena and processes along with the interactions amongst them, form the main basis for the matrix, separate-effects tests, which study single phenomena, are also considered. The scope of this report is limited to the physical boundaries of the intact RPV and its external cooling. Compared with the first version of 1995, the scope has been extended to cover relocation processes into the lower plenum and for debris behaviour in the lower plenum, including the interaction with the vessel wall and heat transfer to the vessel surroundings.

The range of experiments covered and the information provided about them means that the report can also assist code developers in selecting experiments relevant to their activities. The selected experiments are ranked into two categories regarding their perceived usefulness for code validation. Justification regarding selection is provided to aid the code assessor in deciding which of them to use.

This report is the first update of the initial validation matrix in the beyond design basis area. To define the meaning of the dominant phenomena in the context of postulated severe accident sequences of LWRs, now including VVERs, the major accident sequences are described, and key phenomena are explained and classified according to their degree of understanding.

The data base for the early phase has been updated and extended by late phase experiments. It is believed that the resulting data compilation, presented in standard, mainly tabular, form will itself provide a valuable resource and indicate where further information on particular tests can be found. Availability of the data and associated reports has been checked as far as was reasonably practicable. The structure of the data compilation, and indeed of the cross-reference matrix has been kept as before to facilitate the addition of further data as they appear.

Continual updating of the matrix is considered worthwhile on a regular basis to monitor the adequacy and completeness of the experimental database. This is particularly important regarding the late phase, which is currently less well covered than the early phase.

Based on the completeness of the experimental data base necessary for code validation, and reflecting the degree of understanding of phenomena, it is considered that the following parameters or processes are not fully covered or understood only in a limited way:

- Effects of high burn-up, MOX, quenching at high temperature, and air ingress on core degradation;
- Transition from early to late phase, crust failure with subsequent slumping of melt into the lower plenum and quenching;
- Thermal loads to RPV by phase separation in molten pool including metallic layers and their consequences on vessel failure.

Empty page

7. ACKNOWLEDGEMENTS

The authors would like to thank the following additional people who contributed to the production of this report:

Dr P Hofmann, Dr M Steinbrück, Dr A Miassoedov and Dipl-Phys G Schanz of FZ Karlsruhe for providing much detailed technical information on new FZK integral and separate-effects experiments particularly regarding fuel rod quench and materials interactions;

Mr B Clément from IPSN Cadarache providing new material on the Phebus FP experiments.

Dr I Huhtiniemi of JRC Ispra for providing much of the data on the FARO and KROTOS experiments.

Professor J-O Liljenzin of Chalmers University, Dr P Mason of AEA Technology (while on attachment to IPSN Cadarache), Dr T Karjunen of STUK Finland and Dr L Belovsky (consultant to NRI Rez) for providing helpful data regarding oxidation of boron carbide and its interaction with structural materials.

Prof. T G Theofanous of University of California, Santa Barbara, for providing information on the experimental results gained by the Center for Risk Studies and Safety.

Dr. Sang-Baik Kim of Korea Atomic Energy Research Institute for providing detailed information on experiments performed in the frame of SONATA project.

Dr M Veshchunov of IBRAE, Russian Academy of Sciences, for providing valuable information on materials interactions.

Dr J Duspiva of NRI Rez for reviewing the material on VVER-specific plant behaviour.

Dr Th Steinrötter of the Ruhr University of Bochum for providing new figures on the CORA facility.

Mr. P Horner and A Zeisberger of Technical University of Munich for the updates on the experiments performed at the Institut A for Thermodynamics.

Dr. Harri Tuomisto of Fortum and Dr. Gert Sdouz of Austrian Research Centers Seibersdorf for reviewing experimental sections.

Mr. M Bürger and M Buck of University of Stuttgart for their support in collecting reports.

A large part of the new data and understanding obtained since the initial Validation Matrix was written arose out of the European Commission sponsored Fourth Framework programme on Nuclear Fission Safety; the Final Reports of many of these projects are referenced in the current document. One of us (TJH) would also like to thank the JRC for its hospitality during his stay at Ispra as a visiting scientist.

The support of other funding organisations in France (CEA) and Germany (BMWi) is also gratefully acknowledged.

Empty page

APPENDIX A: Summary sheets for experiments

This appendix provides reference information for the experimental series considered for the validation matrix. To facilitate interpretation of the information, a standard format is employed, similar to that used in the Separate Effects Validation Matrix [A1].

For each experimental series, the following information is provided:

- the reference number of the test, in the form n.m:
  - n indicates the kind of test (1 for integral, 2 for separate effects);
  - m indicates the consecutive facility numbering;
- the name, location and country of the test facility;
- the operating period;
  - this is the time during which the test facility was in operation, important for cases where additional information on data, repetition of an experiment or execution of a new experiment is needed or desired by the data user;
- the objectives of the test series;
  - these are the main goals of the test facility and/or the experimental research programme;
- the geometry and construction details of the facility;
  - these are the important geometrical dimensions, geometrical shapes and configurations of the test section, other essential and ancillary components, to help to evaluate:
  - the scaling factors of the test section;
  - the capability of the test facility for establishing the initial and boundary conditions necessary for the investigation of the phenomena of interest;
- the conduct of a typical test;
  - including initial and boundary conditions, the running procedure of the experiment, and the test fluid(s) used;
- the parameter ranges covered;
  - the range of physical parameters (e.g. pressure, temperature, power, mass flow rate etc.) and geometrical parameters (e.g. diameter/cross section, length, surface etc.) varied in the series;
- the measurements made;
  - the parameters measured;
  - the position and kinds of the instrumentation used;
  - differentiation between on-line and post-test measurements;
  - method of acquisition;
  - an evaluation where appropriate;

- a list of the major documentation;
  - overview reports;
  - data reports;
  - data evaluation reports;
- the availability and potential use of the data;
  - whether the data are freely available or proprietary;
- special features;
  - outstanding characteristics concerning facility design, configuration operating capabilities; experiment type and procedure; initial and boundary conditions; parameter range; measurement instrumentation and data qualification and documentation;
- the correctness of the data;
  - statement whether the data as regards the use for code validation is correct and complete;
  - indication of additional phenomena where appropriate;
- an evaluation of the strengths and weaknesses of the test series; and
- any further comments;
  - indicate/emphasise special features or characteristics of facility or experiment;
  - provision of additional information, e.g cross-reference to similar experiments.

The ordering over the facilities is the same as in the main body of the report.

The information provided is intended to assist any analyst wishing to make use of the data for computer code assessment; the parameter ranges, measurements made, documentation reference list, availability of data and evaluation of the series are of particular importance here. Use is made of the evaluations in deciding the preferred tests in the cross-reference validation matrix tables.

Reference

[A1] Aksan N, D'Auria F, Glaeser H, Pochard R, Richards C and Sjoberg A, "OECD/NEA-CSNI Separate Effects Test Matrix for Thermal-Hydraulic Code Validation, Vols. 1 & 2", OCDE/GD(94)82 & 83, September 1993.

No. 1.1	INTEGRAL TEST FACILITY	NIELS
Subject	**Description**	
Test Facility	NIELS (KfK Karlsruhe, Germany)	
- Operating Period	1982 - 1986	
Objectives	Initial investigation of early phase melt progression, including effect of PWR absorber materials, in a single rod and small bundle environment. There were 12 basic single rod tests (ESSI series); 3 additional single rod tests to study the effect of hydrogen (ESA series), 2 3x3 bundle tests with no absorber (ESBU series) and 6 3x3 bundle tests including PWR absorber (ABS series).	
Facility Geometry	The single rods and the bundle, composed of a 3x3 array of fuel simulators, were surrounded by an Al_2O_3 or Zircaloy shroud, respectively which was insulated with a ZrO_2 fibre ceramic wrap. The fuel rod simulator was made of a central tungsten heater of 6 mm diameter, which was surrounded by annular UO_2 pellets and the normal PWR Zircaloy cladding of 10.75 mm outer diameter and a wall thickness of 0.72 mm. The maximum length was 0.25 m for ESSI-1, 2 and 3, and 0.40 m for the others.	
Experimental Conditions	A typical test was conducted in 4 phases: pre-heating in Ar; start of electrical heating and of steam injection; increase of power, leading to oxidation excursion or faster heat-up and to relocation of absorber material (only ABS series) and U/Zr/O melt; and cooling in Ar with power switched off. The transient phase typically lasts 1200 to 5000 s.	
Parameter Range	Parameter ranges are : scale - single rods and 3x3 rod bundles; absorber material - PWR in the ABS series; initial heat-up rate 0.3-4.0 K/s; system pressure 0.1 MPa; internal rod pressure 0.1MPa; atmosphere - argon, steam (in addition one test had a vacuum phase, while another used oxygen); maximum recorded temperature 2073-2523 K.	
Measurements		
- On-line	On-line recordings are made of temperatures of the fuel, simulators, cladding and shroud using thermocouples. Other on-line recordings include heater current, voltage, resistance and power. Temperatures measurements were also made by pyrometers.	

No. 1.1	INTEGRAL TEST FACILITY	NIELS
Subject	**Description**	
- Post-test	Post-test destructive examinations determined axial blockage profiles and material distributions. Aerosol compositions were determined by filter probes.	
- Evaluation	While the experiments provided extremely valuable first insights into the importance of chemical interactions, melt formation and blockage in the early phase of LWR severe accidents, more comprehensive data are available from later tests such as the CORA series.	
- Data Acquisition	On-line acquisition based on a computer system.	
Data Documentation		
- Overview	Hagen S and Hofmann P, "LWR Fuel Behaviour during Severe Accidents", Nuclear Engineering and Design 103 (1987), 85-106, Amsterdam.	
- Data Reports	Hagen S et al.,"Temperature Escalation in PWR Fuel Rod Simulators due to the Zircaloy/Steam Reaction: Tests ESSI-1,2,3 Test Results Report", KfK 3507, August 1983; "Temperature Escalation in PWR Fuel Rod Simulators due to the Zircaloy/Steam Reaction: ESSI-4 to ESSI-10 Test Results Report", KfK 3557, March 1985; "Post-Test Investigation of the Single Rod Tests ESSI 1-11 on Temperature Escalation in PWR Fuel Rod Simulator Bundles due to the Zircaloy/Steam Reaction", KfK 3768, March 1987; Temperature Escalation in Fuel Rod Simulator Bundles due to the Zircaloy/Steam Reaction - Test ESBU-1 Test Results Report", KfK 3508, December 1983; "Post-Test Investigation of Bundle Test ESBU-1 on Temperature Escalation in PWR Fuel Rod Simulator Bundles due to the Zircaloy/Steam Reaction", KfK 3769, August 1986; "Temperature Escalation in PWR Fuel Rod Simulator Bundles due to the Zircaloy/Steam Reaction - Test ESBU-2A Test Results Report", KfK 3509, July 1984; "Temperature Escalation in PWR Fuel Rod Simulator Bundles due to the Zircaloy/Steam Reaction: Post-Test Investigation of Bundle Test ESBU-2A", KfK 3789, November 1986.	

No. 1.1	INTEGRAL TEST FACILITY	NIELS
Subject	**Description**	
- Evaluation	Hagen S and Peck S O," Temperature Escalation of Zircaloy-Clad Fuel Rods and Bundles under Severe Fuel Damage Conditions", KfK 3656, August 1983**;** "Out-of-Pile Bundle Temperature Escalation under Severe Fuel Damage Conditions", KfK 3568, August 1983**;** Fiege A, "Status and Results of the KfK/PNS Research Programs on Severe Fuel Damage", SFD Program Status Meeting, Idaho Falls, USA, April 16-19, 1985**;** Hagen S and Buescher B J, "Out-of-Pile Experiments on PWR Fuel Rod Behaviour under Severe Fuel Damage Conditions", British Nuclear Energy Society Meeting on Nuclear Fuel Performance, London, 1985.	
- Data Availability	The reports listed above are available. Detailed information on the later tests is sparse.	
Use of Data	The data listed above are available for a more detailed analysis.	
Special Features	-	
Correctness of Phenomena	The NIELS tests were invaluable pioneering experiments in determining the major features of early phase melt progression, the results of which have been confirmed and expanded by later experiments such as the CORA series. Non-prototypic features which must be taken into account in interpretation and analysis of the data are given below.	
Overall Evaluation		
- Strengths	A wide range of heat-up conditions is featured in the single rod tests.	
- Weaknesses	The data are limited compared with those available from later test series such as CORA, particularly regarding absorber material behaviour.	
- Miscellaneous	Non-prototypic features such as the temperature dependence of axial power distribution and the very small bundle size must be taken into account when interpreting the test results.	
Comments	-	

No. 1.2	INTEGRAL TEST FACILITY	CORA
Subject	**Description**	
Test Facility	CORA (FZ Karlsruhe, formerly KfK, Germany)	
- Operating Period	1987 - 1992 (VVER tests to 1993)	
Objectives	To investigate out-of-pile the early phases of core degradation in light water reactor systems (PWR and BWR) in a bundle environment. The series was extended (2 further tests) to examine VVER phenomena.	
Facility Geometry	An assembly of fuel rods of heated length 1m is situated within a zirconia-insulated flow shroud of 20mm thickness, with a Zircaloy liner. This assembly is itself situated within a permanently-installed high temperature shield of porous ceramic material; the bypass between the two is accessible to coolant flow. Alternate rods are powered with internal tungsten resistance heaters. The bundle may contain PWR control rods (in place of unheated fuel rods) , a simulated BWR control blade, or a VVER control rod, with prototypic absorber materials. The PWR and BWR test bundles have a square lattice with pitch 14.3 mm; the VVER bundles have hexagonal arrays of side 12.75 mm. A quench cylinder containing water is situated under the heated section. Gas injection (argon and steam) is achieved laterally at the bottom of the heated section.	
Experimental Conditions		
- Initial	In a typical PWR test with 25 rods the bundle is pre-heated in flowing argon (8 g/s) at about 873 K for 3000 s, at a system pressure of 0.2 MPa and internal rod pressures in the range 0.3-0.5 MPa, and with a nominal electrical power. The pre-heating gives near steady-state conditions at the starting time of 3000 s. Similar conditions (scaled) apply to the the BWR and VVER tests and to the PWR test with a large bundle.	
- Boundary	In the typical PWR test, between 3000 s and 4800 s the electrical power is increased linearly with time to give the desired heat-up rate of about 1 K/s. From 3300 s onwards superheated steam (6 g/s) is added to the preheated argon flow. Between about 3700 s and 4800 s temperatures are driven to ~2273 K by the exothermal Zircaloy/steam reaction. The power and coolant flow are suitable scaled in the other types of test. The test is terminated by switching off the electrical power and steam supply and either allowing the bundle to cool in the argon flow, or quenching it by raising the water-filled quench cylinder.	

No. 1.2	INTEGRAL TEST FACILITY	CORA
Subject	**Description**	
Parameter Range	Parameter ranges are for the 17 PWR/BWR tests conducted: bundle size 25 to 59 rods; absorber material - PWR, BWR or none; argon flow 8-16 g/s; steam flow trace-12 g/s, initial heat-up rate 0.2-1.0 K/s; maximum recorded temperature <2300 to 2500 K, system pressure 0.2-1.0 MPa; internal rod pressure 0.3-6.0 MPa; simulated reflood rate none or 10 mm/s. The VVER tests of bundle size 19 rods used VVER-1000 specific fuel and spacer grid materials with a Zr1%Nb shroud liner; one test used a VVER control rod, argon flow was 6g/s and steam flow 4g/s.	
Measurements		
- Online	On-line recordings are made of temperatures of the fuel rods, electrically heated fuel rod simulators, cladding, absorber rods/blade, shroud, high temperature shield, inlet gas and quench water, measured using W/Re and NiCr/Ni thermocouples. Other on-line recordings include heater current, voltage, resistance and power, argon and steam mass flow, system pressure, internal rod pressures (up to 6) and hydrogen production. Video and still cameras record melt progression phenomena in some tests through windows cut in the flow shroud.	
- Post-test	Post-test destructive examinations determine axial blockage profiles and the composition of the refrozen melt, and estimate the maximum temperatures reached beyond thermocouple failure.	
- Evaluation	The available data are of good quality, and strong in the areas of structural temperature and characterisation of the bundle final state. The major lacks are in the thermal hydraulic area, where the fluid temperature distribution and flow split between main channel and bypass is poorly quantified (only the inlet fluid temperature is well known). There are time delay uncertainties regarding steam concentration between the steam generator and the bottom of the test section (where a long pipe intervenes), and in the hydrogen measurements. In addition, only the total rod power is known; the split amongst tungsten heater element, and the molybdenum and copper conductors, must be deduced by modelling. While heat losses, particularly radial, appear to be low, it is hard to quantify them directly from the available data.	
- Data Acquisition	On-line acquisition based on personal computer (PC) system.	

No. 1.2	INTEGRAL TEST FACILITY	CORA
Subject	**Description**	
Data Documentation	The lists below comprise formal KfK reports. Informal reports were made at the CORA Workshops at KfK in September/October annually, for all tests performed.	
- Overview	Hagen S and Hain K, "Out-of-pile Bundle Experiments on Severe Fuel Damage (CORA-Program): Objectives, Test Matrix and Facility Description", KfK 3677, 1986.	
- Data Reports	Hagen S et al.; "Out-of-pile Experiments on LWR Severe Fuel Damage Behaviour - Tests CORA-C and CORA-2", KfK 4404, September 1988**;** "Interactions in Zircaloy/UO_2 Fuel Rod Bundles with Inconel Spacers at Temperatures, above 1200°C (Posttest Results of Severe Fuel Damage Experiments CORA-2 and CORA-3), KfK 4378, September 1990**;** "Results of SFD Experiment CORA-13 (OECD International Standard Problem 31)", KfK 5054, February 1993**;** "BWR Slow Heatup Test CORA-31: Test Results", KfK 5383, December 1994**;** "Dry Core BWR Test 33: Test Results", KfK 5261, December 1994**;** "Behaviour of a VVER Fuel Element Tested under Severe Accident Conditions in the CORA Facility (Test Results of Experiment CORA-W1)", KfK 5212, January 1994**;** "Behaviour of a VVER Fuel Element with Boron Carbide/Steel Absorber Tested under Severe Accident Conditions in the CORA Facility (Test Results of Experiment CORA-W2)", KfK 5363, October 1994**;** ”Pre-oxidised BWR Test CORA-28: Test Results”, FZKA 5571, June 1997**;** ”Pre-oxidised PWR Test CORA-29: Test Results”, FZKA 5928, August 1997**;** ”Cold Lower End Test CORA-10: Test Results”, FZKA 5572, November 1997**;** ”Pre-oxidised PWR Test CORA-29: Test Results”, FZKA 5928, August 1997**;** ”Large Bundle PWR Test CORA-7: Test Results”, FZKA 6030, April 1998**;** ”Large Bundle BWR Test CORA-18: Test Results”, FZKA 6031, April 1998**;** Burbach J, "Ergebnisse von REM Mikrobereichsanalysen des DWR Bündelabschmelzexperiments CORA-13", KfK 5162, April 1993**;** Burbach J, "Ergebnisse von REM Mikrobereichsanalysen des Siedewasserreaktor-Bündelabschmelzexperiments CORA-16", KfK 5282, May 1994**;** Sepold L (ed.), ”Post-test Examination of the VVER-1000 Fuel Bundle CORA-W2”, FZKA 5570, June 1995.	

No. 1.2	INTEGRAL TEST FACILITY	CORA
Subject	**Description**	
- Evaluation	Minato K et al., "Zircaloy Oxidation and Cladding Deformation in PWR-Specific CORA Experiments (2, 5 and 12)", KfK 4827, July 1991; Hagen S et al., "Behaviour of Ag/In/Cd Absorber Material in Zry/UO_2 Fuel Rod Simulator Bundles at High Temperatures (Post-Test Results of Severe Fuel Damage Experiments CORA-5, CORA-12, CORA-15, CORA-9, CORA-7), KfK 4419, 1995; Hagen S et al., "Behaviour of BWR-type Fuel Elements with Boron Carbide/Steel Absorber Tested under Severe Fuel Damage Conditions in the CORA Facility (Post-Test Results of CORA-16, CORA-17, CORA-18), KfK 4560, 1995; Hagen S et al., "Comparison of the Quench Experiments CORA-12, CORA-13, CORA-17", FZKA 5679, August 1996; Firnhaber M et al., "OECD/NEA/CSNI International Standard Problem No. 31: CORA-13 Experiment on Severe Fuel Damage; Comparison Report", NEA/CSNI/R(93)17, GRS-106, KfK 5287, July 1993; Hering W, "Modellierung des Experimentes CORA und Interpretation von Versuchsergebnissen mit dem Erweiterten Kerschmelzcode SCDAP/MOD1", University of Stuttgart thesis, IKE 2-100, February 1993; Firnhaber M et al., " International Standard Problem ISP36: CORA-W2 Experiment on Severe Fuel Damage for a Russian Type PWR; Comparison Report", OCDE/GD(96)19, GRS-120, FZKA 5711, February 1996; Steinrötter Th, "Numerische Analyse und Modellierung des Warmeübergangs durch Konvektion und Gasstrahling in längsdurchströmten Stabbündeln mit Bündelumfassung", Ruhr University of Bochum thesis, 1998.	
- Data Availability	On-line test results and the reports listed above are available. Post-test analysis of the later tests and their formal reporting took place into 1998.	
Use of Data	The data are available for a more detailed analysis.	
Special Features	Video recording of melt progression was a unique feature.	
Correctness of Phenomena	The melt progression phenomena observed (e.g. separation of refrozen melt into an upper ceramic fuel-bearing layer and a lower absorber-bearing layer, and the strong hydrogen production on reflood) are consistent with those observed in the TMI-2 accident and in in-pile experiments. There are various non-prototypic features which must be taken into account in interpretation and analysis of the data, these are given below.	

No. 1.2	INTEGRAL TEST FACILITY	CORA
Subject	**Description**	
Overall Evaluation		
- Strengths	The comprehensive test matrix and detailed post-test analysis are major strengths of the programme. The range of parameters studied is the largest studied in all early phase melt progression integral test series; in particular the database regarding steam availability, pre-oxidation and heat-up rate is usefully extended. Quenching effects are addressed - relevant to accident management. The good organisation of the test programme, and the orderly variation of parameters amongst the tests aids interpretation of the results by inter-test comparison and analysis. The video recordings of melt progression phenomena provided unique information regarding melt progression mechanisms. The VVER tests are the only core degradation experiments to date using VVER-1000 bundles.	
- Weaknesses	The strong dependence on temperature of the electrical resistance of the tungsten heaters means that the electrical power axial profile becomes highly non-linear during the course of the experiments, due to positive feedback effects, this is a significant non-prototypic feature. Simulation of this effect is important when modelling the tests, since the linear electrical heat rating can vary by up to x3 between the hottest and coldest parts of the rods. In addition, the heat source remains static, unlike decay heat in relocating nuclear fuel. The argon flow, always present except during reflood, is untypical of reactor conditions. (These non-prototypic effects are however amenable to modelling.) The tungsten heater elements in the electrically heated rods impose an artificial axial stability to the rod bundles. There are some omissions in thermal hydraulic data, e.g. fluid temperature variation in the bundle and bypass flows are not quantified. The viewing windows, where present, give rise to cross-flow of uncertain magnitude.	
- Miscellaneous	In modelling the tests where ballooning takes place, the non-prototypically small increase in rod pressure as the temperature rises (due to the presence of a large external plenum) must be taken into account.	
Comments	In addition, two preliminary tests (B and C) were carried out with alumina pellets. CORA-13 (PWR, reflood) was selected as CSNI ISP-31, and CORA-W2 (VVER, slow cooling) was selected for ISP-36.	

No. 1.3	INTEGRAL TEST FACILITY	PHEBUS SFD
Subject	**Description**	
Test Facility	PHEBUS SFD (IPSN/CEA - Cadarache, France)	
- Operating Period	1986 - 1989	
Objectives	Investigate in-pile early phase of PWR core degradation in a bundle environment. Experimental data base and odelling of SFD processes in ICARE2 code.	
Facility Geometry	The test bundle with 21 rods has an overall length of 1.3 m with a central 0.8 m long fissile zone. The rods are held in place by two Inconel or Zircaloy spacer-grids. There is a Zircaloy liner on the inner octagonal surface of the shroud. The bundle is located in a SFD loop crossing the central part of the surrounding research PHEBUS reactor. Nuclear power is supplied to the bundle by neutronic coupling with the driver reactor. The bundle may contain PWR control rods with prototypic absorber materials. Only fresh fuel was studied. An independent pressurised water loop (8 MPa, 533 K) works as an external radial cooling circuit of the structures located between the test train and the driver core. Pressurised water and SFD loop are separated by an insulating shroud which includes a thick porous ZrO_2 layer. Three injection lines (steam, hydrogen, helium) and an electric superheating device enable to controlling the gas injection conditions at the bottom of the bundle.	
Experimental Conditions	Thermal-hydraulic conditions (pressure, inlet gas mass flow rate and temperature) are imposed as specified in the test scenario. Typical conditions include a steam injection (a few g/s) at about 528 K during the first oxidation phase and a nuclear power increase with time, continuously or by steps, to give the desired temperature evolution. A second high temperature phase can be performed in steam-starved conditions (pure He injection) in order to facilitate UO_2-clad chemical interactions. Tests are terminated by a scram with steam or helium injection enabling slow cooling (1 K/s) in order to keep intact the final geometry of the bundle reached before the scram (except in the B9R test).	
Parameter Range	Parameter ranges are: 20 or 21 unirradiated fuel rods with or without a central control rod. Steam flow 1-4 g/s, helium flow 0.5-0.05 g/s, initial heat-up before oxidation escalation ~ 0.3 K/s, system pressure: 0.5 to 3.5 MPa, low internal rod pressure and no ballooning, no final quench. Maximum temperature: 2750 K.	

No. 1.3	INTEGRAL TEST FACILITY	PHEBUS SFD
Subject	**Description**	
Measurements		
- On-line	On-line recording are made of temperature of the fuel centreline, cladding, coolant, shroud, control rod guide tube. Different kinds of thermocouples were used, mainly W/Re and chromel / alumel thermocouples. In high temperature areas, W/Re TCs enable measurements up to 2300 K. Other on-line recordings include pressure, steam, He, H_2 mass flowrates, ionisation chambers (power of the driver core) and hydrogen production.	
- Post-test	Non-destructive examinations (radiography and gamma scanning) and destructive examinations based on axial and radial bundle cuttings determine core material and axial blockage profiles and the composition of refrozen melts. When possible, cladding oxidation is quantified by zirconia layer measurements.	
- Evaluation	Great care was taken in controlling the total fission power generated in the bundle (accuracy 5%). Reliable temperature measurements were performed on fuel rods, fluid and shroud. Hydrogen measurements were not possible in the first two tests and were defined with an accuracy not better than 15 to 20% in the following tests. The inlet mass flow rate uncertainty is less than 5%.	
- Data Acquisition	On-line acquisition of all measurements is performed with a computer system.	
Data Documentation		
- Overview	Gonnier C et al., "PHEBUS Severe Fuel Damage Programme. Main Results", ANS Int. Meeting on Safety of Thermal Reactors, Portland, USA, July 1991**;** Grandjean C et al., "Preliminary Specifications for the ISP 28" - IPSN/CEA Report PHEBUS CSD 112/90, March 1990**;** Adroguer B et al., "International Standard Problem n? 28: PHEBUS SFD B9+ Experiment on the Degradation of a PWR Core Type - Comparison Report. Vol. 1 and Vol. 2" - OECD/NEA/CSNI/R(92)17, December 1992**;** Adroguer B et al., "Analysis of the Fuel Cladding Chemical Interaction in PHEBUS SFD Tests using ICARE2 Code", IAEA Tech. Committee Meeting, Aix-en-Provence, France, March 1992.	
- Data Reports	CEA reports (experimental results, post-test examinations, analysis results) exist and have been issued to the PHEBUS SFD partners	

No. 1.3	INTEGRAL TEST FACILITY	PHEBUS SFD
Subject	**Description**	
- Data Availability	Possible under specific agreement with IPSN/CEA. Exceptions are B9+ for which on-line test results and documents listed above are available and B9R available to European Union in the framework of the RCA - Core Degradation Project.	
Use of Data	More detailed analysis, code validation and improvement. Preparation of the new PHEBUS FP tests.	
Special Features	SFD data have been obtained using prototypic reactor materials and realistic heating methods up to a maximum temperature of 2750 K. Unique results on extensive hydriding of Zircaloy were found in the C3 test performed at high pressure and with an H_2 rich atmosphere. This phenomenon became significant with a temperature step of 30 K/s from 850 K to 1350 K.	
Correctness of Phenomena	The melt progression results observed are consistent with those observed in other in-pile experiments. Quantified data have been provided on cladding oxidation, UO_2 dissolution by molten Zr with related rod decladding and on the early degradation stage of a silver-indium-cadmium control rod at 0.7 MPa. These data are consistent with separate-effect tests on chemical interactions between core materials. Non-prototypic features such as deep axial power profiles under the lower spacer-grid, pure helium atmosphere and significant radial heat losses through the shroud must be taken into account in the analysis of the data and the validation of SFD codes.	
Overall Evaluation		
- Strengths	Well-characterised information on the early phase of core degradation has been obtained during the PHEBUS SFD programme performed with a continuous progression in the degradation severity. Each test is specific for a limited number of degradation phenomena enabling a good understanding and quantification of each phenomenon. Destructive PIE gave, for each test, a precise picture of the final state of the bundle. Thermal hydraulic conditions in the cooling fluid and nuclear power source are well controlled.	

No. 1.3	INTEGRAL TEST FACILITY	PHEBUS SFD
Subject	**Description**	
- Weaknesses	Due to the use of low gas flow rates typical of reactor conditions and moderate shroud insulating, a large part of the fission and oxidation power is transmitted through the shroud above 1850 K. The thermal conductivity of the porous zirconia depends significantly on the nature of the shroud filling gas (H_2 ingress resulting of the oxidation of the inner Zircaloy liner can change the filling gas of porosities). This is the main reason for the major experimental uncertainty in the radial heat losses. The impact of the change of the filling gas in porosities has been reduced in the last two tests by using a small helium injection inside the shroud during the transient.	
Comments	Results from Post-Test Examinations of the last two tests B9+ and AIC have been obtained in 1991. Experimental and interpretation reports of these tests have been released in 1993. The B9+ test was selected for ISP-28. On-line qualified measurements for each tests are included in a SFD data bank which has been intensively used for the validation and improvement of the SFD code ICARE2 developed by IPSN/CEA.	

No. 1.4	INTEGRAL TEST FACILITY	PBF-SFD
Subject	**Description**	
Test Facility	PBF-SFD (Power Burst Facility - Severe Fuel Damage), Idaho National Engineering Laboratory (INEL), Idaho Falls, USA	
- Operating Period	1982 - 1985	
Objectives	The specific objectives of the PBF-SFD series of tests were to: (1) investigate fuel rod damage following severe cladding oxidation, melt relocation, and fuel rod fragmentation; (2) measure the release rates, transport, deposition of fission products; (3) determine the magnitude and timing of hydrogen generation; (4) investigate the coolability of test bundles following various types of damage; (5) determine the behavior of irradiated fuel rods compared with fresh fuel rods and to evaluate the effects of control rods.	
Facility Geometry	The fuel rods were 0.9 m long and of representative 17 x 17 PWR design. The rods were arranged in a 6 x 6 square lattice, without the four corner rods. The rods were held in place by Inconel grid spacers. The test bundles were contained in an insulating zirconia shroud, sandwiched between inner and outer Zircaloy walls. The irradiated rods in 1-3 and 1-4 had average burnups of approximately 38 GWd/tU.	
Experimental Conditions	The rods were cooled by a measured coolant flow (water/argon) into the bundle, boiled away by fission heat to produce steam. An independent flow cooled the outer shroud. The entire effluent from the test bundle consisting of superheated steam, argon, hydrogen, fission products, and particulate matter was routed through a heated and insulated line to a sampling and monitoring system containing a variety of instrumentation.	
Parameter Range	Parameter ranges for the four tests: bundle size of 32 rods by 1.0 m, trace and irradiated rods, Inconel spacers, PWR absorber material (one test), 0.4-3.0 K/s heat-up rates (last 3 tests), rapid and slow cooldown rates, steam flow of 0.6 g/s (last 3 tests), system pressure of 6.8 MPa, maximum temperature >2800 K.	

No. 1.4	INTEGRAL TEST FACILITY	PBF-SFD
Subject	**Description**	
Measurements		
- On-line	The test train was instrumented to measure fuel and control rod cladding and centreline temperatures, coolant temperatures, shroud temperatures, fuel and control rod internal pressure, and coolant flow rates and pressures. In addition, a fission product and hydrogen measurement system was also included.	
- Post-test	Post-Test Examination (PTE) included gross gamma scanning, neutron tomography, and destructive sectioning.	
- Data Acquisition	On-line computer-based data acquisition system.	
Data Documentation	-	
- Data Reports	Knipe A D et al., "PBF Severe Fuel Damage Scoping Test - Test Results Report", NUREG/CR-4683, EGG-2413, August 1986**;** Martinson Z R et al., "PBF Severe Fuel Damage Test 1-1 - Test Results Report", Volumes 1 and 2, NUREG/CR-4684, EGG-2463, October 1986**;** Martinson Z R et al., "PBF Severe Fuel Damage Test 1-3 - Test Results Report", NUREG/CR-5354, EGG-2565, October 1989**;** Petti D A et al., "Power Burst Facility (PBF) Severe Fuel Damage Test 1-4 Test Results Report", NUREG/CR-5163, EGG-2542, April 1989.	
- Data Availability	The above reports are available. (The reports contain microfiche of the data.)	
Use of Data	The data are available for a more detailed analysis.	
Special Features	The principal advantages of the tests are that prototypical fuel rod and control rod materials have been used, including both unirradiated and irradiated fuel. The tests, being in-pile, include the effects of internal heating in the fuel during melt relocation.	
Correctness of Phenomena	The PBF-SFD tests were the first fuel damage tests, and they made a significant contribution towards early understanding of degraded core phenomena. The tests are mainly relevant for early phase melt progression phenomena.	

No. 1.4	INTEGRAL TEST FACILITY	PBF-SFD
Subject	**Description**	
Overall Evaluation		
- Strengths	The tests cover a full range of early phase core degradation phenomena (including clad ballooning and the effect of PWR control materials). The ST test is a valuable example of an in-reactor bundle quench test.	
- Weaknesses	Limitations are mainly those common to small bundle tests (i.e., unprototypic small radial scale). There is considerable uncertainty in the radial heat losses after the shroud liner is breached, and the insulating material becomes saturated with steam. In test SFD 1-1 there was some reflux of water back into the bundle due to condensation of steam onto an upper fall-back barrier, creating some uncertainty in the thermal hydraulic conditions and associated heat transfer.	
Comments	All the tests had some unplanned features (for instance, breach of the shroud wall), which have complicated the analysis.	

No. 1.5	INTEGRAL TEST FACILITY	NRU FLHT
Subject	**Description**	
Test Facility	Full-Length High Temperature (FLHT) Tests of the Coolant Boilaway Damage Progression (CBDP) Program were conducted by Pacific Northwest Laboratory (PNL) in the NRU reactor at AECL Chalk River, Ontario, Canada.	
- Operating Period	1985 - 1987	
Objectives	The objectives of the CBDP Programme were to: (1) Obtain well-characterized data for evaluating the effects of coolant boilaway and core damage progression in a LWR; and (2) Investigate integral severe accident phenomena along a full-length bundle.	
Facility Geometry	The CBDP tests were designed to study severe accident conditions using full length fuel rods. The NRU reactor at Chalk River, Ontario, Canada has the required capabilities: (1) For testing highly instrumented, 3.66 m long bundles of fuel rods, up to 12 rods in a bundle, under thermal hydraulic conditions representative of contemporary LWRs; (2) For achieving prototypic power densities and axial power distributions with fuels of commercial enrichment; (3) For providing prototypic coolant mass fluxes at the fluid/vapour interface typical of the conditions in a TMI-2 type boildown.	
Experimental Conditions	FLHT-1 to -5, a 12-rod assembly of full-length rods was subjected to low coolant flow of ~0.1 g/s/rod while operating at 23 or 30 kW, i.e., at ~2% to 3% of normal commercial LWR rod fission power, to simulate decay heat. Exterior cooling for the shroud was provided by a recirculating pressurized water loop. The operating time following the onset of cladding melt temperatures (~2100 K) was increased from test to test, starting with less than 1 min in FLHT-1 and greater than 10 min in FLHT-5.	
Parameter Range	Parameter ranges for the four FLHT tests: bundle size of 11 to 12 full-length (3.66 m) rods, no absorber material, Inconel and Zircaloy spacers, inlet flow of 0.1 to 1.4 g/s/rod, system pressure of 1.38 MPa, internal rod pressure of 0.5 to 2.4 MPa, slow cooldown after the high temperature transient.	

No. 1.5	INTEGRAL TEST FACILITY	NRU FLHT
Subject	**Description**	
Measurements		
- On-line	The test train instrumentation includes the following: thermocouples to monitor the cladding, spacers, and shroud liner; thermocouple pairs in the shroud for radial heat losses and shutdown control; pressure transducers to the fuel rods and shroud cavities; and liquid level detectors. The effluent control module (ECM) contains the valves, instruments, and electronic logic to control the system pressure, sample the effluent, condense the effluent steam, measure hydrogen, and gamma spectra of released fission products.	
- Post-test	Post-test destructive examinations determine axial/radial blockages.	
- Data Acquisition	The output from 250 test train and ECM instruments is scanned and recorded up to five times per second. The data are fed through an analog/digital converter to a super minicomputer.	
Data Documentation		
- Data Reports	Rausch W N et al., "Full-Length High-Temperature Severe Fuel Damage Test 1", PNL-5691, August 1993**;** Lombardo N J et al., "Full-Length High-Temperature Severe Fuel Damage Test 2", PNL-6551, early 1994**;** Lanning D D et al., "Data Report: Full-Length High-Temperature Experiment 4", PNL-6368 (Draft), January 1988**;** Lanning D D et al., "Full-Length High-Temperature Severe Fuel Damage Test 5", PNL-6540, September 1993**;** Lombardo N J et al., "Full-Length Fuel Rod Behavior Under Severe Accident Conditions", NUREG/CR-5876, PNL-8023, December 1992.	
- Data Availability	The above reports are available. Post-test analysis (especially destructive examinations of the bundles) of the tests and formal reporting will continue through 1995. Also, informal reports (presentations) are made at Cooperative Severe Accident Research Program (CSARP) review meetings conducted by the USNRC.	
Use of Data	The data are available for a more detailed analysis.	
Special Features	These tests are the only full-length SFD experiments.	

No. 1.5	INTEGRAL TEST FACILITY	NRU FLHT
Subject	**Description**	
Correctness of Phenomena	The four FLHT tests performed to date have contributed data on severe fuel damage (SFD) behaviour due to a dynamically changing coolant level with full-length fuel and a constant fission power level. The later FLHT tests in the series were held for extended times (up to 1 hr) under severe accident damage conditions, a length of time that exceeded that for any other SFD test. All the FLHT tests conducted to date have resulted in extensive and severe fuel rod damage, with the severity and extent of the damage increasing with each subsequent test. Following the flow reduction that initiated the transient, the coolant boiled away, and the rods dried out and heated until an autocatalytic oxidation reaction began between the steam and Zircaloy cladding. This oxidation reaction concentrated in a "burn front" of limited axial extent (< 0.2 m) that initially moved rapidly downward in the bundle, then travelled slowly upward. Within the burn front, peak temperatures exceeded the Zircaloy melt temperature by as much as 500 K and significant fractions of gaseous and volatile fission products were released. The damage region was as much as 3 m long, encompassing over 80% of the heated length.	
Overall Evaluation		
- Strengths	The test series provides experimental data on full length fuel rods. The comparison of the behaviour of fresh and irradiated fuel is also valuable.	
- Weaknesses	The FLHT-1 test conduct was not well controlled. In this test the upper plenum was not heated and the steam generated in the core condensed and refluxed back into the test section. In all the tests, radial heat losses are large.	
Comments	The outside of the FLHT test section is water cooled throughout the test. The high radial heat losses must be accounted for in test simulations (i.e., with SFD codes).	

No. 1.6	INTEGRAL TEST FACILITY	ACRR-ST
Subject	**Description**	
Test Facility	ACRR-ST Facility: Fission product release tests conducted in the Annular Core Research Reactor (Sandia National Laboratories, Albuquerque, New Mexico, USA)	
- Operating Period	1986 - 1989	
Objectives	Determine effects of temperature, pressure, fuel damage state, gas environment (reducing or oxidizing), clad oxidation state and fuel clad geometry on magnitude and rate of release of fission products from previously irradiated fuels. The scope of the test programme was reduced to the two tests performed.	
Facility Geometry	The Annular Core Research Reactor (ACRR) is a general purpose research reactor capable of steady state, pulse and programmed transient operational modes. The ST experiments comprised a 4-rod bundle with a 150 mm fresh fuel section and a 150 mm irradiated (BR-3) fuel rod section. Tungsten-Rhenium thermocouples were used to measure the test bundle temperatures. A dense ZrO_2 ceramic liner enclosed the test bundle and flow channel. Outside of this, low density ZrO_2 fibre insulation was used. An outer stainless steel pressure vessel contained the insulated test section. Downstream filters, thermal gradient tubes and sampling bottles provided the fission measurement capabilities.	
Experimental Conditions	Test initiation would typically begin with a preconditioning period followed by a stairstep temperature ramp with temperature plateaux at selected values up to ~2400 K where fission product release rates were measured.	
Parameter Range	The main parameter varied in the two ST experiments was pressure. The system pressure in ST-1 was 1.5 MPa whereas in ST-2, the pressure was 3 MPa.	
Measurements		
- On-line	On-line measurements were made of temperatures of the fuel cladding. An array of sampling bottles and fission product deposition tubes was cycled during the test to provide time resolved release data. These instruments were analyzed post-test.	
- Post-test	Post-test destructive examinations were made on the fuel bundles to determine the extent of fuel degradation.	

No. 1.6	INTEGRAL TEST FACILITY	ACRR-ST
Subject	**Description**	
- Evaluation	The data are of good quality, but are limited to release under reducing conditions. A good feature of the test data are that the releases are based on measurement taken just at the exit of the test bundle, and therefore, losses and transport effects are minimized.	
- Data Acquisition	Original on-line acquisition was based on HP computer system. The data has been converted to a DOS (PC) format.	
Data Documentation		
- Data Reports	Allen M D, Stockwell H W, Reil K O and Fisk J W, "Fission Product Release and Fuel Behaviour of Irradiated Light Water Reactor Fuel Under Severe Accident Conditions - The ACRR ST-1 Experiment", NUREG/CR-5345, SAND89-0308, Sandia National Laboratories, Albuquerque, NM, October 1992.	
- Data Availability	On-line test results and the reports listed above are available. Informal reports are made at the USNRC CSARP meetings annually, for all tests to date.	
Use of Data	The data are available for a more detailed analysis.	
Special Features	Video recording of melt progression is a unique feature.	
Correctness of Phenomena	Of principal interest with respect to melt progression processes are the observed fuel swelling behaviour. Since these tests were conducted using prototypic materials, the observed phenomena are considered correct and appropriate for the conditions applied. These data are quite unique in that very little experimentation on irradiated fuels has been carried out.	
Overall Evaluation		
- Strengths	The chief strengths of this work are in the use of prototypic materials and with the excellent quality of the measured data.	
- Weaknesses	The main weaknesses in the ST test programme is that oxidizing conditions were not examined.	

No. 1.7	INTEGRAL TEST FACILITY	ACRR-DF
Subject	**Description**	
Test Facility **- Operating Period**	ACRR-DF Facility: Fuel damage tests conducted in the Annular Core Research Reactor (Sandia National Laboratories, Albuquerque, New Mexico, USA)	
Objectives	To investigate in-pile using prototypic materials the early phases of core degradation in light water reactor systems (PWR and BWR) in a bundle environment. Specific objectives include: (1) characterize initial fuel heat-up and cladding oxidation in flowing steam; (2) measure thermal escalation and hydrogen generation during oxidation transient; (3) characterize fuel damage processes including material interactions with other core materials, formation of flow blockages and loss of rodded geometry	
Facility Geometry	The Annular Core Research Reactor (ACRR) is a general purpose research reactor capable of steady state, pulse and programmed transient operational modes. The DF experiments were conducted using the ACRR as a driver core to control the fission rate within the test fuel. The DF test bundle length is limited to the 0.5 metre height of the ACRR driver core. The test section of the experiment, consisting of from 9 to 14 Zry-clad UO_2 fuel rods, was insulated radially with a porous ZrO_2 insulation material. The insulated bundle was situated within a stainless steel pressure vessel. Steam was injected at a controlled rate into the inlet of the bundle. Bundle temperatures were measured using specially protected W-Re thermocouples and Pt-Rh surface mounted thermocouples. Hydrogen, generated from the oxidation of steam with Zr was measured.	
Experimental Conditions	Test initiation would typically begin with a bundle heating period where only helium gas was present, in order to preheat the test section prior to initiating steam flow into the bundle. When bundle temperatures were above the steam saturation temperature, steam flow was initiated and a slow fission drive heat-up of the fuel rods was begun. This initial heat-up rate was typically ~1 K/s. Reactor power was increased over time to sustain the fuel bundle temperature rise rate. When peak bundle temperatures reached ~1700K, the onset of rapid Zircaloy oxidation was typically observed, as evident from rapidly increasing fuel temperature rise rate and the generation of hydrogen. Test termination was based on detecting a peak in attained fuel temperatures and indications of some degree of melt relocation.	

No. 1.7	INTEGRAL TEST FACILITY	ACRR-DF
Subject	**Description**	
Parameter Range	The time duration of low level oxidation (degree of pre-oxidation) was the primary parameter varied between tests DF-1 and DF-2. Test DF-3 examined the effect of an AIC PWR control rod and test DF-4 examined the behaviour of BWR control blade and channel box structures on the melt progression process.	
Measurements		
- On-line	On-line recordings were made of temperatures of the fuel cladding, absorber rods/blade, shroud, and inlet gas, using W/Re, Pt/Rh and NiCr/NiAl thermocouples. Other on-line recordings include steam mass flow, system pressure and hydrogen production. Video cameras recorded and end-on view of the fuel bundle damage processes.	
- Post-test	Post-test destructive examinations characterize the nature of material interactions and the degree of fuel pellet erosion and blockage formation. Non-destructive radiography, including tomography provide detail where destructive examinations were not performed.	
- Evaluation	The available data are generally of good quality, however, the data are much more useful when consideration of the available post-test thermal analyses are included. The DF-1 test encountered some problems with the exact steam flow history, but the data report on this test resolves the uncertainty and the test data is useful. The DF-3 test experienced a loss of the hydrogen measurement system, so this test has no hydrogen data. The DF-4 test provides the highest quality data and most complete characterization of the series.	
- Data Acquisition	Original on-line acquisition was based on HP computer system. The data has been converted to a DOS (PC) format.	
Data Documentation		
- Overview	Reil K O and Gauntt R O, "Results of the ACRR-DF Experiments", Proc. International ANS/ENS Topical Meeting on Thermal Reactor Safety, San Diego, Ca., February 1986.	

No. 1.7	INTEGRAL TEST FACILITY	ACRR-DF
Subject	**Description**	
- Data Reports	Gasser R D, Fryer C P, Gauntt R O, Marshall A C, Reil K O, and Stalker K T, "Damaged Fuel Experiment DF-l: Results and Analysis", NUREG/CR-4668, SAND86-1030, Sandia National Laboratories, Albuquerque, NM, January 1990; Gasser R D, Fryer C P, Gauntt R O, Marshall A C, Reil K O, and Stalker K T, "Damaged Fuel Relocation Experiment DF-2: Results and Analysis", NUREG/CR-4669, SAND86-1441, Sandia National Laboratories, Albuquerque, NM, September 1992; Fryer C P, Gauntt R O and Cronenberg A W, "Damaged Fuel Experiment DF-3: Test Results", NUREG/CR-6006, SAND87-1212, Sandia National Laboratories, Albuquerque, NM, December 1992; Gauntt R O, Gasser R D and Ott L J, "The DF-4 Fuel Damage Experiment in ACRR with a BWR Control Blade and Channel Box", NUREG/CR-4671, SAND86 -1443, Sandia National Laboratories, Albuquerque, NM, November 1989; Gauntt R O, Gasser R D, Fryer C P and Walker J V, "Results and Phenomena Observed from the DF-4 BWR Control Blade-Channel Box Test", Proc. Intern. ENS/ANS Conf. on Thermal Reactor Safety, Avignon, France, October 2 -7, 1988; Gauntt R O and Gasser R D, "Results of the DF-4 BWR Control Blade-Channel Box Test", Proc. 18th NRC Water Reactor Safety Information Mtg. Rockville, MD, October 22 -24, 1990.	
- Data Availability	On-line test results and the reports listed above are available. Informal reports are made at the USNRC CSARP meetings annually, for all tests to date.	
Use of Data	The data are available for a more detailed analysis.	
Special Features	Video recording of melt progression is a unique feature.	
Correctness of Phenomena	The melt progression phenomena observed generally are consistent with those observed in the TMI-2 accident and in in-pile experiments. The phenomena observed may be specific to that of fresh or low burnup fuel since no irradiated fuel was investigated in this test series.	
Overall Evaluation		
- Strengths	The use of prototypic materials and the external control over steam flow and fission power provide for overall good characterization of the dominant test bundle damage phenomena. The video recordings of melt progression phenomena provide unique information regarding melt progression mechanisms, and the PIE and non-destructive examinations are of good quality.	

No. 1.7	INTEGRAL TEST FACILITY	ACRR-DF
Subject	**Description**	
- Weaknesses	Difficulties in preventing steam condensation in DF-1 and DF-2 (to a much lesser extent) led to some uncertainty in characterizing the steam flow history. Subsequent analyses of the package hydraulic behaviour provided a good estimate of the flow conditions. These data characterizations are documented in the above report, and greatly improve the usefulness of the data. The DF-3 test experienced a failure of the hydrogen measurement equipment, and this data is lacking. The use of fresh fuel only in this test series should be borne in mind when drawing general conclusions about the behaviour of reactor fuels which may have significant burnup.	

No. 1.8	INTEGRAL TEST FACILITY	LOFT LP-FP
Subject	**Description**	
Test Facility	LOFT (Loss of Fluid Test) Facility (Idaho National Engineering Laboratory (INEL), Idaho Falls, Idaho, USA)	
- Operating Period	1976-1982 Period Sponsored by USNRC, 1983-1986 Period Sponsored by OECD	
Objectives	LOFT is a major research programme generally aimed at studying the behaviour of a PWR primary system under LOCA situations. OECD sponsored LOFT after 1983 and decided to undertake an additional matrix of eight tests, of which the last two tests should include fuel damage and fission product release. The specific objectives of the two fuel damage tests were: LP-FP-1 (1) Simulate a large break LOCA sequence with delayed operation of the ECCS. (2) The ECCS should represent a typical 1300 MW German design. (3) Obtain clad rupture and migration of the most volatile FP contained in the gap, and study possible leaching of FP from the fuel during the reflood period. LP-FP-2 (1) Simulate a medium LOCA, V-type sequence, with delayed operation of the ECCS. (2) Attain substantial fuel damage, and maintain maximum fuel temperatures above 2100 K for several minutes. (3) Study FP migration along the leak path, which represents the LPIS pipe connected to the hot leg.	
Facility Geometry	LOFT is a PWR model with a rated power of 50 MW(th), which includes all systems and components needed to simulate the accident under study. A square fuel rod array or Central Fuel Module (CFM) was placed instead of the standard central fuel assembly of the LOFT reactor core. The CFM conformed to the standard 15x15 array, but a thin square Zircaloy shroud was placed surrounding an inner 11x11 array - for the FP-1 test. Fuel temperatures expected for the FP-2 test were much higher, and a 25 mm thick zirconium oxide insulating shroud was used, itself lined with thin Zircaloy layers, in order to limit temperature of standard fuel rods outside the CFM. The CFM contained 100 fuel rods and 21 Zircaloy guide tubes, of which 11 contained stainless steel clad control rods. Pressurized rods with higher than standard enrichment were used in both tests.	

No. 1.8	INTEGRAL TEST FACILITY	LOFT LP-FP
Subject	**Description**	
Experimental Conditions	Both tests were preceded by pre-irradiation in the LOFT core in order to generate a FP inventory. The tests were initiated by scramming the control rods. The blowdown period was initiated 1 sec after scram by opening the valves in the broken loop, the pumps were then turned off and decoupled from their flywheels. The heat-up and fission product transport period followed until the intended fuel degradation goals were obtained. The system discharge was isolated, and finally reflood and recovery ended the tests. Initial conditions were close to those found in a PWR at nominal power: 15 MPa, 550K. Fuel boundary conditions were defined by the evolution of the LOFT system in the accident sequence simulated.	
Parameter Range	The LOFT LP-FP test series did not follow a systematic approach to severe accident phenomenology. The tests are intended to study two specific accident sequences. Therefore test parameters were not varied according to a predefined test matrix. Parameter ranges are: fuel irradiation 0.45-1.40 GWD/tU, steam flow 15-139 g/s, system pressure 15 MPa (initial), 0.1-1.4 MPa (final), fuel rod internal fuel pressure 0.10-2.41 MPa, initial heat-up rate 2.2-50 K/s, maximum temperature 1200-3000 K.	
Measurements		
- On-line	On-line recordings were made of LOFT system pressures, temperatures and other fluid properties. Recordings were also made of CFM fuel clad, fuel centreline, guide tube and shroud temperatures. A Fission Product Measurement System, which included spectrometers, filter sampling, and deposition sampling, was also used.	
- Post-test	Post-test examinations of the LP-FP-2 test were extensive and included neutron radiography, cross-section cuttings, metallographic examination, blockage profiles, and study of the composition of melts.	
- Evaluation	An evaluation of LP-FP-2 will be carried out by the CSNI Principal Working Group 2.	
- Data Acquisition	On-line acquisition of all measurements is performed with a computer system.	

No. 1.8	INTEGRAL TEST FACILITY	LOFT LP-FP
Subject	**Description**	
Data Documentation		
- Data Reports	Many official reports have been published by OECD including pre-test specifications, and experiment analysis and summary reports. International participants have also published a number of reports. Some references are: Carboneau M L et al., "Experiment Analysis and Summary Report for OECD LOFT Experiment LP-FP-2", OECD LOFT-T-3806, OECD, June 1989**;** Jensen S M et al., "PIE Data and Analyses for OECD LOFT LP-FP-2", OECD LOFT-T-3810, Vol. 1, OECD, December 1989**;** Wahba A B, "Thermalhydraulic EASR of OECD LOFT LP-FP-1", OECD LOFT-T-3709, March 1985**;** "Proceedings of the LOFT Open Forum Hold in Madrid in May 1990", published by OECD, 1991. A recent analysis has been published by NRC: Coryell E W, "Summary of Results and SCDAP/RELAP5 Analysis for LP-FP-2", NUREG/CR-6160, April 1994.	
- Data Availability	Reports are easily available. INEL keeps files of data registered on-line.	
Use of Data	Data are available for further analysis.	
Special Features	-	
Correctness of Phenomena	Unintentional water injection to the reactor upper plenum during the LP-FP-1 test reduced the number of failed fuel rods, and rendered thermalhydraulic and fission product behaviour interpretation more difficult. Data obtained from LP-FP-2 (e.g. temperatures, separation of melts, blockages, chemical interactions, damage during reflood) seems of good quality and consistent with results obtained in other test programmes and in TMI-2.	

No. 1.8	INTEGRAL TEST FACILITY	LOFT LP-FP
Subject	**Description**	
Overall Evaluation		
- Strengths	The LP-FP-1 test gave data on volatile fission product release and transport during a large LOCA-type sequence. The LP-FP-2 test gave very interesting data on core degradation and fission product release and transport in a V-type LOCA sequence, under low system pressure, in a decay-heated bundle, and at a larger scale compared with other bundle in-reactor tests. The test confirmed the damage zones observed in TMI-2, showed the inability of blockages to stop fuel oxidation, and showed that significant damage and enhanced hydrogen production can occur during the reflood. Quantitative measurements of FP deposition were made. The test is also unique in the dominance of AgI as chemical form of I. Substantial PIE data are available, and several interpretation reports have been published.	
- Weaknesses	The LP-FP-1 test did not produce many data useful for severe accident research, if compared with test FP-2. The number of failed rods was reduced due to unintentional cooling during the test caused by leakages. The maximum temperature reached was around 1200 K, with strong heterogeneity in the core temperature distribution. The main weakness in LP-FP-2 concerns uncertainty in the thermal hydraulic behaviour, especially in the evaluation of the primary system mass balance and the amount of bypass flow, owing to a lack of instrumentation.	
Comments	Data from the LP-FP-2 test are being used for validation of the latest version of SCDAP/RELAP5 by INEL. The LP-FP-2 test is to be reviewed by a specialist group of the CSNI Principal Working Group 2 Task Group on In-Vessel Degraded Core Behaviour.	

No. 1.9	INTEGRAL TEST FACILITY	PHEBUS FP
Subject	**Description**	
Test Facility	PHEBUS FP (IPSN/CEA - Cadarache, France)	
- Operating Period	Beginning end 1993 (first test FPT0). The sixth and last test is foreseen in 2005.	
Objectives		
- FPT0, FPT1, FPT2	Investigate in-pile the late phase of core degradation and FP release (volatile and non-volatile).	
- FPT4	Investigate in-pile the late phase of core degradation and FP (low volatile) and transuranic nucleides release	
- FPT3	Investigate in-pile the late phase of core degradation and FP (volatile and non-volatile) with carbon compounds release	
- FPT5	Provide qualified experimental data for model improvement and code validation in the field of LWR Source Term analysis.	
Facility Geometry		
- Bundle aspect	The in-pile test train has been modified with respect to PHEBUS SFD in order to perform an initial irradiation phase (~9 days) using the pressurised water cooling circuit of the facility. Just before the test, the closure of the test train foot-valve enables this water (2.5 MPa, 438 K) to by-pass the bundle and to cool the external structures located between the test train and the driver core. An independent gas circuit enables the injection of the selected gas (steam, H_2 or He) at the same temperature as the pressurised cooling water. The wall of the outlet channel is heated at 970K. The bundle is similar to the SFD one except on the following points: fissile length of 1 m (instead of 0.8 m), insulating shroud with an inner cylindrical layer (low porosity ZrO_2 or ThO_2 layer) and an outer cylindrical ZrO_2 layer, two Zircaloy spacer-grids secured to four external Zircaloy stiffeners. The first three tests (FPT0, FPT1, FPT2) are planned with a central Ag-In-Cd control rod. The FPT3 test is planned to be performed with a central B_4C control rod. The FPT4 test starts with a debris bed configuration with quite similar insulating shroud including a neutronic shield (HfO_2) in the lower part.	

No. 1.9	INTEGRAL TEST FACILITY	PHEBUS FP
Subject	**Description**	
Experimental Conditions		
- FPT0, FPT1	Thermal hydraulic conditions (pressure, inlet gas mass flow and temperature for the first two tests are characterised by similar temperature conditions to be applied to fresh fuel (FPT0) and intermediate burn-up fuel (FPT1). The transient is characterised by a first thermal calibration phase (9000 s) involving three temperature plateaux, a heat-up and fuel melting phase (7000 s) obtained with a linear increase of the nuclear power and a final cooling phase (2000 s) characterised by a reactor shutdown and gas injection enabling a moderate cooling (from a few K/s to 1.5 K/s). Significant clad oxidation escalation, FP release and fuel liquefaction were produced during the heat-up phase of FPT0 and FPT-1 tests.	
- FPT2	FPT2 is foreseen with part of the cladding oxidation period in steam starvation, leading to reducing condition at the bundle outlet (low steam mass flow rate). The transient is characterised by a first thermal calibration phase (6500 s : shorter than FPT0 and FPT1) involving two temperature plateaux, a pre-oxidation phase up to a third temperature plateau (around 2270K) including the steam starvation period (from t= 6500 to 11300s), a heat-up and fuel melting phase (2800 s) obtained with a linear increase of the nuclear power and a final cooling phase (2000 s).	
- FPT3	FPT3 is foreseen with B_4C and fuel cladding oxidation and part of the oxidation period in pure reducing condition (probably longer than for FPT2 : H_2O plus H_2/He injection).	
- FPT4	Prefabricated solid debris bed of irradiated UO_2 including ZrO_2 fragments. (H_2O plus H_2 injection), heat-up and fuel melting phase (debris bed to molten pool) obtained by nuclear power increase (7 successive power plateaux) during 18500s	
- FPT5	Air ingress test. Not finalised, conditions currently under investigation.	
Parameter Range		
- FPT0, FPT1	Parameter ranges of these tests are: variable steam flow 0.5 - 3 g/s, initial heat-up of 0.5 K/s before oxidation escalation, system pressure 0.22 MPa, internal rod pressure 2.4 MPa, trace-irradiated fuel (9 days in PHEBUS reactor) for FPT0 and intermediate burn-up fuel for FPT1 (~ 23 GWD/tU). One central Ag-In-Cd control rod.	

No. 1.9	INTEGRAL TEST FACILITY	PHEBUS FP
Subject	**Description**	
- FPT2	Partial oxidation of cladding followed by reducing outlet conditions (steam flow 0.5 g/s), system pressure 0.22 MPa, internal rod pressure 2.4 MPa, intermediate burn-up. One central Ag-In-Cd control rod.	
- FPT4	steam flow 0.4865 g/s - H_2 0.0135 g/s, system pressure 0.22 MPa, intermediate burn-up (~ 33 GWD/tU).	
- FPT3	Partial oxidation of cladding followed by reducing outlet conditions, system pressure 0.22 MPa, intermediate burn-up. One central B_4C rod.	
- FPT5	Not finalised.	
Measurements		
- Pre-test	Non-destructive examinations of the bundle or the debris bed are performed before the test (degradation phase)	
- On-line	Measurements similar to those of the PHEBUS SFD bundle are made. In FPT1 and FPT2 (intermediate burn-up fuel) W/Re fuel centreline thermocouples are used in two fresh fuel rods. In addition, two ultrasonic thermometers are installed in the bundle to measure high temperature levels and fission chambers are located around the test train to detect fuel relocation. Limitations on the number of thermocouples which can be located inside high irradiated fuel bundles lead to reinforcement of temperature measurements inside the surrounding shroud in order to evaluate the thermal conditions inside the bundle and detect fuel movements. An On- Line Aerosol Monitor (OLAM) device enables the detection of severe degradation and FP release events (clad failure, control rod failure, Zr oxidation escalation and melting, significant fuel material relocations). Hydrogen production measurement and various FP/aerosols measurements are performed in the circuit (impactors, filters, capsules, gamma spectrometry, ...).	
- Post-test	Non-destructive examinations are performed before transportation of the bundle to hot cell laboratory (radiography, transmisssion and emission tomography, gamma scanning). Destructive examinations on axial and radial cuts are used to determine core material configuration, axial blockage profiles and the composition of refrozen corium.	
- Data Acquisition	Acquisition of all bundle measurements is performed with several independent computer systems.	

No. 1.9	INTEGRAL TEST FACILITY	PHEBUS FP
Subject	**Description**	
Data Documentation		
- Overview	Von der Hardt P and Tattegrain A, "The PHEBUS Fission Product Project", Journal of Nuclear Materials 188 (1992); Von der Hardt P,Jones AV, Lecomte C, Tattegrain A: "Nuclear Safety Research: The Phebus FP Severe Accident Experimental Programme", Nuclear Safety, Vol 35 n°2 (1994); Von der Hardt P, Schwarz M, "An International Severe Accident Research Programme; PHEBUS PF", Nu-Power, Vol 12 n°3 (1998); Shepherd I et al., "Precalculations for the Bundle for the First PHEBUS-FP Test FPT0", IAEA Technical Committee Meeting, Aix-en-Provence, France, May 1992; Adroguer B et al., "Calculation of the PHEBUS FP Experiments", 3rd Workshop on Severe Accident Research in Japan, Tokyo, Nov. 1992; Tattegrain A et al., "The PHEBUS FP Programme", Third International Conf. on Containment Design and Operation, Toronto, Ontario, Canada, Oct. 19-21, 1994; Repetto G, von der Hardt P, Gonnier C, Haessler M; "The First PHEBUS Fission Product Experiment FPT-0, General Aspects of Experimental Sequence concerning the Fuel Bundle Degradation and FP Release", ANS Int. Topical Meeting on Safety of Operational Reactors, Seattle (Sept. 1995); Jamond C, Bourdon S, Adroguer B, Shepherd I, "Current Analysis of the PHEBUS FPT0 Bundle Behaviour with ICARE2", CSARP Semi-Annual Review Meeting, Bethesda, 1-5 May 1995; Jamond C, Adroguer B, Bourdon S, Ederli S and Repetto G, "Status of the Interpretation of the FPT0 Test with ICARE2: Bundle Degradation", ICHMT Meeting, Çesme, 21-26 May 1995; Schwarz M, Clément B, Ktorza C, Jones AV, Zeyen R, "The Phebus FP International Research Program on Severe Accidents: Status and Main Findings", 26th WRSM, Bethesda (October 1998)	
- Data Reports	FPT-0: Quick Look Report (1993), Preliminary Report (1994), Preliminary Report Addenda (1994). Hanniet-Girault N and Repetto G, "FPT0 Final Report - Final Version", IPSN/DRS/SEA report SEA 1/99 (1999) is now openly available. FPT-1: Quick Look Report (1996), Preliminary Report (1997)	
- Data Availability	Data Reports and associated technical notes are initially restricted to PHEBUS FP partners: European Union, USA (NRC), Canada (COG), Japan (NUPEC and JAERI), South Korea (KAERI). Switzerland (HSK and PSI). Data become generally open for publication one year after the issue of the final Data Report to Phebus partners.	
Use of Data	The data are used by PHEBUS FP partners for a detailed analysis of core degradation, FP and core material releases.	

No. 1.9	INTEGRAL TEST FACILITY	PHEBUS FP
Subject	**Description**	
Special Features	The test matrix focuses on items for which insufficient data exist in the current data banks: late phase of core degradation including significant UO_2 liquefaction, debris bed formation, evolution to a molten pool and core degradation with air ingress. All these severe degradation aspects will be studied with prototypic fuel conditions using high burn-up fuel in order to measure the related FP and core material release. These source term aspects are unique under late core degradation conditions.	
Correctness of Phenomena	It is too soon to discuss this item but it must be pointed out that experience gained from the previous PHEBUS SFD programme on the early phase of core degradation is applied to PHEBUS FP (test operating, instrumentation, analysis of results, ...). A significant effort is devoted to defining prototypic test conditions in the bundle regarding both degradation and FP/core material releases. These conditions are defined on the basis of the current knowledge (TMI-2, other in-pile tests, reactor calculations...).	
Overall Evaluation		
- **Strengths**	Unique data on the transition between the early phase and the late phase and on the late phase and FP/core material releases with prototypic LWR fuel: trace-irradiated and intermediate burn-up, including control rod material.	
- **Weaknesses**	Usual limitations inherent in a small bundle size (1 m long, 20 rods), high temperatures and intermediate burn-ups. In particular limited number of TCs inside the bundle and presence of a thermal shroud. Some non-prototypic PWR core materials are included in the bundle, such as rhenium from TCs.	
Comments	A large international effort is devoted to the definition of objectives, test conditions and to the analyses of results. A parallel effort is also devoted to the development and validation of codes such as ICARE2, intensively used for preparing and analysing PHEBUS results.	

No. 1.10	INTEGRAL TEST FACILITY	ACRR-MP
Subject	**Description**	
Test Facility	ACRR-MP Facility: Fuel damage tests conducted in the Annular Core Research Reactor (Sandia National Laboratories, Albuquerque, New Mexico, USA)	
- Operating Period	1982 - 1989	
Objectives	To investigate late phase melt progression in degraded fuel geometry, this included melting dynamics, molten pool formation, and growth in a debris medium, crust formation and failure and pool migration through blockages and intact rod structure.	
Facility Geometry	The Annular Core Research Reactor (ACRR) is a general purpose research reactor capable of steady state, pulse and programmed transient operational modes. The experiment package consisted of a debris bed zone overlying a preformed metallic/ceramic crust and a free-standing rod-stub zone. The active region was enclosed in melt barriers and insulation and housed in a double containment structure. An axial annular cooling jacket removed excess heat from the package. The experiment was fission heated in the ACRR.	
Experimental Conditions	Test initiation would typically begin with a series of controlled transients followed by steady-state plateau, then a final power boost to initiate bed melting and sustain melting until the molten pool contacts, penetrate, and interacts with the preformed blockage.	
Parameter Range	The principal variation in the MP tests was the degree of melt progression. The MP-1 test progressed to form a molten fuel pool. The MP-2 test continued with growth of the molten pool through the relocation of the pool into the lower rodded region.	
Measurements		
- On-line	Temperature measurements throughout the debris bed, metallic crust and lower rod stub region, as well as good boundary temperature measurements were made in both tests.	
- Post-test	Destructive examinations characterize the nature of material interactions and the degree of melt progression.	
- Evaluation	The available data, combined with the available post-test thermal analyses are excellent.	
- Data Acquisition	Original on-line acquisition was based on HP computer system. The data has been converted to a DOS (PC) format.	

No. 1.10	INTEGRAL TEST FACILITY	ACRR-MP
Subject	**Description**	
Data Documentation		
- Overview	Gasser R D, Dosanjh S S and Gauntt R O, "The DEBRIS Module: An Effective Tool for the Analysis of Melt Progression in LWRs", Presented at the 18th Water Reactor Safety Meeting, Rockville, MD, October 1990.	
- Data Reports	Gasser R D, Gauntt R O and Bourcier S, "Late Phase Melt Progression Experiment - MP-1: Results and Analysis", NUREG/CR-5874, SAND92-0804, June 1993 - to be published**;** Gasser R D, Gauntt R O, Bourcier S, Schmidt R C, Humphries L H and Reil K O, "Late Phase Melt Progression Experiment - MP2: Results and Analysis", NUREG/CR-6167, SAND93-3931, May 1997.	
- Analysis	Tautges T J, "MELCOR 1.8.2 Assessment: The MP-1 and MP-2 Late Phase Melt Progression Experiments", SAND94-0133, May 1994.	
- Data Availability	On-line test results and the reports listed above are available. . Informal reports are made at the USNRC CSARP meetings annually, for all tests to date.	
Use of Data	The data are available for a more detailed analysis.	
Special Features	High temperature melt pool measurements.	
Correctness of Phenomena	The melt progression phenomena observed generally are consistent with those observed in the TMI-2 accident and in in-pile experiments. The phenomena observed may be specific to that of fresh or low burnup fuel since no irradiated fuel was investigated in this test series. Scale limitations preclude direct application where large-scale molten pool convection effects are of direct interest.	
Overall Evaluation		
- Strengths	The use of prototypic materials and realistic heating methods in addition to the extremely high temperatures accomplished in these tests make the tests fairly unique. Additionally, aside from these two tests, virtually no late phase melt progression experiments are currently available	
- Weaknesses	Principal weaknesses include the use of only fresh fuel in the test series and the limited scale (size) of the molten pool.	

No. 1.11	INTEGRAL TEST FACILITY	Sandia Ex-Reactor Experiments
Subject	**Description**	
Test Facility	Ex-Reactor Facility (Sandia National Laboratories, Albuquerque, NM, USA)	
- Operating Period	1993 - 1996	
Objectives	To investigate the behaviour of melting and relocating metallic core materials in ? dry-core? BWR accidents.	
Facility Geometry	A test section including structural details of the lower BWR core region is preheated in an argon-inert environment so that an accident-typical axial thermal gradient exists. Test sections include BWR control blade, channel boxes and fuel rods (XR2-1 pending) in addition to structural features such as fuel canister nose pieces and lower core plate. Metallic melts corresponding to control blade alloy and Zircaloy core components are prepared and introduced to the test section, simulating the melting and draining of core metallic components into the lower metre of the core.	
Experimental Conditions		
- Initial	The test sections are heated so that an axial thermal gradient typical of that in the lower core region under Short Term Station Blackout conditions at the time of incipient melting of the metallic core structures is attained.	
- Boundary	After attaining the desired initial thermal conditions, metallic melts are generated and introduced to the top of the test section over a period of about half an hour, simulating the protracted melting and draining of the stainless steel and Zircaloy core materials.	
Parameter Range	The principal parameter in the XR tests is the axial thermal gradient, which varies between 1000 K/m to 2000 K/m. Other parameters include Zircaloy component surface oxide layer thickness. The metallic melt includes of up to 12 kg stainless steel and B_4C and up to 65 kg Zircaloy; maximum temperatures are in the range 1900 K to 2300 K.	

No. 1.11	INTEGRAL TEST FACILITY	Sandia Ex-Reactor Experiments

Subject	Description
Measurements	
- On-line	On-line measurements of test section temperatures are made prior to and during the metallic melt pour. Additionally, real-time X-ray examination of the test bundle is performed, providing a video record of the melt drainage and blockage processes. The video record provides evidence of intermediate blockages that later fail and reform elsewhere.
- Post-test	Post-test destructive examinations determine the extent of material interactions, blockage distributions and structural damage encountered during the test.
- Evaluation	The data from these tests will provide unique information on an area not covered well in other test programmes. Especially valuable in these tests are the full scale aspects of the tests with respect to the scale of the test section components and with the total mass of molten materials involved in the test conduct. The major test results are still pending at the time of this document preparation.
- Data Acquisition	On-line acquisition based on personal computer (PC) system.
Data Documentation	
- Overview	Gauntt R O et al., "Metallic Core-Melt Behaviour in Dry-Core BWR Accidents: The Ex-Reactor Experiments", Proceedings of the 22nd Water Reactor Safety Meeting, November 1994.
- Data Reports	Gauntt R O et al.,"Data Report on the XR1-1 and XR1-2 BWR Metallic Melt Relocation Experiments", Report NRC FIN L-2452, Sandia National Laboratories (Dept 6423), January 1994**;** Gauntt R O and Humphries L L, "Final Results of the XR2-1 BWR Metallic Melt Relocation Experiment", SAND-97-1039, NUREG/CR-6257, August 1997.
- Evaluation	Griffin F P and Ott L J, "Development of the BWR Dry Core Initial and Boundary Conditiond for the SNL XR2 Experiments", ORNL Letter Report, ORNL/NRC/LTR-94/38, 31 October 1994**;** Ott L J, "Description of the XR/BWR Experiment-Specific Code and Preliminary Posttest Analysis of the XR1 Tests, ORNL Letter Report, ORNL/NRC/LTR-95/5, 28 February 1995.
- Data Availability	On-line test results and the reports listed above are available.

No. 1.11	INTEGRAL TEST FACILITY	Sandia Ex-Reactor Experiments
Subject	**Description**	
Use of Data	The data are available for a more detailed analysis.	
Special Features	Video recording of melt progression and blockage formation is a unique feature.	
Correctness of Phenomena	The phenomena observed in these experiments may be applied to reactor scale issues with minimum analytical augmentation due to the scale of the experiments. Analytical means are required to project the melt progression phenomena to greater time beyond the period of metallic core component melting and relocation.	
Overall Evaluation		
- Strengths	The strengths of the Ex-Reactor experiments are associated with the large scale of the experiments. It must be kept in mind, however that very few experiments in this programme have been conducted, and the most informative of the tests, XR2-1 is pending execution at the time of this document preparation.	
- Weaknesses	The main weakness of the Ex-Reactor experiments are associated with the fact that no internal heating of the fuel rods is maintained following the melt pour. Somewhat countering this deficiency is the fact that the melt delivery system situated just above the test section remains at a very high temperature for a considerably time following the melt pour, and thereby simulates to some degree the continued heat load from the hot core interior region to the lower core geometry. Again, the same note regarding the fact that the test series is currently underway applies here.	
Comments	This information is provided in anticipation of test results that have not yet been obtained.	

No. 1.12	INTEGRAL TEST FACILITY	TMI-2
Subject	**Description**	
Test Facility	TMI-2 reactor, 2720 MW(th), designed and manufactured by Babcock and Wilcox (B&W), Located in Harrisburg, Pa, USA	
- Operating Period	To March 1979	
Objectives	Production Reactor	
Core Geometry	The core contained 93.1 t of fuel in 177 fuel assemblies. A basic assembly consisted of 208 fuel rods, 16 control rod guide tubes and 1 guide, in a 15x15 array. Reactivity was controlled with control rod assemblies and boron dissolved in the coolant. 68 burnable poison assemblies had been included for first cycle reactivity control.	
Accident Conditions	The transient accident sequence is characterised by 4 phases: Phase 1 (0-100 min): PORV opens at 15.7 MPa, reactor scram, PORV fails to close, ECCS manually reduced, void fraction increases, RC pumps stopped, forced flow through the core terminated. Phase 2 (100-174 min): decrease of core level, clad burst and failure, PORV closed manually, clad oxidation, hydrogen production and decrease in primary to secondary heat transfer, eutectic melting of control rods and spacer grids, lower crust, central core blockages, region of partially molten ceramic materials on top of crust, maximum temperature around fuel melting. Phase 3 (174-224 min): water injection by RC pump (174 min), fragmentation, oxidation, melting and ablation of the upper grid, central core heat-up continues, pool of molten materials, HPI partial operation. Phase 4 (224 min-15.5 hours): crust failure (224 min), relocation to the lower head, manual depressurization and venting, one RCS pump restarted, forced flow and heat removal re-established.	
Parameter Range	Fuel irradiation 0.9-6.0 GWD/tU, system pressure 5-15 MPa during heat-up, initial heat-up rate 0.3K/s rising to 0.65 K/s thereafter, maximum temperatures estimated to exceed 3000 K, terminated by quench after 19 t core materials had relocated to the lower plenum.	

No. 1.12	INTEGRAL TEST FACILITY	TMI-2
Subject	**Description**	
Measurements		
- On-line	Only limited on-line data, such as structural temperatures and system pressures, are available.	
- Post-test	Post-test examinations of samples extracted from the core and lower vessel debris has been carried out by several international laboratories. Their results have been integrated in a OECD document. Post-test examination is the main analysis tool used to estimate the accident scenario.	
- Evaluation	TMI-2 was not a well-instrumented test facility. One of the main difficulties when analyzing the TMI-2 accident is the lack of recorded data. Although the operational sequence of events is well-known, times for phenomenological events are based on indirect data and analyses. A limitation is the lack of recorded boundary flows. Parametric calculations have to be made to infer the effect of uncertainties in the boundary conditions.	
- Data Acquisition	See above.	
Data Documentation	Many official reports have been published by OECD including analysis and summary reports. International participants have also published a number of reports. Some references are: Golden D W, "TMI-2 Analysis Exercise Final Report", ref. DWG-07-90, published by EG&G, May 1990**;** "TMI-2 Examination Results from the OECD Programme", several authors, EGG-OECD-9168 document, August 1990**;** Wolf J R et al., "TMI-2 Vessel Investigation Project Integration Report", NUREG/CR-6197, March 1994.	
- Data Availability	Reports are easily available. INEL keeps files of data registered on-line.	
Use of Data	Data are available for further analysis.	
Special Features		
Correctness of Phenomena	An important international effort has been undertaken, through analyses and PIE evaluation, to define a "best- estimate TMI-2 scenario". This scenario is considered a reference against which results from test programmes are often compared.	

No. 1.12	INTEGRAL TEST FACILITY	TMI-2
Subject	**Description**	
Overall Evaluation		
- Strengths	The TMI-2 accident is unique in that it gives the only full-scale data available on LWR severe accident phenomena. A broad spectrum of phenomena is represented in the accident scenario, including late phase degradation, relocation to the lower plenum and attack on the lower vessel head. Data gathered from the accident analysis are very valuable for designing late phase test programmes, and for validation of late phase models.	
- Weaknesses	The lack of instrumentation and recording of some important parameters makes the interpretation of the accident more uncertain. The phenomenological sequence during the last phases of the accident can only be inferred from PIE data and results of analysis. The analyst should be aware of the remaining uncertainties, when using the "TMI-2 best estimate scenario".	
Comments	-	

No. 1.13	INTEGRAL TEST FACILITY	SCARABEE BF
Subject	**Description**	
Test Facility **- Operating Period**	SCARABEE (IPSN/CEA - Cadarache, France) 1985 - 1988: for the BF test series	
Objectives	Investigate the evolution of a solid debris bed to a molten pool. Study the heat transfer between a molten or a boiling pool with surrounding walls.	
Facility Geometry	The in-pile test train which crosses the SCARABEE reactor has been used to study the evolution of a fast reactor sub-assembly with a supposed blockage at the entrance preventing the circulation of a cooling sodium. The first test BF1 started with a pre-fabricated solid debris bed of UO_2 pellets (~5 kg of UO_2) in a 0.06 m diameter SS crucible cooled by flowing sodium from the outside and brought to different power plateaux. The initial height of the debris bed is 0.26 m. BF2 has been made in the same way but under different conditions: lower pressure, higher nuclear power leading to a boiling pool in a Niobium crucible. BF3 started from an initial 37 fuel rod bundle with stainless-steel cladding (6 kg UO_2 and 2 kg SS) located inside a nickel crucible. It enabled studying of the evolution of a UO_2-SS boiling pool. Mainly the BF1 test performed at low power is of interest for studying molten pool situations representative of LWR.	
Experimental Conditions	Thermal hydraulic conditions (pressure, mass flow rate and temperature) of the flowing sodium along the external surface of the SS crucible are well-controlled enabling to measure the heat flux profile. The power is increased by steps enabling six temperature plateaux (specific power of 5.9 W/g for the 1st plateau and of 17 W/g for the last one).	
Parameter Range	A maximum temperature of ~3230 K was measured during the first plateau. The crust thickness at the last plateau was deduced from the post-test examinations (1 to 2 mm). A small erosion of 0.1 mm has been observed locally on the crucible wall. The maximum experimental lateral heat fluxes between the pool and the crust are 66 W/cm^2 (1st plateau in laminar regime) and 190 W/cm^2 (last plateau in turbulent regime) leading to a flux concentration factor of 1.72 and 1.38 respectively. Substantial cooling of the pool by radiation across the upper surface was found. About 25% of the power was removed through the upper surface of the pool.	

No. 1.13	INTEGRAL TEST FACILITY	SCARABEE BF
Subject	**Description**	
Measurements		
- On-line	The external cooling fluid and the crucible wall are well-controlled at different locations by thermocouples. One of the two ultrasonic thermometers measured the inner debris bed temperature evolution up to 3230 K (1st plateau). Then this thermometer failed and no more pool temperatures are available for the following plateaux. Post-test examinations enabled clear characterisation of the final molten pool, the remaining solid debris, the upper dome and the surrounding crust.	
- Data Acquisition	Acquisition of all on-line measurements was performed with a computer system.	
Data Documentation		
- Overview	Kayser G, "Synthesis of Molten Pool Test BF1", IPSN/CEA Report - NT DRS/SEMAR 93/02 - May 1994**;** Kayser G, "The Scarabee BF1 Experiment with a Molten UO_2 Pool and its Interpretation", OECD/CSNI/NEA Workshop on Large Molten Pool Heat Transfer, Grenoble, NEA/CSNI/R(94)11, March 1994**;** Livolant M, Dadillon J, Kayser G and Moxon D, "Scarabee: A Test Reactor and Programme to Study Fuel Melting and Propagation in Connection with Local Faults. Objectives and Results", International Fast Reactor Meeting, Snowbird, Utah, USA, 12-16 August, 1990**;** Seiler J M, Petrel H, Perret C and Bede M, "One Component, Volume Heated, Boiling Pool Thermohydraulics", NURETH-5, Salt Lake City, Utah, USA, 21-24 September 1992. The BAFOND separate-effect tests on water pools have been used as a supporting programme in the framework of the BF1 analysis. Seiler J M, "Cooling of a Molten Material Liquid Pool Submitted to Volumetric Heating. New Correlations for Various Cooling Conditions", International Conf. on Thermal Reactor Safety, Avignon - Oct. 1988.	
- Data Reports	Additional internal IPSN/CEA reports exist and are available.	
- Data Availability	Test results of BF1 are available to the European Community in the framework of RCA/Core Degradation Project.	
Use of Data	Validation and improvement of models describing the transition between a debris bed to a pool and the natural convection in molten pools.	

No. 1.13	INTEGRAL TEST FACILITY	SCARABEE BF
Subject	**Description**	
Special Features	UO_2 molten pool. FP simulants have been added in the debris bed (4.3% in mass). They do not play a role in the heat transfer mechanism and the corresponding analysis of results did not allow so far to draw firm conclusions about any migration. Ultrasonic thermometers gave measurements at 4 levels up to the end of the first plateau with an experimental uncertainty of ?0? C.	
Correctness of Phenomena	Heat exchanges measured are consistent with evaluations deduced using BAFOND correlations adapted to take into account axial heat radiation transfer. (BAFOND was a separate effect test programme with water in a cylindrical volume heated cavity devoted to studying natural convection heat exchanges). Laminar and turbulent convection regimes have been investigated.	
Overall Evaluation		
- Strengths	Well-characterized information on the heat flux distribution around a volume heated molten pool has been obtained in the SCARABEE BF1 test performed with experimental conditions enabling valuable applications for LWR situations. Nuclear power evolution and distribution and the final state of the pool, in particular the crust distribution, were well characterized.	
- Weaknesses	The main difficulty is related to the measurement of temperature of the molten UO_2. This could be made only for the first plateau. For other plateaux the ultrasonic TC did not work. The second difficulty is linked to the uncertainties in pool temperature measurement (60 K for a level of 3230 K) which induce an uncertainty range up to 50% on the evaluation of the radial heat exchange coefficient between the pool and the surrounding wall. Nevertheless this evaluation must be considered as valuable compared to the very large uncertainty in this field.	
Comments	Axial heat exchange due to radiative transfer was found to be greater than expected: 25% of the total power.	

No. 1.14	INTEGRAL TEST FACILITY	ACRR-DC
Subject	**Description**	
Test Facility	ACRR-DC Facility: Dry debris bed coolability and melt dynamics tests conducted in the Annular Core Research Reactor (Sandia National Laboratories, Albuquerque, New Mexico, USA)	
- Operating Period	1982 - 1989	
Objectives	To heat up and melt down a dry core debris bed to determine the heat transfer characteristics of a debris medium and to study the melt formation in a debris medium.	
Facility Geometry	The Annular Core Research Reactor (ACRR) is a general purpose research reactor capable of steady state, pulse and programmed transient operational modes. The DC test capsule was made up of a debris bed enclosed in a tungsten crucible insulated in radial direction and actively cooled top and bottom. The crucible was contained within a steel containment structure 0.9 m high and 0.23 m in diameter cooled by helium gas flow and fission heated in the ACRR.	
Experimental Conditions	Test initiation would typically begin by heating the test section and attaining a specified steady-state temperature to measure the heat transfer characteristics. Three such steady-state conditions were attained followed by a resumed transient to take the bed to melting and melt ~1/2 of the original bed inventory.	
Parameter Range	Bed composition from pure UO_2 to 75% UO_2 25% SS by wt. Temperature range 100 - 3400 K.	
Measurements		
- On-line	Thermocouple - W/Re + Ultrasonic T/C.	
- Post-test	Post-test destructive examinations.	
- Evaluation	The available data are generally of good quality.	
- Data Acquisition	At this time only hard copies of the measured temperature data exist.	

No. 1.14	INTEGRAL TEST FACILITY	ACRR-DC
Subject	**Description**	
Data Documentation		
- Data Reports	Hitchcock J T and Kelly J E, "The DC-1 and DC-2 Debris Bed Coolability and Melt Dynamics Experiments", NUREG/CR-4060, SAND84-1367, Sandia National Laboratories, Albuquerque, NM, April 1985**;** Fryer C P and Hitchcock J T, "The Postirradiation Examination of the DC Melt Dynamics Experiments", NUREG/CR-4625, SAND86-1102, Sandia National Laboratories, Albuquerque, NM, August 1987.	
- Data Availability	On-line test results and the reports listed above are available. . Informal reports are made at the USNRC CSARP meetings annually, for all tests to date:	
Use of Data	The data are available for a more detailed analysis.	
Special Features	Ultrasonic thermocouples provided continuous measurements to above 3300 K.	
Correctness of Phenomena	The phenomena observed in the tests are reasonable for the applied conditions, although the later MP tests extend the phenomenological area well beyond the regime covered in the DC tests.	
Overall Evaluation		
- Strengths	The DC tests were unprecedented in their time and were carefully instrumented and characterized. The strengths include the use of prototypic materials and the attainment of extremely high temperatures. The data provided benchmarking for state-of-the-art models for high temperature thermal conductivity in porous media.	
- Weaknesses	The main weaknesses of the DC tests are the use of only fresh fuel and the simple geometry of the fuel debris. No reactor-typical structures were investigated in these materials properties oriented tests.	

No. 1.15	INTEGRAL TEST FACILITY	CODEX
Subject	**Description**	
Test Facility	CODEX (AEKI, Budapest, Hungary)	
- Operating Period	The main series started in December 1995, the programme is ongoing	
Objectives	To investigate early-phase core degradation in light water reactors (Western LWR and VVER designs). The series of 5 tests to date has investigated the effects of quench in VVER geometry, and the effect of of air ingress on pre-oxidised Western LWR bundles.	
Facility Geometry	A fuel rod bundle of representative Western PWR or VVER-440 design of overall cladded length 1.15 m (heated length 0.6 m) is surrounded by a permanently-installed high temperature shield. Decay heat is simulated by electrical heating with tungsten heaters installed within all but the central rod (9-rod square array with pitch 14.3 mm for PWR; 7-rod hexagonal array with pitch 12.2 mm for VVER). Coolant (superheated steam, argon or argon/oxygen mixture) is injected laterally at the bottom of the heated section, while cold air or a fast, cold argon flow (for rapid cooling) can be injected into the bottom of the heated section. In the tests not involving air ingress, quench can be effected by injection of water into the bottom of the bundle.	
Experimental Conditions		
- Initial	A typical test was started by pre-heating the bundle in hot flowing argon (4 g/s) at ~923 K to about 800-900 K, and with a nominal electrical power. This pre-heating typically for ~6000 s gives near steady-state conditions prior to the start of the pre-oxidation and/or transient phase.	
- Boundary	In the VVER tests the bundle was then ramped initially at 0.5-0.6 K/s in steam until the desired maximum temperature of up to ~2300K was reached (in some cases following an oxidation excursion), then cooled in warm argon or quenched by water, with power switched off. In the air ingress tests the bundle was pre-oxidised in an argon/25%oxygen mixture or steam before the transient phase in air was entered. The air ingress tests were terminated from the desired maximum temperature (2200-2300K) by rapid cooling in a high flow of argon at room temperature, again with power switched off.	

No. 1.15	INTEGRAL TEST FACILITY	CODEX
Subject	**Description**	
Parameter Range	Parameter ranges are for the 5 tests conducted: absorber material - none; heated argon flow 1.5-4 g/s; cold argon (quench) flow ~25g/s; argon/25%oxygen flow 3.5-4g/s; steam flow 1-1.5 g/s, air flow 2.5-3.5g/s; initial heat-up rate 0.5-0.6K/s; maximum recorded temperature <1450 to 2300 K, system pressure 0.2 MPa; internal rod pressure 0.22 MPa; simulated reflood rate none or 6-8 mm/s.	
Measurements		
- On-line	On-line recordings are made of temperatures of the fuel rods, electrically heated fuel rod simulators, cladding, shroud, high temperature shield, inlet and outlet gas, measured using W/WRe, NiCr/Ni and Pt/PtRh thermocouples and pyrometers; also the gas flows and system pressures are recorded continuously. In the second air ingress test a video camera recorded melt progression phenomena through a window cut in the flow shroud. In the air ingress tests there are on-line measurements of the aerosol rate and size distribution.	
- Post-test	Destructive post-test examinations determine such quantities as blockage formation and material distribution,. In the air ingress tests the aerosol composition is determined by analysis of impactor and filter data.	
- Evaluation		
- Data Acquisition	On-line acquisition based on personal computer (PC) system.	
Data Documentation		
- Overview	The air ingress tests to 31st January 1999 formed part of the EC 4th Framework shared cost action project ”Oxidation Phenomena in Severe Accidents” (OPSA project), and its conclusions are included in its Final Report, EUR 19528 EN, 2000.	
- Data Reports	Hózer Z, Maróti L, Nagy I, Windberg P: CODEX-2 Experiment: Integral VVER-440 Core Degradation Test, KFKI-2000-02/G, Internal data reports have been produced for AIT1 and AIT2	
- Evaluation	Hózer Z, Maróti L, Tóth B and Windberg P, ”VVER Core Degradation Experiment”, Proc. NURETH-8 Conference, Kyoto, 30 September - 4 October 1997, pp 605-611**;** Hózer Z, Maróti L and Windberg P, ”Quenching of High Temperature VVER Bundle”, accepted for the NURETH-9 Conference, October 1999.	

No. 1.15	INTEGRAL TEST FACILITY	CODEX
Subject	**Description**	
- Data Availability	On-line test results and the reports listed above are available, however the Test Data Reports referred to above are of the nature of quick-look reports and may not be freely available.	
Use of Data	The data are available for a more detailed analysis.	
Correctness of Phenomena		
Overall Evaluation		
- Strengths	The air ingress tests, carried out with real fuel, are unique, with the aerosol measurements being a valuable additional feature. CODEX-2 and 3 are the only core degradation tests to date using VVER-440 bundles.	
- Weaknesses	The strong dependence on temperature of the electrical resistance of the tungsten heaters means that the electrical power axial profile becomes highly non-linear during the course of the experiments, due to positive feedback effects, this is a significant non-prototypic feature. Simulation of this effect is important when modelling the tests. In addition, the heat source remains static, unlike decay heat in relocating nuclear fuel. The argon flow is untypical of reactor conditions. (These non-prototypic effects are however amenable to modelling.) The tungsten heater rods in the electrically heated rods impose an artificial axial stability to the rod bundles. The overall scale of the experiments is smaller than that of CORA. In the AIT air ingress tests, there was unmonitored and unexpected additional cold air flow into the test section, in the heatup phase in AIT1 and in the pre-oxidation phase of AIT2. These flows lead to uncertainties in the boundary conditions, which however can be reduced by analysis taking into account gas temperature and bundle pressure drop measurement.	
Comments	A VVER scoping test CODEX-1 was performed with alumina pellets, but data are not available so it is not discussed further here. Extension of the series to include further air ingress tests, further quench tests and tests involving control materials (especially boron carbide) are being considered.	

No. 1.16	INTEGRAL TEST FACILITY	QUENCH
Subject	**Description**	
Test Facility	QUENCH (FZ Karlsruhe, formerly KfK, Germany)	
- Operating Period	The series started with commissioning tests in October 1997, the programme is ongoing.	
Objectives	Investigation of the physico-chemical behaviour of overheated water reactor fuel elements in rod-like geometry under different flooding conditions. More detailed aims are the determination of a failure criterion for oxidised cladding and of the hydrogen source term. The bundle experiments are supplemented by an extensive series of single-rod quench experiments and by measurements of hydrogen absorption and release by Zircaloy cladding.	
Facility Geometry	An assembly of 21 fuel rods of heated length 1m is situated within a porous zirconia-insulated flow shroud of 35mm thickness, with a Zircaloy liner, without coolant bypass. In addition, a small solid rod is positioned in three of the corners of the rod array, with a hollow instrumentation tube in the fourth. The solid rods can be withdrawn during an experiment, to check on the amount of pre-oxidation. The high temperature shield is itself surrounded by a stainless steel cooling jacket, whose annulus of 7mm thickness is cooled by argon. Each rod apart from the central one is powered by an internal tungsten resistance heater, and all contain sintered annular zirconia pellets. Above the heated zone both test bundle and shroud are uninsulated, and this part of the cooling jacket is cooled by water. Both the absence of ZrO_2 insulation above the heated region and water cooling are to force the axial temperature maximum downward. Superheated steam with argon as a carrier gas is injected at the bottom of the test section; the quench water (or cold steam) for cooling enters through a separate line at the bottom. At the inlet of the test section quench water reaches approx. 395 K, i.e. saturation temperature at 0.2 MPa. In tests from QUENCH-02 onwards the argon fill gas of the fuel rod simulators has 5% krypton added to enable measurement of the time of cladding failure (by the on-line mass spectrometer).	
Experimental Conditions		
- Initial	In a typical test the bundle is pre-heated in a heated argon/steam mixture (3 g/s + 4.5g/s) by stepwise increases of electrical power to about 823 K for 3000 s, at a system pressure of 0.2 MPa. This pre-heating for typically 4800s gives near steady-state conditions before the pre-oxidation phase (if required) and the onset of the transient phase.	

No. 1.16	INTEGRAL TEST FACILITY	QUENCH
Subject	**Description**	
- Boundary	The main test sequence begins with an optional and pre-oxidation phase in a heated argon/steam mixture (3 g/s + 3 g/s) (if required, typically at 1400-1600K); then a transient phase during which an uncontrolled oxidation excursion may occur; and finally a quench phase induced by reflooding the bundle from the bottom or by injection of cold steam (top injection is being considered for future tests). Reflood with water is in two phases; in the first water is injected at a high rate to fill the lower plenum rapidly; in the second the desired injection rate for the bundle section is employed. Additional calibration phases may be used; this was particularly the case during commissioning.	
Parameter Range	Parameter ranges for the 4 main tests conducted: bundle size 21 rods; system pressure 0.2 MPa; pre-oxidation none-500µm oxide thickness; initial heat-up rate 0.45-1.5K/s; temperature at onset of quenching ~1773-~2273K; maximum recorded temperature <1773 to 2500 K; water flooding rate 1.0–2.8 cm/s, cold steam injection (570K) 50g/s.	
Measurements		
- On-line	Extensive on-line recordings are made of temperatures of the fuel rod cladding, shroud, high temperature shield, inlet and outlet gas, quench water, measured using W-5Re/W-26Re and NiCr/Ni thermocouples. The cladding thermocouples lie at elevations from 250 mm below the start of the heated section to 350 mm above, and are in four different orientations. Other on-line recordings include heater current, voltage, resistance and power, argon and steam mass flow rates, quench water flow rate, system pressures, liquid levels, and hydrogen production (rate and total). The hydrogen is analysed by two different instruments: (1) a mass spectrometer located behind the test section, (2) a ”Caldos” hydrogen detection system located downstream of the condenser. Due to the different locations of the hydrogen measurement devices the mass spectrometer responds almost immediately whereas the delay time for the response of the Caldos system is around 100 s (as determined by calibration tests).	
- Post-test	Comprehensive destructive post-test examinations determine such quantities as extent of oxidation, crack pattern in the oxide films, blockage formation and material distribution.	

No. 1.16	INTEGRAL TEST FACILITY	QUENCH
Subject	**Description**	
- Evaluation	The available data are of good quality, and strong in the areas of cladding temperature response, hydrogen production (a major aim of the programme) and characterisation of the bundle final state. Lessons learnt from the CORA series have led to significant improvements in the instrumentation; for example better survival of thermocouples at high temperature, reduction of uncertainties in the hydrogen production rates, and better characterisation of thermal hydraulic parameters with no unquantified bypass flows. As in CORA, only the total rod power is known; the split amongst tungsten heater element, and the molybdenum and copper conductors, must be deduced by modelling.	
- Data Acquisition	On-line acquisition based on personal computer (PC) system.	
Data Documentation		
- Overview	The programme to 31st January 1999 formed part of the EC 4th Framework shared cost action project "Investigation of Core Degradation" (COBE project), and its conclusions are included in its Final Report EUR 18982 EN, 1999.	
- Data Reports	Hofmann P et al.; "Results of the QUENCH Commissioning Tests", FZKA 6099, August 1998**;** "QUENCH-01 Experimental and Calculational Results", FZKA 6100, November 1998**;** Sepold L et al.; "Quench Commissioning Tests Test Data Report", FZKA Interner Bericht 4/97, December 1997**;** "QUENCH-01 Test Data Report", FZKA Interner Bericht 2/98, PSF 3291, March 1998**;** "QUENCH-02 Test Data Report", FZKA Interner Bericht HIT 9/98, PSF 3303, July 1998**;** "QUENCH-03 Test Data Report", FZKA Interner Bericht HIT 2/99, PSF 3316, March 1999; "QUENCH-04 Test Data Report", FZKA Interner Bericht 421/99, PSF 3327, July 1999**;** "Experimental and Calculational Results of the Experiments QUENCH-02 and QUENCH-03", FZKA 6295, 2000.	
- Data Availability	On-line test results and the formal reports listed above are available, however the Test Data Reports referred to above are of the nature of quick-look reports and may not be freely available. Informal reports are made at the QUENCH Workshops at FZ Karlsruhe in the Autumn of each year, for all tests to date.	
Use of Data	The data are available for a more detailed analysis.	

No. 1.16	INTEGRAL TEST FACILITY	QUENCH
Subject	**Description**	
Correctness of Phenomena	There are various non-prototypic features which must be taken into account in interpretation and analysis of the data, these are given below.	
Overall Evaluation		
- Strengths	The facility provides the most detailed data on quench behaviour of oxidised Zircaloy-clad bundles yet achieved. The comprehensive associated programme of single rod separate-effect quench tests and hydrogen absorption/release experiments aids in test definition and in interpretation of the results. Scaling studies helped to ensure that the test conditions were relevant to the envelope of possible plant transients.	
- Weaknesses	The strong dependence on temperature of the electrical resistance of the tungsten heaters means that the electrical power axial profile becomes highly non-linear during the course of the experiments, due to positive feedback effects, this is a significant non-prototypic feature. Simulation of this effect is important when modelling the tests, since the linear electrical heat rating can vary by up to x3 between the hottest and coldest parts of the rods. The thermophysical properties of he zirconia fuel peelets differ fro those of UO_2 pellets. The argon flow is untypical of reactor conditions. (These non-prototypic effects are however amenable to modelling.). The use of zirconia pellets means that quench behaviour beyond clad melting may be affected since the melts will not be of prototypic composition (no U present, as in the typical U/Zr/O eutectic formed in-reactor). Data acquisition was incomplete in QUENCH-02.	
- Miscellaneous		
Comments	There are plans to extend the series for example by including control materials, ballooning the cladding, using higher system pressures (to the facility limit of ~1.0MPa), and quenching from the top. These extensions would enable further coverage of the range of possible plant conditions, though system pressures expected at the onset of reflood in some plant transients (over 1MPa) still fall outside the current facility limit.	

No. 1.17	INTEGRAL TEST FACILITY	FARO LWR
Subject	**Description**	
Test Facility	FARO (EC-JRC-Ispra, Italy)	
- Operating Period	Beginning end 1991 (test L-06). End mid-1999 (test L-33).	
Objectives	Investigate core melt quenching when slump into water in lower head and cavity and provide qualified experimental data for model improvement and code validation in the field of FCI analysis	
- L-06, L-08, L-14, L-19	Quenching at 5.0 MPa in saturated water, different melt masses and water depths	
- L-11	Influence of metallic zirconium in oxidic melt	
- L-20, L-24, L-27	Influence of lowering the pressure on the quenching process	
- L-28	Core melt quenching in long pour	
- L-29, L-31	Core melt quenching in subcooled water	
- L-33	Steam explosion work output in 3-D configuration	
- L-26S, L-32S	Core melt spreading for advanced core catcher concepts	
Facility Geometry		
- FCI tests	The experimental set-up includes, in a vertical arrangement, an interaction vessel connected to the UO_2-ZrO_2 melting furnace via a release channel and isolated from it during interaction by a high pressure valve. After melting in the FARO furnace (by direct heating), the melt is first delivered to a release vessel in just the time to isolate the furnace from the interaction vessel, and then released into the water. The release vessel, located in the upper head (so-called dome) of the test vessel, can contain Zr wire distributed in the volume. In that case (L-11 test) the superheated oxide melt coming from the furnace induced the melting of the zirconium and the formation of a UO_2-ZrO_2-Zr mixture. The tests are performed in a closed volume.	

No. 1.17	INTEGRAL TEST FACILITY	FARO LWR
Subject	**Description**	
	The test vessel is connected downstream to a condenser via a steam/water separator and exhaust valves. The condenser can condense up to 200 kg of steam at a rate of 24 kg/s. The purpose of this unit is to vent and condense part of the steam produced during the melt quenching should the pressure in the interaction vessel exceed a pre-established value (e.g., 9.3 MPa for the tests performed at 5 MPa). Non-condensable gases (such as the hydrogen produced by oxidation of the melt or the argon possibly initially present in the test vessel) can be stored in the 2.5 m^3 free-board volume of the condenser for further evaluation of the gas composition. The overall height of the facility is10 m and the lateral extension 2 m, plus the venting unit. Two test vessels designed for 10 MPa and 600 K were used, which differed by their diameter (0.71 m for TERMOS and 1.5 m for FAT).	
- **Spreading tests**	The FCI test vessel is substituted by a horizontal box (SARCOFAGO, 1.2x1.2x4 m), which houses the spreading plate.	
Experimental Conditions and parameter range	The melt was released by gravity. In all tests but L-11, 80wt%UO_2 – 20wt%ZrO_2 corium melt was used. In FCI tests up to and including L-27, a melt delivery nozzle of 100 mm was used. The TERMOS vessel was used up to test L-24, then the FAT vessel was used with an internal cylinder reducing the diameter of the water pool to the same as in TERMOS vessel (i.e., 0.71 m). The SARCOFAGO vessel (1.2x1.2.4 m) was used for the spreading tests.	
- **L-06, L-08, L-14, L-19**	The tests were performed basically at the same pressure (~5.MPa) and water temperature (near to saturation). They specifically reproduced TMI-2 type of melt relocation. They mainly differed by the melt mass (18 to 157 kg) and the water depth (typically, 1 and 2 m). There were performed in the TERMOS vessel (in L-06, an internal test section reduced the diameter of the water pool form 0.71 to 0.47 m).	
- **L-11**	6 kg of Zr were added to 145 kg of oxidic melt. Water depth 2 m.	
- **L-20, L-24, L-27**	The tests were performed in nearly saturated water, and 2.0 MPa (L-20, 96 kg of melt) and 0.5 MPa (L-24, L-27). L-20 and L-24 were performed in TERMOS and L-27 in FAT. Tests L-24 and L-27 differed by the mass of melt (177 kg in L-24 and 129 kg in L-27), by the water depth (2 m in L-24 and 1.5 m in L-27) and by the free-board volume (1.26 m^3 in L-24 and 3.52 m^3 in L-27). Water depth was 2 m in tests L-20.	

No. 1.17	INTEGRAL TEST FACILITY	FARO LWR
Subject	**Description**	
- L-28	175 kg of melt. Melt delivery nozzle of 50 mm giving a melt pour duration of 6 s, sufficient to reach steady state conditions. System pressure 0.5 MPa, water at saturation.	
- L-29, L-31	Tests in subcooled water: 0.2 MPa, water at ambient temperature. Melt delivery nozzle of 50mm. 39 kg of melt in L-29 and 92 kg in L-31. Water depth 1.5 m.	
- L-33	Steam explosion test in subcooled water at 0.4 MPa, water at ambient temperature. Trigger applied at the bottom of the water column. Melt mass in water at the time of the trigger ~25 kg. Total melt mass released 100 kg.	
- L-26s	Dry spreading experiment. 160 kg of melt released to a horizontal stainless steel 17° sector through a nozzle of 30 mm in diameter.	
- L-32s	Wet spreading experiment. Same conditions as L-26s with 130 kg of melt and 10 mm water layer on the spreading plate.	
Measurements		
- On-line	The principal quantities measured in the test vessel during corium quenching are pressures and temperatures both in the freeboard volume and in the water, and temperatures in the debris catcher bottom plate. Tungsten ultrasonic temperature sensors are mounted in the release vessel for measuring the melt temperature. About 250 signals are loaded to 6 different recorders of the data acquisition system and recorded at 3 different rates (low, medium, fast). Piezoresistive, 5-kHz frequency response pressure transducers measure the vessel pressurisation. Piezoelectric, 100-kHz frequency response pressure transducers are located at four different elevations in the water for rapid transient records in case of energetic FCI. K-thermocouples are distributed at different axial and radial locations in cover gas and water. K- are imbedded into the bottom plate of the debris catcher for measuring the thermal load on the plate. The level swell is measured by means continuous level-meters based on the time domain reflectrometry method (Ispra patent).	

No. 1.17	INTEGRAL TEST FACILITY	FARO LWR
Subject	**Description**	
	The instrumentation includes also absolute pressure transducers and thermocouples in the separator and in the condenser. A mass spectrometer is connected to the condenser for a qualitative indication of the gas composition. Visualisation of melt entry conditions in water and of melt/water mixing are performed by using high speed video cameras up to 2000 f/s.	
- **Post-test**	Non-destructive examination of the debris bed configuration and topology. Determination of the debris morphology and particle size distribution.Determination of the quantity of hydrogen produced by venting the test section gas inventory into the condenser and applying the partial pressure method.	
- **Data Acquisition**	Acquisition of all measurements is performed with several independent computer systems at different acquisition rates.	
Data Documentation		
- **Overview**	D.Magallon, H.Hohmann, "High Pressure Corium Melt Quenching Tests in FARO", CSNI-FCI Specialist Meeting, Santa Barbara (Ca) USA, January 5-8, 1993; D.Magallon, I.Huhtiniemi, H.Hohmann, ”In-Vessel Loads Resulting from Molten Fuel Coolant/Structure Interactions”, ASME PVP-1995 Conf., Honolulu, HI, July 23-27, 1995, Journal of Pressure Vessel Technology, Vol.303, p.159; Magallon D., Hohmann H, "High pressure Corium Melt Quenching Tests in FARO", Nucl. Eng. Des. 155 (1995), 253-270; D.Magallon, H.Hohmann, ”Experimental Investigation of 150-kg-Scale Corium Melt Quenching in Water", Nucl. Eng. Des. 177 (1997), 321-337; M.Corradini, D.Cho, D.Magallon, S.Basu, "FCI Experiments and Analysis: Contributions to Basic Understanding", OECD/CNSI Specialist Meeting on Fuel Coolant Interactions, JAERI-Tokai, Japan 19-21 May, 1997; D.Magallon, I.Huhtiniemi, H. Hohmann, "Lessons Learnt from FARO/TERMOS Corium Melt Quenching Experiments", Nucl. Eng. Des. 189 (1999), 223-238; D.Magallon, I.Huhtiniemi, "Corium Melt Quenching Tests at Low Pressure and Subcooled Water in FARO", NURETH-9, San Francisco, October 1999; D.Magallon, S.Basu, M.Corradini, ”Implications of FARO and KROTOS experiments for FCI and debris coolability”, OECD Workshop on Ex-Vessel Debris Coolability, FZK, 16-18 November 1999; W.Tromm, D.Magallon, ”Corium Melt Spreading Tests in FARO.” OECD Workshop on Ex-Vessel Debris Coolability, FZK, 16-18 November 1999.	

No. 1.17	INTEGRAL TEST FACILITY	FARO LWR
Subject	**Description**	
- Data Reports	Data Reports:Quick Look Reports: available for all FCI tests. Experimental Data Reports: available for L-06, L-08, L-11, L-14, L-26s, L-28, L-29, L-31, L-32s; being edited for the other tests	
- Evaluation	A. Annunziato, C. Addabbo, "COMETA (Core Melt Thermal-hydraulic Analysis) a Computer Code for Melt Quenching Analysis ", Pisa 1994, June 94; C.Addabbo, A.Annunziato, R.Silverii, D.Magallon, "COMETA Analysis of System Effect in FARO Melt Quenching Tests", ICONE-6 Conference , May 1998; ISP-39 on FARO L-14:A. Annunziato, C. Addabbo, A. Yerkess, R. Silverii, W. Brewka, G. Leva,"FARO Test L-14 on Fuel Coolant Interaction and Quenching: OECD/CSNI International Standard Problem 39", NEA/CSNI/R(97)31, May 98.	
- Data Availability	Data Reports and associated Technical Notes are initially restricted to FARO LWR partners European Union and USA (NRC).. Data are also available in electronic form to partners upon written request. Data are generally summarised in international conferences and/or published in international journals at a variable rate.	
Use of Data	The data are used by FARO LWR partners and other national organisations throughout the world (when disclosed) for FCI modelling improvement, and code validation and verification.	
Special Features	The tests focus on items where insufficient knowledge and data exist in the current data banks: quenching and spreading of large masses of prototypical corium melts in saturated and subcooled water, debris bed formation, high and low pressure scenarios, 3-D configurations close to reactor conditions. These aspects are unique using prototypic corium.	

No. 1.17	INTEGRAL TEST FACILITY	FARO LWR
Subject	**Description**	
Correctness of Phenomena	The quenching tests at high pressure and saturated water are directly relevant to TMI-2 type of accident scenario: melt pool formation in the core with subsequent release in water through a breach in the pool crust and collection on the reactor pressure vessel lower head. Lower pressure tests in saturated conditions cope with present accident management strategies, which include the RPV depressurisation prior to melt relocation in the lower head. Test in subcooled water are relevant to possible melt relocation in a flooded cavity in case of lower head failure. The tests implicitly address the issue of spontaneous steam explosion with corium in 3-D configurations. In one test, the potential for corium melt/water mixtures to be externally triggered and the subsequent mechanical loading structures in a 3-D environment was assessed. The spreading tests are relevant to the testing of advanced core catcher concepts based on the spreading and cooling of the core melt in the reactor cavity.	
Overall Evaluation		
- Strengths	Unique data on FCI involving at experimental level large masses of corium melts in 3-D configurations and prototypical conditions for the melt composition and temperature, system pressure and temperature, water depth.	
- Weaknesses	No direct measurement of some local parameters important for detailed modelling (e.g., component fraction during mixing) and of hydrogen production.	
Comments	A large international effort was devoted to the definition of objectives, test conditions and to the analyses of results through the FARO Experts Group. All FCI codes in the world are being assessed using the FARO data. The early closure of the programme will not allow to confirm some encouraging findings concerning the mitigating role of some reactor features (3-D, venting possibilities) on mechanical dynamic loading of the structures.	

No. 1.18	INTEGRAL TEST FACILITY	KROTOS
Subject	**Description**	
Test Facility	KROTOS (EC-JRC-Ispra, Italy)	
- Operating Period	From 1991 tests with alumina and corium. Prior to 1991 tests with tin (KROTOS pre-test series)	
Objectives		
- General	Investigate all the phases of steam explosion. Determine the conditions for corium melt to generate an energetic steam explosion and provide qualified experimental data for model improvement and code validation in the field of FCI analysis.	
- K-26 - K-30, K-32 - K-36	Steam explosions in narrow 1-D test geometry with alumina melt with and without external trigger.	
- K-37, K-45 - K47, K-52, K-53	Conditions for corium melt to generate an energetic steam explosion and measure its yield.	
- K-38 - K-44, K-49	Reasons for difference between the yields of explosions of alumina and corium melts.	
- K-56 - K-58	Mixing behaviour of corium melt by means of visualisation.	
- K-63	Influence of external trigger.	
Facility Geometry	The crucible containing the melt is released from the furnace and falls by gravity through a ~5.2 m long release tube. Half-way down the tube, a fast isolation valve separates the furnace from the test section below. The crucible strikes a retainer ring at the end of the tube where a conical-shaped spike pierces the bottom of the crucible and penetrates into the melt allowing the melt to pour out through the openings in the puncher. The injection diameter of the melt jet is defined by guiding it through a funnel of high temperature refractory material with an exit diameter of 30 mm. The jet pours into the test section filled with water (up to about 1.3 m). The test section is made of strong stainless steel tube of inner diameter 200 mm and outer diameter 240 mm. The bottom of the test section is closed with a plain closing plate or with plate housing a trigger device.	

No. 1.18	INTEGRAL TEST FACILITY	KROTOS
Subject	**Description**	
	The trigger device consists either of a gas chamber (volume of 29.5 cm^3) which can be charged to a pressure of up to 20 MPa (nitrogen) and is closed by a 0.25 mm thick steel membrane or an explosive charge. The purpose of the trigger device is to produce a well-defined pressure pulse that is capable initiating a steam explosion. The test section is inserted into a pressure vessel is which designed for 4.0 MPa at 493 K. It is a cylindrical vessel of 0.57 m inner diameter and 2.0 m in height (volume: ~0.35 m^3) with a flanged flat upper head plate.	
Experimental Conditions and parameter range	All the tests were performed with 30 mm exit nozzle. Injection speed is determined by the gravity. However, the fall height varied depending on whether a so-called brake disk was used (to temporarily arrest the melt at the nozzle). The average injection speed in most tests was on the order of a few metres per second. All the tests were performed with helium cover gas and with about 1 metre of water.	
- **K-26 - K-30**	Alumina tests (1.5 kg) with near saturated and subcooled water at ambient pressure. With and without external trigger.	
- **K-32 - K36**	Corium tests (3 kg) with near saturated and subcooled water at ambient pressure. With and without an external trigger.	
- **K-37, K-45 - K47, K-52, K-53**	Corium tests (3-5.5 kg) with near saturated and subcooled water at ambient and elevated pressure (up to 0.36 MPa). With and without an external trigger.	
- **K-38 - K-44, K-49, - K-51**	Alumina tests (1.5 kg) with near saturated and subcooled water at ambient and elevated pressure (up to 0.37 MPa). With and without an external trigger. Alumina superheat was varied from 150 K to 750 K.	
- **K-56, K-58**	Corium tests (4.5 kg) with subcooled water at elevated initial pressure of 0.37 MPa. With and without an external trigger. Viewports to gas phase and mixing zone allowed visualisation.	
- **K-57**	Subcooled alumina (1.5 kg) test at ambient pressure with visualisation. External trigger not used.	
- **K-63**	Subcooled corium tests at elevated initial pressure of 0.21 MPa triggered with a different type of external trigger.	

No. 1.18	INTEGRAL TEST FACILITY	KROTOS
Subject	**Description**	
Measurements		
- On-line	The principal quantities measured in the test vessel during the melt/water interaction are pressures and temperatures both in the freeboard volume and in the water, and the water level. A bi-chromatic pyrometer is mounted in the furnace for measuring the temperature of the melt. Piezoresistive, 5-kHz frequency response pressure transducers measure the vessel pressurisation. Piezoelectric, >100-kHz frequency response pressure transducers are located up to seven different elevations in the water for measuring dynamic pressures generated during steam explosion. K-type thermocouples are distributed at different axial and radial locations in the water and gas phase. The level swell is measured by means continuous level-meters based on the time domain reflectrometry method. Visualisations of melt entry conditions in water and of melt/water mixing are performed by using high speed video cameras up to 1000 f/s.	
- Post-test	Determination of the debris morphology and particle size distribution.	
- Data Acquisition	Acquisition of all measurements is performed with several independent computer systems at different acquisition rates (up to 50 kHz).	

No. 1.18	INTEGRAL TEST FACILITY	KROTOS
Subject	**Description**	
Data Documentation		
- Overview	D.Magallon, I.Huhtiniemi, H.Hohmann, ”In-Vessel Loads Resulting from Molten Fuel Coolant/Structure Interactions”, ASME PVP-1995 Conf., Honolulu, HI, July 23-27, 1995, Journal of Pressure Vessel Technology, Vol.303, p.159**;** H.Hohmann, D.Magallon, H.Schins, A.Yerkess, ”FCI Experiments in the Aluminium Oxide/Water System”, Nucl. Eng. Des. 155 (1995), 391-403**;** I.Huhtiniemi, D.Magallon, A.Yerkess, H.Hohmann, B.Shamoun, M.Corradini, ”Test Results and Analysis of Recent KROTOS FCI Experiments”, National Heat Transfer Conference, ASME/AIChE/ANS, Houston, Aug. 1996**;** I.Huhtiniemi, H.Hohmann, D.Magallon, ”FCI Experiments in the Corium/Water System”, Nucl. Eng. Des. 177 (1997), 339-349**;** M.Corradini, D.Cho, D.Magallon, S.Basu, "FCI Experiments and Analysis: Contributions to Basic Understanding", OECD/CNSI Specialist Meeting on Fuel Coolant Interactions, JAERI-Tokai, Japan 19-21 May, 1997**;** I.Huhtiniemi, D.Magallon, H. Hohmann, "Results of Recent KROTOS FCI Tests: Alumina versus Corium Melts", Nucl. Eng. Des. 189 (1999), 379-389**;** I.Huhtiniemi, D.Magallon, ”Insight into Steam Explosions with Corium Melts in KROTOS”, NURETH-9, San Francisco, October 1999**;** D.Magallon, S.Basu, M.Corradini, ”Implications of FARO and KROTOS Experiments for FCI and Debris Coolability”, OECD Workshop on Ex-Vessel Debris Coolability, FZK, 16-18 November 1999.	
- Data Reports	There are data Reports for all KROTOS FCI experiments.	
- Data Availability	Data Reports and associated Technical Notes are initially restricted to FARO/KROTOS LWR partners European Union and USA (NRC). Data are also available in electronic form to partners upon written request. Data are generally summarised in international conferences and/or published in international journals at a variable rate.	
Use of Data	The data are used by FARO/KROTOS LWR partners and other national organisations throughout the world (when disclosed) for FCI modelling improvement, and code validation and verification.	
Special Features	Tests provide interaction data with high temperature prototypical corium melt. Facility is well-suited for testing melt/water interactions with a variety of different melt compositions at small scale. The test geometry is well-suited for model validation and determination of main phenomena during pre-mixing and steam explosion.	

No. 1.18	INTEGRAL TEST FACILITY	KROTOS
Subject	**Description**	
Correctness of Phenomena	The test condition range is within expected ex-vessel the thermohydraulic conditions. The mass scaling cannot be addressed in KROTOS tests alone. All the relevant phenomena (premixing, triggering, propagation, expansion, structural loading) involved in steam explosion are simulated experimentally in small-scale for modelling purposes. The tests can be used to determine the dominant integral phenomena with different melt types and conditions. However, the test section geometry is believed to influence the magnitude of the energetics and therefore particular care has to be taken to apply KROTOS results directly to reactor case.	
Overall Evaluation		
- Strengths	Unique data on steam explosions with prototypical melt under well-defined conditions.	
- Weaknesses	Melt masses limited thereby KROTOS tests alone are not suited to address mass scaling. No direct measurement of some local parameters important for detailed modelling (e.g., component fraction during mixing) and of hydrogen production.	
Comments	Worldwide all steam explosion codes/models are being assessed using the KROTOS data. KROTOS tests continue to provide data to help to close the steam explosion issue.	

No. 2.1	SEPARATE EFFECTS TEST FACILITIES	Clad Ballooning

Subject	Descrtipion
Test Facilities	REBEKA - FZ Karlsruhe, Germany PHEBUS - CEA Cadarache, France NRU MT (Materials Test) - AECL Chalk River, Canada MRBT (Multi Rod Burst Test) - Oak Ridge National Laboratories (ORNL), USA JAERI bundle burst experiments - JAERI, Japan PBF/LOC (Power Burst Facility/Loss of Coolant) - Idaho National Engineering Laboratories (INEL), USA AEKI bundle burst experiments - AEKI, Hungary
Objectives	The general objectives of ballooning experiments are to measure the amount of cladding strain and coolant channel blockage which occurs when cladding deforms at high temperatures (over 1000K) under loss-of-coolant accident (LOCA) conditions.
Facility Geometry	In a typical test section, a bundle of pressurised fuel rods (typically 25 to 49 in a large bundle) is positioned inside a shroud which provides mechanical restraint, and which may be heated to minimise the radial temperature differences. Heated lengths vary from 0.8m to 3.9m (full length). A guard ring of unpressurised rods may serve a similar purpose. In nuclear heated tests, the rods are filled with UO_2 fuel pellets and the assembly is loaded into a reactor to be driven by fission power. In an electrically heated test, the rods contain internal resistance heaters which may be fabricated to impose an axial power profile typical of that experienced in-reactor.
Experimental Conditions	In electrically heated tests, the bundle is heated in flowing steam at decay heat powers (which give heat-up rates of typically 7K/s), until ballooning and clad rupture occurs. There may be a simulated refill/reflood phase before or after the clad deformation. A similar procedure may be followed in-reactor, alternatively a full LOCA transient may be simulated, with blowdown, refill and reflood phases included. If there is no reflood phase, the power is switched off at the end of the transient phase and the bundle is allowed to cool to room temperature.
Parameter Range	REBEKA tests 5, 6 and 7: 49 rods, electrically heated over length 3.9m, internal/system pressures 6.00/0.45MPa, initial heatup 7K/s, burst temperatures 1048-1073, 1038-1063 and 1028-1063K, burst strain ranges (mean) 39-88(49), 32-64(42) and 42-87(55)%. PHEBUS tests 215P, 215R, 216, 218 and 219: 25 rods, nuclear (fission) heated over length 0.8m, internal pressures 4.00, 4.00, 3.00, 3.35, 3.00 MPa with variable system pressure (LOCA simulation), initial heatup 8K/s, burst temperatures 1073-1133, 1073-1133, 1173, 1123 and 1153K, burst strain ranges (mean) 20-54(38), 20-50(38), 20-30, 14-27(20) and 19-46(28)%.

No. 2.1	SEPARATE EFFECTS TEST FACILITIES	Clad Ballooning
Subject	**Descrtipion**	
	NRU MT tests 3 and 4: 32 rods (20 unpressurised in guard ring), electrically heated over length 3.66m, internal/system pressures 3.80 and 4.62/0.2MPa, initial heatup 7K/s, burst temperatures 1049-1088 and 1033-1200K, burst strain ranges (mean) 38-94(55) and 53-99(72)%. MRBT tests B3, B5 and B6: 16, 64 and 64 rods, electrically heated over length 0.915m, internal/system pressures 11.6, 11.6 and 3.20/0.2MPa, initial heatup 9.5, 9.8 and 3.5K/s, burst temperatures 1020-1052, 1033-1057 and 1192-1210K, burst strain ranges 42-77, 32-95 and 21-56%. JAERI tests - 20 bundles, of which 13, 17 and 24: 49 rods (4 unpressurised in test 24), electrically heated over length 0.85m, internal/system pressure 4.9/0.1MPa to give rod burst in the high α-phase of Zircaloy, initial heatup 0.7, 7.6 and 7.0K/s, burst temperatures 1020-1052, 1033-1057 and 1192-1210K burst strain ~60%. PBF/LOC tests 3, 5 and 6: 4 rods (some irradiated), nuclear (fission) heated over length 0.91m, internal pressures 2.4-4.9, 2.4-4.9 and 2.4-4.8 MPa, initial heatup 4-20, 0-100 and 0-100K/s, burst temperatures 1110-1300, 1160-1350 and 1066-1098K, burst strain ranges 20-42, 19-48 and 31-74%. AEKI tests 6 and 8: 7 rods, in electrically heated furnace, length 0.15m, internal/system pressures (at burst) 0.1/5.5MPa and 0.1/2.0MPa, initial heatup 1.2K/s and 0.6 K/s, burst temperatures 1143-1173 and 1073-1173 K, burst strain ranges (mean) 18-31(22) and 24-31(27) %.	
Measurements		
- On-line	On-line recordings of temperatures of the cladding, fuel (or electrical simulator) and fluid using thermocouples. Other on-line recordings may include system pressure, internal rod pressures and coolant flows.	
- Post-test	Post-test destructive examinations determine axial profiles of cladding strains and flow channel blockage.	
Data Documentation		
- Overview	Parsons P D, Hindle E D and Mann C A, "The deformation, oxidation and embrittlement of PWR fuel cladding in a Loss-of-Coolant Accident", ND-R-1351(S), CSNI Report 129, September 1986. **;** Karwat H, "International Standard Problem 14: Behaviour of a fuel bundle simulator during a specified heatup and flooding period (REBEKA experiment)", CSNI Report 98, February 1985.	

No. 2.1	SEPARATE EFFECTS TEST FACILITIES	Clad Ballooning

Subject	Descrtipion
- **Data Reports**	REBEKA: Wiehr K, "REBEKA-Bündelversuche Untersuchungen zur Wechselwirkung zwischen aufblähenden Zircaloyhüllen und einsetzender Kernnotkühlung : Abschlußbericht, KfK 4407, May 1988**;** Harten U and Wiehr K, "Datenbericht REBEKA-5", KfK 3842, March 1985**;** Wiehr K and Harten U, "Datenbericht REBEKA-6", KfK 3986, March 1986**;** Wiehr K and Harten U, "Datenbericht REBEKA-7", KfK 4145, February 1987 PHEBUS: Réocreux M and Scott de Martinville E F, "A study of fuel behaviour in PWR design basis accident: an analysis of results from the PHEBUS and EDGAR experiments", Nucl. Eng. & Design **124**, 363-378, 1990**;** Scott de Martinville E F and Gonnier C R, "Thermomechanics of a nuclear fuel bundle submitted to a L.B. LOCA evaluation transient Lessons drawn from the Phebus Loca Program", Volume C of Trans. 9th Int. Conf. on Structural Materials in Reactor Technology, Lausanne, August 1987**;** Adroguer B, Hueber C and Trotabas M, "Behaviour of PWR fuel in LOCA Conditions, PHEBUS test 215P", OECD/NEA/CSNI Specialists meeting on water reactor fuel safety and fission product release in off-normal and accident conditions, Risø, Denmark, Summary Report IWGFPT/16, May 1983**;** Scott de Martinville E and Pignard M, "International Standard Problem 19: Behaviour of a fuel rod bundle simulator during a large break LOCA transient with a two peaks temperature history (PHEBUS experiment)", CSNI Report 131, 1987. NRU MT: Mohr C L et al., "LOCA simulation in the National Research Universal Reactor Program. Data report for the third materials experiment (MT3), NUREG/CR-2528, PNL-4916, April 1983**;** Rausch W N, "LOCA simulation in the National Research Universal Reactor Program. Postirradiation examination results for the third materials experiment (MT3), NUREG/CR-3350, PNL-4933, April 1984**;** Wilson C L et al., "LOCA simulation in the NRU program: data report MT-4", NUREG/CR-3272, PNL 4669, July 1983. ORNL MRBT: Chapman R H et al., "Multi rod burst test program: Bundle B-3 test data", ORNL/NUREG/TM-360, January 1980**;** Longest A W et al., "Experiment data report for multirod burst test (MRBT) bundle B-5", NUREG/CR-3459 (ORNL/TM-8889), August 1984**;** Chapman R H et al., "Experiment data report for multirod burst test (MRBT) bundle B-6", NUREG/CR-3460 (ORNL/TM-8890), July 1984. JAERI: Kawasaki S et al., "Effect of non-heated rods on the ballooning behaviour in a fuel assembly under loss-of-cooling conditions", ANS/ENS Topical Meeting on Reactor Safety aspects of Fuel Behaviour, Sun Valley, Idaho, USA, August 1981**;** Kawasaki et al., "Multi-rod burst tests under loss-of-coolant conditions", OECD/NEA/CSNI Specialists meeting on water reactor fuel safety and fission product release in off-normal and accident conditions, Risø, Denmark, Summary Report IWGFPT/16, May 1983**;** Kawasaki S et al., "Effect of burst temperature on coolant channel restriction in multirods burst tests", J. Nucl. Science and Technology **20(3)**, pp.246-253, March 1983.

No. 2.1	SEPARATE EFFECTS TEST FACILITIES	Clad Ballooning
Subject	**Descrtipion**	
- Evaluation	PBF LOC: Broughton J M et al., "PBF LOCA test series LOC-3 and LOC-5 fuel behaviour report", NUREG/CR-2073, June 1981; Broughton J M et al., "PBF LOCA test LOC-6 fuel behaviour report", NUREG/CR-3184, April 1983. AEKI: Windberg P, Nagy I, Hózer Z, Horváth M,"Ballooning Experiments with VVER Bundle", Nucl. Energy in Central Europe, 11-14 September 2000, Bled, Slovenia, Proceedings (to be published) Nuclear/electrical comparison: Healey T et al., "Ballooning response of nuclear and electrically heated PWR fuel rods tested in the Halden reactor and under laboratory simulation conditions", Proc. BNES conference on nuclear fuel performance, Stratford-on-Avon, UK, British Nuclear Energy Society, London, March 1985. Effect of oxidation at high temperatures: Hunt C E L et al., "The effect of steam oxidation on the strain of fuel sheathing at high temperatures", AECL-5559, August 1976; Hindle E D and Mowat J A S, "The effect of oxygen uptake on the deformation and rupture of SGHWR fuel cladding", UKAEA TRG-2899(S), August 1976; Hunt C E L, "The growth of necks in fuel sheaths during high temperature transients in steam", AECL-6783, February 1980; Sagat S et al., "Deformation and failure of Zircaloy fuel sheaths under LOCA conditions", 6th Int. Conf. on Zirconium in the Nuclear Industry, Vancouver, Canada, ASTM STP-824, October 1982.	
- Data Availability	The above reports are available. On-line data may be available on demand to the owning organisations.	
Use of Data	As above.	
Correctness of Penomena	The tests above are chosen to give a representative range of data from large bundle experiments, both electrically and nuclear heated. Bundle tests are preferable to single rod tests since they reproduce rod-to-rod mechanical interactions giving subchannel geometries of prototypic shape, and in reflood tests such as REBEKA-6 give more prototypic thermal hydraulic conditions. The IFA-54X series in the Halden reactor (reference above) showed differences in the burst strains experienced in nuclear and electrical tests (nuclear heated tests gave slightly larger strains than electrically heated tests under otherwise the same conditions). This was explained mechanistically by differences in the heat source/cladding eccentricity leading to different azimuthal temperature gradients on the cladding. Account can be taken of this in design basis calculations; in severe accident situations where ballooning is treated as a separate effect the difference is probably small compared with other uncertainties.	

No. 2.1	SEPARATE EFFECTS TEST FACILITIES	Clad Ballooning

Subject	Descrtipion
Overall Evaluation	
- Strengths	REBEKA**:** The series provides well-qualified large bundle data including the effect of different reflood methods (compares cold leg and cold leg + hot leg reflooding). Detailed test reports available. PHEBUS**:** In-reactor data with two-peak LOCA transients simulated by suitably varying the loop conditions. NRU**:** MT3 provides data for ballooning under 2-phase flow conditions (as in the reflood phase of a LOCA); MT4 provides similar data under single phase (steam) conditions, in-reactor. Detailed test reports available. MRBT**:** Effect of bundle size studied - 8*8 is the largest bundle tested in any facility reviewed. B6 test extends database into the Zircaloy phase change region where lower strains are found. Detailed test reports available. JAERI**:** Extensive series of large bundle tests. PBF LOC**:** Both unirradiated and irradiated fuel used. Detailed test reports available. AEKI**:** hexagonal arrangement of rods, VVER material
- Weaknesses	PHEBUS**:** Some uncertainties in thermal hydraulic conditions, e.g. coolant enthalpy. Openly available detailed test reports not found (except for test 218 - ISP-19). MRBT**:** Some problems with non-uniform steam flow leading to untypical cross-bundle temperature differences. JAERI**:** Few reports of the data are found in the literature in English, mostly in Japanese. PBF/LOC**:** Small number of rods. AEKI**:** small number of rods, short length
- Miscellaneous	The multi-rod experiments reviewed here reflect the conditions likely to be found in PWR design basis accidents. In some severe accidents ballooning may occur at higher temperatures (over ~1100K) where increasing oxidation (if there is sufficient steam availability) reduces the rate of deformation and the burst strains achieved. The net effect can be severely reduced coolant channel blockage. These conditions are not addressed in the PWR bundle database; recourse must be made to single rod tests such as those carried out at CRNL (references above) for suitable data (which are relevant to the design basis in reactor types such as CANDU and SGHWR). Since in general the strains found are not sufficient to cause rod-to-rod contact, there is less disadvantage in using single rod data than there would be at lower temperatures.
Comments	REBEKA-6 (electrically heated) was selected as CSNI ISP-14, and PHEBUS 218 was selected for ISP-19.

No. 2.2.1	SEPARATE EFFECTS TEST FACILITIES	Material Oxidation

Subject	Descrtipion
Test Facilities	Zircaloy/steam Argonne National Laboratory (ANL), USA Atomic Energy of Canada Limited (AECL), Canada Oak Ridge National Laboratories (ORNL), USA Kernforschungszentrum Karlsruhe (KfK), Germany Battelle Memorial Institute (BMI)/Pacific Northwest Laboratories (PNL), USA AEA Technology/Springfields Nuclear Power Development Laboratories (SNPDL), UK AEA Technology/Risley Nuclear Laboratories (RNL), UK Japanese Atomic Energy Research Institute (JAERI), Japan. KFKI Atomic Energy Research Institute (AEKI), Hungary. Stainless steel/steam General Electric (GE)/Ohio, USA Argonne National Laboratory (ANL), USA Boron carbide/steam Union Carbide (UC), USA Battelle, Pacific NW Laboratories (BMI/PNWL), USA Sandia National Laboratories (SNL), USA Nordic Liaison Committee for Atomic Energy (NKA), Sweden JAERI, Japan STUK/VTT, Finland
Objectives	The general objectives of metal oxidation experiments are to measure the reaction rates of the metals over a range of temperatures and to quantify them, usually in the form of correlations (which are usually parabolic with time; for the Zircaloy/steam reaction this changes to cubic below about 1250K). Breakaway (linear) oxidation is observed for Zircaloy at long times, e.g. over 30min. at 1200K. The aims of the boron carbide oxidation experiments are similar, but the oxidation kinetics are more complex and a simple description in mechanistically-based terms is not at present possible.

No. 2.2.1	SEPARATE EFFECTS TEST FACILITIES	Material Oxidation

Subject	Descrtipion
Facility Geometry	For Zircaloy, electrically-heated tube specimens are generally used, over which superheated steam is passed. For other materials, the specimen geometry is more varied Zircaloy/steam ANL: zirconium and Zry-3 wire, capacitor discharge heating in water. AECL: Zry-2 and Zry-4 tube, induction furnace. ORNL: Zry-4 tube, infra-red furnace. FZKA: Zry-4 tube, resistance furnace. PNL: Zry-4 disc, laser heated. SNPDL: Zry-4 tube, resistance heated. RNL: Zry-4 tube, resistance heated. JAERI: Zry-4 tube, resistance furnace and infra-red furnace. AEKI: Zr1%Nb tube, resistance furnace Stainless steel/steam GE: SS 304L cylinder, resistance furnace. ANL: fuel rod clad in SS 304, resistance furnace. Boron carbide /steam UC: 0.5g B_4C powder 1mm deep on a platinum disk, ϕ=25mm, B_4C surface area 0.44m^2/g, continuous weight measurement by thermogravimetric balance, electric globar furnace, specimen in a quartz tube BMI/PNWL: borated graphite (5wt% B), 7x13x3mm parellipipeds, tube furnace, continuous weight measurement SNL: thin B_4C coupons 38x1.5x7mm, and particle bed with particle ϕ=0.8-3.0mm, reaction tube, offgas analysis NKA: solid pieces of B_4C, 3x11x15mm, irregular surface of ~11cm^2, placed on stainless steel slabs JAERI: B_4C and B_4C+graphite pellets, ϕxh=10x10mm, B content 30, 40, 50% and pure B_4C (78%), tubular furnace, offgas analysis STUK/VTT: electric heating (1) 1g B_4C powder; (2) prototypic B_4C pellets from EdF, ~1g, ϕxh=7.5x13.8mm
Experimental Conditions	The specimen is heated rapidly to the test temperature, allowed to react for the desired period, and allowed to cool. The highly exothermic nature of the Zircaloy/steam reaction requires a high degree of fast-acting temperature control to keep the test conditions steady.

No. 2.2.1	SEPARATE EFFECTS TEST FACILITIES	Material Oxidation

Subject	Descrtipion
Parameter Range	Zircaloy/steam ANL: system pressure 0.1MPa, temperature 1373-2125K. AECL: system pressure 0.1MPa, temperature 1323-2123K, reaction times to 7100s. ORNL (1): system pressure 0.1MPa, temperature 1173-1773K, reaction times 8-2089s. ORNL (2): system pressure 3.45-10.34MPa, temperature 1173-1373K, reaction times 35-2711s. FZKA: system pressure 0.1MPa, temperature 873-1873K, reaction times 120-90000s. PNL: system pressure 0.1MPa, temperature 1573-2673K, reaction times not defined. SNPDL: system pressure 0.1MPa, temperature 873-1573K, reaction times 60-8000s, different Zry-4. RNL: system pressure 0.1-18.6MPa, temperature 1023-1273K, reaction times 240-2500s. JAERI: system pressure 0.1MPa, temperature 1273-1763K, reaction times 120-14400s. AEKI: system pressure 0.1MPa, temperature 1173-1473K, reaction times 100-10000s Stainless steel/steam GE: system pressure 0.1MPa, temperature 1273-1648K, reaction times 240-7200s. ANL: system pressure 0.1-1.1MPa, temperature 1773-1873K, reaction times 600-10800s, variation in steam flowrate. Boron carbide /steam UC: system pressure 0.1MPa, temperature 470-1020K, steam/argon and air/argon mixtures, reaction times to 10h BMI/PNWL: system pressure 0.1MPa, temperature 1100-1200K, helium/steam mixture with 5000-30000 vpm (volume parts per million) steam, reaction time to 150min SNL: system pressure 0.1MPa, temperature 1270K, 620 torr steam pressure, reaction time to 390min NKA: low pressure, temperature 1097-1328K, water vapour pressure 3.19-14.5mbar, reaction times typically 3-5hr JAERI: system pressure 0.1MPa, temperatures 823, 923, 1023, 1123 and 1273K, He with 0.65% water vapour, reaction times to 9hr STUK/VTT: system pressure 0.1MPa; (1) temperature 1073K, steam, time ~ 3h; (2) temperature 1273K, Ar/steam and 50%steam/50%hydrogen, time ~1hr
Measurements **- On-line**	The specimen temperatures are measured on-line, sometimes the hydrogen production is measured also (for metals) and offgas composition (for boron carbide).

No. 2.2.1	SEPARATE EFFECTS TEST FACILITIES	Material Oxidation
Subject	**Descrtipion**	
- Post-test	For metals, post-test destructive examinations determine the reacted layer thicknesses (oxide and oxygen-stabilised alpha-zirconium layers for Zircaloy) and weight gains. For boron carbide, weight loss/gain.	
Data Documentation		
- Overview	General (metals)**:** Parsons P D, Hindle E D and Mann C A, "The Deformation, Oxidation and Embrittlement of PWR Fuel Cladding in a Loss-of-Coolant Accident", ND-R-1351(S), CSNI Report 129, September 1986. General (B_4C)**:** Belovsky L, "Heat Release from B_4C Oxidation in Steam and Air'", Proceedings IAEA- TCM, Dimitrovgrad, Russia, October 1995; Mason P K, "Preliminary Assessment of Boron Carbide Control Rod Release and Consequences for Fission Products ", AEA Technology/IPSN Cadarache unpublished work, March 1999.	
- Data Reports	<u>Zircaloy/steam</u> ANL**:** Baker L and Just L C, "Studies of Metal-Water Reactions at High Temperatures - III - Experimental and Theoretical Studies of the Zirconium-Water Reaction", ANL-6548, May 1962; AECL**:** Urbanic V F and Heidrick T R, "High Temperature Oxidation of Zircaloy-2 and Zircaloy-4 in Steam", J. Nucl. Mat. **75(2)**, 251-261, August 1978; ORNL**:** Cathcart J V et al., "Zirconium Metal-Water Oxidation Kinetics IV**:** Reaction Rate Studies", ORNL/NUREG-17, August 1977**;** Pawel R E, "Zirconium Metal-Water Oxidation Kinetics V: Oxidation of Zircaloy in High Pressure Steam", ORNL/NUREG-31, November 1977; FZKA**:** Liestikow S, Schanz G and v Berg H, "Comprehensive Presentation of Extended Zircaloy-4 Steam Oxidation Results (600-1600°C)", OECD/NEA/CSNI Specialists Meeting on Water Reactor Fuel Safety and Fission Product Release in Off-Normal and Accident Conditions, Risø, Denmark, Summary Report IWGFPT/16, May 1983**;** Liestikow S, Schanz G and Berg H V, "Kinetics and Morphology of Isothermal Steam Oxidation of Zircaloy-4 at 700-1300°C", KfK 3587, March 1978**;** Aly A E, "Oxidation of Zircaloy-4 Tubing in Steam at 1350 to 1600°C", KfK 3358, May 1982; PNL**:** Prater J T and Courtright E L, "High-temperature Oxidation of Zircaloy-4 in Steam and Steam-Hydrogen Environments", NUREG/CR-4476, PNL-5558, February 1986. SNPDL**:** Haste T J, Harrison W R and Hindle E D, "Zircaloy Oxidation Kinetics in the Temperature Range 700-1300°C", IAEA Technical Committee Meeting on Water Reactor Fuel Element Modelling in Steady-State, Transient and Accident Conditions, Preston, UK, IAEA-TC-657/4.7, September 1988.	

No. 2.2.1	SEPARATE EFFECTS TEST FACILITIES	Material Oxidation

Subject	Descrtipion
	RNL**:** Bramwell I L, Haste T J, Worswick D A and Parsons P D, "An Experimental Investigation into the Oxidation of Zircaloy-4 at Elevated Pressures in the Temperature Range 750-1000°C", AEA RS 5438, Presented at the 10th Int. Symposium on Zirconium in the Nuclear Industry, Baltimore, June 1993. JAERI**:** Uetsuka H and Otomo T, "High Temperature Oxidation of Zircaloy-4 in Diluted Steam", J. of Nucl. Science and Technology, **26(2)**, pp240-248, February 1989**;** Uetsuka H, Otomo T and Kawasaki S, "Zircaloy-4 Oxidation Behaviour in Steam-Argon Mixtures from 1000 to 1500°C", IAEA/NEA Int. Symp. on Severe Accidents in Nuclear Power Plants, Sorrento, 21-25 March 1988; Suzuki M et al., "Zircaloy-Steam Reaction and Embrittlement of the Oxidised Zircaloy Tube under Postulated Loss of Coolant Accident Conditions", JAERI-M 6879, January 1977. AEKI**:** Frecska J, Konczos G, Maróti L, Matus L: ”Oxidation and Hydriding of Zr1%Nb Alloys by Steam”, KFKI-1995-17/G. Stainless steel/steam GE**:** Bittel J T, Sjodahl L H and White J F, "Oxidation of 304L Stainless Steel by Steam and Air", Corrosion **25(1)**, 7-14, January 1969**;** Brassfield et al., "Recommended Property and Reaction Kinetic Data for Use in Evaluating a Light-Water-Cooled Reactor Loss-of Coolant Accident involving Zircaloy-4 or 304 SS Clad UO_2", GEMP 482, 1968. ANL**:** Hesson J C et al., "Laboratory Simulation of Cladding-Steam Reactions following Loss-of-Coolant Accident in Water-Cooled Reactors", ANL-7609, 1970. Boron carbide/steam UC**:** Litz L M and Mercuri R A, "Oxidation of Boron Carbide by Air, Water and Air-Water Mixtures at Elevated Temperatures", J. Electrochem. .Soc. **110(8)** (1963), 921-925 BMI/PNWL**:** Woodley R E, 'The Reaction of Boronated Graphite with Water Vapour", Carbon, **7**(1969), 609-613 SNL:. Elrick R M, Sallach R A, Ouellette A L and Douglas S C, "Boron Carbide-Steam Reactions with Caesium Hydroxide and Cesium Iodide at 1270 K in an Inconel 600 System", NUREG/CR-4963, 1987 NKA**:** Alenljung R, Johansson L G, Lindquist O, Hammar L, Hautojarvi A, Jokiniemi J, Liljenzin J-O, Omtvedt J P, Raunemaa T, Koistinen K, Pasanen P and. Steiner Jensen U, 'The Influence of Chemistry on Melt Core Accidents**:** Final Report of the NKA Project ATKI-150", Sept. 1990 JAERI**:** Fujii K, Nomura S, Imai H and Shindo M, "Oxidation Behaviour of Boronated Graphite in Helium, containing Water Vapour", J. Nucl. Mat. **187**(1992), 32-38

No. 2.2.1	SEPARATE EFFECTS TEST FACILITIES	Material Oxidation
Subject	**Descrtipion**	
- Evaluation	STUK/VTT: Auvinen A and Jokiniemi J K, "Organic Iodide: B_4C-Steam Reaction Studies. Interim Report", VTT Energia Report No. 1/98, Jan. 1998, and private communications to Mason PK. The work was performed in the framework of the EC 4th Framework shared cost action project "Organic Iodine Chemistry (OIC)" which was summarised in the symposium "FISA-99 – EU Research in Reactor Safety", Luxembourg, 29 November – 1 December 1999, proceedings to be published as Report EUR 19532 EN. Hohorst J K (ed.), "MATPRO, A Library of Materials Properties for Light-Water-Reactor Accident Analysis", Volume 4 of NUREG/CR-6150, November 1993 and Revision 1, October 1997, reviews both Zircaloy and SS oxidation data and recommends correlations (the Zry/steam correlation combines those of ORNL (Cathcart/Pawel) and AECL (Urbanic/Heidrick)).	
- Data Availability	The above reports are available.	
Use of Data	As above.	
Special Features	-	
Correctness of Phenomena	The metal oxidation experiments correctly represent the respective oxidation reactions. The situation regarding boron carbide oxidation is less clear; several reactions have been identified but their relative importance under given severe accident conditions has not been firmly established.	
Overall Evaluation		
- Strengths	Zircaloy/steam FZKA: Wide temperature and time ranges, covering transitions amongst parabolic, cubic and linear regimes. ORNL: Effect of system pressure studied. PNL: Measurements extend to highest temperature studied (2673K). RNL: Effect of system pressure studied to beyond normal RCS pressures. JAERI: Effect of steam starvation studied. AEKI: Hydrogen up-take measurements, use of VVER cladding	
- Weaknesses	No studies of the oxidation of liquefied Zircaloy, nor of cladding/fuel mixtures (U/Zr/O), relevant to oxidation of relocating and relocated core materials, are reported.	

No. 2.2.1	SEPARATE EFFECTS TEST FACILITIES	Material Oxidation
Subject	**Descrtipion**	
- Miscellaneous	The ANL correlation (Baker/Just) has been widely used in licensing work. A similar Russian conservative correlation is used for Zr1%Nb cladding.	
Comments	The chief use of the metal oxidation work reported here is in the development of models for mechanistic melt progression codes, currently mainly using correlations derived from these steady-state measurements. The MATPRO evaluation is widely used; the SNPDL correlation extends this to lower temperatures. Zircaloy oxidation increases with system pressure, but no models for this effect are reported in the literature. Validation of these models is best carried out independently of the basic measurements, using data from the integral tests (which are transient in nature). Currently, the MATPRO correlation is widely used in severe accident modelling codes, giving acceptable agreement with the integral data, however sometimes the PNL correlation (Prater/Courtright) is reported to give better agreement. Concerning boron carbide oxidation, it is premature to recommend specific correlations as the reactions are not sufficiently well quantified. Further separate-effects tests under typical severe accident conditions and detailed evaluation of the results thereof appear necessary.	

No. 2.2.2	SEPARATE EFFECTS TEST FACILITIES	Structural Material Interactions

Subject	Descrtipion
Test Facilities	FZ Karlsruhe (FZKA) material interaction experiments, Germany JAERI material interaction experiments - Japan AEKI material interaction experiments - Hungary
Objectives	The general objectives of material interaction experiments are to measure the reaction rates of the metals over a range of temperatures and to quantify them, usually in the form of Arrhenius correlations (which are usually parabolic with time). In the experiments reviewed, the effect of oxide films between the components in delaying the onset of the main material interactions is also investigated.
Facility Geometry	Generally, a crucible is formed of the higher melting-point component, containing the sample of the other component. The compatibility specimens were contained in an argon-filled quartz ampoule during heat treatment (annealing) in a muffle or tube furnace. Protection against oxidation. The Zircaloy used in the reviewed experiments is always Zircaloy-4. FZKA**:** electric heating in Ar atmosphere; AIC/SS, SS (AISI 316) crucible, ϕ= 6/11mm, 1.8g AIC; AIC/Zry, Zry crucible, ϕ= 6/11mm, 1.8g AIC; SS/Zry, Zry crucible, ϕ= 6/11mm, 1.5g SS; Incl/Zry, Zry crucible, ϕ= 6/11mm, 1.5g Incl-718; B_4C/SS, SS crucible, ϕ= 6/11mm, 0.5g B_4C (powder, 180-250μm); B_4C/Zry, Zry crucible, ϕ= 6/11mm, 0.5g B_4C (powder, 180-250μm). JAERI**:** electric heating in Ar atmosphere; Ag/Zry, quartz crucible, ϕ= 10mm, Zry, ϕ= 12,h=5mm, 3g Ag; AIC/Zry, quartz crucible, ϕ= 12mm, Zry, ϕ= 10,h=5mm, 3g AIC; SS/Zry, Zry crucible, ϕ= 8/16mm, SS-304, ϕ= 8,h=5mm; Incl/Zry, Zry crucible, ϕ= 8.5/16,h=10mm, Incl-718, ϕ= 8.5,h=5mm; B_4C/SS, SS crucible, ϕ= 10/16mm, B_4C pellet ϕ= 9.5,h=5mm or 0.5g B_4C powder; B_4C/Zry, B_4C powder and pellets; B_4C+SS/Zry, 80wt% SS 304+20wt% B_4C. AEKI**:** electric heating in Ar atmosphere; SS/Zr1%Nb, quartz tube,Zr1%Nb ϕ= 9mm h=4mm, SS ϕ= 9mm h=4mm; B_4C/SS, SS crucible, ϕ= 7.6/9.1mm, B_4C pellet ϕ= 7.6mm h=10mm; B_4C/Zr1%Nb, Zr1%Nb crucible, ϕ= 7.6/9.1mm, B_4C pellet ϕ= 7.6mm h=10mm.
Experimental Conditions	The specimen is heated to the test temperature, allowed to react for the desired period, and allowed to cool.

No. 2.2.2	SEPARATE EFFECTS TEST FACILITIES	Structural Material Interactions
Subject	**Descrtipion**	
Parameter Range	FZKA**:** system pressure 0.1MPa; AIC/SS, temperature 1673-1723K, reaction time 1200s; AIC/Zry, temperature 1273-1473K, reaction time 60-1800s, Zry preoxidation 0,10μm oxide; SS/Zry, temperature (1) 1273-1473K and (2) 1273-1673K, reaction time (1) 60-1800s and (2) 60-18000s, Zry preoxidation (1) 0,10-100μm and (2) 0,10,20,50μm oxide; Incl/Zry, temperature 1273-1473K, reaction time 60-18000s, Zry preoxidation 0,20,45μm oxide; B_4C/SS, temperature 1073-1473K, reaction time 6000-10^6s; B_4C/Zry, temperature 1073-1873K, reaction time 300-10^6s. JAERI**:** system pressure 0.1MPa; Ag/Zry, temperature 1273-1473K, reaction time 30-7200s; AIC/Zry, temperature 1273-1473K, reaction time 30-7200s; SS/Zry, temperature 1273-1573K, reaction time 30-28800s, Zry preoxidation 0,20,50μm oxide; Incl-718/Zry, temperature 1223-1523K, reaction time 30-28800s, Zry preoxidation 0,20,50μm oxide; B_4C/SS, temperature 1073-1623K, reaction time 30-3.6x10^6s; B_4C/Zry, temperature 1173-1953K; B_4C+SS/Zry, temperature 1473-1703K. AEKI**:** system pressure 0.1MPa (vacuum in SS/Zr1%Nb tests) SS/Zr1%Nb, temperature 1333-1453K, reaction time 30-3000s, Zr1%Nb preoxidation 0,3,9,30μm oxide; B_4C/SS, temperature 1073-1473K, reaction time 1800-90000s; B_4C/Zr1%Nb, temperature 1473-1873K, reaction time 300-90000s.	
Measurements **- On-line**	The specimen temperatures are measured on-line.	
- Post-test	Post-test destructive examinations determine the reacted layer thicknesses. Metallography and analytical examination of the reaction zones by Scanning Electron Microscope (SEM)/Energy Dispersive X-ray (EDX) methods determine material characteristics.	

No. 2.2.2	SEPARATE EFFECTS TEST FACILITIES	Structural Material Interactions

Subject	Descrtipion
Data Documentation **- Data Reports**	FZKA: Hofmann P and Markiewicz M, "Chemical Behaviour of (Ag,In,Cd) Absorber Alloys in Severe LWR Accidents", KfK 4670, 1990; Hofmann P and Markiewicz M, "Interactions between As-received and Pre-oxidised Zircaloy-4 and Stainless Steel and High Temperatures", KfK-5106, 1994; Hofmann P, Markiewicz M E and Spino J L, "Reaction Behavior of B_4C Absorber Material with Stainless Steel and Zircaloy in Severe Light Water Reactor Accidents", KfK 4598, 1989 and Nuclear Technology **90** (1990), pp. 226-244; Veshchunov M S and Hofmann P, "Modelling of the Interactions between B_4C and Stainless Steel at High Temperatures", J. Nucl. Mater. **226** (1995), pp. 72-91; Veshchunov M S and Hofmann P, "Modelling of B_4C Interactions with Zircaloy at High Temperatures", J. Nucl. Mater. **210** (1994), pp. 11-20; Garcia E A, Hofmann P and Denis A, "Analysis and Modelling of the Chemical Interactions between Inconel Grid Spacers and Zircaloy Cladding of LWR Fuel Rods; Formation of Liquid Phases due to Chemical Interactions", KfK 4921, 1992; Hofmann P and Markiewicz M, "Chemical Interactions between As-Received and Pre-Oxidised Zircaloy-4 and Inconel 718 at High Temperatures", KfK 4729, 1994; Hofmann P and Markiewicz M, "Liquefaction of Zircaloy-4 by Molten (Ag,In,Cd) Absorber Alloy", J. Nucl. Mat. **209** (1994), pp. 92-106; Veshchunov M S and Hofmann P, "Modelling of Zircaloy Dissolution by Molten (Ag,In,Cd) Absorber Alloy", J. Nucl. Mat. **228** (1996), pp. 318-329 and National Heat Transfer Conference, Houston, Texas, 3-6 August 1996. JAERI: Nagase F, Otomo T, Uetsuka H and Furuta T, "Interaction between Zircaloy Tube and Inconel Spacer Grid at High Temperatures", JAERI-M-90-165, 1990; Nagase F, Otomo T, Uetsuka H and Furuta T, "Interaction between Silver-Indium-Cadmium Control Rod Alloy and Zircaloy-4 at High Temperatures", JAERI-M-92-001, 1992; Interaction between Silver and Zircaloy-4 at High Temperatures", JAERI-M-92-179, 1992; "Interaction between Stainless Steel and Zircaloy-4 at High Temperatures", JAERI-M-04-256, 1993; Uetsuka H, Nagase F and Otomo T, "Chemical Interactions between Control Material and Zircaloy or Stainless Steel", Trans. of ANS 1993 Winter Meeting, pp. 309-310; Uetsuka H and Nagase F, "Material Interaction during Severe Accidents of LWRs", Proc. of PHEBUS FP Information Meeting, pp263-272, November 1994; Nagase F, Uetsuka H and Otomo T, "Chemical Interactions between B_4C and Stainless Steel at High Temperatures", J. Nucl. Mat. **245** (1997), pp. 52; Uetsuka H, Nagase F and Otomo T, "High Temperature Interaction between Zircaloy-4 and Inconel-718", J. Nucl. Mat. **246** (1997), pp. 180-188. AEKI: Maróti L, Windberg P, ”Interaction of B_4C Pellets with Zr1%Nb and Stainless Steel”, KFKI-1995-16/G, Frecska J, Maróti L, Matus L,”Kinetics of Chemical Interactions between Zirconium Alloys and Stainless Steels”, KFKI-1995-18/G

No. 2.2.2	SEPARATE EFFECTS TEST FACILITIES	Structural Material Interactions
Subject	**Descrtipion**	
- Evaluation	Hofmann P and Hering W, "Material Interactions during Severe LWR Accidents", KfK 5125, April 1994**;** Belovsky L, Vrtílková V and Valach M, "Failure Behaviour of B_4C-filled PWR Control Rod Segments at Temperatures above 1000°C", NRI Rez report ÚJV 10833-M, January 1997**;** Maróti L,"Chemical Interactions between VVER Core Components under Accidental Condition", Nucl. Eng. Design **172** (1997) pp.73-81	
- Data Availability	The above reports are available.	
Use of Data	As above.	
Special Features		
Correctness of Phenomena	The crucible geometry differs from that in fuel rods, and also in the relative mass of materials present. Differences observed between FZKA and JAERI measurements of reaction rates for the SS/Zry and Incl/Zry systems may be explained in terms of the higher Zry mass inventory used at JAERI (Hering and Hofmann, reference above). Mass and volume ratios must be considered when applying the derived parabolic correlations in severe accident modelling codes.	
Overall Evaluation		
- Strengths	FZKA and JAERI**:** Well-reported measurements are available for the major structural materials interactions relevant to severe accident analysis, covering the temperature and time ranges of interest. AEKI**:** unique set of tests with Russian core materials	
- Weaknesses	-	
- Miscellaneous	There are no transient separate-effects tests reported.	
Comments	The chief use of the work reported here is in the development of models for mechanistic melt progression codes, currently mainly using correlations derived from these steady-state measurements, both for the materials interactions themselves and for the delays in the onset of the reactions caused by the presence of pre-formed ZrO_2 layers (in the case of couples involving Zry). Validation of these models is best carried out independently of the basic measurements, using data from the integral tests (which are transient in nature).	

No. 2.2.3	SEPARATE EFFECTS TEST FACILITIES	Metal/Ceramic Interactions

Subject	Descrtipion
Test Facilities	MONA - FZ Karlsruhe (FZKA), Germany LAVA - FZ Karlsruhe (FZKA), Germany JAERI material interaction experiments, Japan AECL material interaction experiments, Chalk River National Laboratories (CRNL), Canada Lawrence Berkeley Laboratory/University of California, Berkeley (LBL), USA Skoda-UJP and IPSN cooperative experiments, Czech Republic and France JRC/ITU experiments, Karlsruhe, Germany JRC Ispra and ENEA cooperative experiments, Italy FZ Karlsruhe and AECL cooperative experiments, Germany and Canada AEKI material interaction experiments, Hungary FZ Karlsruhe breach criterion experiments, Germany
Objectives	The general objectives of material interaction experiments are to measure the reaction rates of the metals over a range of temperatures and to quantify them, usually in the form of Arrhenius correlations
Facility Geometry	MONA**:** Zry/UO_2 (95%TD UO_2, Zry-4), electric inductive heating, single fuel rod segment (fill gas He), ϕ=9.1/10.7mm, L=150mm, with (1) atmosphere 25%O_2/75%Ar and (2) atmosphere Ar. LAVA**:** (1) Zry/UO_2 (95%TD UO_2, Zry-4), electric inductive heating, UO_2 crucible of 170g, A=5.8cm^2, 10g of Zry, atmosphere Ar and (2) Zry/ZrO_2 (97.3%ZrO_2/2.7%CaO, 75%TD ZrO_2, Zry-4), ZrO_2 crucible of A=7.6cm^2, 10g of Zry, atmosphere Ar. JAERI**:** Zry+Ag/UO_2 (50wt%Zry-4, 50wtAg%), electric heating, UO_2 pellet/metal tube, atmosphere Ar. CRNL**:** Zry/UO_2 (CANDU fuel), radiant energy heating, with (1) fuel rod segment, ϕ=15.25/14.4mm, L=9mm, (2) fuel rod trefoil segment, ϕ=15.25/14.4mm, L= 9mm, (3) UO_2 crucible, ϕ=12.1/6.7mm, L=16.6mm, 13mm deep, and (4) UO_2 crucible, ϕ=14.4/6.7mm, L= 18.4mm, 15mm deep, with atmospheres (1)&(2) steam and (3)&(4) ultra-high purity Ar. LBL**:** Zry/UO_2 (95%TD UO_2, Zry-4), electric inductive heating, UO_2 disks 2mm thick and spheres ϕ=3mm, atmosphere Ar/5%H_2 in (1) thoria crucible, ϕ=10.4/4.7mm; (2) UO_2 crucible, ϕ=10.4/4.9mm, L=10.4mm. Skoda/IPSN**:** Ag-Zry-Fe/UO_2, electric heating, UO_2 and ZrO_2 crucibles inner ϕ=4 or 6 mm, atmosphere Ar. JRC/ITU**:** Zry/unirradiated and irradiated UO_2 (53GWd/tU), electric heating, mainly with graphite crucibles, at.Ar. JRC Ispra/ENEA**:** molten FeO/UO_2, inductive electric heating, UO_2 crucibles, FeO pellets of ϕ=12/14mm, 1mm deep, atmosphere Ar.

No. 2.2.3	SEPARATE EFFECTS TEST FACILITIES	Metal/Ceramic Interactions

Subject	Descrtipion
	FZKA/AECL (FZKA in the LAVA facility): Zry/(UO_2 and ZrO_2 both separately and simultaneously), UO_2 and ZrO_2 crucibles for the separate dissolution tests, UO_2 crucible with a CaO stabilised ZrO_2 central rod for the FZKA simultaneous dissolution tests. Crucible dimensions for ZrO_2 dissolution (1) early FZKA, ϕ=27mm, t=4.7mm, CaO stabilised, 75%TD, (2) late FZKA, as (1) but 93%TD, (3) AECL, ϕ=14mm, t=3.5mm, Y_2O_3 stabilised, 100%TD. Series (2) includes 1-dimensional dissolution tests with a 2mm thick yttria disc on the inside base of the crucible and 2-dimensional dissolution tests with no yttria disc. Crucible dimensions for UO_2 tests, ϕ=14mm, t=5mm, L=16.8mm, ZrO_2 rod (if present) ϕ=6.45mm, again with or without a yttria disc. Electric induction heating for the ZrO_2 tests, tungsten resistance furnace for tests involving UO_2. Inert atmosphere which can be up to 3 bar in LAVA. AEKI: Zr1%Nb/UO_2 (Russian UO_2, Zr1%Nb), electric inductive heating, single fuel rod segment, ϕ=7.6/9.1mm, L=30mm, with atmosphere 25%O_2/75%Ar. FZKA breach criterion: electric inductive heating, single rod, ZrO_2 pellets, ϕ=14mm, l=50mm, Zircaloy-4 cladding, Ar/O_2 atmosphere
Experimental Conditions	The specimen is heated to the test temperature, allowed to react for the desired period, and allowed to cool.
Parameter Range	MONA: Zry/UO_2, system pressure 0.1-4.0MPa with (1) temperature 1173-1673K, reaction times 360-1800s, and (2) temperature 1273-1973K, reaction times 60-3600s. LAVA: system pressure 0.1-0.3MPa, (1) Zry/UO_2, temperature 2223-2523K, reaction times 60-7200s, and (2) Zry/ZrO_2 temperature 2073-2673K, reaction times 60-3600s. JAERI: Zry+Ag/UO_2, temperature 1473-1703K. CRNL: Zry/UO_2, (1) temperature 2143-2193K, reaction times 80-120s, (2) temperature 2143-2193K, reaction times 80-120s, (3) temperature 2273-2473K, reaction times 0-3600s, O-free Zry and Zry/25% O_2, (4) temperature 2473-2773K, reaction times 0-3600s, O-free Zry and Zry/25% O_2. LBL: Zry/UO_2, oxygen concentrations 0.1% (as-received), 2.5% and 5.0%, (1) temperature 2173-2473K, reaction times 10-200s, (2) temperature 2223-2473K, reaction times 15-600s. Skoda/IPSN: various alloys used, pure Zry, Zry-stainless steel (SS), Zry-Ag, Zry-SS-Ag, designed to represent AIC control rod melts, temperatures 1573-2273K, times to 5000s. JRC/ITU: Zry/UO_2, fixed temperature of 2273K, reaction times 25-200s, comparison of dissolution rates of irradiated and unirradiated fuel. JRC Ispra/ENEA: temperature 1573-2273K, reaction times to 300s.

No. 2.2.3	SEPARATE EFFECTS TEST FACILITIES	Metal/Ceramic Interactions

Subject	Descrtipion
	FZKA/AECL**:** for ZrO_2 dissolution, temperature 2273-2673K, reaction times overall 60-7200s (varies amongst series); for UO_2 dissolution, temperature 2373-2573K, reaction times 100-1800s; for simultaneous dissolution fixed temperature of 2373K, reaction time 108-554s. AEKI**:** Zr1%Nb/UO_2, system pressure 4 MPa with temperature 1273-1873K, reaction times 180-7200s. FZKA breach criterion**:** system pressure 0.1MPa, pre-oxidation for 2-9 minutes at 1673K, ramp at 2-10K/s until meltthrough is observed, maximum temperatures 2073-2573K.
Measurements **- On-line** **- Post-test**	The specimen temperatures and the system pressure are measured on-line. Post-test destructive examinations determine the reacted layer thicknesses. Metallography and analytical/chemical examination of the reaction zones by Scanning Electron Microscope (SEM), Energy Dispersive X-ray (EDX) and X-ray Fluorescence Spectroscopy (XFS) methods determine material characteristics.
Data Documentation **- Data Reports**	FZKA**:** Hofmann P and Kerwin-Peck D K, "UO_2/Zircaloy-4 Chemical Interactions and Reaction Kinetics from 1000 to 1700°C under Isothermal Conditions", KfK 3552, 1983**;** Hofmann P and Kerwin-Peck D K, "UO_2/Zircaloy-4 Chemical Interactions and Reaction Kinetics from 1000 to 1700°C under Isothermal and Transient Conditions", J. Nucl. Mater. **124**, pp80-105, 1984**;** Hofmann P, Neitzel H J amd Garcia E A, "Chemical Interactions of Zircaloy-4 Tubing with UO_2 Fuel and Oxygen at Temperatures between 900 and 2000°C**;** Experiments and PECLOX Code", KfK 4422, 1988**;** Hofmann P, Uetsuka H, Wilhelm A N and Garcia A, "Dissolution of Solid UO_2 by Molten Zircaloy and its Modelling", Int. Symposium on Severe Accidents in Nuclear Power Plants", Sorrento, Italy, IAEA-SM-2986/1, 21-25 March 1988**;** Hofmann P et al., "Dissolution of Solid ZrO_2 by Molten Zircaloy", KfK 4100, 4200/0, 1987. AECL**:** Hayward P J and George M, "Dissolution of UO_2 in Molten Zircaloy-4, Part 1: Solubility from 2000 to 2200°C", J. Nucl. Mater. **208**, pp 35-42, 1994 and "Dissolution of UO_2 in Molten Zircaloy-4, Part 2: Phase Evolution during Dissolution and Cooling", ibid. pp 43-52, 1994**;** "Dissolution of UO_2 in Molten Zircaloy-4, Part 3: Solubility from 2000 to 2500°C", J. Nucl. Mater. **232**, pp 1-12, 1996 and "Dissolution of UO_2 in Molten Zircaloy-4, Part 4: Phase Evolution during Dissolution and Cooling of 2000 to 2500°C Specimens", ibid. pp 13-22, 1996. Also available in proprietary reports are UO_2 solubilities in molten Zircaloy and Zry/25%O in the temperature range 2000-2500°C.

No. 2.2.3	SEPARATE EFFECTS TEST FACILITIES	Metal/Ceramic Interactions

Subject	Descrtipion
- **Evaluation**	LBL**:** Kim K T and Olander D R, "Dissolution of Uranium Dioxide by Molten Zircaloy, (I) Diffusion-controlled Reaction", J. Nucl. Mat. **154**, pp85-101, 1988**;** Kim K T and Olander D R, "Dissolution of Uranium Dioxide by Molten Zircaloy, (II) Convection-controlled Reaction", J. Nucl. Mat. **154**, pp102-115, 1988. CIT project**:** The reports of the EC 4th Framework shared cost action project "Corium Interactions and Thermochemistry (CIT)" include details of the Skoda/IPSN, JRC/ITU, JRC Ispra and FZKA/AECL work, see for example the summary in the symposium "FISA-99 – EU Research in Reactor Safety", Luxembourg, 29 November – 1 December 1999, proceedings published as Report EUR 19532 EN. Hofmann P and Stuckert J, "UO_2 and ZrO_2 Dissolution by Molten Zircaloy", Proc. 5th International Quench Workshop, Karlsruhe, 19-22 October 1999, FZ Karlsruhe Interner Bericht 32.21.08, November 1999. The experimental work on dissolution is described in Hayward P J et al., "UO_2 Dissolution by Molten Zircaloy - New Experimental Results and Modelling", FZKA 6379, December 1999, while the breach criteria experiments are described in Hofmann P et al., "ZrO_2 Dissolution by Molten Zircaloy and Cladding Oxide Shell Failure - New Experimental Results and Modelling", FZKA 6383, December 1999. Further details are given in the Final Report of CIT, published by IPSN, which is proprietary. AEKI**:** Maróti L, Windberg P, "Chemical Interaction of Zr1%Nb Cladding with UO_2 and Steam", KFKI-1995-15/G. Veshchunov M S and Hofmann P, "Dissolution of Solid UO_2 by Molten Zircaloy", J. Nucl. Mater. **209** (1994) pp. 27-40**;** Olander DR, "Interpretation of Laboratory Crucible Experiments on UO_2 Dissolution by Molten Zircaloy", J. Nucl. Mater. **224** (1995) pp. 254-265**;** Veshchunov M S, Hofmann P and Berdyshev AV, "Critical Evaluation of Uranium Oxide Dissolution by Molten Zircaloy in Different Crucible Tests", J. Nucl. Mater. **231** (1996) pp. 1-19**;** Veshchunov M S and Berdyshev AV, "Modelling of Chemical Interactions of Fuel Rod Materials at High Temperatures, I Simultaneous Dissolution of UO_2 and ZrO_2 by Molten Zr in an Oxidising Atmpsphere", J. Nucl. Mater. **252** (1998) pp. 98-109 and "Modelling of Chemical Interactions of Fuel Rod Materials at High Temperatures, II Investigation of Downward Relocation of Molten Materials", ibid. pp. 110-120 (1998).
- **Data Availability**	The above reports are available, except where indicated proprietary.
Use of Data	As above.
Special Features	

No. 2.2.3	SEPARATE EFFECTS TEST FACILITIES	Metal/Ceramic Interactions

Subject	Descrtipion
Correctness of Phenomena	The crucible geometry differs from that in fuel rods, and also in the relative mass of materials present. Differences in reaction rates are observed. Veshchunov and Hofmann (reference above) have developed a theoretical model which describes the material behaviour during different stages of the chemical interaction process before and after liquid phase saturation. It is shown that the main cause of the discrepancy amongst the different experimental results found in the literature is connected with different dimensions of the UO_2 crucibles and different UO_2/Zircaloy mass ratios used in the experiments.
Overall Evaluation	
- Strengths	MONA/LAVA**:** Wide temperature and time ranges for Zry/UO_2 reaction. LAVA**:** Unique data on the Zry/ZrO_2 reaction. JAERI**:** Unique data on the Zry+Ag/UO_2 reaction. CRNL**:** Comparison of behaviour in different atmospheres, and with different oxygen concentrations in Zircaloy. LBL**:** Comparison of diffusion-controlled and convection-controlled reactions. CIT project**:** Wide range of materials interactions investigated in a coordinated manner with accompanying analytical efforts. Unique dissolution data for irradiated UO_2. AEKI**:** Unique data with Russian VVER-specific core materials
- Weaknesses	JAERI**:** Data unreported in the literature.
Comments	The chief use of the work reported here is in the development of models for mechanistic melt progression codes, currently mainly using correlations derived from these steady-state measurements. Validation of these models is best carried out independently of the basic measurements, using data from the integral tests (which are transient in nature). UO_2 dissolution tests with irradiated fuel show that the irradiated material is dissolved by Zircaloy more quickly than is unirradiated fuel, by an amount equivalent to a temperature difference of 150K. The preliminary FZKA simultaneous dissolution tests show a faster ZrO_2 dissolution rate and a larger extent of UO_2 and ZrO_2 dissolution than would be expected from separate dissolution tests. The oxide shell failure experiments help to reduce a dominant uncertainty in modelling the progress a severe accident - the transition from mainly rod-like to debris bed geometry. However, the fact that simultaneous dissolution of ZrO_2 and UO_2 together may be faster than expected (see previous sentence) must be taken into account in interpreting these results. Experiments planned in the 5^{th} Framework shared cost action COLOSS, using prototypic materials, may resolve these matters.

No. 2.3	SEPARATE EFFECTS TEST FACILITIES	Reflood
Subject	**Descrtipion**	
Test Facilities	JAERI single rod quench experiments - JAERI, Japan QUENCH programme of single rod tests - FZ Karlsruhe, Germany	
Objectives	In general, quench tests address safety issues relevant to accident management measures which involve water injection into a degrading core. The specific stated objectives of the FZ Karlsruhe and JAERI programmes, which involve quenching of single, oxidised Zircaloy rods, are as follows. JAERI**:** investigation of the conditions of fuel fracture by quenching as parameters of oxide layer thickness on cladding tube and of cladding temperature before quenching; investigation of the characteristics of cladding fracturing by quenching; and investigation of the effect of steam generated during reflooding on fuel quenching behaviour. FZKA**:** examination of the physico-chemical behaviour of a core during quench; provision of improved understanding of the effects of water addition to different stages of a core in the early phase of degradation; and provision of an extensive experimental database for the development of detailed mechanistic models for quench of a degraded core in a rod-like geometry. Both test series are ongoing.	
Facility Geometry	JAERI**:** single rod containing fuel pellets, specimen length 37cm, pellet stack length 32cm, nuclear fission heating. FZKA**:** single rod, empty or containing zirconia pellets, specimen length 10-15cm, electric inductive heating.	
Experimental Conditions	In both facilities, the specimen is heated to the test temperature, then quenched by water. Specific points are: JAERI**:** the specimen is heated in steam or an inert atmosphere (helium), water is injected into the bottom of the test section. The radial heat transfer boundary condition is adiabatic. FZKA**:** pre-oxidation to the desired extent takes place in an Ar/oxygen mixture (20%vol. O_2) or an Ar/steam mixture, the specimen is heated or cooled to the test temperature, quench is achieved by raising a water-filled cylinder over the sample, or rapid cooling is induced by injection of cold steam. The radial heat transfer boundary condition is defined largely by thermal radiation.	
Parameter Range	JAERI**:** system pressure 0.1MPa, rod pressure 0.4/0.5MPa helium, pre-oxidation to 40%, quench temperature range 1273-2073K, reflood rate 7.0-8.0 cm/s. FZKA**:** system pressure 0.1MPa, pre-oxidation at 1673Kto 50%, quench temperature range 1273-1873K, reflood rate 0.3-3.0 cm/s, steam injection at 423K for cooldown possible to 2 g/s (present data to 1 g/s).	

No. 2.3	SEPARATE EFFECTS TEST FACILITIES	Reflood
Subject	**Descrtipion**	
Measurements		
- On-line	JAERI**:** specimen temperatures are measured on-line at six places on the tube. FZKA**:** specimen temperatures are measured on-line at three places on the tube, hydrogen production is also continuously recorded and the outside of the tube is monitored by a video camera.	
- Post-test	Post-test destructive examinations determine the reacted layer thicknesses and microstructures (by metallography and scanning electron microscopy). In the FZKA tests the hydrogen concentration in the metal can be measured, in the LAVA facility, and much attention is paid to the measurement of crack density and patterns.	
Data Documentation		
- Data Reports	JAERI**:** Katanishi S et al., "Quenching Degradation In-Pile Experiment on an Oxidised Fuel Rod in the Temperature Range of 1000 to 1260°C", Nucl. Eng. and Design **132**(1991), pp239-251. FZKA**:** Hofmann P and Noack V, "Physico-Chemical Behavior of Zircaloy Fuel Rod Cladding Tubes During LWR Severe Accident Reflood. Part I: experimental results of single rod quench experiments", FZKA 5846, May 1997**;** Hofmann P, Miassoedov A, Steinbock L, Steinbrück M, Veshchunov MS, Berdyshev AV, Boldyrev AV, Palagin AV and Shestak VE, "Quench Behaviour of Zircaloy Fuel Rod Cladding Tubes: Small Scale Experiments and Modelling of the Quench Phenomena", FZKA 6208, March 1999.	
- Data Availability	Data may be available by agreement with the institution concerned.	
Use of Data	As above.	
Correctness of Phenomena	The main quench phenomena which would occur in-core are represented in the facilities, although the detailed subchannel geometry is not reproduced and the overall balance of heat transfer may not be prototypic.	

No. 2.3	SEPARATE EFFECTS TEST FACILITIES	Reflood
Subject	**Descrtipion**	
Overall Evaluation		
- Strengths	JAERI**:** In-reactor facility. FZKA**:** Video-recording , continuous measurement of hydrogen production, detailed data on crack morphology. Comprehensive parameter range.	
- Weaknesses	JAERI**:** No detailed data reports openly available. FZKA**:** High radial heat losses due to thermal radiation. Limitation to 1873K quench temperature, which is below that for which oxidation excursions are observed on reflood in the CORA and QUENCH facilities for example.	
Comments	The aim of the work reported here is mainly to investigate the mechanisms of quenching of Zircaloy-clad fuel rods, rather than to provide data directly for code validation. The FZ Karlsruhe experiments are closely linked to the QUENCH bundle test programme, see table 1.16.	

No. 2.4	SEPARATE EFFECTS TEST FACILITIES	Melt Pool Thermal Hydraulics

Subject	Descrtipion
Test Facilities	Technische Universität Hannover (TUH), Germany Ohio State University (OSU), USA, sponsored by the US Nuclear Regulatory Commission AEA Technology (AEAT), Culham Laboratory, UK, funded by the UK Health and Safety Executive COPO, Fortum, Finland ACOPO, University of California, Santa Barbara (UCSB), USA University of California, Los Angeles (UCLA), USA BALI, STR/CEN Grenoble, France RASPLAV, Russian Research Institute "Kurchatov Institute", Moscow, Russia, supported by countries in the Organisation of Economic Cooperation and Development (OECD) SIMECO, Royal Institut of Technology (RIT), Division of Nuclear Power Safety, Sweden
Objectives	The general objectives of melt pool thermohydraulics experiments are to measure heat flux distributions in different geometries over a wide range of internal heat generation and to quantify them, usually in the form of correlations Nu = f(Ra) (Nusselt number as a function of Rayleigh number) for averaged and local heat transfer coefficients between melted fuel and crust or surroundings. The melt pool may be formed in the core region or in the lower plenum. Recent experiments explore solidification and crust formation too.
Facility Geometry	TUH: (1) rectangular slab, hxbxs=5x8x2 cm; (2) semicircular slab, rxs=3 to 28x1 cm, h/r=1 to 0.25 cm. OSU: (1) rectangular slab, hxbxs=<25x50x50 cm; (2) cylinder+spherical segment, r=46 cm , h_{spher}=12 cm, $h_{cyl} \leq$ 52 cm. AEAT: rectangular tank, hxbxs=10x20x20cm. COPO I: slice of VVER-440 lower head, hxbxs=80x177x10 cm. COPO II-Lo: slice of VVER-440 lower head, hxbxs=95x178x9 cm. COPO II-AP: slice of a PWR lower head (semicircular slab), rxs=100x9 cm. ACOPO: Axisymmetry moke-up of AP600 lower head (~hemisphere), r = 200cm UCLA: hemisphere, r=7.5 to 22 cm, h/r=1 to 2.6 cm. BALI: semicircular slab, rxs=200x10 cm.

No. 2.4	SEPARATE EFFECTS TEST FACILITIES	Melt Pool Thermal Hydraulics

Subject	Descrtipion
	RASPLAV AW200: semicircular slab, rxs= 40x10 cm. RASPLAV Salt: semicircular slab, r = 20 cm; s = 11 - 17 cm. SIMECO: semicircular slab and vertical section, r = 26.5 cm; s = 9 cm; h/r < 2.35.
Experimental Conditions	TUH: electrical resistance heating, test fluid is water. OSU: electrical resistance heating, test fluid is (1) silver nitrate solution; (2) copper sulphate solution. AEAT: heating by conduction from walls, test fluid is sodium sulphate and sodium nitrate solution. COPO: electrical resistance heating, test fluid is zinc sulphate ($ZnSO_4$) solution. ACOPO: transient cool-down of preheated water, no sustained heating. UCLA: microwave heating, test fluid is Freon R-113. BALI: electrical resistance heating, test fluid is water+salt+glycerine. RASPLAV AW200: heating by conduction from side wall, test materials are U/Zr/O mixture: U/Zr molar ration = 1.6 and 1.2, Zr-Oxidation = 22, 32, 100% RASPLAV Salt: heating by conduction from side wall and direct by electrical resitance, test materials are salts NaF(8%) - $NaBF_4$, NaF(25%) - $NaBF_4$, LiF(46.5%) - NaF(11.5%) - KF (% are relative to molar concentration). SIMECO: internally by electric wires, test fluid biary salt ($NaNO_3$ - KNO_3)
Parameter Range	TUH: temperature 300 K; (1) heat source of <4.2 W/cm³, Rayleigh number (Ra)=10^6 to 10^9; (2) heat source <0.4 W/cm³, Ra=10^7 to 10^{10} , with jet penetration. OSU: temperature 300 K; (1) heat source of <0.04 W/cm³, Ra=10^4 to 10^{12}; (2) heat source ? W/cm³, Ra=10^8 to 10^{14}. AEAT: temperature 270/290 K, no internal heat source, Ra=10^8 to 10^9, some precipitation of salt crystals. COPO I: temperature 350 K, heat source of 0.04 W/cm³, Ra=10^{14} to 10^{15}. COPO II: temperature 350 K, heat source of 0.1 W/cm^3, Ra=10^{14} to 10^{15}. ACOPO: temperature 350 K, pre-heated, Ra=10^{16} to 10^{17}. UCLA: temperature 300 K, heat source of <0.006 W/cm³, Ra=10^{11} to 10^{14}. BALI: temperature 200-300 K, crust simulation by ice , Ra = 10^{16} to 10^{17}

No. 2.4	SEPARATE EFFECTS TEST FACILITIES	Melt Pool Thermal Hydraulics

Subject	Descrtipion
	RASPLAV AW200: temperature <2800 K, side wall heated, corium mass = 200 kg, Ra = 10^{11} to 10^{12} four experiments have been performed in the large scale facility, two tests with low oxidation and significant Carbon content showed strong phase separation, the test with complete oxidation did not separate, the forth test with 32% oxidation and low carbon content was highly uniform during the high temperature phase. RASPLAV Salt: temperature <1000 K, side wall heated and direct heated < 1 W/cm³, Ra = $2 \cdot 10^{11}$ to $2 \cdot 10^{13}$; Pr = 4 - 8, 6 test series have been performed in the first phase ofproject, and two in the second. SIMECO: temperature < 700 K, internally heated 2 - 4 W/cm³, Ra ~ 3 10^{13}.
Measurements **- On-line**	The all tests are performed under steady-state conditions, except ACOPO without internal or external heat sources (constant temperatur diference by cooldown of external heat sink). Temperature field and heat flux distributions are measured either directly by thermocouples and pyrometers or indirectly by holograhic interferometry (TUH). The internal heat source can be derived from electrical power input. In one test facility (BALI) local crust thickness, velocities and void fractions will be measured by laser doppler anemometry and gamma absorption. In the AEAT experiments the boundary layer concentration profile is measured via the refractive index. Local crust thickness was also measured in RASPLAV Salt experiments. In RASPLAV AW200 test 4 material probes have been taken during the heigh temperature transient to distiguish between heat-up, steady state and cool-down effects on concebtration profile and phase separation..
- Post-test	RASPLAV AW200: Corium composition profile and melt separation, ablation and crust formation was estimated by metallographic investigations
Data Documentation **- General Reports**	TUH: Mayinger F, Reineke H H and Jahn M, "Bestimmung der Thermohydraulischen Vorgänge in einer Kernschmelze", BMFT RS 48/1, T. U. Hannover, 1973; Mayinger F et al., "Theoretische und experimentelle Untersuchung des Verhaltens eines geschmolzenen Kerns im Reaktorbehälter und auf dem Betonfundament", Band 5, BMFT RS 166-79-05, T. U. Hannover, February 1980. OSU: Kulacki F A and Goldstein R J, "Thermal Convection in a Horizontal Fluid Layer with Uniform Volumetric Energy Sources", Journal of Fluid Mechanics, **55** Part 2, pp 271-287, 1972; Min J H and Kulacki F A, "An Experimental Study of Thermal Convection with Volumetric Energy Source in a Fluid Layer Bounded from Below by a Segment of a Sphere", 6th International Heat Transfer Conference, Toronto, Canada, 1978.

No. 2.4	SEPARATE EFFECTS TEST FACILITIES	Melt Pool Thermal Hydraulics

Subject	Descrtipion
	AEAT**:** :Schneider S B and Turland B D, "Experiments on Convection and Solidification in a Binary System", Proceedings of the Workshop on Large Molten Pool Heat Transfer, Grenoble, NEA/CSNI/R(94)11, March 1994. COPO I**:** Hongisto O, Kymäläinen O, Tuomisto H and Theofanous T G, "Heat Flux Distribution from a Volumetrically Heated Pool with High Rayleigh Number", Proceedings of NURETH-6, Grenoble, France, pp47-53, 1993 and Proceedings of the Workshop on Large Molten Pool Heat Transfer, Grenoble, NEA/CSNI/R(94)11, March 1994; Kymäläinen O, Tuomisto H, Hongisto O and Theofanous T G, ”Heat Flux Distribution from a Volumetrically Heated Pool with High Rayleigh Numbers”, Nuclear Engineering and Design **149** (1994) 401-408. COPO II**:** Helle M., O. Kymäläinen, H. Tuomisto, "Experimental Data on Heat Flux Distribution from a Volumetrically Heated Pool with frozen Boundaries", OECD/CSNI Workshop on In-Vessel Core Debris Retention and Coolability, Garching, Germany, 3.-6. March, 1998; Helle M, Kymäläinen O and Tuomisto H, ”Experimental COPO II Data on Natural Convection in Homogemous and Stratified Pools”, Ninth International Topical Meeting on Nuclear Reactor Thermal Hydraulics (NURETH-9) San Francisco, California, October 3 - 8, 1999. ACOPO**:** Theofanous T G and Angelini S, ”Natural Convection for In-Vessel Retention at Prototypic Rayleigh Numbers”, Proc. NURETH-8, Kyoto, Japan, 1997. UCLA**:** Asfia F J, "Natural Convection in Volumetrically Heated Spherical Segments", Ph. D. Dissertation, University of California, Los Angeles**;** Frantz B and Dhir V K, ”Experimental Investigations of Natural Convection in Spherical Segments of Volumetrically Heated Pools”, ASME Proc. National Heat Transfer Conference, San Diego, CA, August 1992; Asfia F J and Dhir V K, "Natural Convection Heat Transfer in Volumetrically Heated Spherical Pools", Proceedings of the Workshop on Large Molten Pool Heat Transfer, Grenoble, NEA/CSNI/R(94)11, March 1994. BALI**:** Bonnet J M, Rouge S and Seiler J M, "Large Scale Experiments for Core Melt Retention", Proceedings of the Workshop on Large Molten Pool Heat Transfer, Grenoble, NEA/CSNI/R(94)11, March 1994; Bernaz L., J.-M. Bonnet, B. Spindler, C. Villermaux, "Thermal Hydraulic Phenomena in Corium Pools**:** Numerical Simulation with TOLBIAC and Experimental Validation with BALI", OECD/CSNI Workshop on In-Vessel Core Debris Retention and Coolability, Garching, Germany, 3.-6. March, 1998, Bonnet J M and Seiler J M, ”Thermal Hydraulic Phenomena in Corium Pools**:** the BALI experiments”, ICONE7, Tokyo, Japan, April 19-23, 1999.

No. 2.4	SEPARATE EFFECTS TEST FACILITIES	Melt Pool Thermal Hydraulics

Subject	Descrtipion
- **Data Availability**	RASPLAV**:** Strizhov V, "OECD RASPLAV Project", Proceedings of the Workshop on Large Molten Pool Heat Transfer, Grenoble, NEA/CSNI/R(94)11, March 1994; Asmolov V., "Latest Findings of Rasplav Project", OECD/CSNI Workshop on In-Vessel Core Debris Retention and Coolability, Garching, Germany, 3.-6. March, 1998; Tuomisto H. et al, "Application of the OECD Rasplav Project Results to Evaluations at Prototypic Accident Conditions", OECD/CSNI Rasplav Seminar 2000, Garching, Germany, 14.-15. Nov. 2000; Asmolov V, Ponomarev-Stepnoy N N, Strizhov V and Sehgal R, "Challenges left in the Area of Molten Corium Coolability", FISA99 EU Research in Reactor Safety, Luxembourg, Luxembourg, 29 November - 1 December 1999; De Cecco L, Montanelli P and Spindler B, "TOLBIAC Code Simulation of some Molten Salt RASPLAV Experiments". OECD Workshop on In-Vessel Core Debris Retention and Coolability, Garching, Germany, 3-6 March, 1998, NEA/CSNI/R(98)18, February 1999. SIMECO:Sehgal B R et al., "Core Melt Pressure Vessel Interaction during a Light Water Reactor Severe Accident (MVI)". FISA99 EU Research in Reactor Safety, Luxembourg, Luxembourg, 29 November - 1 December 1999; Sehgal,B R, Bui V A, Dinh T N, Green J A, Kolb G, "SIMECO Experiments on In-Vessel Melt Pool Formation and Heat Transfer with and without a Metallic Layer", OECD Workshop on In-Vessel Core Debris Retention and Coolability, Garching, Germany, 3-6 March, 1998, NEA/CSNI/R(98)18, February 1999. The above reports are available. On-line data may be available on demand to the owning organisations.
Use of Data	As above.
Special Features	The experiments mentioned herein differ in geometry, size, material, heating method, temperature, heat source density and Rayleigh number and bear special conditions. Geometry: Rectangular, fundamental investigation**:** UH(1), OSU(1), AEAT Two-dimensional flow, slab geometry**:** TUH(2), COPO, BALI, RASPLAV AW200, RASPLAV Salt Three-dimensional flow, hemisphere**:** UCLA Three-dimensional flow, cylindrically**:** OSU(2) Size: Small (< 2 dm**3)**:** TUH, AEAT Medium**:** OSU(1), UCLA, RASPLAV AW200, RASPLAV Salt Large (> 50 dm**3)**:** OSU(2), COPO, BALI

No. 2.4	SEPARATE EFFECTS TEST FACILITIES	Melt Pool Thermal Hydraulics

Subject	Descrtipion
	Material: Aqueous solution: TUH, OSU, AEAT, COPO, BALI Frigene: UCLA Salt: RASPLAV Salt Ceramic: RASPLAV AW200 Heating Method: Electrical resistance: TUH, OSU, COPO, BALI, RASPLAV Salt (one series) Microwave: UCLA Heat conduction from side walls: AEAT, RASPLAV AW200, RASPLAV Salt (all except one series) Internal electric resistance wires: SIMECO Transient cool-down: ACOPO Temperature: Low (< 400 K): TUH, OSU, AEAT, COPO, ACOPO, UCLA, BALI Medium: RASPLAV Salt, SIMECO High (> 2400 K): RASPLAV AW200 Heat source density: Low (< 0.1 W/cm**3): OSU, UCLA, BALI, COPO I Medium: TUH(2), COPO II, RASPLAV Salt High (> 1.0 W/cm**3): TUH(1), RASPLAV AW200, SIMECO Rayleigh number: Low (< 1.e12): TUH, OSU(1), AEAT, RASPLAV AW200 Medium: OSU(2), COPO, UCLA, RASPLAV Salt, SIMECO High (> 1.e15): ACOPO, BALI Special Condition: Jet penetration: TUH(2) Precipitation of salt crystals: AEAT Phase separation, stratification: RASPLAV AW200 Crust formation, wall interaction: RASPLAV AW200 Multi layer melt pool: RASPLAV AW200, SIMECO Crust simulation: BALI, COPO II, RASPLAV Salt, SIMECO

No. 2.4	SEPARATE EFFECTS TEST FACILITIES	Melt Pool Thermal Hydraulics
Subject	**Descrtipion**	
Correctness of Phenomena	The correct simulation of natural convection in an internally heated melt pool of reactor core material requires high Rayleigh numbers (> 1.e16); which is determined by heat source density and geometrical dimensions, in conjunction with solidification and liquefaction of multi-phase systems (ceramic melt with metallic components U/Zr/O). This goal has not been reached up to now. Extrpolation to reactor scale and condions need computer tools	
Overall Evaluation		
- Strengths	One particular process has been simulated and quantified to generate a data base for code modelling: Heat transfer coefficient as function of Rayleigh number (< 1.e15) and local position for different geometries with and without phase change. First results on phase secretion are provided by the RASPLAV project. With simulate material high Rayleigh number have been reached including crust formation (ice in BALI). Test in RASPLAV AW200 with real corium melt indicated some limited material interaction with wall structures. The RASPLAV project was acompied by many use full small scale material investigations.	
- Weaknesses	Either the tests are performed with unprototypical materials or the estimation of heat transfer coefficients is not possible due to the lack of appropriate measurements. A direct transposition to reactor conditions is therefore inpossible. Not judging the quality of numerical simulation of free convection in melt pools, the indirect transposition of experimental results to the reactor case by means of computer codes is handicapped by the lack of adequate data of material properties. Since the formation of the melt pool either by continous melt relocation (candling) or core slump or by dry out and subsequent melting of particulate debris has not been studied up to now, the initial melt pool conditions are unknown. Furthermore the material composition (metal content) and local material distribution due to precipitation, secretion or accumulation are not completely understood.	
Comments	Melt pool phenomena are typically for the late phase. They need more theoretical and experimental investigations. The PHEBUS FP and MASCA (Continuation of RASPLAV) projects should be carefully observed to gain further experience.	

No. 2.5	SEPARATE EFFECTS TEST FACILITIES	Gap Thermal Hydraulics

Subject	Descrtipion
Test Facilities	CHFG: Korea Atomic Energy Research Institut (KAERI), Korea BENSON test rig : operated by Siemens, Erlangen, and supported by BMWi, Germany KC-CTF: Russian Research Institute "Kurchatov Institute" (RRC-KI), Moscow, Russia CORCOM: operated by Technical University Munich and supported by BMWi, Germany
Objectives	The general objectives of gap thermal hydraulics experiments are to explore the cooling potential of a gap between core debris (solid or molten) and RPV wall. Further application is the extrapolation to in-vessel core retention and coolability for present and future reactor design (core catcher).
Facility Geometry	CHFG: Hemisphere, r = 250 mm, s = 0.5, 1.0, 2.0, 5.0, 10.0 mm BENSON test rig: spherical 30 ° section, r = 2000 mm, s = 1.0 - 10.0 mm KC-CTF: rectangular, vertical or inclined, h =< 400 mm, b = 200 mm, s = 0.5 - 5.0 mm CORCOM(1): rectangular, inclined 0, 5, 10, 15, 20, 25°, l =260, 380, 480 mm, b = 140 mm, s = 1, 2, 3, 6, 11 mm CORCOM(2): rectangular, inclined 10°, debris above gap h = 140 mm, l = 480 mm, b = 140 mm, s = 0.5, 2.0 mm
Experimental Conditions	CHFG: electrical resistance heated wall, test fluid water or Freon 113, quasi steady state condition BENSON test rig: electrical resistance heated wall, test fluid water, quasi steady state condition KC-CTF: electrical resistance heated wall(s), test fluid water, quasi steady state condition CORCOM(1): electrical resistance heated wall, test fluid R134a, quasi steady state condition CORCOM(2): inductive (3.3 kHz) heated debris, test fluid water or R134a, transient & quasi steady state cond.
Parameter Range	CHFG: temperature < 600 K, wall heat flux < 500 kW/m², pressure = 0.1 - 1.0 MPa BENSON test rig: temperature < 750 K, wall heat flux < 550 kW/m², pressure = 1.0 - 12.0 MPa KC/CTF: temperature < 600 K, wall heat flux < 1000 kW/m², pressure = 0.1 - 8.0 MPa CORCOM(1): temperature < 620 K, wall heat flux < 750 kW/m², pressure = 0.8 - 1.8 MPa CORCOM(2): debris heat source / debris cross section < 600 kW/m², pressure(R134a) = 0.8 - 1.8 MPa, pressure(water) < 10 MPa

No. 2.5	SEPARATE EFFECTS TEST FACILITIES	Gap Thermal Hydraulics

Subject	Descrtipion
Measurements	
- On-line	CHFG**:** Pressure, temperature field and heater power. BENSON test rig**:** Total pressure, pressure difference beteen gap center and periphery, temperature field and average heat flux. KC-CTF**:** Pressure, temperature field and average heat flux. CORCOM(1)**:** Pressure, temperature field, local heat flux, local void fraction and visual observation (high speed). CORCOM(2)**:** Pressure, temperature field, average heat flux, local void fraction, visual observation (high speed)
- Post-test	No examinations, except visual inspection of debris in CORCOM(2)
Data Documentation	
- General Reports	CHFG**:** J. H. Chung, R. J. Park, and S. B. Kim, "Visualisation Experiments of the Two Phase Flow inside Hemispherical Gap", Int. Communications Heat & Mass Transfer, Vol. 25, No 5, pp.693-700, July 1998; J. H. Chung, R. J. Park, and S. B. Kim, Thermal-hydraulic Phenomena Relevant to Global Dryout in a Hemispherical Narrow Gap, Heat & Mass Transfer 3, pp. 325-328, 1998; R. J. Park, S. J. Lee, K. H. Kang, J. H. Kim, S. B. Kim, H. D. Kim, J. H. Jeong, "An Experimental Study on critical Heat Flux in a Hemispherical Narrow Gap", SARJ-99(Workshop on Severe Accident Research), Tokyo, Japan, November 8-10, 1999; J. H. Chung, R. J. Park, K. H. Kang, S. B. Kim, and H. D. Kim, "Experimental Study on CHF in a Hemispherical Narrow Gap", OECD/CSNI Workshop on In-Vessel Core Debris Retention and Coolability, Technical University of Munich, Garching, Germany, March 3-6, 1998 BENSON test rig**:** Köhler W., H. Schmidt, O. Herbst, W. Krätzer, "Experiments on Heat Removal in a Gap between Debris Crust and RPV Wall", OECD/CSNI Workshop on In-Vessel Core Debris Retention and Coolability, Technical University of Munich, Garching, Germany, March 3-6, 1998 KC-CTF: Asmolov V., L. Kobzar, V. Nickulshin, V. Strizhov, "Experimental Studies of Heat Transfer in the Slotted Channels at the CTF Facility", OECD/CSNI Workshop on In-Vessel Core Debris Retention and Coolability, Technical University of Munich, Garching, Germany, March 3-6, 1998.

No. 2.5	SEPARATE EFFECTS TEST FACILITIES	Gap Thermal Hydraulics

Subject	Descrtipion
- **Data Reports**	CORCOM**:** Zeisberger A., P. Horner, F. Mayinger, "Cooling Mechanisms at the bottom of relocated Porous Debris", ANS Winter Meeting, Albuquerque, NM, USA, 16.-20. Nov. 1997, Transactions of ANS (77) 1997, pp 270-271; Horner P., A. Zeisberger, F. Mayinger, " Evaporation and Flow of Coolant at the Bottom of a Particle-Bed modelling Relocated Debris", OECD/CSNI Workshop on In-Vessel Core Debris Retention and Coolability, Garching, Germany, 3.-6. March, 1998; Horner P., A. Zeisberger, F. Mayinger, "Simulating Gap Cooling Phenomena of a Melt in the Lower Head of a RPV", SARJ'98, Tokyo, Japan, 4.-6- Nov. 1998; Zeisberger A., P. Horner, F. Mayinger, "Boiling in Particle Beds with Internal Heat Sources", NURETH9, San Francisco, 3.-8. Oct. 1999; Horner P., A. Zeisberger, F. Mayinger, " Boiling and Flow Regimes in a Gap with Adjustable Inclination and Heating from the Top", NURETH9, San Francisco, 3.-8. Oct. 1999. BENSON test rig**:** Köhler W., H. Schmidt, O. Herbst, W. Krätzer, "Thermal-hydraulic Investigations of Debris/Wall-Interaction", Final Report, Siemens Erlangen, Nov 1998
- **Data Availability**	On request from the authors or operating institution
Use of Data	The large scale tests in the BENSON test rig can be used for direct application to reactor scale (TMI-2) or core catcher devise. The small scale experiment are used for model develpoment for the thermal hydraulics and heat transfer in small gaps respective for flooded debris.
Special Features	BENSON test rig**:** large scale and high pressure. It represents reactor conditions. CORCOM (2): includes debris heat transfer with and without gap underneeth, test with flooding of over heated debris bed
Correctness of Phenomena	Most experiments employ a gap with defined geometry (except some in CORCOM 1). This may represent some special conditions (core catcher devise) but it does not represent the reactor conditions with areas of direct contact between debris or melt with the RPV wall or with the developing of a gap due to wall creeping and/or crust movement.
Overall Evaluation	
- **Strengths**	A wide range of gap thickness and inclination have been explored, usefull for model development and verification.
- **Weaknesses**	Most experiments does not reach high local heat fluxes or high temperatures typical for severe accident conditions. Small scale test facilities do not allow extrapolation to multi dimemsional flow. Same uncertainties have to considered as in usual thermal hydraulic experiments

No. 2.6	SEPARATE EFFECTS TEST FACILITIES	Ex-vessel Thermal Hydraulics

Subject	Descrtipion
Test Facilities	SULTAN: operated by CEA Grenoble and supported by CEA, EdF and FRAMATOME, France SBLB: operated by Pennsylvania University and supported by USNRC CYBL: operated by Sandia national Laboratory (SNL) and supported by USNRC, USA UPLU: operated by University of California, Santa Barbara (UCSB), USA, supported by FORTUM and US DOE
Objectives	Investigation of ex-vessel cooling as accident management measure, to enlarge the data base on critical heat flux for model development and to verify the cooling capability under reactor typical condions
Facility Geometry	SULTAN: rectangular gap, vertical or inclined, lenght = 400 cm, width = 15 cm, thickness = 3 - 15 cm SBLB: 1/15 linear scaled RPV mock-up with thermal insulation and cavity, RPV: radius = 15 cm, $heigth_{cyl}$ = 70 cm, insulation radius = 23 cm, adustable minimum gap width between RPV and insulation, CYBL: 1/1 scale of RPV mock-up, torispherical and cylidrical part, radius = 185 cm, height = 500 cm, submerged in large water tank ULPU: full height natural convection loop with heating device to represent conditions of Loviisa NPP
Experimental Conditions	All facilities have water as test fluid and electrically heated surfaces except the second heating device of CYBL, where the heat flux was imosed by radiative heating. Test are quasi steady state with variable electric power and flow conditions.
Parameter Range	SULTAN: Fluid pressure 0.1 - 0.5 MPa, Fluid temperature < 400 K, heat flux ≤ 2000 kW/m² SBLB: Pressure =.1 MPa, water saturated or subcooled according to hyrdostatic pressure, heat flux ≤ 1200 kW/m² CYBL: Pressure =.1 MPa, water saturated or subcooled according to hyrdostatic pressure, heat flux ≤ 500 kW/m² ULPU: Pressure =.1 MPa, water saturated or subcooled according to hyrdostatic pressure, heat flux ≤ 1400 kW/m²
Measurements **- On-line**	SULTAN: total pressure and power, local wall and fluid temperature, differential pressure, and void fraction, flow visualisation SBLB: local wall temperature and heat flux, total power, flow visualisation CYBL: local wall temperature and heat flux, total power, flow visualisation ULPU: local wall temperature and heat flux, total power, flow visualisation

No. 2.6	SEPARATE EFFECTS TEST FACILITIES	Ex-vessel Thermal Hydraulics

Subject	Descrtipion
Data Documentation	
- Data Reports	SULTAN: Rougé S, I Dor, G Geffraye, "Reactor Vessel External Cooling for Corium Retention, SULTAN Experimental Program and Modelling with CATHARE Code", OECD/CSNI Workshop on In-Vessel Core Debris Retention and Coolability, Garching, Germany, 3.-6. March, 1998. SBLB: Cheung F B, Y C Liu,"Natural Convection Boiling on the Outer Surface of a Hemispherical Vessel Surrounded by a Thermal Insulation Structure", OECD/CSNI Workshop on In-Vessel Core Debris Retention and Coolability, Garching, Germany, 3.-6. March, 1998. CYBL: Chu T Y, J H Benz, S E Slezak, W F Pasedag, "Ex-vessel Boiling Experiments - Laboratory and Reactor Scale Testing of the Flooded Cavity Concept for In-vessel Core Retention", Nucl. Engng. & Des., **169**, 88-99 UPLU: Theofanous T G, "In-vessel Retention as a Severe Accident Management Scheme", OECD/CSNI Workshop on In-Vessel Core Debris Retention and Coolability, Garching, Germany, 3.-6. March, 1998. Kymäläinen O., Tuomisto H., Theofanous T.G, "Critical Heat Flux on Thick Walls of Large Naturally Convecting Loops", Proceedings of 1992 National Heat Transfer Conference, San Diego, California, August 9-12, 1992; Theofanous T G et al, "Critical Heat Flux through Curved, Downward Facing, Thick walls", Nucl. Engng. & Des., **151**, 247-258 (1994); Theofanous T G, "In-vessel Retention as a Severe Accident Management Scheme", OECD/CSNI Workshop on In-Vessel Core Debris Retention and Coolability, Garching, Germany, 3.-6. March, 1998.
- Data Availability	On request from the authors or operating institution
Use of Data	The large and medium scale tests are directly used or extrapolated for the application to reactor scale. The SULTAN experimental data are used for develpoment and verification of the thermal-hydraulic and heat transfer models for flooded cavity or ex-vessel core catcher to be implemented in system codes.
Correctness of Phenomena	No restrictions for intact or not serverely damaged structures or thermal insulation and not too much soiled water
Overall Evaluation	
- Strengths	With SULTAN a wide range of gap thickness and inclination as well subcooling and heat flux have been explored, usefull for model development and verification. Results of the other experiments are applicable to reactor scale and can be used for specific code validation.
- Weaknesses	Natural circulation flow is strongly depended on the design of containment structures, compartments, heat sinks etc.

No. 2.7	SEPARATE EFFECTS TEST FACILITIES	Gap Formation
Subject	**Descrtipion**	
Test Facilities	FOREVER: Royal Institut of Technology (RIT), Division of Nuclear Power Safety, Sweden LAVA: Korea Atomic Energy Research Institut (KAERI), Korea	
Objectives	Investigation of the gap formation between the debris and the lower head vessel wall and evaluation for the effect of the gap on the cooling characteristics of the lower head vessel.	
Facility Geometry	FOREVER: themispherical test section with 1/10 linear scale mock-up of lower plenum, RPV: cylindrical height = 40 cm, inner radius = 20 cm, wall thickness = 1.5 cm, melt volume = 20 dm^3, wall material: carbon steel. LAVA: hemispherical test section with 1/8 linear scale mock-up of lower plenum, RPV: cylindrical height = 80cm, inner radius = 25 cm, wall thickness = 2.5 cm, melt volume = 10 dm^3, wall material: carbon steel.	
Experimental Conditions	FOREVER: The vessel is pre-heated, the melt ($CaO-B_2O_3$ or $CaO-WO_3$), generated in an external furnace, is poured into the vessel and the system pressurized. With this the test phase is initiated. The melt temperature is controlled by an nternal heater device. LAVA: The vessel is filled with water and pre-heated, the melt is generated by thermite reaction .(40kg of molten Al_2O_3/Fe or 30kg of Al_2O_3) and drained into the water within the lower vessel head, the system is pressurized. With this the transient test phase is initiated and messurments taken.	
Parameter Range	FOREVER: internal pressure load on the lower head vessel < 4 MPa, melt temperature < 1700 K LAVA: internal pressure load on the lower head vessel < 1.6MPa, melt temperature < 2500 K, water subcooling = 5.5 to 55 K, water height = 0.25 to 0.5 m	
Measurements **- On-line**	FOREVER: pressure, local temperatures of the lower head vessel wall and melt or debris, vessel deformation and creep, electric power input LAVA: pressure, local temperatures of the lower head vessel wall and melt, deformation of the lower head vessel wall	
- Post-test	FOREVER: plastic deformation of lower vessel head LAVA: check on the existence and the spatial distribution of the gap using an ultrasonic pulse echo method, metallurgical inspections of the debris and the lower head vessel specimen to observe the permanent structural deformations of the vessel and the microscopic characteristics focused on the porosity and permeability within the solidified debris.	

No. 2.7	SEPARATE EFFECTS TEST FACILITIES	Gap Formation
Subject	**Descrtipion**	
Data Documentation **- Overview** **- Data Reports** **- Data Availability**	FOREVER**:** Sehgal B R et al, "FOREVER Experiments on Thermal and Mechanical Behaviour of a Reactor Pressure Vessel during a Severe Accident", OECD/CSNI Workshop on In-Vessel Core Debris Retention and Coolability, Garching, Germany, March 3-6, 1998 LAVA**:** K. H. Kang et al., ”Experimental Investigation on In-vessel Debris Coolability through Inherent Cooling Mechanisms”, OECD/CSNI Workshop on In-Vessel Core Debris Retention and Coolability, Garching, Germany, March 3-6, 1998**;** J. H. Kim et al., ”Experimental Study on Inherent In-Vessel Cooling Mechanism during a Severe Accident”, ICONE-7, Tokyo, Japan, April 19-23, 1999.	
Use of Data		
Special Features		
Correctness of Phenomena		
Overall Evaluation **- Strengths** **- Weaknesses**		
Comments	No experimental data available yet	

No. 2.8	SEPARATE EFFECTS TEST FACILITIES	Fuel Coolant Interaction

Subject	Descrtipion
Test Facilities	WFCI**:** University of Wisconsin, USA MAGICO 2000**:** University of California, Santa Barbara (UCSB), USA SIGMA 2000**:** University of California, Santa Barbara (UCSB), USA
Objectives	The general objectives of these separate effects tests are to explore various aspects of fuel coolant interactions, including premixing, energetigs of explosions and the effect of material properties and coolant conditions. The results are used for model development and verification.
Facility Geometry	WFCI(1)**:** One dimensional shock tube (inner diameter = 8.7 cm, volume = 8.7 dm^3), trigger device, expansion tube (volume = 34.3 dm^3), furnace and melt pouring device above test section WFCI(2): as WFCI(1) but larger test section (inner diameter = 17.3 cm, volume = 34.3 dm^3) MAGICO 2000**:** Rectangular water tank, water volume hxbxs = 8x10x2 dm^3, debris pouring device above test tank. SIGMA 2000**:** One dimensional shock tube (inner diameter = ? cm, volume = ? dm^3), trigger device
Experimental Conditions	WFCI(1)**:** Super heated tin melt is poured into subcooled water, micro fragmetation initiated by trigger. WFCI(1)**:** Superheated iron oxide melt is poured into subcooled water, micro fragmetation initiated by trigger. MAGICO 2000**:** Preheated particles are poured into saturated or subcooled water, SIGMA 2000**:** Super heated tin or iron melt is poured into subcooled water, micro fracmentation initated by shock wave.
Parameter Range	WFCI(1)**:** Melt mass 0.72 - 4.48 kg, melt temperature 760 - 1250 K, water subcooling 7 - 75 K WFCI(2)**:** Melt mass 1.2 kg, melt temperature ~ 1900 K, water subcooling 15 - 75 K MAGICO 2000**:** Particle: diameter 2; 7 mm, mass 2.6 - 5.7 kg, temperature 300; 1670 - 2270 K, water subcooling 0; 10 K SIGMA 2000**:** Single droplets: diameter 5 - 7 mm, mass ~ 1 g, temperature 1270 - 2070; 1680 - 1920 K, water subcooling 10; 80 K, shock wave pressure 6.8; 20.5; 27.2 MPa.

No. 2.8	SEPARATE EFFECTS TEST FACILITIES	Fuel Coolant Interaction
Subject	**Descrtipion**	
Measurements		
- On-line	WFCI**:** melt and water temperature, local pressure, thermic to mechanical energy conversation MAGICO 2000**:** Void and particle distribution and void fraction (X-ray), swell level SIGMA 2000: Pressure, mixing region and mass distribution	
- Post-test	Debris formation	
Data Documentation		
- Overview	MAGICO 2000: Angelini S, T G Theofanous, W W Yuen, "On the Regime of Premixing", OECD/CSNI Spec. Mtg. On Fuel Coolant Interaction, May 1997, Tokai-Mura, Japan SIGMA 2000: "Experimental Simulation of Microinteractions in Large Scale Explosions", OECD/CSNI Spec. Mtg. On Fuel Coolant Interaction, May 1997, Tokai-Mura, Japan	
- Data Reports	WFCI**:** Park H S, R Champman, M L Corradini, "Vapor Explosions in a One-Dimensional Large-Scale Geometry with Simulant Materials", NUREG/CR 6623, Oct. 1999	
- Data Availability	On request from the authors or operating institution	
Use of Data	Development and verification of FCI codes	
Special Features		
Correctness of Phenomena	See below "Comments"	
Overall Evaluation	See below "Comments"	
- Strengths		
- Weaknesses		
Comments	See Magallon D et al: "MFCI Project, Final Report", European Commission report INV-MFCI(99)-P007, 1999. "Technical Opinion Paper on Fuel Coolant Interactio", NEA/CSNI/R(99)24, Apr. 2000	